UNIVERSITEIT GENT

FACULTY OF SCIENCES

Unraveling molecular mechanisms regulating leaf growth under drought:

It's all about timing

Marieke Dubois

October 6, 2015

Promotor: Prof. Dr. Dirk Inzé

Dissertation submitted in partial fulfillment of the
requirements to obtain the degree of
Doctor of Philosophy (Ph.D)
in Biotechnology

UNIVERSITEIT GENT

VIB

PSB
A VIB-UGENT DEPARTMENT

Ghent University - Department of Biotechnology and Bioinformatics
VIB - Department of Plant Systems Biology

Examination board

Chair

Prof. Dr. Geert De Jaeger
Ghent University – Department of Plant Biotechnology and Bioinformatics
VIB – Department of Plant Systems Biology

Secretary

Prof. Dr. Dirk Inzé
Ghent University – Department of Plant Biotechnology and Bioinformatics
VIB – Department of Plant Systems Biology

Members

Prof. Dr. Patrick Achard *
CNRS/IBMP – Department of Molecular Mechanisms of Phenotypic Plasticity

Prof. Dr. Bruno Cammue *
K.U. Leuven – Centre of Microbial and Plant Genetics
VIB – Department of Plant Systems Biology

Dr. Stijn Dhondt
Ghent University – Department of Plant Biotechnology and Bioinformatics
VIB – Department of Plant Systems Biology

Dr. Nathalie Gonzalez
Ghent University – Department of Plant Biotechnology and Bioinformatics
VIB – Department of Plant Systems Biology

Prof. Dr. Frank Van Breusegem *
Ghent University – Department of Plant Biotechnology and Bioinformatics
VIB – Department of Plant Systems Biology

Prof. Dr. Filip Vandenbussche *
Ghent University – Department of Physiology

* These members are also members of the reading commission.

Table of Contents

List of abbreviations

ABA	Abscisic acid
ACC	1-aminocyclopropane-1-carboxylic acid
ACS	ACC SYNTHASE
ACO	ACC OXIDASE
ANOVA	Analysis of variance
APC/C	ANAPHASE PROMOTING COMPLEX / CYCLOSOME
bHLH	Basic helix-loop-helix
C_2H_4	Ethylene
CCA1	CIRCADIAN CLOCK ASSOCIATED
CDK	CYCLIN DEPENDENT KINASE
CDR	Cell division rate
CKI	CDK INHIBITOR
CPL3	C-terminal domain PHOSPHATASE-LIKE
CYC	CYCLIN
DAS	Days after stratification
DEL1	DP-E2F-LIKE1
DEX	Dexamethasone
Dr	Drought
DREB	DROUGHT-RESPONSIVE ELEMENT BINDING
ERF	ETHYLENE RESPONSE FACTOR
EGM	ENHANCED GROWTH on MANNITOL
GA	Gibberellin
GA2-OX6	GA 2-OXIDASE6
GAI	GA INSENSITIVE
GO	Gene ontology
GR	Glucocorticoid receptor
IOE	Inducible overexpression
JA	Jasmonic Acid
KRP	KIP-RELATED PROTEIN
LEA	LATE EMBRYOGENESIS ABUNDANT
LHY1	LONG HYPOCOTYL1

LUC	LUCIFERASE
Mann	Mannitol
M(A)PK	MITOGEN-ACTIVATED PROTEIN KINASE
miRNA	Micro-RNA
MKK	MAPK KINASE
MS	Murashige and Skoog
MYB51	MYB-containing domain transcription factor 51
OSCA	OSMOLALITY-INDUCED CA^{2+}
PCC	Pearson Correlation Coefficient
PEG	Poly-ethylene glycol
p*GENE*	Promoter *of a gene*
PIF	PHYTOCHROME INTERACTING FACTOR
PIP	PLASMAMEMBRANE INTRINSIC PROTEIN
qRT-PCR	Quantitative Real-Time Polychain Reaction
RBOH	RESPIRATORY BURST OXIDASE HOMOLOG
RCER	Relative cell expansion rate
RGA	REPRESSOR OF *ga1-3*
RGL	RGA-LIKE
RGR	Relative growth rate
ROS	Reactive oxygen species
RST1	RESURRECTION1
SAM	Shoot apical meristem
SAM	S-adenosyl-methionine
SE	Standard error
SIM	SIAMESE
SMR	SIM-RELATED
STZ	SALT-TOLERANT Zn-FINGER
TF	Transcription factor
TOC1	TIMING OF CAB 1
UVI4	UV-B-INSENSITIVE 4
WW	Well-watered
Y2H	Yeast-2-hybrid

Aims and thesis outline

With a rapidly growing world population and an increasing demand for food, the importance of stabilizing plant yield even under adverse environmental conditions is evident. One of the most destructive factors for agriculture worldwide is drought stress. As illustrated by the drought period of last summer, drought stress in moderate climates does not often threaten the survival of plants, but has a clear negative impact on plant growth. During vegetative growth, even when the water availability has only slightly decreased, mechanisms are quickly induced to repress the growth of plant organs such as leaves. It has been shown that exposure of crop to drought during their vegetative growth period leads to a decrease in final seed yield. Therefore, understanding this leaf growth inhibition at the molecular level forms a first major step towards future engineering of plants with reduced yield penalties under drought.

With this ultimate goal in mind, our group explored the mechanisms underlying leaf growth inhibition in Arabidopsis by exposing plants to *in vitro* medium supplemented with an osmotic compound thought to mimic drought stress. When I started my PhD it was already clear that (i) the response to stress is extremely fast, (ii) this response is highly depending on the developmental stage of the leaf, and (iii) the plant hormones ethylene and gibberellins (GA) might be important in the youngest leaves. Specifically in these young, actively growing leaves ethylene triggered a very prompt response involving several ETHYLENE RESPONSE FACTORs (ERFs) and, a bit later, repression of the GA-pathway is responsible for the inhibition of the growth machinery. However, a major question remained unsolved and would become the common thread throughout my research:

What are the molecular networks connecting ethylene accumulation and the GA-pathway, thereby regulating leaf growth inhibition under stress?

To explore this, we first opted for the routinely-used *in vitro* osmotic stress assays as they offer multiple advantages to uncover such rapid responses. We first identified a simple pathway, connecting one ERF to leaf growth inhibition. Next, we linked it to another ERF, and it soon became clear that actually a whole network of regulatory

proteins is orchestrating leaf growth under osmotic stress. However, the question whether these mechanisms would be relevant during drought stress in soil still triggered our curiosity, and the exploration of it formed the last part of my PhD. This thesis presents the major results, bundled in four results chapters, which are preceded by two introduction chapters to clarify the context of the work:

- In **Chapter 1**, we reviewed the complex and sometimes contradictory roles of ethylene in leaves, with an emphasis on its role in growth.

- In **Chapter 2**, we clarify the reasons why osmotic stress assays were ever introduced to mimic drought stress, and we provide an overview of the rapid stress responses unraveled using such setups.

- In the first results chapter, **Chapter 3**, we provide the first piece of the puzzle and present the ERF6 as a central regulator of leaf growth under stress. We show that ERF6 regulates the inactivation of the growth-stimulating GA-pathway and induces multiple other stress-related mechanisms.

- In **Chapter 4**, we characterize in more detail the relationship between ERF6 and one of its target genes, *ERF11*. By inducing *ERF11*, ERF6 activates a negative feedback mechanism to fine-tune the stress response.

- As growth regulation of leaves under stress is supposed to be more complex than the presented ERF6/ERF11-centered pathway, we performed a large scale screen for new genes potentially involved in this growth-regulatory network, the results of which are presented in **Chapter 5**.

- In the last part of my PhD, we established a new experimental setup to capture similar growth-regulatory mechanisms in plants exposed to drought stress in soil. To our surprise, the response to real drought is incredibly complex and highly depending on the timing of the measurement. We present these unexpected results in **Chapter 6**.

- We conclude this thesis with **Chapter 7**, providing a broader general discussion about these growth-regulatory mechanisms uncovered *in vitro* and in soil, and how they compare. Additionally, we discuss possible future paths to further understand the fascinating mechanisms underlying leaf growth under drought.

Part 1:

INTRODUCTION

Chapter 1

DIVERSE AND CONTRADICTORY ROLES OF ETHYLENE IN LEAVES

Marieke Dubois [a,b] and Dirk Inzé [a,b]

[a] Department of Plant Systems Biology, VIB, Ghent, Belgium
[b] Department of Plant Biotechnology and Bioinformatics, Ghent University, Belgium

Contributions: M.D. performed the literature study and was the main author of the chapter. D.I. supervised the project and contributed to the writing of the manuscript.

Leaves grow and move, adapting the rate and amplitude of both processes during their development, but also depending on the time of day or on the environmental conditions to which the plant is exposed. The phytohormone ethylene plays a crucial role in these responses, functioning as a hub integrating endogenous developmental, diurnal, and stress-related signals. In this chapter, we provide an overview of the highly diverse and sometimes contradictory roles of ethylene in leaves, with emphasis on the molecular mechanisms underlying these different processes. Ethylene is a well-known repressor of leaf growth, able to inhibit both cell division and cell expansion when environmental conditions are unfavorable. Since the levels of ethylene fluctuate during the day, it could also have a role in diel leaf growth rhythms. We therefore speculate about a possible mechanism by comparing diurnal ethylene oscillations and dynamic growth patterns. By stimulating the growth of specific cells, ethylene also triggers hyponastic leaf movements. We discuss the roles of ethylene in this process, under stress but also under control conditions, since leaves also move in a diurnal manner.

Ethylene in brief: how it is synthesized and what it triggers

Phytohormones, small molecules synthesized by and transported through the plant, serve as communication signals between the organs. Ethylene, the smallest phytohormone with the simple C_2H_4 structure, is gaseous and capable of plant-to-plant communication. Since its discovery around one century ago (Knight et al., 1910 ; Gane, 1934), this hormone and its multiple facets has fascinated scientists, and consequently, the biosynthesis and signaling pathway of ethylene are well-documented. Decades of research enabled the identification of various functions of ethylene, which is involved in both endogenously controlled developmental processes such as root and leaf development, senescence, and fruit ripening, as well as in plant responses to the environment, such as stimulation of germination by light, but also responses to both biotic and abiotic stress.

The biosynthesis pathway of ethylene has been unraveled since the 1980s (Yang and Hoffman, 1984), and consists of a simple, three-step process (Figure 1.1). In the first step, the amino acid methionine is used as a substrate by S-adenosyl methionine (SAM)-synthases and is converted to SAM (Adams and Yang, 1977). SAM is further converted to 1-aminocyclopropane-1-carboxylic acid (ACC) by a family of ACC-synthases (ACS), of which 10 members are found in Arabidopsis thaliana (Tsuchisaka et al., 2004). In this step, which is considered the rate-limiting step of ethylene biosynthesis, the released methylthioadenosine residue is recycled into methionine. This maintains the cellular

methionine balance and enables rapid ethylene biosynthesis when necessary (Murr and Yang, 1975; Sauter et al., 2013). In the final step, ACC is converted to ethylene by ACC-oxidases (ACO), also known as ethylene forming enzymes (Dong et al., 1992). As this last step is an exothermic reaction requiring only the presence of O_2 (Sallmann et al., 2015), the levels of the precursor ACC are tightly regulated (Yoon, 2015). Besides regulation at the level of conjugation and release from conjugates such as malonyl-ACC or jasmonyl-ACC (Van de Poel and Van Der Straeten, 2014), the rate of ACC biosynthesis is controlled at gene expression level of ACSs; *ACS8* transcript profiles, for example, coincide with the rhythms of ACC levels (Thain et al., 2004). ACC biosynthesis is also regulated by posttranslational control of ACS protein levels, as reported for ACS2, ACS5, ACS6 and ACS9 (Yoon, 2015). Targeted for ubiquitin-mediated degradation under control conditions, several ACSs, such as ACS2 and ACS6 are phosphorylated by the MPK3/6-cascade in adverse conditions, stabilizing the proteins (Liu and Zhang, 2004; Joo et al., 2008). The biosynthesis of ethylene occurs in almost all plant organs, including roots, leaves, flowers, and fruits, and ACC has also been found in the xylem sap, indicating that it is likely transported through the plant (Perez-Alfocea et al., 2011).

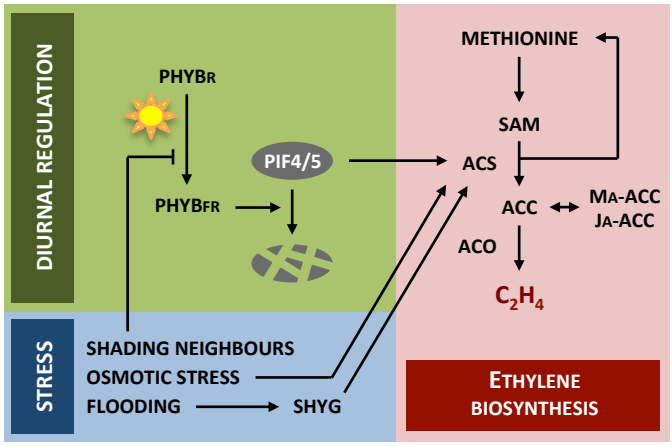

Figure 1.1. Overview of the ethylene biosynthesis pathway and the environmental factors influencing it. Ethylene is synthesized from the amino acid methionine by a 3-step pathway, with recycling of the methylthioadenosine residue. The intermediate product, ACC, can be conjugated into malonyl-ACC (Ma-ACC) or Jasmonyl-ACC (Ja-ACC). In control conditions, the ethylene biosynthesis is regulated in a diurnal way by the red:far red light ratio, reflected by the $PHYB_{FR}$:$PHYB_R$ ratio. Light-activated PHYB ($PHYB_{FR}$) binds and degrades PIF4/5, which can no longer induce *ACS* transcription. Several stress conditions stimulate ethylene biosynthesis; shading by neighboring plants decreases the red:far red ratio, thereby influencing the PHYB-PIF4/5 pathway, flooding stress induces the expression of the SHYG transcription factor, and osmotic stress likely triggers ACC biosynthesis in roots. $PHYB_R$ = red-light absorbing form of PHYTOCHROME B, FR = far red, PIF = PHYTOCHROME INTERACTING PROTEIN, SHYG = SPEEDY HYPONASTIC GROWTH, SAM = S-adenosyl-methionine, ACC = 1-aminocyclopropane-1-carboxylic acid, C_2H_4 = ethylene, ACS = ACC-SYNTHASE, ACO = ACC-OXIDASE

In the destination organ, ethylene triggers a signaling cascade initiated by the ethylene receptors, of which 5 different members are known: ERS1 (ETHYLENE RESPONSE SENSOR1), ERS2, ETR1 (ETHYLENE RESISTANCE1), ETR2 and EIN4 (ETHYLENE INSENSITIVE4) (reviewed in Gallie, 2015). These receptors are located in the membrane of the endoplasmatic reticulum and are able to bind ethylene (Schaller and Bleecker, 1995; Hall et al., 2000; O'Malley et al., 2005; Lacey and Binder, 2014). They all have kinase activity, either His-kinase (ETR1) or Ser/Thr kinase (ERS2, ETR2, and EIN4), or both (ERS1), which is active in the absence of ethylene and repressed upon binding of the gaseous molecule (Gamble et al., 1998; Gamble et al., 2002; Moussatche and Klee, 2004). Downstream, the major identified target of the receptors is CTR1 (CONSTITUTIVE TRIPLE REPSONSE1), which binds the receptors in the absence of ethylene, and is activated by phosphorylation (reviewed in Lacey and Binder, 2014). It is thus active in the absence of ethylene. The levels of receptor/CTR1 complexes are directly regulated both at transcriptional and posttranslational level to fine-tune the response (Shakeel et al., 2015). When mutated, CTR1 confers the constitutive triple response, a signature phenotype of ethylene-treated dark-grown seedlings characterized by a less elongated and thickened hypocotyl and a curling apical hook. CTR1 is also a kinase that, when active, represses its downstream target EIN2, and ER-located membrane protein. When this repression is released by the presence of ethylene, the EIN2 protein is cleaved, releasing a C-terminal fragment that moves to the nucleus to activate the expression of the two central primary ethylene-responsive transcription factors EIN3 and EIL1 (An et al., 2010; Bisson and Groth, 2010). The latter then induce numerous downstream secondary ETHYLENE-RESPONSE FACTORS, transcription factors collectively called ERFs because they share a common APETALA2/ERF DNA-binding domain through which they can bind Ethylene Responsive Elements (ERE)(Nakano et al., 2006). EIN3 and EIL1 protein levels are further controlled by two E3-ligases, EBF1 and EBF2, which target EIN3 and EIL1 for degradation by the 26S-proteasome (Guo and Ecker, 2003; Potuschak et al., 2003). In turn, EBF1 and EBF2 transcript levels are controlled by an RNA-exoribonuclease, EIN5 (Olmedo et al., 2006; Potuschak et al., 2006). Besides this classical ethylene signaling pathway, a secondary EIN2-independent pathway has been shown to be involved in the ethylene response. This secondary pathway includes a MAPK-phosphorylation cascade involving MKK9 and MPK3/6. Through phosphorylation, MPK3/6 activate ACS proteins for further ethylene biosynthesis as well as several downstream ERFs in specific conditions (Yoo et al., 2008; Yoo and Sheen, 2008; Son et al., 2012).

The overall effect of ethylene in leaves

In dicot plants, leaf primordia emerge from the shoot apical meristem as an organized clump of highly proliferating cells. Cell division continues to drive the growth of these very young leaves for about three to four days after emergence (Donnelly et al., 1999; Andriankaja et al., 2012; Gonzalez et al., 2012). Then, cells start to expand, a process initiated at the tip of the leaf and gradually progressing toward the leaf base. Finally, with the exception of several dispersed proliferating cells called meristemoids, all cells only grow through expansion until leaf maturity. In Arabidopsis, this process from emergence until maturity takes about one month (Aguirrezabal et al., 2006). From a physiological point of view, the growth of leaves is driven by the availability of three crucial elements: carbon as building blocks for cellular structures, nitrogen as limiting component for DNA and protein biosynthesis, and water to provide the necessary turgor for cell growth. Sunlight constitutes an additional essential factor for plants to grow, since it is necessary for the photosynthesis reactions. To increase the growth potential and photosynthesize efficiently, plants developed mechanisms to optimize the capture of light. Under unfavorable light conditions, leaves are set upwards a reaction called hyponasty (Pierik et al., 2004). Hyponastic movements are actually a consequence of cellular growth in the petioles. In Arabidopsis, ethylene controls the growth of both the cells in the leaves and in the petioles, and thus regulates both leaf growth and leaf movements.

Plants overproducing ethylene are generally dwarfed, and plant growth is repressed by exposure to this phytohormone. Consequently, when the positive regulators of the ethylene signaling pathway are mutated, plants are generally found to exhibit larger rosette phenotypes with larger leaves (Zhou et al., 2006; Meng et al., 2013; Feng et al., 2015). Increased growth has been observed upon mutation of either the receptors ERS1 and ETR1, EIN2, or several ERFs (Qu et al., 2007; Meng et al., 2013; Feng et al., 2015). Also, some rhizosphere bacteria that promote plant growth do so by expressing *ACC-DEAMINASE*, decreasing the levels of ACC in plants exposed to stress, which has a positive effect on growth (Chen et al., 2013). Moreover, mutants not directly linked to ethylene signaling or biosynthesis, but in which the ethylene sensitivity is reduced, generally also produce larger leaves (Cao et al., 2015; Tao et al., 2015). This negative correlation between ethylene sensitivity and leaf growth has led to the classification of ethylene as a growth-repressing hormone. However, despite an overall growth-repressing effect, examples exist where ethylene stimulates Poa leaf growth when present in concentrations just slightly higher than ambient concentrations (Fiorani et al., 2002). Interestingly, ethylene is known to stimulate cell growth in specific cell types of the leaf, contributing to the hyponastic leaf movements of plants exposed to stress (Pierik et al., 2004; Pierik et al., 2004). The role for ethylene in growth can thus be both

negative and positive within the same plant organ, depending on the specific cell type and specific conditions.

Effects of ethylene on cell division

Initial leaf growth is driven by active proliferation of the cells. In plants and other organisms, the core cell cycle is composed of four consecutive phases: duplication of nuclear DNA (S-phase), separation of the sister chromatids to the daughter cells during cell division (M-phase), and two gap phases (G1 and G2) between the S- and M-phase. The transition between the first gap phase (G1) and the S-phase is strictly controlled as it is a crucial step in the initiation of a new cell division cycle (Gutierrez, 2005; De Veylder et al., 2007). E2F factors are key in the induction of this step, and their positive regulatory effect is counteracted by the RETINOBLASTOMA-RELATED (RBR1) proteins, repressing the E2F target genes (Desvoyes et al., 2006). Also CYCLIN-DEPENDENT KINASES (CDKs) are important in triggering G1-to-S transition. They are subjected to multi-level regulation by phosphorylation/dephosphorylation, interaction with CDK activating kinases (CAKs), and with CDK inhibitory proteins (CKIs), of which KIP-related proteins (KRP) and SIAMESE-related proteins (SMR) are the most well-known (reviewed in Komaki and Sugimoto, 2012). The transition from proliferation to expansion is accompanied by a shift from mitotic cell cycle to endoreduplication. During endoreduplication, the S-phase still takes place but not the M-phase, resulting in a doubling of DNA amount per cell. The shift between mitotic cell cycle and endocycle is mainly controlled by the balance between the anaphase promoting complex APC/C and the DEL1/UVI4 proteins (Heyman et al., 2011).

The role of ethylene on the cell cycle is generally negative, and the first inhibitory effect of ethylene on cell division was observed more than 40 years ago (Apelbaum and Burg, 1972). Actually, only three studies currently report a positive effect of ethylene on cell division. First, ethylene stimulates the cell cycle in the cambial meristems of poplar trees, but the molecular mechanisms remain unclear (Love et al., 2009). Second, ethylene promotes cell division during vasculature development in Arabidopsis stems, through the activation of the *ERF018* and *ERF109* (Etchells et al., 2012). Third, the cell divisions responsible for the apical hook formation are also stimulated by ethylene, and ethylene overproducing mutants have exaggerated apical hooks due to increased cell division, although cell expansion is also affected (Raz and Koornneef, 2001). This shows that, similarly to what was discussed for the overall effect on growth, ethylene can stimulate cell division in specific contexts, although it generally acts as a negative regulator.

In leaves, only few studies report on the link between ethylene and the cell cycle, likely because the study of young leaves in which cells are still in the proliferative stage is technically challenging. Overproduction of ethylene or overexpression of a transcription factor downstream of the ethylene signaling pathways is always associated with smaller leaves with fewer cells (and smaller cells, see next section). Ethylene thus constitutes a negative regulator of cell division in leaves, mainly in response to stress, where it can have short-term and long-term effects. In first instance, ethylene mediates a temporary and reversible stop of the cell cycle, which can occur under short term unfavorable conditions, e.g. when plants are exposed to less than 10 hours osmotic stress. This "pause" of the cell cycle is achieved through inactivation of the CDKA by phosphorylation, likely through the ethylene-MPK3/6 pathway, as the process is ethylene-mediated but independent from EIN3/EIL1 (Figure 1.2) (Skirycz et al., 2011).

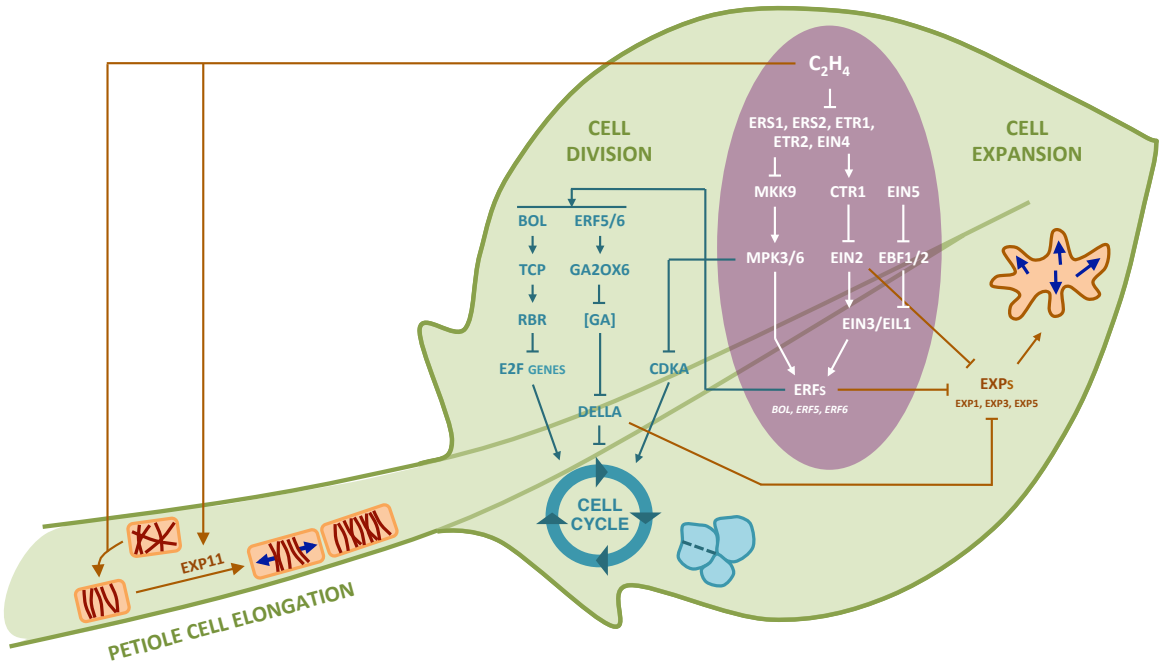

Figure 1.2. The ethylene signaling pathway and molecular mechanisms regulating cell division, cell expansion, and petiole cell elongation. In actively growing Arabidopsis leaves, ethylene regulates cellular growth and division through different pathways. In the leaf blade, proteins of the ethylene signaling pathway and downstream Ethylene Response Factors inhibit cell division and cell expansion when environmental conditions are unfavorable. Ethylene also stimulates the elongation of the abaxial petiole cells, causing hyponasty. See main text for the description of the pathways. C_2H_4 = ethylene, ERS = ETHYLENE RESPONSE SENSOR, ETR = ETHYLENE RECEPTOR, EIN = ETHYLENE INSENSITIVE, MKK9 = MAP-KINASE KINASE9, MPK3/6 = MAP-KINASE 3/6, CTR1 = CONSTITUTIVE TRIPLE RESPONSE1, EBF1/2 = EIN-BINDING F-BOX, ERF = ETHYLENE RESPONSE FACTOR, BOL = BOLITA, EXP = EXPANSIN, TCP = TEOSINTE BRANCHED1-CYCLOIDEA-PCF, RBR = RETINOBLASTOMA RELATED, GA2OX6 = GA-2-OXIDASE 6, GA = Gibberellic acid, CDKA = CYCLIN-DEPENDENT KINASE A

When adverse conditions require the inhibition of the cell cycle for a longer time, three mechanisms exist, in leaves, to exit cell division and stimulate endoreduplication and differentiation. First, accumulation of ethylene and the upregulation of several ERFs, particularly the *BOLITA* transcription factor, have been shown to trigger the induction of type II *TCP* (TEOSINTE BRANCHED1/CYCLOIDEA/PCF) genes (Figure 1.2) (Marsch-Martinez et al., 2006). These TCP proteins bind on the promoter of *RBR1*, which is also upregulated in these conditions and which represses the transcription of the E2F-target genes, thereby inhibiting progression into S-phase and cell division. Second, ethylene as triggered by osmotic stress induces the activity and the expression of *ERF5* and *ERF6*, two homologous transcription factors activated specifically in actively growing Arabidopsis leaves of plants exposed to mild stress (Skirycz et al., 2011; Dubois et al., 2013). ERF6 further induces the expression of a GA-inactivating enzyme, *GA2-OX6*, which likely triggers a reduction in bioactive GA levels and consequent accumulation of the DELLA proteins (Figure 1.2). Under such stress conditions, the DELLA proteins further repress the expression of the *UVI4* and *DEL1* genes, thereby shifting the balance between cell division and endoreduplication towards endoreduplication, and thus causing a premature exit out of the cell cycle (Claeys et al., 2012). Leaf growth inhibition mediated by this mechanism can be rescued by increasing GA levels, for instance through upregulation of their biosynthesis or by treatment with GA (Dubois et al., 2013; Plett et al., 2014). Finally, a third cell cycle inhibitory mechanism relies on the downregulation of the *CYCLIN* genes. Overexpression of *ACS8* in poplar leaves, causing elevation of ethylene levels, results in smaller leaves through the downregulation of *CDK1* and several *CYCLINs* (*CYCLIN-B1*, *CYCLIN-A*), but the molecular mechanisms remain unclear (Plett et al., 2014). This decrease in cyclin activity might not form a general mechanism as other studies, for example tracking growth inhibition under osmotic stress, did not find any indication of reduced *CYCB* expression or activity (Skirycz et al., 2011). Notably, in roots, where ethylene also reduces cell cycle at the root apical meristem, the transcript levels of *CYCB* are not affected by ethylene, but the activity of the CYCB1;1:GUS-Dbox reporter construct is decreased. As this Dbox-construct enables visualization of CYCB1;1 at protein level, this decrease indicates CYCB1;1 degradation, and thus highlights a posttranslational regulatory mechanism (Street et al., 2015). Finally, it should be noted that in roots, ethylene has been shown to induce the expression of *ICK1/KRP1*, thereby providing a fourth mechanisms of action which has not been observed in leaves yet (Street et al., 2015).

Effects of ethylene on cell expansion

In a simplified view, cellular growth is the result of the uptake of water when the cell wall is extensible. Cell expansion thus requires two basic actions: the relaxation of the

cell wall, mediated by cell wall remodeling enzymes (Fleming, 2006), and the import of water under favorable water potential, mainly through aquaporins. Additionally, when cell growth is to occur in a specific direction (also called cell elongation), for example during hypocotyl growth in the light, the corticular microtubules (CMTs) need to be re-oriented in the direction opposite from growth (Smith, 2003; Bashline et al., 2014). Similarly as for cell division, the overall effect of ethylene on cell expansion is negative, but several examples exist of ethylene's involvement in the positive regulation of cell expansion, such as in petioles (see below) and hypocotyls grown in light (Smalle et al., 1997). Ethylene does so by directly acting on the microtubule orientation and on the genes of the *EXPANSIN* family, which are remodeling enzymes loosening the cell wall (Cosgrove et al., 2002; Polko et al., 2012). In *Sagittaria pygmaea* and grape berry, ethylene induces the expression of xyloglucan endotransglycolases/hydrolases (XTHs), also stimulating cell wall loosening and cell expansion (Ookawara et al., 2005; Chervin et al., 2008).

Similarly as for cell division, the role of ethylene on cell growth in leaves is however almost exclusively negative. The only positive effect of ethylene on cell expansion in leaves, to our knowledge, is upon treatment with Harpin, an ethylene-inducing protein secreted by the blight pathogen of rice (Li et al., 2014). The underlying molecular mechanism was proposed to be the expression of two expansin genes, but as Harpin induces both ethylene and GA simultaneously, these genes might not be directly induced by ethylene. In general however, overproduction of ethylene in plants or overexpression of proteins of the signaling cascade results in smaller leaves due to restricted cell expansion, as illustrated by overexpression of *ACS8* (Plett et al., 2014), *EIN2* (Feng et al., 2015), *BOLITA* (an ERF)(Marsch-Martinez et al., 2006), *TINY* (another ERF)(Wilson et al., 1996), *ERF6* (Dubois et al., 2013), and *ERF11* (Dubois et al., 2015). In contrast, mutants with reduced ethylene sensitivity have increased leaf size due to enhanced cell expansion, as recently demonstrated in *ein2* (Feng et al., 2015).

Molecularly, the connection between the proteins downstream of the ethylene signaling and the effectors of cell expansion is not entirely clear, but the available data point toward convergence at the level of EXPANSINs. *EXP3* and *EXP5* are downregulated in 35S:EIN2 and upregulated in *ein2*, and *EXP1* and *EXP5* are strongly repressed in dwarfed *bol-D*, BOLITA gain-of-function plants (Figure 1.2) (Marsch-Martinez et al., 2006; Feng et al., 2015). In the dwarfed plants overexpressing *ERF6*, no EXPANSINs were identified amongst the possible direct targets of ERF6 (Dubois et al., 2013). Instead, DELLA proteins were shown to be stabilized by ERF6-overexpression within 24h, and the inhibition of cell expansion might therefore be regulated by the DELLA proteins. Numerous molecular mechanisms connect DELLAs to inhibition of cell expansion (reviewed in Claeys and Inzé, 2013), but notable mechanisms are the DELLA-mediated

degradation of the PIF4 and PIF5 proteins, which activate genes involved in cell wall remodeling (Castillon et al., 2007; de Lucas et al., 2008). Moreover, DELLAs interact with BOS1 INTERACTOR (BOI)-type proteins, which act directly on and repress the promoter of genes encoding EXPANSINs (Park et al., 2013). Because in the studies of Feng (2015) and Marsch-Martinez (2006) the expression measurements were performed at steady state without validation of the direct effect of EIN2 and BOLITA on the *EXPANSIN* genes, it cannot be excluded that also in these lines the observed effect on the *EXPANSIN* genes is mediated by DELLA proteins.

Involvement of ethylene in leaf movements

Besides growing, leaves also move up and down to optimize light capture in changing environments. This phenomenon, called hyponasty (up) and epinasty (down), has been observed in multiple plant species but is most pronounced in rosette plants such as Arabidopsis. Leaves move in a diurnal way, moving upwards during day-time to reach their most vertical position at dusk, and subsequently back to their original position at dawn (Hangarter, 1997; Millenaar et al., 2005; Dornbusch et al., 2014). Leaves also move upwards when plants are in the shadow of neighboring plants in an attempt to capture more red light, a stress-response named shade avoidance (Pierik et al., 2004). Besides light stress, flooding stress of roots (waterlogging) or shoots also triggers upward leaf movements in several species, constituting for the plant a mechanism to escape the flooding (Blom and Voesenek, 1996; Voesenek et al., 2003; Cox et al., 2006). Ethylene has since long been known to be the principal regulator of hyponastic leaf movements under shade and submergence. Ethylene insensitive tobacco mutants, generated by transformation with the mutant *etr1-1* gene from Arabidopsis (Tetr), have reduced shade avoidance responses (Pierik et al., 2004), and Arabidopsis *aco5* mutants show reduced hyponasty during flooding stress (Rauf et al., 2013).

Upstream, ethylene accumulation is triggered by the reduced availability of red light (Figure 1.1). Under shade, changing red:far red ratios are reflected by the ratios of Pr and Pfr forms of phytochrome proteins, of which PHY-B plays the dominant role (Reed et al., 1993). In shade and in comparison to plants directly exposed to sunlight, PHY-B proteins are less light-activated and interact less with PIF4/5 proteins. PIF4/5 proteins are thereby stabilized and induce the expression of downstream *ACS* genes (Nomoto et al., 2013). Consistently, *phyB* mutants show more hyponastic leaves (Mullen et al., 2006) with higher amplitudes of leaf movements, which can be attenuated by reducing the ethylene levels, as in the *phyB-acs2* double mutant (Bours et al., 2013). In contrast, PIF4 and PIF5 were shown to indeed influence the amplitude of the movement, although they do not seem to be essential for the movement *in se* (Dornbusch et al., 2014). This is likely because another canopy shade-induced gene, *HFR1* (long hypocotyl under far red

light) triggers the transcriptional expression of *ACS8* as well (Stamm and Kumar, 2010). Under flooding stress, a NAC transcription factor, SHYG (SPEEDY HYPONASTIC GROWTH) is transcriptionally induced in petioles and is responsible for the downstream ethylene accumulation, by direct activation of the *ACS5* promoter (Figure 1.1) (Rauf et al., 2013). *shyg* mutants have less hyponasty under waterlogging, and overexpression lines show increased hyponasty. Both types of stress thus result, through two distinct pathways, in the accumulation of ethylene (Finlayson et al., 1999; Thain et al., 2004; Nomoto et al., 2013).

At the cellular level, hyponasty is established by elongation of the cells at the lower side of the petiole (Figure 1.2) (Stamm and Kumar, 2010). To enable elongation, cortical microtubuli (CMTs), which strengthen the cell wall and inhibit growth in their orientation, are re-oriented from longitudinal to transverse, enabling longitudinal growth (Figure 1.2). This re-orientation is stimulated by ethylene, specifically in the proximal abaxial petiole cells, and coincides with ethylene-mediated transcriptional induction of *EXPANSIN11* (Polko et al., 2012). Detailed molecular connections underlying this cellular expansion currently remain unknown, but the response downstream of ethylene might involve alterations in brassinosteroid and auxin metabolism (Stamm and Kumar, 2010; Polko et al., 2013). This response is moreover thought to diverge between different Arabidopsis ecotypes, as *Landsberg* plants do not show hyponastic responses to ethylene, and most likely lack an essential component in the downstream signaling (Millenaar et al., 2005).

Recently, this elongation-mediated petiole growth and the involvement of ethylene in it has been modeled mathematically, highlighting also a role for cell division in this process (Polko et al., 2015). The model suggests that the elongation should be larger than was actually observed, unless the cell elongation increase was compensated by a repression of cell division in the proximal abaxial petiole cells. Experimental validation indeed showed that besides stimulating cell expansion, ethylene also moderates the level of hyponasty by negatively acting on the cell cycle of petiole cells (Polko et al., 2015).

Diurnal fluctuations in ethylene levels: an effect on diurnal leaf growth and rhythmic leaf movements ?

Molecular mechanisms behind ethylene oscillations

Interestingly, ethylene levels are not stable throughout the day but instead fluctuate in a diurnal manner. Diurnal oscillations of ethylene levels have been observed in numerous plants species, such as sorghum (Finlayson et al., 1999), *Stellaria longipes* (longstalk

starwort) (Kathiresan et al., 1996), *Chenopodium rubrum* (Machackova et al., 1997), the potato subspecies Andigena (Chincinska et al., 2013), cotton (Rikin et al., 1984), and Arabidopsis (Thain et al., 2004). In general, ethylene levels are low at dawn, increase during the day, and decrease again during the night (Figure 1.3), but the peak shows slight shifts depending on the species; midday in Arabidopsis and sorghum (Finlayson et al., 1999; Thain et al., 2004) and evening in potato and *Chenopodium rubrum* (Machackova et al., 1997; Chincinska et al., 2013). Interestingly, with the exception of *Chenopodium rubrum*, these oscillations are maintained when plants are transferred to continuous light or dark, pointing to an endogenously controlled rather than a pure light/dark response (Machackova et al., 1997; Thain et al., 2004).

The level at which these ethylene oscillations are regulated, at the level of ACC biosynthesis or at the level of conversion of ACC to ethylene, has long been debated and might also be depending on the species. Several studies observed oscillating ACC levels, as a result of fluctuating ACS transcript levels (Rikin et al., 1984; Machackova et al., 1997; Thain et al., 2004). In contrast, other studies observed stable ACC levels throughout the day, and explained the oscillating ethylene levels by the diurnal changes in ACO transcript levels and activity (Kathiresan et al., 1996; Machackova et al., 1997; Finlayson et al., 1999; Chincinska et al., 2013). In Arabidopsis, however, it is clear that the fluctuating levels of ACC in seedlings are resulting from oscillating expression patterns of several ACS genes, *ACS8*, *ACS5* and *ACS9* (Thain et al., 2004). Upon transfer to continuous darkness, only *ACS8* levels continue to oscillate similarly as the ethylene levels, thereby forming the best candidate for regulating the diurnal ethylene levels. Moreover, when treating Arabidopsis seedlings with ACC, or in ACC-overproducing mutants such as *eto2*, the rhythmicity in ethylene production upon transfer to darkness disappears, indicating that diurnal ethylene levels are not regulated at the level of ACO (Thain et al., 2004).

More upstream, the diurnal ethylene rhythms are entrained by both core circadian clock mechanisms and by photoperiodic response (Figure 1.1). In Arabidopsis, the *ACS8* promoter contains an element which is also found in the CAB (chlorophyll a/b-binding proteins) promoter, where it is necessary for its diurnal regulation by the clock (Piechulla et al., 1998). *ACS8* is thus likely also a target of the circadian clock (Thain et al., 2004). *ACS8* transcript levels are also controlled by PIF4 (Phytochrome B Interacting Factor), which nicely integrates the endogenous clock and environmental light signals, as PIF4 is transcriptionally controlled by the clock but posttranslationally by light/dark (Nomoto et al., 2013). Consistently, *ACS8* transcript levels are induced in *phyB* mutants and by FR light, when PIF4 proteins are no longer degraded by the light-form of PHY-B. This induction is less pronounced in *pif4pif5* mutants (Nomoto et al., 2012). These findings suggest that diurnal ethylene oscillations in Arabidopsis are regulated by ACS8,

the levels of which are in turn regulated by both the circadian clock and the PHY-B-mediated light/dark response (Figure 1.3). Accordingly, ethylene oscillations are altered in the clock mutants *toc1-1* (shortened period) and *CCA1*-overexpressor (CCA1-OX) (arrhythmic ethylene) (Thain et al., 2004), and in *phyB* mutants of sorghum (increased amplitude) (Finlayson et al., 1999).

Oscillating leaf growth rate and diurnal movements: a match with ethylene levels?

Even under optimal growth conditions, leaves move up and down within a diel period, and also leaf growth rate does depend on the time of day (Nozue and Maloof, 2006). This time-dependent growth effect is highly related to the developmental stage of the leaf. Young leaves grow more during the day and old leaves grow more during the night (Pantin et al., 2011). Similarly as the ethylene oscillations, this growth rhythm is maintained even when light/dark conditions are perturbed, indicating that endogenous mechanisms controlled by the circadian clock are regulating these dynamics (Poire et al., 2010).

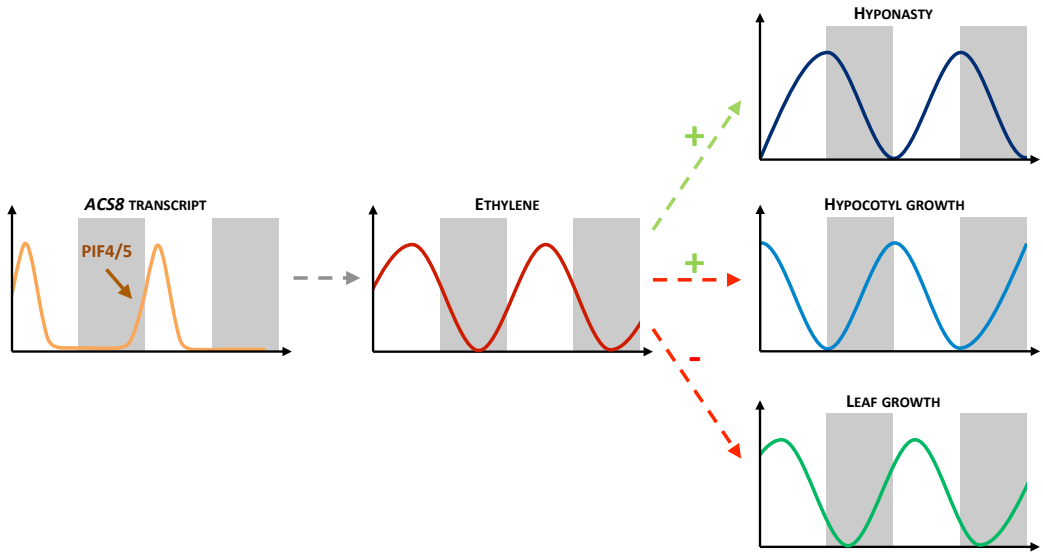

Figure 1.3. Diurnal oscillations in ethylene level, leaf movements and growth. Oscillations in ethylene levels in seedlings are triggered by a clear peak of *ACS8* levels at dawn. Peaking ethylene levels during the day could explain (green arrow) hyponastic leaf movements, as ethylene stimulates this process (+). However, diurnal ethylene levels do not explain (red arrow) rhythms in hypocotyl growth; while ethylene stimulates (+) hypocotyl elongation, growth decreases when ethylene levels are peaking. Growth rhythms of young leaves correlate with ethylene oscillations, but in this context ethylene has a repressive function (-); thus, diurnal leaf growth rhythms cannot be explained by ethylene levels (red arrow). See main text for references.

If and how the oscillating ethylene levels connect to the diurnal growth rhythms observed in young Arabidopsis leaves, is however not yet clear, as measurements of ethylene levels in young leaves throughout the day are technically very challenging. However, studies attempted to link the ethylene levels with hypocotyl growth, and this data can shed light on possible involvement of ethylene in diurnal leaf growth. The unidirectional growth of young hypocotyls is regulated in a diurnal way, and the rhythmicity is, similarly to ethylene, depending on both the circadian clock and maintained photoperiodic rhythms (Nozue et al., 2007). Hypocotyl growth has long been studied only under continuous light conditions, when maximal growth rates were observed at subjective dusk, but under light/dark cycles, the elongation rate of hypocotyls is highest at dawn (Figure 1.3) (Nozue et al., 2007; Michael et al., 2008). Amongst the phytohormones significantly correlating with the growth rhythms of hypocotyls, ethylene showed the most pronounced and coinciding oscillation, with a clear peak in *ACS8* expression level at dawn (Figure 1.3) (Michael et al., 2008). The observation that *ACS8* transcript levels are the highest at the moment of maximal growth is in accordance with the old observation that ethylene stimulates hypocotyl growth in the light (Smalle et al., 1997). However, ethylene levels are further increasing throughout the day, while hypocotyl growth is low in the light (Figure 1.3) (Michael et al., 2008; Thain et al., 2004). Moreover, the rhythmicity of hypocotyl growth was not disturbed in ethylene insensitive mutants, indicating that ethylene rhythms are not important for diurnal growth (Thain et al., 2004).

Similarly as for hypocotyls, leaf growth has recently been reported to be maximal in the morning, several hours after dawn (Dornbusch et al., 2014). As in growing leaves ethylene has a growth-repressive function, the oscillations in ethylene levels do not explain the diurnal leaf growth pattern (Figure 1.3). However, diurnal ethylene levels were never measured in growing Arabidopsis leaves. Expression analysis in young leaves showed an increase in the expression of two genes encoding ETHYLENE RESPONSE FACTORs (*ERF5* and *ERF6*) throughout the day, a stable high level at night, and an abrupt decrease in the morning (Dubois et al., 2015). As *ERF5* and *ERF6* are known to be induced by ethylene within 45 minutes, this expression pattern does not correlate with the diurnal ethylene levels observed in seedlings, and could indicate that ethylene oscillations in leaves differ from those in whole seedlings. If the ethylene levels are reflected by the *ERF5* and *ERF6* expression level, we can speculate that diurnal ethylene levels could be involved in leaf growth rhythms: low ethylene levels in the morning enabling leaf growth, and high levels at night, repressing leaf growth. Further investigations of this purely speculative model would be highly valuable to better understand a possible role for ethylene in the regulation of growth under non-stress conditions.

Under control conditions, the position of leaves is highly dynamic, with leaves moving upwards around midday until the evening, and back to their original position in the morning. Interestingly, the pattern of these movements, stimulated by ethylene, matches with the ethylene oscillations, reaching a peak at midday (Thain et al., 2004; Dornbusch et al., 2014). However, the rhythmicity of movements of cotyledons was shown to not be affected in several ethylene insensitive mutants, such as *etr1* and *ein2* (Thain et al., 2004). These results are contradictory to those of a later study (Bours et al., 2013), where it has been demonstrated that *etr1-1* and *ein2* mutants indeed showed clear reductions in leaf movement amplitudes. This observation was further supported by analysis of the *acs2* mutant, which produce less ethylene and shows reduced hyponastic movements throughout the day (Bours et al., 2013). Overall, these results indicate that ethylene is clearly capable of regulating hyponasty, and likely does so to regulate diurnal leaf movements under favorable conditions, although the exact role of ethylene in this process certainly deserves further consideration.

CONCLUSION

The roles of the phytohormone ethylene in Arabidopsis leaves has mainly been characterized under non-optimal environmental conditions, including shade, submergence, and growth-repressive conditions such as osmotic stress. In these conditions, ethylene has a negative effect on leaf growth and reduces cell division and cell expansion through diverse molecular pathways, some of them converging to the DELLA proteins. In contrast, ethylene positively influences cell elongation of the abaxial petiole cells, thereby stimulating hyponastic movements under stress. As ethylene levels are not constitutively low in the absence of stress, but instead show fluctuations throughout the day, ethylene likely also has similar roles in leaves under control conditions. These roles are much less studied but would deserve further exploration, since several pieces of evidence suggest that ethylene could also influence the diurnal rhythms of leaf growth and leaf movements when plants are not exposed to stress.

ACKNOWLEDGEMENTS

We thank Dr. Hannes Claeys, Dr. Hannes Vanhaeren and Lisa Van den Broeck for the fruitful discussions and helpful suggestions to improve this chapter. This work was supported by the Interuniversity Attraction Poles Program (IUAP P7/29 "MARS") initiated by the Belgian Science Policy Office, by Ghent University (‘Bijzonder

Onderzoeksfonds Methusalem Project' no. BOF08/01M00408, Multidisciplinary Research Partnership "Biotechnology for a Sustainable Economy" Project no. 01MRB510W).

REFERENCES

Adams DO, Yang SF (1977) Methionine metabolism in apple tissue: implication of s-adenosylmethionine as an intermediate in the conversion of methionine to ethylene. Plant Physiol 60: 892-896

Aguirrezabal L, Bouchier-Combaud S, Radziejwoski A, Dauzat M, Cookson SJ, Granier C (2006) Plasticity to soil water deficit in Arabidopsis thaliana: dissection of leaf development into underlying growth dynamic and cellular variables reveals invisible phenotypes. Plant Cell Environ 29: 2216-2227

An F, Zhao Q, Ji Y, Li W, Jiang Z, Yu X, Zhang C, Han Y, He W, Liu Y, Zhang S, Ecker JR, Guo H (2010) Ethylene-induced stabilization of ETHYLENE INSENSITIVE3 and EIN3-LIKE1 is mediated by proteasomal degradation of EIN3 binding F-box 1 and 2 that requires EIN2 in Arabidopsis. Plant Cell 22: 2384-2401

Andriankaja M, Dhondt S, De Bodt S, Vanhaeren H, Coppens F, De Milde L, Mühlenbock P, Skirycz A, Gonzalez N, Beemster GTS, Inzé D (2012) Exit from proliferation during leaf development in Arabidopsis thaliana: a not-so-gradual process. Developmental Cell 22: 64-78

Apelbaum A, Burg SP (1972) Effect of Ethylene on Cell Division and Deoxyribonucleic Acid Synthesis in Pisum sativum. Plant Physiol 50: 117-124

Bashline L, Lei L, Li S, Gu Y (2014) Cell wall, cytoskeleton, and cell expansion in higher plants. Mol Plant 7: 586-600

Bisson MM, Groth G (2010) New insight in ethylene signaling: autokinase activity of ETR1 modulates the interaction of receptors and EIN2. Mol Plant 3: 882-889

Blom CW, Voesenek LA (1996) Flooding: the survival strategies of plants. Trends Ecol Evol 11: 290-295

Bours R, van Zanten M, Pierik R, Bouwmeester H, van der Krol A (2013) Antiphase light and temperature cycles affect PHYTOCHROME B-controlled ethylene sensitivity and biosynthesis, limiting leaf movement and growth of Arabidopsis. Plant Physiol 163: 882-895

Cao YR, Chen HW, Li ZG, Tao JJ, Ma B, Zhang WK, Chen SY, Zhang JS (2015) Tobacco ankyrin protein NEIP2 interacts with ethylene receptor NTHK1 and regulates plant growth and stress responses. Plant Cell Physiol 56: 803-818

Castillon A, Shen H, Huq E (2007) Phytochrome Interacting Factors: central players in phytochrome-mediated light signaling networks. Trends Plant Sci 12: 514-521

Chen L, Dodd IC, Theobald JC, Belimov AA, Davies WJ (2013) The rhizobacterium Variovorax paradoxus 5C-2, containing ACC deaminase, promotes growth and development of Arabidopsis thaliana via an ethylene-dependent pathway. J Exp Bot 64: 1565-1573

Chervin C, Tira-Umphon A, Terrier N, Zouine M, Severac D, Roustan JP (2008) Stimulation of the grape berry expansion by ethylene and effects on related gene transcripts, over the ripening phase. Physiol Plant 134: 534-546

Chincinska I, Gier K, Krugel U, Liesche J, He H, Grimm B, Harren FJ, Cristescu SM, Kuhn C (2013) Photoperiodic regulation of the sucrose transporter StSUT4 affects the expression of circadian-regulated genes and ethylene production. Front Plant Sci 4: 26

Claeys H, Inzé D (2013) The agony of choice: how plants balance growth and survival under water-limiting conditions. Plant Physiology 162: 1768-1779

Claeys H, Skirycz A, Maleux K, Inzé D (2012) DELLA signaling mediates stress-induced cell differentiation in Arabidopsis leaves through modulation of anaphase-promoting complex/cyclosome activity. Plant Physiology 159: 739-747

Cosgrove DJ, Li LC, Cho HT, Hoffmann-Benning S, Moore RC, Blecker D (2002) The growing world of expansins. Plant Cell Physiol 43: 1436-1444

Cox MC, Peeters AJ, Voesenek LA (2006) The stimulating effects of ethylene and auxin on petiole elongation and on hyponastic curvature are independent processes in submerged Rumex palustris. Plant Cell Environ 29: 282-290

de Lucas M, Daviere JM, Rodriguez-Falcon M, Pontin M, Iglesias-Pedraz JM, Lorrain S, Fankhauser C, Blazquez MA, Titarenko E, Prat S (2008) A molecular framework for light and gibberellin control of cell elongation. Nature 451: 480-484

De Veylder L, Beeckman T, Inze D (2007) The ins and outs of the plant cell cycle. Nat Rev Mol Cell Biol 8: 655-665

Desvoyes B, Ramirez-Parra E, Xie Q, Chua NH, Gutierrez C (2006) Cell type-specific role of the retinoblastoma/E2F pathway during Arabidopsis leaf development. Plant Physiol 140: 67-80

Dong JG, Fernandez-Maculet JC, Yang SF (1992) Purification and characterization of 1-aminocyclopropane-1-carboxylate oxidase from apple fruit. Proc Natl Acad Sci U S A 89: 9789-9793

Donnelly PM, Bonetta D, Tsukaya H, Dengler RE, Dengler NG (1999) Cell cycling and cell enlargement in developing leaves of Arabidopsis. Dev Biol 215: 407-419

Dornbusch T, Michaud O, Xenarios I, Fankhauser C (2014) Differentially phased leaf growth and movements in Arabidopsis depend on coordinated circadian and light regulation. Plant Cell 26: 3911-3921

Dubois M, Skirycz A, Claeys H, Maleux K, Dhondt S, De Bodt S, Vanden Bossche R, De Milde L, Yoshizumi T, Matsui M, Inzé D (2013) ETHYLENE RESPONSE FACTOR6 acts as a central regulator of leaf growth under water-limiting conditions in Arabidopsis. Plant Physiology 162: 319-332

Dubois M, Van den Broeck L, Claeys H, Van Vlierberghe K, Matsui M, Inze D (2015) The ETHYLENE RESPONSE FACTORS ERF6 and ERF11 antagonistically regulate mannitol-induced growth inhibition in Arabidopsis. Plant Physiol

Etchells JP, Provost CM, Turner SR (2012) Plant vascular cell division is maintained by an interaction between PXY and ethylene signalling. PLoS Genet 8: e1002997

Feng G, Liu G, Xiao J (2015) The Arabidopsis EIN2 restricts organ growth by retarding cell expansion. Plant Signal Behav 10: e1017169

Finlayson SA, Lee IJ, Mullet JE, Morgan PW (1999) The mechanism of rhythmic ethylene production in sorghum. The role of phytochrome B and simulated shading. Plant Physiol 119: 1083-1089

Fiorani F, Bogemann GM, Visser EJ, Lambers H, Voesenek LA (2002) Ethylene emission and responsiveness to applied ethylene vary among Poa species that inherently differ in leaf elongation rates. Plant Physiol 129: 1382-1390

Fleming AJ (2006) The co-ordination of cell division, differentiation and morphogenesis in the shoot apical meristem: a perspective. J Exp Bot 57: 25-32

Gallie DR (2015) Ethylene receptors in plants - why so much complexity? F1000Prime Rep 7: 39

Gamble RL, Coonfield ML, Schaller GE (1998) Histidine kinase activity of the ETR1 ethylene receptor from Arabidopsis. Proc Natl Acad Sci U S A 95: 7825-7829

Gamble RL, Qu X, Schaller GE (2002) Mutational analysis of the ethylene receptor ETR1. Role of the histidine kinase domain in dominant ethylene insensitivity. Plant Physiol 128: 1428-1438

Gane R (1934) Production of ethylene by some ripening fruits. Nature 134: 1008-1008

Gonzalez N, Vanhaeren H, Inze D (2012) Leaf size control: complex coordination of cell division and expansion. Trends Plant Sci 17: 332-340

Guo H, Ecker JR (2003) Plant responses to ethylene gas are mediated by SCF(EBF1/EBF2)-dependent proteolysis of EIN3 transcription factor. Cell 115: 667-677

Gutierrez C (2005) Coupling cell proliferation and development in plants. Nat Cell Biol 7: 535-541

Hall AE, Findell JL, Schaller GE, Sisler EC, Bleecker AB (2000) Ethylene perception by the ERS1 protein in Arabidopsis. Plant Physiol 123: 1449-1458

Hangarter RP (1997) Gravity, light and plant form. Plant Cell Environ 20: 796-800

Heyman J, Van den Daele H, De Wit K, Boudolf V, Berckmans B, Verkest A, Alvim Kamei CL, De Jaeger G, Koncz C, De Veylder L (2011) Arabidopsis ULTRAVIOLET-B-INSENSITIVE4 maintains cell division activity by temporal inhibition of the anaphase-promoting complex/cyclosome. Plant Cell 23: 4394-4410

Joo S, Liu Y, Lueth A, Zhang S (2008) MAPK phosphorylation-induced stabilization of ACS6 protein is mediated by the non-catalytic C-terminal domain, which also contains the cis-determinant for rapid degradation by the 26S proteasome pathway. Plant J 54: 129-140

Kathiresan A, Reid DM, Chinnappa CC (1996) Light- and temperature-entrained circadian regulation of activity and mRNA accumulation of 1-aminocyclopropane-1-carboxylic acid oxidase in Stellaria longipes. Planta 199: 329-335

Knight LI, Rose RC, Crocker W (1910) Effects of various gases and vapors upon etiolated seedlings of the sweet pea. Science 31: 635-636

Komaki S, Sugimoto K (2012) Control of the plant cell cycle by developmental and environmental cues. Plant Cell Physiol 53: 953-964

Lacey RF, Binder BM (2014) How plants sense ethylene gas--the ethylene receptors. J Inorg Biochem 133: 58-62

Li X, Han B, Xu M, Han L, Zhao Y, Liu Z, Dong H, Zhang C (2014) Plant growth enhancement and associated physiological responses are coregulated by ethylene and gibberellin in response to harpin protein Hpa1. Planta 239: 831-846

Liu Y, Zhang S (2004) Phosphorylation of 1-aminocyclopropane-1-carboxylic acid synthase by MPK6, a stress-responsive mitogen-activated protein kinase, induces ethylene biosynthesis in Arabidopsis. Plant Cell 16: 3386-3399

Love J, Bjorklund S, Vahala J, Hertzberg M, Kangasjarvi J, Sundberg B (2009) Ethylene is an endogenous stimulator of cell division in the cambial meristem of Populus. Proc Natl Acad Sci U S A 106: 5984-5989

Machackova I, Chauvaux N, Dewitte W, Van Onckelen H (1997) Diurnal Fluctuations in Ethylene Formation in Chenopodium rubrum. Plant Physiol 113: 981-985

Marsch-Martinez N, Greco R, Becker JD, Dixit S, Bergervoet JH, Karaba A, de Folter S, Pereira A (2006) BOLITA, an Arabidopsis AP2/ERF-like transcription factor that affects cell expansion and proliferation/differentiation pathways. Plant Mol Biol 62: 825-843

Meng X, Xu J, He Y, Yang KY, Mordorski B, Liu Y, Zhang S (2013) Phosphorylation of an ERF transcription factor by Arabidopsis MPK3/MPK6 regulates plant defense gene induction and fungal resistance. Plant Cell 25: 1126-1142

Michael TP, Breton G, Hazen SP, Priest H, Mockler TC, Kay SA, Chory J (2008) A morning-specific phytohormone gene expression program underlying rhythmic plant growth. PLoS Biol 6: e225

Millenaar FF, Cox MC, van Berkel YE, Welschen RA, Pierik R, Voesenek LA, Peeters AJ (2005) Ethylene-induced differential growth of petioles in Arabidopsis. Analyzing natural variation, response kinetics, and regulation. Plant Physiol 137: 998-1008

Moussatche P, Klee HJ (2004) Autophosphorylation activity of the Arabidopsis ethylene receptor multigene family. J Biol Chem 279: 48734-48741

Mullen JL, Weinig C, Hangarter RP (2006) Shade avoidance and the regulation of leaf inclination in Arabidopsis. Plant Cell Environ 29: 1099-1106

Murr DP, Yang SF (1975) Inhibition of in Vivo Conversion of Methionine to Ethylene by l-Canaline and 2,4-Dinitrophenol. Plant Physiol 55: 79-82

Nakano T, Suzuki K, Fujimura T, Shinshi H (2006) Genome-wide analysis of the ERF gene family in Arabidopsis and rice. Plant Physiology 140: 411-432

Nomoto Y, Kubozono S, Miyachi M, Yamashino T, Nakamichi N, Mizuno T (2013) Circadian clock and PIF4-mediated external coincidence mechanism coordinately integrates both of the cues from seasonal changes in photoperiod and temperature to regulate plant growth in Arabidopsis thaliana. Plant Signal Behav 8: e22863

Nozue K, Covington MF, Duek PD, Lorrain S, Fankhauser C, Harmer SL, Maloof JN (2007) Rhythmic growth explained by coincidence between internal and external cues. Nature 448: 358-361

Nozue K, Maloof JN (2006) Diurnal regulation of plant growth. Plant Cell Environ 29: 396-408

O'Malley RC, Rodriguez FI, Esch JJ, Binder BM, O'Donnell P, Klee HJ, Bleecker AB (2005) Ethylene-binding activity, gene expression levels, and receptor system output for ethylene receptor family members from Arabidopsis and tomato. Plant J 41: 651-659

Olmedo G, Guo H, Gregory BD, Nourizadeh SD, Aguilar-Henonin L, Li H, An F, Guzman P, Ecker JR (2006) ETHYLENE-INSENSITIVE5 encodes a 5'-->3' exoribonuclease required for regulation of the EIN3-targeting F-box proteins EBF1/2. Proc Natl Acad Sci U S A 103: 13286-13293

Ookawara R, Satoh S, Yoshioka T, Ishizawa K (2005) Expression of alpha-expansin and xyloglucan endotransglucosylase/hydrolase genes associated with shoot elongation enhanced by anoxia, ethylene and carbon dioxide in arrowhead (Sagittaria pygmaea Miq.) tubers. Ann Bot 96: 693-702

Pantin F, Simonneau T, Rolland G, Dauzat M, Muller B (2011) Control of leaf expansion: a developmental switch from metabolics to hydraulics. Plant Physiol 156: 803-815

Park J, Nguyen KT, Park E, Jeon JS, Choi G (2013) DELLA proteins and their interacting RING Finger proteins repress gibberellin responses by binding to the promoters of a subset of gibberellin-responsive genes in Arabidopsis. Plant Cell 25: 927-943

Perez-Alfocea F, Ghanem ME, Gomez-Cadenas A, Dodd IC (2011) Omics of root-to-shoot signaling under salt stress and water deficit. OMICS 15: 893-901

Piechulla B, Merforth N, Rudolph B (1998) Identification of tomato Lhc promoter regions necessary for circadian expression. Plant Mol Biol 38: 655-662

Pierik R, Cuppens ML, Voesenek LA, Visser EJ (2004) Interactions between ethylene and gibberellins in phytochrome-mediated shade avoidance responses in tobacco. Plant Physiol 136: 2928-2936

Pierik R, Voesenek LA, de Kroon H, Visser EJ (2004) Density-induced plant size reduction and size inequalities in ethylene-sensing and ethylene-insensitive tobacco. Plant Biol (Stuttg) 6: 201-205

Pierik R, Whitelam GC, Voesenek LA, de Kroon H, Visser EJ (2004) Canopy studies on ethylene-insensitive tobacco identify ethylene as a novel element in blue light and plant-plant signalling. Plant J 38: 310-319

Plett JM, Williams M, LeClair G, Regan S, Beardmore T (2014) Heterologous over-expression of ACC SYNTHASE8 (ACS8) in Populus tremula x P. alba clone 717-1B4 results in elevated levels of ethylene and induces stem dwarfism and reduced leaf size through separate genetic pathways. Front Plant Sci 5: 514

Poire R, Wiese-Klinkenberg A, Parent B, Mielewczik M, Schurr U, Tardieu F, Walter A (2010) Diel time-courses of leaf growth in monocot and dicot species: endogenous rhythms and temperature effects. J Exp Bot 61: 1751-1759

Polko JK, Pierik R, van Zanten M, Tarkowska D, Strnad M, Voesenek LA, Peeters AJ (2013) Ethylene promotes hyponastic growth through interaction with ROTUNDIFOLIA3/CYP90C1 in Arabidopsis. J Exp Bot 64: 613-624

Polko JK, van Rooij J, Vanneste S, Pierik R, Ammerlaan AM, Vergeer-van Eijk MH, McLoughlin F, Guhl K, van Isterdael G, Voesenek LA, Millenaar FF, Beeckman T, Peeters A, Maree AF, Van Zanten M (2015) Ethylene-mediated regulation of A2-type CYCLINs modulates hyponastic growth in Arabidopsis thaliana. Plant Physiol

Polko JK, van Zanten M, van Rooij JA, Maree AF, Voesenek LA, Peeters AJ, Pierik R (2012) Ethylene-induced differential petiole growth in Arabidopsis thaliana involves local microtubule reorientation and cell expansion. New Phytol 193: 339-348

Potuschak T, Lechner E, Parmentier Y, Yanagisawa S, Grava S, Koncz C, Genschik P (2003) EIN3-dependent regulation of plant ethylene hormone signaling by two arabidopsis F box proteins: EBF1 and EBF2. Cell 115: 679-689

Potuschak T, Vansiri A, Binder BM, Lechner E, Vierstra RD, Genschik P (2006) The exoribonuclease XRN4 is a component of the ethylene response pathway in Arabidopsis. Plant Cell 18: 3047-3057

Qu X, Hall BP, Gao Z, Schaller GE (2007) A strong constitutive ethylene-response phenotype conferred on Arabidopsis plants containing null mutations in the ethylene receptors ETR1 and ERS1. BMC Plant Biol 7: 3

Rauf M, Arif M, Fisahn J, Xue GP, Balazadeh S, Mueller-Roeber B (2013) NAC transcription factor speedy hyponastic growth regulates flooding-induced leaf movement in Arabidopsis. Plant Cell 25: 4941-4955

Raz V, Koornneef M (2001) Cell division activity during apical hook development. Plant Physiol 125: 219-226

Reed JW, Nagpal P, Poole DS, Furuya M, Chory J (1993) Mutations in the gene for the red/far-red light receptor phytochrome B alter cell elongation and physiological responses throughout Arabidopsis development. Plant Cell 5: 147-157

Rikin A, Chalutz E, Anderson JD (1984) Rhythmicity in ethylene production in cotton seedlings. Plant Physiol 75: 493-495

Sallmann M, Oldenburg F, Braun B, Reglier M, Simaan AJ, Limberg C (2015) A Structural and Functional Model for the 1-Aminocyclopropane-1-carboxylic Acid Oxidase. Angew Chem Int Ed Engl

Sauter M, Moffatt B, Saechao MC, Hell R, Wirtz M (2013) Methionine salvage and S-adenosylmethionine: essential links between sulfur, ethylene and polyamine biosynthesis. Biochem J 451: 145-154

Schaller GE, Bleecker AB (1995) Ethylene-binding sites generated in yeast expressing the Arabidopsis ETR1 gene. Science 270: 1809-1811

Shakeel SN, Gao Z, Amir M, Chen YF, Rai MI, Haq NU, Schaller GE (2015) Ethylene Regulates Levels of Ethylene Receptor/CTR1 Signaling Complexes in Arabidopsis thaliana. J Biol Chem 290: 12415-12424

Skirycz A, Claeys H, De Bodt S, Oikawa A, Shinoda S, Andriankaja M, Maleux K, Eloy NB, Coppens F, Yoo S-D, Saito K, Inzé D (2011) Pause-and-stop: the effects of osmotic stress on cell proliferation during early leaf development in Arabidopsis and a role for ethylene signaling in cell cycle arrest. Plant Cell 23: 1876-1888

Smalle J, Haegman M, Kurepa J, Van Montagu M, Straeten DV (1997) Ethylene can stimulate Arabidopsis hypocotyl elongation in the light. Proc Natl Acad Sci U S A 94: 2756-2761

Smith LG (2003) Cytoskeletal control of plant cell shape: getting the fine points. Curr Opin Plant Biol 6: 63-73

Son GH, Wan J, Kim HJ, Nguyen XC, Chung WS, Hong JC, Stacey G (2012) Ethylene-responsive element-binding factor 5, ERF5, is involved in chitin-induced innate immunity response. Molecular Plant-Microbe Interactions 25: 48-60

Stamm P, Kumar PP (2010) The phytohormone signal network regulating elongation growth during shade avoidance. J Exp Bot 61: 2889-2903

Street IH, Aman S, Zubo Y, Ramzan A, Wang X, Shakeel S, Kieber JJ, Schaller GE (2015) Ethylene Inhibits Cell Proliferation of the Arabidopsis Root Meristem. Plant Physiol

Tao JJ, Cao YR, Chen H, Wei W, Li QT, Ma B, Zhang WK, Chen SY, Zhang JS (2015) Tobacco TCTP interacts with ethylene receptor NTHK1 and enhances plant growth through promotion of cell proliferation. Plant Physiol

Thain SC, Vandenbussche F, Laarhoven LJ, Dowson-Day MJ, Wang ZY, Tobin EM, Harren FJ, Millar AJ, Van Der Straeten D (2004) Circadian rhythms of ethylene emission in Arabidopsis. Plant Physiol 136: 3751-3761

Tsuchisaka A, Theologis A (2004) Unique and overlapping expression patterns among the Arabidopsis 1-amino-cyclopropane-1-carboxylate synthase gene family members. Plant Physiol 136:2982-3000

Van de Poel B, Van Der Straeten D (2014) 1-aminocyclopropane-1-carboxylic acid (ACC) in plants: more than just the precursor of ethylene! Front Plant Sci 5: 640

Voesenek LA, Benschop JJ, Bou J, Cox MC, Groeneveld HW, Millenaar FF, Vreeburg RA, Peeters AJ (2003) Interactions between plant hormones regulate submergence-induced shoot elongation in the flooding-tolerant dicot Rumex palustris. Ann Bot 91 Spec No: 205-211

Wilson K, Long D, Swinburne J, Coupland G (1996) A Dissociation insertion causes a semidominant mutation that increases expression of TINY, an Arabidopsis gene related to APETALA2. Plant Cell 8: 659-671

Yang SF, Hoffman NE (1984) Ethylene biosynthesis and its regulation in higher plants. Annu Rev Plant Physiol Mol Biolog 35: 155-189

Yoo SD, Cho YH, Tena G, Xiong Y, Sheen J (2008) Dual control of nuclear EIN3 by bifurcate MAPK cascades in C2H4 signalling. Nature 451: 789-795

Yoo SD, Sheen J (2008) MAPK signaling in plant hormone ethylene signal transduction. Plant Signal Behav 3: 848-849

Yoon GM (2015) New Insights into the Protein Turnover Regulation in Ethylene Biosynthesis. Mol Cells 38: 597-603

Zhou HL, Cao WH, Cao YR, Liu J, Hao YJ, Zhang JS, Chen SY (2006) Roles of ethylene receptor NTHK1 domains in plant growth, stress response and protein phosphorylation. FEBS Lett 580: 1239-1250

Chapter 2

STUDYING DROUGHT: FROM IN SOIL TO IN VITRO TO UNRAVEL EARLY STRESS RESPONSES

Marieke Dubois [a,b] and Dirk Inzé [a,b]

[a] Department of Plant Systems Biology, VIB, Ghent, Belgium
[b] Department of Plant Biotechnology and Bioinformatics, Ghent University, Belgium

Contributions: M.D. performed the literature study and was the main author of the chapter. D.I. supervised the project and contributed to the writing of the manuscript.

Drought stress forms a major environmental constraint during the life cycle of plants, often decreasing plant yield and in extreme cases threatening survival. The molecular responses induced by drought have therefore been the topic of extensive research from the 1970s onward. As soil-based approaches to study drought response are often inconvenient due to low throughput and insufficiently precise control of the conditions, *in vitro* setups were developed to mimic drought. Addition of compounds such as NaCl, mannitol, sorbitol, or polyethylene glycol to controlled growth media has become increasingly popular since it offers the advantages of accurate control of stress level and onset. These approaches enabled the discovery of very early stress responses, occurring within seconds and minutes following stress exposure. In this chapter, we used this main advantage of *in vitro* setups to construct a detailed time line of early responses to osmotic stress based on the available literature. We further discuss the specific responses triggered by different types and severities of osmotic stress. Finally, we made the comparison between transcriptome datasets generated using either *in vitro* approaches or in soil drought assays, and question the usefulness of these *in vitro* proxies.

From in soil to in vitro: when, why, and how

About forty years ago, people started to become aware of the rising problems of the drastically increasing world population and the upcoming effects of global warming (Broecker, 1975). It became clear that drought stress would form a major constraint for worldwide agriculture and therefore scientists started to extensively study drought stress responses in plants (extensively reviewed first in Hsiao and Acevedo, 1974), as reflected by the exponentially increasing amount of drought-related publications from the 1960s onward (Figure 2.1). Drought stress experiments were performed in soil either by progressive drying of the soil or by transplantation to pots with reduced moisture levels (Boyer, 1971; Saunier et al., 1968). These methods were however rapidly found inappropriate, as it was impossible to exactly control the stress levels and, most importantly, because they were unsuitable to screen or harvest large numbers of plants, as in soil approaches are very space-consuming. Therefore, during the seventies and eighties, alternative approaches to study drought response were investigated, and the step was made to mimic drought stress *in vitro* first on cell cultures, and not much later on plants (Kaufman and Eckard, 1971). By adding osmotic compounds to the artificial growth medium, the water potential (ψ_w) was lowered to simulate what happens under drought, making it harder for the plants to take up water from the substrate (Claes et al., 1990; Heyser and Nabors, 1981; Nguyen and Lamant, 1989).

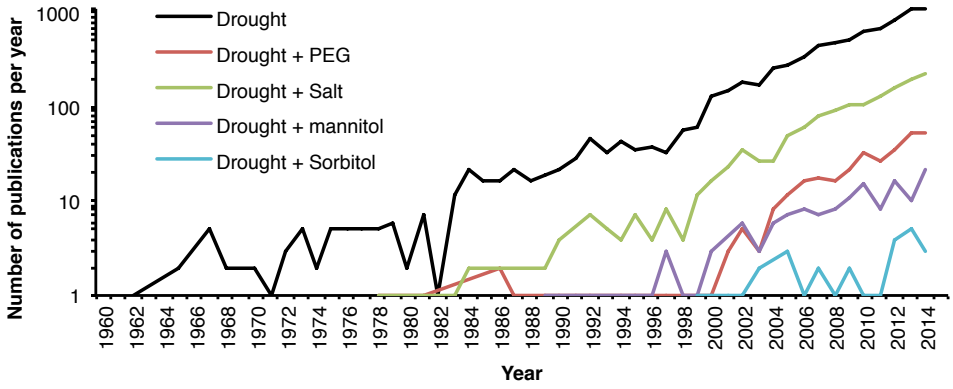

Figure 2.1. Historical overview of the use of osmotic compounds to study drought stress. Amount of publications containing the indicated keywords accepted each year from 1961 until 2014, according to the Pubmed litterature database.

Four major osmotic compounds were introduced to lower ψ_w, of which sodium chloride (NaCl) is most commonly used, followed by polyethylene glycol (PEG), mannitol, and sorbitol (Claeys et al., 2014; Verslues et al., 2006) (Figure 2.1). Mannitol and sorbitol are low molecular weight osmotica, sharing a common chemical structure only differing in steric C-atom conformation, and are non-metabolizable sugar analogs. Because of their low molecular weight, they offer the advantage of being easily and equally dissolved in the growth medium, but the disadvantage of being taken up by the plant, potentially triggering plasmolysis. Moreover, mannitol was recently reported to putatively activate mannitol-specific downstream responses, which will be discussed in more detail later (Trontin et al., 2014). In contrast, high molecular weight polyethylene glycols (PEG6000 or higher) are not taken up by plants, and do not trigger, to our current knowledge, PEG-specific downstream responses (Hesyer and Lamant, 1981; Kaufman and Eckard, 1971). Because PEG cannot be dissolved in the medium but has to infiltrate solidified medium through diffusion (Verslues et al., 2006), it is less equally distributed within one plate than small compounds, which might be problematic for studies using mild concentrations to trigger subtle stress effects (Skirycz et al., 2010). As most studies however focus on response to severe osmotic stress, with clear symptoms, PEG forms the best and most commonly used osmoticum for *in vitro* studies. In contrast to the compounds described so far, which are mainly used to mimic drought stress, NaCl is often used in parallel to drought stress. NaCl is known to trigger a dual stress, consisting of an osmotic component which might mimic drought, but also of an ionic stress component caused by the high levels of Na^+. These ions are toxic by themselves as they inhibit enzymatic activities, and because they trigger the uptake of other toxic and positive ions such as Li^+ and K^+ (Xiong and Zhu, 2002). In low concentrations and particularly when considering the short term plant responses to NaCl, within hours, the

ionic component might be less pronounced and NaCl could still mimic drought (Munns, 2002). As compared to in soil drought assays, *in vitro* setups are easy to use and suitable to expose large amounts of plants simultaneously to stress, as well as to precisely control the stress levels, onset, and duration.

Control of stress onset enables to build a time line of short term stress response

One of the main advantages of *in vitro* setups is the possibility to apply short term stress assays. For this purpose, young seedlings can either be grown in liquid medium or hydroponics cultures to which the compound can be added at the preferred moment. Alternatively, seedlings can be grown on solid control medium overlaid with a mesh, which can be transferred to medium supplemented with the osmoticum at the desired time point (Verslues et al., 2006). The possibility to precisely control the onset of the stress using these methods offers two major benefits. First, the exact time point at which the stress will be applied can be chosen. As the response to stress in different plant organs has been shown to highly depend on the developmental stage of the tissue (Skirycz et al., 2010), it might be suitable to expose plants to stress at a particular moment during development. Second, because the moment of stress exposure is chosen and precisely known, the short term stress response can be followed by harvesting the tissue of interest after hours, minutes, or even seconds upon stress exposure. Here, we combined the available osmotic stress studies that investigated this short term response to construct a time line of the response of *Arabidopsis thaliana* to osmotic stress. Ideally, an individual time line should be constructed per type of stress, per organ, per developmental stage and per level of stress, as all of these factors were shown to differently affect the stress response (Claeys et al., 2014; Dinneny et al., 2008; Ma et al., 2014; Skirycz et al., 2010, Verelst et al., 2013). However, since too few studies are available to enable such an analysis, we combined here the different types and levels of stresses but mentioned, when available, the specificity of the responses. As the abiotic stresses discussed here are achieved by adding compounds to the growth medium, the response in the roots is expected to be faster and different from the response in shoot and, therefore, the presented time line makes a distinction between root and shoot responses.

1 - Detection of the stress in roots: endocytosis and Ca^{2+} initiate the response

When roots are exposed to environments with a water potential (ψ_w) lower than the one of the root cells, water is passively exported (Figure 2.2a) (Zonia and Munnik,

2007). This lowers the intracellular turgor pressure and has three direct consequences. First, the surface-to-volume ratio of cells is increased, generating a surplus of plasma membrane which is internalized by clathrin-mediated endocytosis (Figure 2.2b) (Leshem et al., 2007; Zwiewka et al., 2015). This vesicle internalization has been observed under both ionic and non-ionic osmotic stresses even under relatively mild concentrations (75mM mannitol or sorbitol, 50mM KCl, 100mM NaCl) and occur within 10 minutes of stress exposure (Zwiewka et al., 2015). Consistently, mutants defective in clathrin components or in regulators of vesicle trafficking are unable to adapt their growth when exposed to osmotic stress and show clear stress symptoms such as necrosis (Leshem et al., 2007; Zwiewka et al., 2015).

Second, the decrease in cellular ψ_w increases the relative concentration of free Ca^{2+} molecules, which will act as a primary signal to induce more Ca^{2+} uptake (Figure 2.2c). The accumulation of Ca^{2+} has been reported to occur under salt, mannitol, sorbitol and PEG-mediated osmotic stress and occurs in waves of which the first peak was observed already within five seconds following stress exposure (Kiegle et al., 2000; Yuan et al., 2014). The Ca^{2+} peak is extremely short and only lasts for about one minute but, in specific cell-types in roots, repetitive peaks can trigger sustained signals (Kiegle et al., 2000). Within five minutes following stress exposure, the Ca^{2+} accumulation completely disappears (Yuan et al., 2014).

Although the observation that Ca^{2+} accumulates in response to osmotic stress is more than forty years old (Kaufman and Eckard, 1971) and despite the fact that the importance of Ca^{2+} has been widely studied during the last 20 years (Knight et al., 1998), the first dehydration-mediated molecular players responsible for Ca^{2+} sensing and further signal transmission were identified only recently (Yuan et al., 2014). Forward genetics screens enabled the identification of OSCA1 (OSmolality-induced CA^{2+}-increase), a Ca^{2+}-gated osmosensor which senses Ca^{2+} and stimulates influx channels for further Ca^{2+} accumulation. Consistently, in *osca1* mutants, the Ca^{2+} wave is weaker, resulting in impaired osmotic stress responses. Ca^{2+} molecules can further be recognized and bound by different families of proteins such as calmodulin and the calmodulin-binding transcription factors (CATMA) to further elicit transcriptional responses, or by Ca^{2+}-dependent protein kinases (CDPKs) and calmodulin-dependent kinases (CCaMKs) to trigger post-translational responses (Figure 2.2d) (Dodd et al., 2010; Finkler et al., 2007; Kaplan et al., 2006).

Finally, changes in cytoskeleton dynamics were reported to be the third process initiated within minutes upon stress, but are specific for severe salt stress (250mM, but not 150mM and below) (Wang et al., 2007; 2011). In Arabidopsis root epidermis cells, the actin and microtubule cytoskeleton is highly dynamic and filaments polymerize,

assemble, elongate, etc. Upon exposure of roots to high salt stress, actin depolymerization and bundle fragmentation is stimulated within 10 minutes of stress exposure (Liu et al., 2012) as one of the responses to the Ca^{2+} signal, but the exact mechanisms are poorly understood (Figure 2.2e) (Wang et al., 2011).

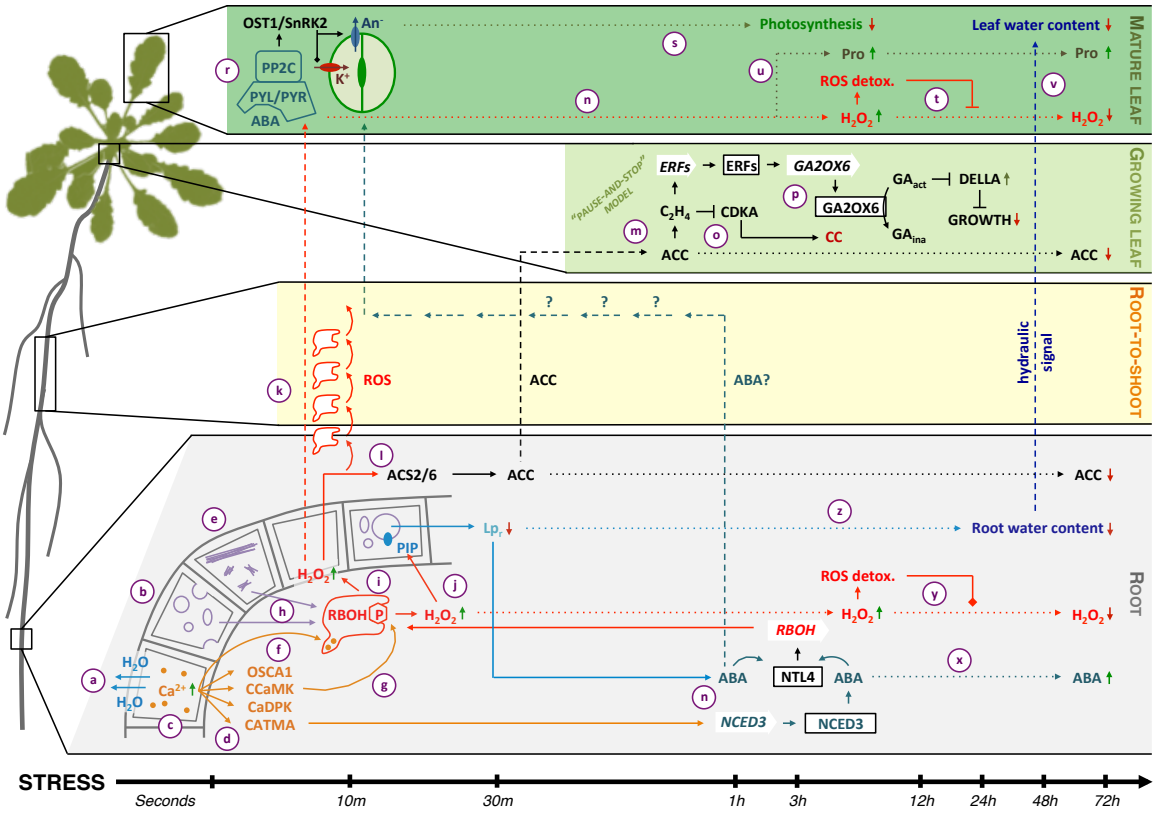

Figure 2.2. Overview of the osmotic stress responses over time following stress. Osmotic stress decreases the cellular water potential (a), which triggers internalization of the plasma membrane (b) and the increase of cytosolic Ca^{2+} levels (c). Ca^{2+}-triggered cascades are indicated in orange and comprise activation of Ca^{2+}-dependent kinases and transcription factors (d). Stress also triggers cytoskeleton changes (e). Ca^{2+}, cytoskeleton changes and membrane internalization are also involved in the activation of RBOH enzymes (f, g and h). RBOH enzymes are involved in the biosynthesis of the ROS species (red) (i), which rapidly induce aquaporin internalization (j). The ROS-signal is transduced to the shoot through a ROS-wave in which RBOH enzymes are subsequently activated (k). ROS can also activate ACC-biosynthesis enzymes (l). This triggers the accumulation of ACC, which is transported to the shoot and triggers ethylene-response in growing leaves within 1 hour (black) (m). This response causes leaf growth arrest and is denominated the "pause-and-stop" model, as leaf growth is first transiently arrested through CDKA phosphorylation (o) and later stopped by acting on the GA/DELLA pathway (p). As a result, leaf growth is inhibited within 24 hours (q). In fully-grown leaves, ABA (blue/grey) triggers closure of the stomata (r), which on longer term block photosynthesis (s). ABA also triggers further ROS generation in roots and leaves (n), which activates proline biosynthesis (u). ROS detoxifying mechanisms are induced to buffer the increasing ROS levels in shoot and root (t and y). Further dehydration also reduces root and leaf water content (v and z). After days of stress, ACC levels decrease again (w), while ABA and proline levels remain high (x). Full lines indicate activation/inhibition, dashed lines transport, and dotted lines evolution over time. See main text for abbreviations and references.

2 - Production of ROS within minutes following stress

One of the longer-term effects of Ca^{2+} accumulation is the posttranslational activation of the ROS-producing enzymes RESPIRATORY BURST OXIDASE HOMOLOGs (RBOHs). RBOH proteins posses EF-hand motifs at the N-terminus through which they might bind Ca^{2+} and thereby be activated (Figure 2.2f) (Canton and Grinstein, 2014). Moreover, some RBOHs are known to have phosphorylation domains which are targeted by Ca^{2+}-calmodulin-dependent kinases (Figure 2.2g) (Kadota et al., 2015). Although less characterized at the molecular level, several lines of evidence also suggest that the RBOH enzymes are stimulated by stress-induced endocytosis and by actin depolymerization (Figure 2.2h) (Hao et al., 2014; Tian et al., 2015; Wang et al., 2011).

RBOH proteins are a class of NADPH oxidases of which 10 members are known in Arabidopsis (Ma et al., 2012; Xie et al., 2011). Following short term stress exposure, they produce O_2^- in the apoplast of root cells (Gill and Tuteja, 2010), which is further converted to H_2O_2 by superoxide dismutase (SOD) (Figure 2.2i) (Suzuki et al., 2011). Each RBOH produces ROS in a different context; RBOH-D and E are responsible for ROS production under osmotic stress (Ma et al., 2012; Xie et al., 2011). While in high concentrations ROS can damage proteins and inactivate enzymes, low concentrations of ROS species, particularly H_2O_2, act as signaling molecules (Foyer and Noctor, 2009).

Upon exposure to salt stress, ROS accumulate in all cell layers of Arabidopsis roots within 5 minutes of stress (Leshem et al., 2007), likely as a direct consequence of the Ca^{2+} wave which occured after seconds. Upon initiation in the roots, the ROS-mediated signal further spreads systemically through the so-called ROS-wave (see later). It should be noted, however, that although mannitol and PEG response are also generally thought to involve ROS, the molecular mechanisms described above were up to now only reported for salt and drought stress, and the ionic component of the salt stress appears to be the determinant for fast ROS production (Leshem et al., 2007). Several studies report the absence or even downregulation of this NADPH-mediated ROS-production under mannitol or PEG (Leshem et al., 2007; Tamas et al., 2010; Uzilday et al., 2014). It is thus still unclear whether the described mechanisms occurr under all types of osmotic stress.

3 - A signal from root to shoot: what is the time delay?

Upon exposure to osmotic stress, root growth is affected but numerous changes also occur in the shoot, mainly to reduce growth, redirect energy metabolism, and minimize water loss, requiring a fast and mobile signal from root to shoot. Whether this signal has

a hydraulic origin or is a chemical, such as a hormone-related molecule, has been debated for a long time. Root conductivity is affected within minutes by osmotic stress, through ROS-induced internalization of the aquaporins (Figure 2.2j) (Boursiac et al., 2008). As a result, water transport is downregulated, and this could potentially initiate a hydraulic signal along the root up to the shoot, where this decrease in water potential is perceived. However, several lines of evidence suggest that root-to-shoot signaling following stress still occurs when the water potential is maintained by watering parts of the roots or by adjusting the osmotic potential (Bonhomme et al., 2012; Davies and Zhang, 1991; Nonami et al., 1997; Parent et al., 2010; Tang and Boyer, 2002), thereby suggesting the presence of non-hydraulic signals. The current view is that the early response to mild stress is dominated by chemical/hormonal signals, while the more long term response (week(s) following stress), when the stress is more severe, is mostly triggered by hydraulic signals (Perez-Alfocea, 2011; Schachtman and Goodger, 2008). In this context of the rapid stress response, only chemical/hormonal signals will thus be considered.

Multiple signals are candidates for being transported from root to shoot via the xylem. Classically discussed root-to-shoot signals include the stress hormone abscisic acid (ABA), the ethylene precursor 1-aminocyclopropane-1-carboxylic acid (ACC), and ROS (reviewed by Schachtman and Goodger, 2008; Skirycz and Inzé, 2010), but in the last years jasmonate (JA) is also being considered as a candidate to either function as or trigger the signal (Correia et al., 2014; Hasegawa et al., 2011; Ollas et al., 2015). It is expected for early root-to-shoot signals that biosynthesis or accumulation of the signals in the roots, transport to the shoot, and subsequent accumulation in the shoot occur in subsequent order and thus with a certain delay in timing. As the first responses in shoots were captured between 10 minutes and one hour upon exposure of the root to stress (see next section), this series of steps is expected to be extremely fast. It is thus rather unlikely that the earliest signals are synthesized by enzymes that are regulated at the transcriptional level; posttranslational activation of biosynthetic enzymes that are present in the exposed cells or release of stored or conjugated molecules is more plausible.

As described earlier, posttranslational mechanisms activate ROS biosynthesis, and ROS might thus be amongst the earliest root-to-shoot signals. ROS species are not transported through the xylem but are transmitted through a ROS wave, in which ROS induce RBOH activity in adjacent cells, which in turn produce ROS (Figure 2.2k) (Mittler et al., 2011). As this wave can reach a speed of 8 cm per minute, it likely reaches the shoot of small petri dish-grown seedlings within minutes following stress exposure.

Accumulation of ROS in roots can activate ACC biosynthesis in a posttranslational manner. Although it is not clear whether this mechanism is occurring under osmotic stress, ROS are known to activate a phosphorylation cascade involving MKK9, MPK3 and MPK6 in an ABA-independent manner (Chang et al., 2012; Liu et al., 2010; Tsugama et al., 2012; Yuasa et al., 2001). MPK3 and MPK6 were previously found to phosphorylate and thereby activate ACS2 and ACS6, two ACC synthase enzymes regulating the rate-limiting step of ACC biosynthesis (Figure 2.2l) (Liu and Zhang, 2004), but conflicting results exist about the precise involvement of ROS in this process (Xu et al., 2014). The first ethylene-related transcriptional responses in shoots were already measured after 45 minutes following stress (see further) (Dubois et al., 2015), indicating that ACC should be transported within the first half hour of osmotic stress (Figure 2.2m). This timing is consistent with what is known on short term signaling under biotic stress, where wounding of the roots triggers activation of ethylene-responsive genes in the shoot within 30 minutes (Hasegawa et al., 2011).

In contrast, the enzymes regulating ABA and JA biosynthesis are, to our knowledge, regulated at transcriptional level (Hu et al., 2009; Ollas et al., 2015). Upstream, Ca^{2+} induces the expression of *NCED3* (NINE-CIS-EPOXYCAROTENOID DIOXYGENASE 3; rate limiting for ABA biosynthesis) and of several JA biosynthesis genes, and also here ROS might be involved (Hu et al., 2009; Kang et al., 2006). ABA and JA levels were increased in Arabidopsis, wheat and eucalyptus roots following exposure to drought (Correira et al., 2014; Du et al., 2013; Liu et al., 2015). However, when considering the timing, the accumulation of ABA and JA (60 minutes) precedes the induction of their respective biosynthesis genes (90 minutes), pointing towards a feedback mechanism rather than a causal effect (Figure 2.2n) (Ellouzi et al., 2014). Several other studies questioned the importance of a root-sourced ABA signal in osmotic stress response, and currently the role of ABA as a root-to-shoot signal is still controversial. Grafting experiments showed that the ABA responsible for stomatal closure is likely synthesized in the shoot (Holbrook et al., 2002), and it was also demonstrated that the concentrations of ABA moving from root to shoot are too low to trigger stomatal closure (Munns and King, 1988). As ABA was recently even shown to accumulate more rapidly in the shoot (10 minutes) than in the roots (Yuan et al., 2014; Liu et al., 2015), it is hypothesized that the previously observed increasing levels of ABA in the xylem (Correira et al., 2014; Perez-Alfocea et al., 2011) might result from secondary re-circulation rather than from early stress-responsive root-to-shoot transport (Schachtman and Goodger, 2008; Zeevaart and Boyer, 1984). Thus, for ROS and ACC, mechanisms for a rapid induction of biosynthesis enzymes do exist and might occur under osmotic stress, while JA and ABA are synthesized more slowly and might thus not be part of the earliest root-to-shoot signals but rather belong to the more long-term signals.

4 - Response in the leaves within the first hour

After a short delay of a few minutes to about ½ hour following stress exposure of Arabidopsis roots, the early stress signal reaches the shoot and triggers responses which are known to be highly dependent on the developmental stage of each leaf, the tissue, and even the cell type (Dinneny et al., 2008; Skirycz et al., 2010; Verelst et al., 2013). In young, actively growing Arabidopsis leaves whose cells did not yet start to expand but are still proliferating, 57 genes responded to mild osmotic stress treatment within 1.5h (Skirycz et al., 2011a), and several of these genes were confirmed to be induced even earlier, within one hour (Dubois et al., 2015). These genes are mainly involved in ethylene responses, and consistently osmotic stress was shown to trigger a 30% increase in ACC levels in young seedlings after 1h (Figure 2.2m) (Skirycz et al., 2011a). The role of ACC in young leaves of plants exposed to stress is summarized by the "pause-and-stop model" (Figure 2.2o) (Skirycz et al., 2011a). Within hours following stress, the accumulation of ACC triggers, likely through the MPK3/6-cascade, the phosphorylation and inactivation of CYCLIN-DEPENDENT KINASE A (CDKA). The inhibition of this positive regulator of the cell cycle results in a transient and reversible "pause" of the cell cycle, which is further converted to "stop" when the stress lasts more than 10 hours (Skirycz et al., 2011a). This permanent exit out of the cell cycle, which constitutes the basis of leaf growth inhibition upon stress, is caused by the ETHYLENE RESPONSE FACTOR (ERF)-mediated activation of gibberellin (GA) degradation by the GA2-OXIDASE6 enzyme, thereby stabilizing DELLA proteins, which further push cells into differentiation (Figure 2.2p) (Claeys et al., 2012; Claeys and Inzé, 2013; Dubois et al., 2013). The subsequent steps linking ACC accumulation to inhibition of the GA/DELLA pathway will be discussed in detail in the next chapters. In the end, the ACC-triggered activation of leaf growth inhibition causes reductions in leaf growth that were observed 24 hours following exposure to mild stress (Figure 2.2q) (Skirycz et al., 2011a).

In contrast to young, actively growing leaves, ACC does not accumulate in fully-grown leaves before 72h after stress onset (Ellouzi et al., 2014), and the ERFs activated in growing tissue and likely involved in control of leaf growth are not induced by osmotic stress in mature leaves (Lisa Van den Broeck, personal communication). Although transcriptomics in leaves were extensively performed upon desiccation stress, there is to our knowledge no data available about genome-wide transcriptional changes in full-grown leaves within one hour of exposure of osmotic stress to roots, but expression analysis on individual genes showed that gene expression is affected within this time frame (Gamboa et al., 2015; Li et al., 2014). In contrast, fast physiological responses such as stomatal closure were reported. The aperture of stomata has been shown to decrease within 10 minutes following treatment of roots with PEG or sorbitol (Figure 2.2r) (Yuan

et al., 2014). In short (reviewed in Joshi-Saha et al., 2011), stomatal closure is mediated by ABA, which binds to a family of PYL/PYR (PYRABACTIN-RESISTANCE(-LIKE)) soluble receptors, thereby changing their conformation, causing them to bind to PROTEIN-PHOSPHATASE 2Cs (PP2C). PP2C can then no longer inhibit downstream kinases such as OST1 (OPEN STOMATA 1) and SnRK2 (SNF-RELATED KINASE 2), which are free to phosphorylate on the one hand K^+ influx channels, thereby inhibiting them, and on the other hand anions efflux channels, activating them. In general, ABA functions as the major hormone regulating stress-induced responses in mature leaves.

In the longer term, within hours following stress, closure of stomata enables a reduction in leaf transpiration but also limits CO_2 uptake, thereby lowering photosynthesis, and chlorophyll contents decrease on middle-long term, within 4 hours following osmotic stress (Figure 2.2s) (Ellouzi et al., 2014). Also within 4 hours, and likely as a result of the ABA increase which stimulates RBOH-mediated ROS accumulation, H_2O_2 levels are induced by about 8-fold and further increase progressively (Figure 2.2t) (Ellouzi et al., 2014). ROS triggers the biosynthesis of proline, of which accumulation in the leaves was observed with a similar timing (Figure 2.2u) (Ben Rejeb et al., 2015a; Ellouzi et al., 2014). Finally, as a result of all these responses, leaf water content and osmotic potential are only mildly affected during the first 2 days, but showed a clear reduction 72 hours following exposure to severe salt stress (and might thus take longer when the stress is milder), with reductions of 54% and 68%, respectively (Figure 2.2v) (Ellouzi et al., 2014; Ben Rejeb et al., 2015b).

5 - In the mean time in roots

After the rapid accumulation of root-to-shoot signals in the roots, levels of ACC rapidly decrease again between 4 and 16 hours following stress (Figure 2.2w) (Ellouzi et al., 2014). In contrast, ABA levels continue to increase progressively (Figure 2.2x) (Ellouzi et al., 2014), in accordance with previous reports that ABA would play increasing importance when the stress levels get more severe (Schachtman and Goodger, 2008). As a result of increased ABA accumulation, *RBOH* genes are transcriptionally activated through the ABA-responsive NTL4 (NAC WITH TRANSMEMBRANE MOTIF-LIKE4) transcription factor, maintaining further ROS production (Figure 2.2y) (Lee et al., 2012). *RHOB-D* is induced in Arabidopsis roots from 3h upon stress onwards (Suzuki et al., 2011) and H_2O_2 levels continue to increase until 24 hours before they reach a plateau (Ellouzi et al., 2014). The H_2O_2 accumulation triggers, together with the previously described increase in endocytosis, the internalization of plasma membrane-localized aquaporins mediating water transport (Figure 2.2j) (Boursiac et al., 2008). This causes a decrease in root hydraulic conductance, which is observed in many species, and in

Arabidopsis occurs within 1 hour of treatment with osmotic stress (Kaneko et al., 2015). As a consequence, the root water content rapidly decreases after 16 hours, and together with osmotic potential, is reduced by half after 72 hours (Figure 2.2z) (Ellouzi et al., 2014).

Responses overlooked in longer term stress assays

During the 20th century, "short term" responses (in terms of hormone levels, gene expression levels or physiological measurements) to sudden osmotic stress was mainly studied after 2 or 3 days following stress exposure, without taking into account earlier time points (Kalantari et al., 2000; Kaufmann and Eckard, 1971). Since the years 2000, however, numerous studies report time series measurements following stress exposure, with a range and resolution varying depending on the type of experiment. Ca^{2+} measurements are, for example, always performed within minutes following stress with up to 1-second resolution (Kiegle et al., 2000; Knight et al., 1998; Yuan et al., 2014), while physiological processes such as stomatal closure or chlorophyll-measurements are taken with intervals of few minutes, from on average 5 minutes following stress until maximum 3 hours upon stress (Bu et al., 2014; Luo et al., 2013; Yuan et al., 2014). Finally, expression analysis, hormone and ROS level measurements are often performed from 1h until 2 or 3 days following stress, with typically 2 additional time points between the start and the end measurement (e.g. Zhao et al., 2015, Gamboa et al., 2015). Earlier measurements on expression levels are rare, but do show that transcriptional responses occur within 30 to 45 minutes upon exposure to mild stress, so it might be useful to consider measurements before 1h upon stress (Ding et al., 2014; Dubois et al., 2015).

Time course experiments made it possible to distinguish between two types of processes. On the one hand, certain processes are induced shortly upon stress and further maintained or enhanced over time, such as proline and ABA accumulation, contributing to their widely accepted role as main stress response factors (Zeller et al., 2009). On the other hand, multiple processes are only transiently induced following stress, but might be equally important even if they are not further stimulated while stress levels or duration increase. For example, the very short term signal Ca^{2+} that initiates a large part of the response becomes fully undetectable within minutes following stress (Yuan et al., 2014). Also the ROS-mediated stress-signaling, induced within minutes and peaking after hours upon stress, is decreasing back to control levels after on average 24 hours due to the activation of multiple ROS-scavenging enzymes (Figure 2.2t and y) (Ben Rejeb et al., 2015b). The ACC accumulation, orchestrating the short-term growth-inhibitory response of growing Arabidopsis leaves, is also just a transient signal, and decreases back to control levels after days following stress

exposure (Figure 2.2m) (Kalantari et al., 2000). Finally, also at transcriptome level genes induced within hours following stress might be overlooked when transcriptomics are performed at later time points. Although only few studies performed transcriptomics at multiple time points following osmotic stress, on average about 1/4 of the genes differentially expressed at the most early time points (1h to 3h) are not longer affected by the stress at later time points (10h to 24h)(Kreps et al., 2002; Matsui et al., 2008; Skirycz et al., 2011a; Zeller et al., 2009). Thus, by sampling only at later time points, for example around 24 hours following stress, a considerable part of the stress response, likely mainly corresponding to early stress avoidance responses, is highly overlooked.

Importance of controlling stress levels

Besides exact control of the stress onset, *in vitro* stress setups give the possibility to expose plants to a wide range of stress levels by varying the concentrations of the osmotic compound. Similarly to what has been done in soil by using dehydration stress or survival assays, *in vitro* research mainly focused, and nowadays still focus, on rather severe stress levels (Claeys et al., 2014). High levels of stress (>25 mM mannitol, >100 mM sorbitol, >50 mM salt) trigger huge transcriptional responses and easily visible and measurable phenotypic effects, such as bleaching, alterations in leaf shape, inhibition of root growth, or germination defects, and are therefore used in the majority of stress studies (Claeys et al., 2014). However, more sensitive traits, such as rosette growth, are already affected by much milder stress, inhibiting only shoot growth while other symptoms remain absent (Claeys et al., 2014). Thus, low levels of osmotic stress also induce stress responses in plants, affecting growth mechanisms without threatening survival. Plants react according to the stress level to balance growth and survival and, consequently, different mechanism control growth under moderate stress and survival to life-threatening, severe stress (for a review, see Claeys and Inzé, 2013). As a result, mutants reported to survive better under severe stress, in soil, are not performing better when measuring rosette growth under milder drought (Skirycz et al., 2011b). An interesting recent study showed similar results in flowers of soil-grown Arabidopsis plants which were exposed to either moderate drought, not affecting development but only growth, or to severe drought (Ma et al., 2014). Although severe drought induced transcriptional changes of a much larger number of genes, about 15% of the genes differentially expressed by moderate drought were not affected by severe drought. Interestingly, these 277 moderate drought-specific genes were enriched for processes linked with growth, e.g. down-regulation of the GA pathway, known to be important for stem elongation (Ma et al., 2014). The currect idea is thus that different stress levels do not only quantitatively affect the gene expression by increasing/decreasing the number

of differentially expressed genes or their expression level, but rather trigger specific responses qualitatively depending on stress severity.

Compound-specific early responses

While all described types of osmotic stress share a common feature in lowering the water potential of the growth medium, several compounds, in particular salt and mannitol, are also known to elicit specific responses. As mentioned above, salt specifically induces amongst the most early signals multiple changes in cytoskeleton structure and prevents actin bundle polymerization, a response that has never been observed upon exposure to other types of osmotic stress (Liu et al., 2012; Wang et al., 2007; Wang et al., 2011). Another primary stress signal, cytosolic Ca^{2+} accumulation, is common to all types of osmotic stresses, as well as to biotic stress and temperature stress, but nevertheless plays a major role in the establishment of stress-specific responses. The specificity is achieved through the Ca^{2+}-signature, determined by the speed, amplitude, frequency, and duration of the Ca^{2+}-peak (Chinnusamy et al., 2004). For example, mannitol induces in the root endodermis a low primary Ca^{2+}-peak (1.1 μM) but with a long duration (50 sec), while salt stress induces a higher primary peak (1.8 μM) that lasts shorter (30 to 40 sec) (Kiegle et al., 2000). The speed with which the peak occurs correlates mainly with the strength of the stress (Zhu et al., 2013). The speed, strength, and duration of the secondary peak also contribute to this signature, and the combination of each profile across the different cell types forms an additional characteristic contributing to the specificity (Kiegle et al., 2000).

The secondary signals, the ROS, are induced through binding of RBOH enzymes to Ca^{2+} molecules (Canton and Grinstein, 2014; Kadota et al., 2015). As different RBOH-enzymes are induced depending on the type of environmental stress, the specificity of the Ca^{2+}-signature is also likely to be involved in this process. RBOHs D and E have been shown to be induced only by salt, but not by non-ionic osmotic stress such as mannitol and PEG, and it still remains unclear whether the latter induce ROS accumulation (Leshem et al., 2007).

More downstream, the Ca^{2+} signatures are recognized by specific receptors, but the exact mechanisms through which the different characteristics of the wave are captured at cellular level are not yet fully understood. The salt-induced Ca^{2+} signature triggers the activation of the well-known Salt Overly Sensitive pathway: the SOS3 receptor binds and is activated by Ca^{2+}-molecules and in turn induces the SOS2 kinase, which further phosphorylates and activates the SOS1 protein, a transmembrane channel exporting the toxic Na^{+} molecules (Chinnusamy et al., 2004). This SOS pathway has been observed under salt-induced osmotic stress, but not under non-ionic osmotic stress.

Finally, recent research also demonstrated compound-specific response pathways for mannitol (Trontin et al., 2014). In Arabidopsis *Col-0*, two putative mannitol receptors, *EGM1* and *EGM2* (Enhanced Growth on Mannitol) are thought to recognize mannitol molecules in a specific manner. They were suggested to activate the downstream responses, including ERF-mediated signaling. Consequently, the growth of mutants lacking one of these EGMs is less affected by mannitol. Whether EGM-proteins are necessary and sufficient for the induction of the ERF-pathway is however still under debate and might occur only under rather high mannitol concentration and/or under long term mannitol-stress (Dubois et al., 2015).

Severe in vitro setups are a good proxy for sudden dehydration

Although specific pathways exist for different types of osmotic stresses, these pathways converge towards general responses (Chinnusamy et al., 2004). Particularly when high levels of stress are used (> 100mM NaCl, > 200mM mannitol and > 20% PEG6000), the overlaps in short term (within 48h) transcriptional responses induced by the different types of stresses are extensive. The datasets of Kreps (2002) and Matsui (2008) were used to calculate overlaps between transcriptome changes in shoot tissue under short term severe mannitol-, salt-, and dehydration-induced stress. All datasets correlated significantly with each other and notably high correlations ($CC_{Spearman}$ = 0.74) were found between salt and dehydration response (Matsui et al., 2008). Thus, high levels of stress trigger survival responses in the shoot (Claeys and Inzé, 2013) that are common to different types of hyperosmotic stress and with very severe forms of drought, such as sudden dehydration.

Accordingly, numerous mutants were reported to be more tolerant to more than one type of severe osmotic stress (Bu et al., 2014; Cidade et al., 2012; Liu et al., 2013; Ma et al., 2014; Sousa et al., 2014; Wang et al., 2014). These mutants often carry mutations in genes involved in general stress response pathways, both ABA-regulated mechanisms and ABA-independent pathways such as ROS- and Ca^{2+}-signaling. Importantly, many of these mutants with increased tolerance to severe osmotic stress also survive better when grown in soil and exposted to dehydration stress in which water is withheld for weeks before rewatering (Cai et al., 2014, 2015; Cho et al., 2014; Gamboa et al., 2015; Kim et al., 2014; Li et al., 2014; Liu et al., 2013; Lu et al., 2013; Qin et al., 2014; Song et al., 2013; Xiao et al., 2013; Zhao et al., 2015). Thus, severe *in vitro* stress assays elicit general tolerance responses and are suitable to mimic severe dehydration stress in soil. However, these general pathways that provide tolerance to osmotic and drought stress (as a typical example, by reduced stomatal aperture) often interfere with normal plant development and these mutants thus often show growth penalties under control conditions or milder, sub-lethal drought stress (Skirycz et al., 2011b). This is supported

by the observation that the transcriptome changes upon severe osmotic or dehydration stress do not correlate or even show weak anti-correlation with expression changes measured under sub-lethal drought stress (Baerenfaller et al., 2012; Harb et al., 2010).

The relevance of mild in vitro assays to mimic mild drought is uncertain

Although the relevance of using milder stress levels to study stress responses is widely accepted, as even low levels of osmotic stress affect plant growth, and particularly rosette growth (Claeys et al., 2014), such studies are still uncommon. In striking contrast with the short-term severe stress response, mild salt levels (50mM; Shen et al., 2014) and mild mannitol levels (25mM; Skirycz et al., 2011a) trigger very different responses in growing shoot tissue. Significant anti-correlation ($CC_{Spearmann}$ = -0.38) was observed between 48h-salt and 24h-mannitol response, and the anti-correlation was most pronounced at the last time point, indicating that the responses to salt and mannitol stress diverge over time. Accordingly, genes identified as important regulators for growth under mild mannitol-mediated stress, such as *ERF5* and *ERF6*, are not affected by mild salt, and consequently the corresponding mutants, which grow better than wild type on low concentrations of mannitol, do not perform better under mild salt stress (Dubois et al., 2013). Growth under mild stress thus seems to be specifically regulated depending on the type of stress, even within *in vitro* setups.

Recently, a study reported transcriptome changes in actively growing leaves upon exposure to mild drought stress in soil. This forms the most suitable dataset published thus far to compare with the mild osmotic stress data and estimate translatability towards real drought (Clauw et al., 2015). Surprisingly, although the plant tissue used in both studies is highly comparable, no correlation or weak but significant anti-correlation ($CC_{Spearmann}$ = -0.19) was observed between the different mannitol datasets and this drought dataset. Although this observation might point toward strongly different responses under *in vitro* stress and in soil mild drought, these results should be interpreted with care: the stress level and mainly the stress duration, which greatly affect the molecular stress response, differ in both studies. While the *in vitro* transcriptomics were performed within hours after sudden mannitol treatment, the expression analysis in the drought stress study was done one week upon transfer to dry soil, and thus mainly reflects longer term stress response. It thus remains uncertain whether mild osmotic stress forms an appropriate proxy for mild drought when aiming to unravel short term stress reponses. To explore this, early stress-responsive molecular pathways in specific organs can first be unraveled taking advantage of the *in vitro* assays and the ease they provide to apply mild stress levels and to control stress onset. Subsequently, an appropriate setup enabling detection of short term drought response needs to be established, in order to perform in soil assays that ressemble as much as

possible the conditions used *in vitro*, in terms of stress level and duration. Such a setup would enable to reliably test the involvement of the *in vitro* identified molecular players under in soil mild drought, or to uncover new regulators of short term mild drought response. This approach was taken in the research presented hereafter: molecular pathways orchestrating leaf growth under short term osmotic stress were first unraveled *in vitro*, as presented in Chapters 3, 4, and 5, and subsequently investigated in soil with a new experimental setup enabling comparison (Chapter 6).

ACKNOWLEDGEMENTS

We thank Dr. Hannes Claeys for the critical comments and helpful suggestions to improve this chapter. This work was supported by the Interuniversity Attraction Poles Program (IUAP P7/29 "MARS") initiated by the Belgian Science Policy Office, by Ghent University ('Bijzonder Onderzoeksfonds Methusalem Project' no. BOF08/01M00408, Multidisciplinary Research Partnership "Biotechnology for a Sustainable Economy" Project no. 01MRB510W).

REFERENCES

Baerenfaller K, Massonnet C, Walsh S, Baginsky S, Buhlmann P, Hennig L, Hirsch-Hoffmann M, Howell KA, Kahlau S, Radziejwoski A, Russenberger D, Rutishauser D, Small I, Stekhoven D, Sulpice R, Svozil J, Wuyts N, Stitt M, Hilson P, Granier C, Gruissem W (2012) Systems-based analysis of Arabidopsis leaf growth reveals adaptation to water deficit. Mol Syst Biol 8: 606

Ben Rejeb K, Abdelly C, Savoure A (2015a) How reactive oxygen species and proline face stress together. Plant Physiol and Biochemistry 80 : 278–284

Ben Rejeb K, Benzarti M, Debez A, Bailly C, Savoure A, Abdelly C (2015b) NADPH oxidase-dependent H2O2 production is required for salt-induced antioxidant defense in Arabidopsis thaliana. J Plant Physiol 174: 5-15

Bonhomme L, Valot B, Tardieu F, Zivy M (2012) Phosphoproteome dynamics upon changes in plant water status reveal early events associated with rapid growth adjustment in maize leaves. Mol Cell Proteomics 11: 957-972

Boursiac Y, Prak S, Boudet J, Postaire O, Luu DT, Tournaire-Roux C, Santoni V, Maurel C (2008) The response of Arabidopsis root water transport to a challenging environment implicates reactive oxygen species- and phosphorylation-dependent internalization of aquaporins. Plant Signal Behav 3: 1096-1098

Boyer JS (1971) Nonstomatal Inhibition of Photosynthesis in Sunflower at Low Leaf Water Potentials and High Light Intensities. Plant Physiology 48: 532-&

Broecker WS (1975) Climatic Change - Are We on Brink of a Pronounced Global Warming. Science 189: 460-463

Bu Q, Lv T, Shen H, Luong P, Wang J, Wang Z, Huang Z, Xiao L, Engineer C, Kim TH, Schroeder JI, Huq E (2014) Regulation of drought tolerance by the F-box protein MAX2 in Arabidopsis. Plant Physiol 164: 424-439

Cai G, Wang G, Wang L, Liu Y, Pan J, Li D (2014) A maize mitogen-activated protein kinase kinase, ZmMKK1, positively regulated the salt and drought tolerance in transgenic Arabidopsis. J Plant Physiol 171: 1003-1016

Cai W, Liu W, Wang WS, Fu ZW, Han TT, Lu YT (2015) Overexpression of Rat Neurons Nitric Oxide Synthase in Rice Enhances Drought and Salt Tolerance. PLoS One 10: e0131599

Canton J, Grinstein S (2014) Priming and activation of NADPH oxidases in plants and animals. Trends Immunol 35: 405-407

Chang R, Jang CJ, Branco-Price C, Nghiem P, Bailey-Serres J (2012) Transient MPK6 activation in response to oxygen deprivation and reoxygenation is mediated by mitochondria and aids seedling survival in Arabidopsis. Plant Mol Biol 78: 109-122

Chinnusamy V, Schumaker K, Zhu JK (2004) Molecular genetic perspectives on cross-talk and specificity in abiotic stress signalling in plants. J Exp Bot 55: 225-236

Cho HY, Lee C, Hwang SG, Park YC, Lim HL, Jang CS (2014) Overexpression of the OsChI1 gene, encoding a putative laccase precursor, increases tolerance to drought and salinity stress in transgenic Arabidopsis. Gene 552: 98-105

Cidade LC, de Oliveira TM, Mendes AF, Macedo AF, Floh EI, Gesteira AS, Soares-Filho WS, Costa MG (2012) Ectopic expression of a fruit phytoene synthase from Citrus paradisi Macf. promotes abiotic stress tolerance in transgenic tobacco. Mol Biol Rep 39: 10201-10209

Claes B, Dekeyser R, Villarroel R, Vandenbulcke M, Bauw G, Vanmontagu M, Caplan A (1990) Characterization of a Rice Gene Showing Organ-Specific Expression in Response to Salt Stress and Drought. Plant Cell 2: 19-27

Claeys H, Inze D (2013) The Agony of Choice: How Plants Balance Growth and Survival under Water-Limiting Conditions. Plant Physiology 162: 1768-1779

Claeys H, Skirycz A, Maleux K, Inze D (2012) DELLA Signaling Mediates Stress-Induced Cell Differentiation in Arabidopsis Leaves through Modulation of Anaphase-Promoting Complex/Cyclosome Activity. Plant Physiology 159: 739-+

Claeys H, Van Landeghem S, Dubois M, Maleux K, Inzé D (2014) What is stress? Dose-response effects in commonly used *in vitro* stress assays. Plant Physiology 165: 519-527

Clauw P, Coppens F, De Beuf K, Dhondt S, Van Daele T, Maleux K, Storme V, Clement L, Gonzalez N, Inze D (2015) Leaf responses to mild drought stress in natural variants of Arabidopsis. Plant Physiol 167: 800-816

Correia B, Pinto-Marijuan M, Castro BB, Brossa R, Lopez-Carbonell M, Pinto G (2014) Hormonal dynamics during recovery from drought in two Eucalyptus globulus genotypes: from root to leaf. Plant Physiol Biochem 82: 151-160

Davies WJ, Zhang JH (1991) Root Signals and the Regulation of Growth and Development of Plants in Drying Soil. Annual Review of Plant Physiology and Plant Molecular Biology 42: 55-76

Ding ZJ, Yan JY, Xu XY, Yu DQ, Li GX, Zhang SQ, Zheng SJ (2014) Transcription factor WRKY46 regulates osmotic stress responses and stomatal movement independently in Arabidopsis. Plant J 79: 13-27

Dinneny JR, Long TA, Wang JY, Jung JW, Mace D, Pointer S, Barron C, Brady SM, Schiefelbein J, Benfey PN (2008) Cell identity mediates the response of Arabidopsis roots to abiotic stress. Science 322: 44-44

Dodd AN, Kudla J, Sanders D (2010) The Language of Calcium Signaling. Annual Review of Plant Biology, Vol 61 61: 593-620

Du H, Liu H, Xiong L (2013) Endogenous auxin and jasmonic acid levels are differentially modulated by abiotic stresses in rice. Front Plant Sci 4: 397

Dubois M, Skirycz A, Claeys H, Maleux K, Dhondt S, De Bodt S, Vanden Bossche R, De Milde L, Yoshizumi T, Matsui M, Inze D (2013) Ethylene Response Factor6 acts as a central regulator of leaf growth under water-limiting conditions in Arabidopsis. Plant Physiol 162: 319-332

Dubois M, Van den Broeck L, Claeys H, Van Vlierberghe K, Matsui M, Inze D (2015) The ETHYLENE RESPONSE FACTORS ERF6 and ERF11 antagonistically regulate mannitol-induced growth inhibition in Arabidopsis. Plant Physiol

Ellouzi H, Ben Hamed K, Hernandez I, Cela J, Muller M, Magne C, Abdelly C, Munne-Bosch S (2014) A comparative study of the early osmotic, ionic, redox and hormonal signaling response in leaves and roots of two halophytes and a glycophyte to salinity. Planta 240: 1299-1317

Finkler A, Ashery-Padan R, Fromm H (2007) CAMTAs: Calmodulin-binding transcription activators from plants to human. Febs Letters 581: 3893-3898

Foyer CH, Noctor G (2009) Redox regulation in photosynthetic organisms: signaling, acclimation, and practical implications. Antioxid Redox Signal 11: 861-905

Gamboa MC, Baltierra F, Leon G, Krauskopf E (2013) Drought and salt tolerance enhancement of transgenic Arabidopsis by overexpression of the vacuolar pyrophosphatase 1 (EVP1) gene from Eucalyptus globulus. Plant Physiol and Biochemistry 73 :99e105

Gill SS, Tuteja N (2010) Reactive oxygen species and antioxidant machinery in abiotic stress tolerance in crop plants. Plant Physiol Biochem 48: 909-930

Hao H, Fan L, Chen T, Li R, Li X, He Q, Botella MA, Lin J (2014) Clathrin and Membrane Microdomains Cooperatively Regulate RbohD Dynamics and Activity in Arabidopsis. Plant Cell 26: 1729-1745

Harb A, Krishnan A, Ambavaram MM, Pereira A (2010) Molecular and physiological analysis of drought stress in Arabidopsis reveals early responses leading to acclimation in plant growth. Plant Physiol 154: 1254-1271

Hasegawa S, Sogabe Y, Asano T, Nakagawa T, Nakamura H, Kodama H, Ohta H, Yamaguchi K, Mueller MJ, Nishiuchi T (2011) Gene expression analysis of wounding-induced root-to-shoot communication in Arabidopsis thaliana. Plant Cell Environ 34: 705-716

Heyser JW, Nabors MW (1981) Growth, Water-Content, and Solute Accumulation of 2 Tobacco Cell-Lines Cultured on Sodium-Chloride, Dextran, and Polyethylene-Glycol. Plant Physiology 68: 1454-1459

Holbrook NM, Shashidhar VR, James RA, Munns R (2002) Stomatal control in tomato with ABA-deficient roots: response of grafted plants to soil drying. J Exp Bot 53: 1503-1514

Hsiao TC, Acevedo E (1974) Plant Responses to Water Deficits, Water-Use Efficiency, and Drought Resistance. Agricultural Meteorology 14: 59-84

Hu X, Li W, Chen Q, Yang Y (2009) Early signal transduction linking the synthesis of jasmonic acid in plant. Plant Signal Behav 4: 696-697

Joshi-Saha A, Valon C, Leung J (2011) A brand new START: abscisic acid perception and transduction in the guard cell. Sci Signal 4: re4

Kadota Y, Shirasu K, Zipfel C (2015) Regulation of the NADPH Oxidase RBOHD During Plant Immunity. Plant Cell Physiol 56: 1472-1480

Kalantari KM, Smith AR, Hall MA (2000) The effect of water stress on 1-(malonylamino)cyclopropane-1-carboxylic acid concentration in plant tissues. Plant Growth Regulation 31: 183-193

Kaneko T, Horie T, Nakahara Y, Tsuji N, Shibasaka M, Katsuhara M (2015) Dynamic regulation of the root hydraulic conductivity of barley plants in response to salinity/osmotic stress. Plant Cell Physiol 56: 875-882

Kang S, Kim HB, Lee H, Choi JY, Heu S, Oh CJ, Kwon SI, An CS (2006) Overexpression in Arabidopsis of a plasma membrane-targeting glutamate receptor from small radish increases glutamate-mediated Ca2+ influx and delays fungal infection. Mol Cells 21: 418-427

Kaplan B, Davydov O, Knight H, Galon Y, Knight MR, Fluhr R, Fromm H (2006) Rapid transcriptome changes induced by cytosolic Ca2+ transients reveal ABRE-related sequences as Ca2+-responsive cis elements in Arabidopsis. Plant Cell 18: 2733-2748

Kaufmann MR, Eckard AN (1971) Evaluation of Water Stress Control with Polyethylene Glycols by Analysis of Guttation. Plant Physiology 47: 453-&

Kiegle E, Moore CA, Haseloff J, Tester MA, Knight MR (2000) Cell-type-specific calcium responses to drought, salt and cold in the Arabidopsis root. Plant Journal 23: 267-278

Kim H, Lee K, Hwang H, Bhatnagar N, Kim DY, Yoon IS, Byun MO, Kim ST, Jung KH, Kim BG (2014) Overexpression of PYL5 in rice enhances drought tolerance, inhibits growth, and modulates gene expression. J Exp Bot 65: 453-464

Knight H, Brandt S, Knight MR (1998) A history of stress alters drought calcium signalling pathways in Arabidopsis. Plant Journal 16: 681-687

Kreps JA, Wu Y, Chang HS, Zhu T, Wang X, Harper JF (2002) Transcriptome changes for Arabidopsis in response to salt, osmotic, and cold stress. Plant Physiol 130: 2129-2141

Lee S, Seo PJ, Lee HJ, Park CM (2012) A NAC transcription factor NTL4 promotes reactive oxygen species production during drought-induced leaf senescence in Arabidopsis. Plant J 70: 831-844

Leshem Y, Seri L, Levine A (2007) Induction of phosphatidylinositol 3-kinase-mediated endocytosis by salt stress leads to intracellular production of reactive oxygen species and salt tolerance. Plant Journal 51: 185-197

Li XL, Yang X, Hu YX, Yu XD, Li QL (2014) A novel NAC transcription factor from Suaeda liaotungensis K. enhanced transgenic Arabidopsis drought, salt, and cold stress tolerance. Plant Cell Rep 33: 767-778

Liu H, Sultan MA, Liu XL, Zhang J, Yu F, Zhao HX (2015) Physiological and comparative proteomic analysis reveals different drought responses in roots and leaves of drought-tolerant wild wheat (Triticum boeoticum). PLoS One 10: e0121852

Liu SG, Zhu DZ, Chen GH, Gao XQ, Zhang XS (2012) Disrupted actin dynamics trigger an increment in the reactive oxygen species levels in the Arabidopsis root under salt stress. Plant Cell Rep 31: 1219-1226

Liu W, Tai H, Li S, Gao W, Zhao M, Xie C, Li WX (2014) bHLH122 is important for drought and osmotic stress resistance in Arabidopsis and in the repression of ABA catabolism. New Phytol 201: 1192-1204

Liu XM, Kim KE, Kim KC, Nguyen XC, Han HJ, Jung MS, Kim HS, Kim SH, Park HC, Yun DJ, Chung WS (2010) Cadmium activates Arabidopsis MPK3 and MPK6 via accumulation of reactive oxygen species. Phytochemistry 71: 614-618

Liu Y, Zhang S (2004) Phosphorylation of 1-aminocyclopropane-1-carboxylic acid synthase by MPK6, a stress-responsive mitogen-activated protein kinase, induces ethylene biosynthesis in Arabidopsis. Plant Cell 16: 3386-3399

Lu P, Kang M, Jiang X, Dai F, Gao J, Zhang C (2013) RhEXPA4, a rose expansin gene, modulates leaf growth and confers drought and salt tolerance to Arabidopsis. Planta 237: 1547-1559

Luo X, Bai X, Sun X, Zhu D, Liu B, Ji W, Cai H, Cao L, Wu J, Hu M, Liu X, Tang L, Zhu Y (2013) Expression of wild soybean WRKY20 in Arabidopsis enhances drought tolerance and regulates ABA signalling. J Exp Bot 64: 2155-2169

Ma L, Zhang H, Sun L, Jiao Y, Zhang G, Miao C, Hao F (2012) NADPH oxidase AtrbohD and AtrbohF function in ROS-dependent regulation of Na(+)/K(+)homeostasis in Arabidopsis under salt stress. J Exp Bot 63: 305-317

Ma T, Li ML, Zhao AG, Xu X, Liu GS, Cheng LQ (2014) LcWRKY5: an unknown function gene from sheepgrass improves drought tolerance in transgenic Arabidopsis. Plant Cell Reports 33: 1507-1518

Matsui A, Ishida J, Morosawa T, Mochizuki Y, Kaminuma E, Endo TA, Okamoto M, Nambara E, Nakajima M, Kawashima M, Satou M, Kim JM, Kobayashi N, Toyoda T, Shinozaki K, Seki M (2008) Arabidopsis transcriptome analysis under drought, cold, high-salinity and ABA treatment conditions using a tiling array. Plant Cell Physiol 49: 1135-1149

Mittler R, Vanderauwera S, Suzuki N, Miller G, Tognetti VB, Vandepoele K, Gollery M, Shulaev V, Van Breusegem F (2011) ROS signaling: the new wave? Trends Plant Sci 16: 300-309

Munns R (2002) Comparative physiology of salt and water stress. Plant Cell and Environment 25: 239-250

Munns R, King RW (1988) Abscisic Acid is not the only stomatal inhibitor in the transpiration stream of wheat plants. Plant Physiol 88: 703-708

Nguyen A, Lamant A (1989) Variation in Growth and Osmotic Regulation of Roots of Water-Stressed Maritime Pine (Pinus-Pinaster Ait) Provenances. Tree Physiology 5: 123-133

Nonami H, Wu Y, Boyer JS (1997) Decreased Growth-Induced Water Potential (A Primary Cause of Growth Inhibition at Low Water Potentials). Plant Physiol 114: 501-509

Ollas CD, Arbona V, Gomez-Cadenas A (2015) Jasmonoyl isoleucine accumulation is needed for abscisic acid build-up in roots of Arabidopsis under water stress conditions. Plant Cell Environ

Parent B, Suard B, Serraj R, Tardieu F (2010) Rice leaf growth and water potential are resilient to evaporative demand and soil water deficit once the effects of root system are neutralized. Plant Cell Environ 33: 1256-1267

Perez-Alfocea F, Ghanem ME, Gomez-Cadenas A, Dodd IC (2011) Omics of root-to-shoot signaling under salt stress and water deficit. OMICS 15: 893-901

Qin LX, Li Y, Li DD, Xu WL, Zheng Y, Li XB (2014) Arabidopsis drought-induced protein Di19-3 participates in plant response to drought and high salinity stresses. Plant Mol Biol 86: 609-625

Saunier RE, Hull HM, Ehrenrei.Jh (1968) Aspects of Drought Tolerance in Creosotebush (Larrea Divaricata). Plant Physiology 43: 401-&

Schachtman DP, Goodger JQ (2008) Chemical root to shoot signaling under drought. Trends Plant Sci 13: 281-287

Shen X, Wang Z, Song X, Xu J, Jiang C, Zhao Y, Ma C, Zhang H (2014) Transcriptomic profiling revealed an important role of cell wall remodeling and ethylene signaling pathway during salt acclimation in Arabidopsis. Plant Mol Biol 86: 303-317

Skirycz A, Claeys H, De Bodt S, Oikawa A, Shinoda S, Andriankaja M, Maleux K, Eloy NB, Coppens F, Yoo S-D, Saito K, Inzé D (2011a) Pause-and-stop: the effects of osmotic stress on cell proliferation during early leaf development in Arabidopsis and a role for ethylene signaling in cell cycle arrest. Plant Cell 23: 1876-1888

Skirycz A, De Bodt S, Obata T, De Clercq I, Claeys H, De Rycke R, Andriankaja M, Van Aken O, Van Breusegem F, Fernie AR, Inzé D (2010) Developmental stage specificity and the role of mitochondrial metabolism in the response of Arabidopsis leaves to prolonged mild osmotic stress. Plant Physiology 152: 226-244

Skirycz A, Inze D (2010) More from less: plant growth under limited water. Current Opinion in Biotechnology 21: 197-203

Skirycz A, Vandenbroucke K, Clauw P, Maleux K, De Meyer B, Dhondt S, Pucci A, Gonzalez N, Hoeberichts F, Tognetti VB, Galbiati M, Tonelli C, Van Breusegem F, Vuylsteke M, Inze D (2011b) Survival and growth of Arabidopsis plants given limited water are not equal. Nat Biotechnol 29: 212-214

Song JB, Gao S, Sun D, Li H, Shu XX, Yang ZM (2013) miR394 and LCR are involved in Arabidopsis salt and drought stress responses in an abscisic acid-dependent manner. BMC Plant Biol 13: 210

Sousa AO, Assis ET, Pirovani CP, Alvim FC, Costa MG (2014) Phosphate-induced-1 gene from Eucalyptus (EgPHI-1) enhances osmotic stress tolerance in transgenic tobacco. Genet Mol Res 13: 1579-1588

Suzuki N, Miller G, Morales J, Shulaev V, Torres MA, Mittler R (2011) Respiratory burst oxidases: the engines of ROS signaling. Curr Opin Plant Biol 14: 691-699

Tamas L, Mistrik I, Huttova J, Haluskova L, Valentovicova K, Zelinova V (2010) Role of reactive oxygen species-generating enzymes and hydrogen peroxide during cadmium, mercury and osmotic stresses in barley root tip. Planta 231: 221-231

Tang AC, Boyer JS (2002) Growth-induced water potentials and the growth of maize leaves. J Exp Bot 53: 489-503

Tian M, Lou L, Liu L, Yu F, Zhao Q, Zhang H, Wu Y, Tang S, Xia R, Zhu B, Serino G, Xie Q (2015) The RING finger E3 ligase STRF1 is involved in membrane trafficking and modulates salt-stress response in Arabidopsis thaliana. Plant J 82: 81-92

Trontin C, Kiani S, Corwin JA, Hématy K, Yansouni J, Kliebenstein DJ, Loudet O (2014) A pair of receptor-like kinases is responsible for natural variation in shoot growth response to mannitol treatment in Arabidopsis thaliana. Plant Journal 78: 121-133

Tsugama D, Liu S, Takano T (2012) Drought-induced activation and rehydration-induced inactivation of MPK6 in Arabidopsis. Biochem Biophys Res Commun 426: 626-629

Uzilday B, Turkan I, Ozgur R, Sekmen AH (2014) Strategies of ROS regulation and antioxidant defense during transition from C(3) to C(4) photosynthesis in the genus Flaveria under PEG-induced osmotic stress. J Plant Physiol 171: 65-75

Verelst W, Bertolini E, De Bodt S, Vandepoele K, Demeulenaere M, Pe ME, Inze D (2013) Molecular and Physiological Analysis of Growth-Limiting Drought Stress in Brachypodium distachyon Leaves. Molecular Plant 6: 311-322

Verslues PE, Agarwal M, Katiyar-Agarwal S, Zhu J, Zhu J-K (2006) Methods and concepts in quantifying resistance to drought, salt and freezing, abiotic stresses that affect plant water status. Plant Journal 45: 523-539

Wang C, Li J, Yuan M (2007) Salt tolerance requires cortical microtubule reorganization in Arabidopsis. Plant Cell Physiol 48: 1534-1547

Wang C, Zhang LJ, Huang RD (2011) Cytoskeleton and plant salt stress tolerance. Plant Signal Behav 6: 29-31

Wang J, Ding B, Guo Y, Li M, Chen S, Huang G, Xie X (2014) Overexpression of a wheat phospholipase D gene, TaPLDalpha, enhances tolerance to drought and osmotic stress in Arabidopsis thaliana. Planta 240: 103-115

Xiao Y, Huang X, Shen Y, Huang Z (2013) A novel wheat alpha-amylase inhibitor gene, TaHPS, significantly improves the salt and drought tolerance of transgenic Arabidopsis. Physiol Plant 148: 273-283

Xie YJ, Xu S, Han B, Wu MZ, Yuan XX, Han Y, Gu Q, Xu DK, Yang Q, Shen WB (2011) Evidence of Arabidopsis salt acclimation induced by up-regulation of HY1 and the regulatory role of RbohD-derived reactive oxygen species synthesis. Plant J 66: 280-292

Xiong L, Zhu JK (2002) Molecular and genetic aspects of plant responses to osmotic stress. Plant Cell and Environment 25: 131-139

Xu J, Xie J, Yan C, Zou X, Ren D, Zhang S (2014) A chemical genetic approach demonstrates that MPK3/MPK6 activation and NADPH oxidase-mediated oxidative burst are two independent signaling events in plant immunity. Plant J 77: 222-234

Yuan F, Yang HM, Xue Y, Kong DD, Ye R, Li CJ, Zhang JY, Theprungsirikul L, Shrift T, Krichilsky B, Johnson DM, Swift GB, He YK, Siedow JN, Pei ZM (2014) OSCA1 mediates osmotic-stress-evoked Ca2+ increases vital for osmosensing in Arabidopsis. Nature 514: 367-+

Yuasa T, Ichimura K, Mizoguchi T, Shinozaki K (2001) Oxidative stress activates ATMPK6, an Arabidopsis homologue of MAP kinase. Plant Cell Physiol 42: 1012-1016

Zeevaart JA, Boyer GL (1984) Accumulation and transport of abscisic Acid and its metabolites in ricinus and xanthium. Plant Physiol 74: 934-939

Zeller G, Henz SR, Widmer CK, Sachsenberg T, Ratsch G, Weigel D, Laubinger S (2009) Stress-induced changes in the Arabidopsis thaliana transcriptome analyzed using whole-genome tiling arrays. Plant J 58: 1068-1082

Zhao X, Xu M, Wei R, Liu Y (2015) Expression of OsCAS (Calcium-Sensing Receptor) in an Arabidopsis Mutant Increases Drought Tolerance. PLoS One 10: e0131272

Zhu X, Feng Y, Liang G, Liu N, Zhu JK (2013) Aequorin-based luminescence imaging reveals stimulus- and tissue-specific Ca2+ dynamics in Arabidopsis plants. Mol Plant 6: 444-455

Zonia L, Munnik T (2007) Life under pressure: hydrostatic pressure in cell growth and function. Trends in Plant Science 12: 90-97

Zwiewka M, Nodzyński T, Robert S, Vanneste S, Friml J (2015) Osmotic Stress Modulates the Balance between Exocytosis and Clathrin-Mediated Endocytosis in Arabidopsis thaliana. Mol Plant 8(8):1175-87

Part 2:

RESULTS

Chapter 3

ETHYLENE RESPONSE FACTOR6 ACTS AS A CENTRAL REGULATOR OF LEAF GROWTH UNDER OSMOTIC STRESS CONDITIONS IN ARABIDOPSIS

Marieke Dubois [a,b,*], Aleksandra Skirycz [a,b,*], Hannes Claeys [a,b], Katrien Maleux [a,b], Stijn Dhondt [a,b], Stefanie De Bodt [a,b], Robin Vanden Bossche [a,b], Liesbeth De Milde [a,b], Takeshi Yoshizumi [c], Minami Matsui [c], and Dirk Inzé [a,b]

[a] Department of Plant Systems Biology, VIB, Ghent, Belgium
[b] Department of Plant Biotechnology and Bioinformatics, Ghent University, Belgium
[c] RIKEN Plant Science Center, Tsurumi-ku, Yokohama, Kanagawa 230–0045, Japan
[*] These authors contributed equally to the work.

This chapter is based on a research article published in:
Plant Physiology, 2013, 162(1): 319–332

Contributions: M.D. designed and performed most experiments, and was the main author of the manuscript. A.S. and D.I. supervised the project and contributed to the writing of the manuscript. H.C. performed the experiments shown in Figure S6, was involved in the discussions throughout the project and contributed to the writing of the manuscript. K.M., R.V.B. and L.D.M. provided technical assistance. S.D. developed the automated platform for phenotyping and analyzed the data. S.D.B. performed the statistical analysis of the micro-array data. T.Y. and M.M. provided plant material.

Leaf growth is a complex developmental process that is continuously fine-tuned by the environment. Various abiotic stresses, including mild osmotic stress, have been shown to inhibit leaf growth in Arabidopsis (*Arabidopsis thaliana*), but the underlying mechanisms remain largely unknown. Here, we identify the redundant Arabidopsis transcription factors ETHYLENE RESPONSE FACTOR5 (ERF5) and ERF6 as master regulators that adapt leaf growth to environmental changes. *ERF5* and *ERF6* expression is induced very rapidly and specifically in actively growing leaves after sudden exposure to osmotic stress. Subsequently, enhanced *ERF6* expression inhibits cell proliferation and leaf growth by a process involving gibberellin and DELLA signaling. Using an inducible ERF6-overexpression line, we demonstrate that the gibberellin-degrading enzyme GIBBERELLIN 2-OXIDASE6 is transcriptionally induced by ERF6 and that, consequently, DELLA proteins are stabilized. As a result, ERF6 gain-of-function lines are dwarfed and hypersensitive to osmotic stress, while the growth of *erf5erf6* loss-of-function mutants is less affected by stress. Besides its role in plant growth under stress, ERF6 also activates the expression of a plethora of osmotic stress-responsive genes, including the well-known stress tolerance genes *STZ*, *MYB51*, and *WRKY33*. Interestingly, activation of the stress tolerance genes by ERF6 occurs independently from the ERF6-mediated growth inhibition. Together, these data fit into a leaf growth regulatory model in which ERF5 and ERF6 form a missing link between the previously observed stress-induced 1-aminocyclopropane-1-carboxylic acid accumulation and DELLA-mediated cell cycle exit and execute a dual role by regulating both stress tolerance and growth inhibition.

INTRODUCTION

Drought stress is one of the most destructive environmental cues that affect plant growth and crop productivity (Boyer, 1982; Yang et al., 2010). In response to water deprivation, leaf growth is shut down by a fast and active mechanism initiated in order to save energy, as the duration and extent of the stress are unknown (Skirycz and Inzé, 2010; Skirycz et al., 2011a). This growth inhibition upon stress, however, is expected to cause yield losses that are unnecessary when the stress only lasts for short periods or when the stress is too mild to threaten the plant's survival.

The molecular processes by which mature plant organs respond to water shortage are extensively documented and are characterized by increasing abscisic acid levels activating stress-avoidance mechanisms (Xiong et al., 2002; Verslues et al., 2006; Seki et al., 2007; Schachtman and Goodger, 2008). However, the mechanisms by which stress

affects actively growing plant organs are largely unknown. Although there have been many reports of transgenic Arabidopsis (*Arabidopsis thaliana*) lines with enhanced survival after severe water stress, an analysis of 27 of these showed no improved growth under milder, nonlethal drought conditions (Skirycz et al., 2011b). Thus, tolerance to severe drought stress and the ability of plants to continue to grow under mild stress conditions are very different traits mediated by different molecular processes. Furthermore, recent studies pointed out the importance of analyzing stress responses at the organ or tissue level, as the responses to stress both at the transcriptional level (Harb et al., 2010; Skirycz et al., 2010) and at the protein level (Baerenfaller et al., 2012) are much dependent on organ developmental stage or even on cell type identity (Dinneny et al., 2008).

In Arabidopsis, leaf development consists of three major phases during which cell proliferation, driving the growth of very young leaves, gradually switches toward cell expansion. The transition between cell proliferation and cell expansion occurs gradually, from leaf tip to leaf base, and is generally paired with a switch from the mitotic cell cycle to endoreduplication (Donnelly et al., 1999; Vlieghe et al., 2005; Anastasiou and Lenhard, 2007; Andriankaja et al., 2012; Gonzalez et al., 2012). In plants undergoing mild osmotic stress, both cell proliferation and cell expansion are affected, and as a result, leaves have fewer and smaller cells (Skirycz et al., 2010; Tardieu et al., 2011). Proliferating leaves were shown to be affected in a two-step process, previously denominated the "pause-and-stop" mechanism (Skirycz et al., 2011a). In Arabidopsis, when stress occurs during early leaf development (leaves approximately 0.1 mm^2 in size), cell cycle progression is first arrested in a reversible manner by posttranslational inhibition of CYCLIN-DEPENDENT KINASE A (CDKA) activity. Only later, if the stress persists, the cell cycle pause will be converted into a definitive cell cycle exit. Cells then enter cell expansion, which is accompanied by the well-documented activation of endoreduplication and an increased DNA copy number. The exit out of the cell cycle was previously shown to be dependent on GA and DELLAs (Achard et al., 2009; Claeys et al., 2012).

In the first phase of a mild osmotic stress response in growing leaves ("pause"), we previously observed an early stress-induced increase in 1-aminocyclopropane-1-carboxylic acid (ACC) levels. ACC is the direct precursor of ethylene, a gaseous plant hormone that previously has been implicated in regulating, either positively or negatively, growth upon stress treatments. For example, ethylene was shown to either stimulate or inhibit primary root growth under low phosphate availability or under deficiency of other nutrients, respectively (Ma et al., 2003; Pierik et al., 2007). Shoot growth was shown to be positively regulated by ethylene during flooding as well as during shade avoidance, the latter as a result of increased cell expansion (Bailey-Serres

and Voesenek, 2008; Jackson, 2008; Pierik et al., 2011). On the other hand, using mutants in the ethylene signaling pathway, ethylene was reported to confer growth inhibition. The *ctr1* mutant, in which the ethylene signaling pathway is constitutively active, has a dwarf phenotype due to a reduction of both cell size and cell number (Roman et al., 1995; Kieber, 1997). Moreover, ethylene-insensitive mutants are generally reported to be larger than wild-type plants (Roman et al., 1995). Consistently, overexpression of the ethylene receptors increases rosette size (Cao et al., 2006, 2007; Wuriyanghan et al., 2009). Together, these seemingly contradictory observations can be explained by a biphasic model (Pierik et al., 2006), presenting ethylene as a growth-stimulating hormone until an optimal concentration is reached, after which ethylene inhibits growth. This optimum varies according to environmental signals, internal signals, and species-dependent factors.

Here, we identify a transcription factor, ETHYLENE RESPONSE FACTOR 6, as being a central regulator of leaf growth inhibition upon mild osmotic stress. ERF6, and its close homolog ERF5 belong to the class of APETALA2 (AP2)/ERF transcription factors (Fujimoto et al., 2000; Nakano et al., 2006) and are situated downstream of the ethylene signaling cascade, where they regulate ethylene-responsive genes (Yoo et al., 2009). Recently, these two transcription factors were shown to be able to interact with each other at the protein level, although further investigations are necessary to confirm an *in planta* interaction (Son et al., 2012). Although ERF5 and ERF6 have not yet been extensively characterized, they recently have been described as being important regulators of biotic stress defense (Moffat et al., 2012; Son et al., 2012). Besides its function in response to biotic stress, ERF6 was recently shown to control the expression of reactive oxygen species-responsive genes after activation by MPK3/MPK6 (Wang et al., 2013).

In this study, we focus on one of these ERFs, ERF6, demonstrating that it affects cell cycle exit by triggering the expression of the *GA2-OXIDASE6 (OX6)* gene and consequently the inactivation of GAs. Thus, ERF6 provides a link between ACC and DELLA signaling in the cell cycle pause-and-stop model, improving our understanding of growth inhibition in the proliferating leaf primordia of plants subjected to water limitation. In addition, ERF6 regulates, in a GA- and DELLA-independent manner, the expression of multiple genes associated with abiotic and biotic stress conditions, such as genes encoding the transcription factors WRKY33, MYB51, and STZ (for salt tolerance zinc finger). Thus, ERF6 plays a dual role under stress, as it activates both stress tolerance and growth inhibition, and importantly, these two roles occur independently from each other.

RESULTS

ERF5 and ERF6 are transcriptionally induced in actively growing leaves within 1 h of stress exposure

We recently investigated the effects of mild osmotic stress on the transcriptome of very young, small (approximately 0.1 mm^2 in size), and thus still actively growing leaves (Skirycz et al., 2010, 2011a). Among the more than 1,500 genes differentially expressed following exposure to mild osmotic stress, the transcription factors *ERF5* (AT5G47230) and *ERF6* (AT4G17490) were induced very early after stress onset, already 1 h after stress exposure specifically in actively growing leaves, and their induction was further maintained over time (Supplemental Figure S1A). Furthermore, analysis of publicly available transcriptome data revealed that *ERF5* and *ERF6* are induced by several other, often severe abiotic stresses, including drought (Supplemental Figure S1B; Hruz et al., 2008). These data prompted us to investigate the role of ERF5 and ERF6 in integrating environmental signals into leaf growth regulation.

Within the large class of more than 120 AP2/ERF transcription factors, ERF5 and ERF6 belong to group IXb, a small group of transcriptional activators containing several other stress-responsive ERFs, such as ERF1 and ERF2 (Supplemental Figure S2; Nakano et al., 2006; Skirycz et al., 2010). ERF5 and ERF6 share 51% amino acid similarity, with high conservation of three functional domains: CMIX-2, CMIX-5, and the AP2/ERF domain (Thompson et al., 1994).

erf5erf6 loss-of-function mutants grow better under osmotic stress

To investigate the importance of ERF5 and ERF6 in leaf growth under various conditions, we used single and double mutants. Single *erf5* and *erf6* mutants were obtained from the SALK collection and have transfer DNA insertions in the 3′ untranslated region and coding sequence, respectively (Supplemental Figure S3A; Alonso et al., 2003; Wang et al., 2013). The *ERF5* and *ERF6* expression levels were strongly decreased both under normal and osmotic stress conditions (Supplemental Figure S3B). The *erf5* and *erf6* single mutants had no obvious growth phenotype, most likely because of functional redundancy; thus, the *erf5erf6* double mutant was used for further analysis.

First, we explored how *erf5erf6* plants behave under standard conditions and when exposed to various long-term abiotic stress conditions. As we were interested in measuring growth dynamics in response to stress instead of limiting our analysis to

end-point measurements, we chose to grow the *erf5erf6* mutant and the wild-type line on an automated phenotyping platform named the In Vitro Growth Imaging System (IGIS; see "Materials and Methods"). The IGIS platform allows for a continuous measurement of projected rosette area of *in vitro*-grown Arabidopsis plants by taking photographs every hour from germination onward until 20 d after stratification (DAS) and extracting the projected rosette area. The *erf5erf6* mutant and the wild type were exposed to different mild abiotic stresses: osmotic stress (25 mM mannitol, mimicking mild drought stress; Skirycz et al., 2011a), oxidative stress (1.5 mM hydrogen peroxide), and salt stress (50 mM NaCl). Interestingly, growth curves representing projected rosette area over time (Figure 3.1A) demonstrate that under standard conditions on the IGIS system, the *erf5erf6* mutant tends to grow faster than the wild type. At the end point (20 DAS), *erf5erf6* was 13% larger (Supplemental Table S1). When grown on osmotic stress from germination onward, *erf5erf6* mutants tolerated the stress better than wild-type plants. The *erf5erf6* mutants were less affected by the stress-induced growth inhibition and showed an increase in final projected rosette area of 33% compared with wild-type plants exposed to this stress (Supplemental Table S1). Importantly, the same tendency was observed for *erf5erf6* plants exposed to long-term oxidative stress and was consistent in two out of the three experiments. However, the long-term hydrogen peroxide treatment introduced significant variability between the experiments, making them poorly reproducible and thus rather difficult to interpret (details per experiment are provided in Supplemental Table S1). Finally, when exposed to long-term mild salt stress (50 mM NaCl), the *erf5erf6* plants were not larger than wild-type plants, suggesting that both transcription factors have no role in tolerance to salt stress. This hypothesis is further supported by the observation that exposure of plants to 50 mM NaCl does not induce *ERF5* and *ERF6* expression in very young, small proliferating leaves (Supplemental Figure S4). Together, these data show that ERF5 and ERF6 are central regulators that orchestrate leaf growth under long-term mild osmotic and possibly oxidative stress conditions but not under salt stress.

Next we investigated the growth of *erf5erf6* when exposed to a short-term mild osmotic stress (25 mM mannitol). Briefly, the assay consists of growing plants on a nylon mesh covering control Murashige and Skoog (MS) medium until the third leaf has completely emerged from the shoot apical meristem but is still in a fully proliferative stage, at 9 DAS. At this time point, the mesh is transferred to MS medium containing 25 mM mannitol, and the effect of the stress is analyzed daily by measuring the growth of the third leaf. As previously shown, wild-type plants exposed to 25 mM mannitol show a reduction of leaf area of about 50%, caused by a reduction of both cell number and cell size (Skirycz et al., 2010, 2011a; Figure 3.1B). Importantly, the growth of *erf5erf6* was significantly ($P = 0.0004$) less affected than that of the wild type (Figure 3.1B): on average, wild-type plants showed a 42% leaf size reduction, while the leaf size of

erf5erf6 was only decreased by 11% (Supplemental Table S2, C and D). As a consequence, third leaves harvested at 19 DAS from *erf5erf6* plants exposed to stress are 59% larger in comparison with those of wild-type plants exposed to stress (P = 0.025). Thus, the third leaf of *erf5erf6* plants exposed to short-term mild osmotic stress continued to grow almost indistinguishably from that of wild-type plants grown on standard medium. Interestingly, this reduced leaf growth inhibition is already visible at 12 DAS (Figure 3.1B), suggesting that ERF5 and ERF6 act early in leaf development.

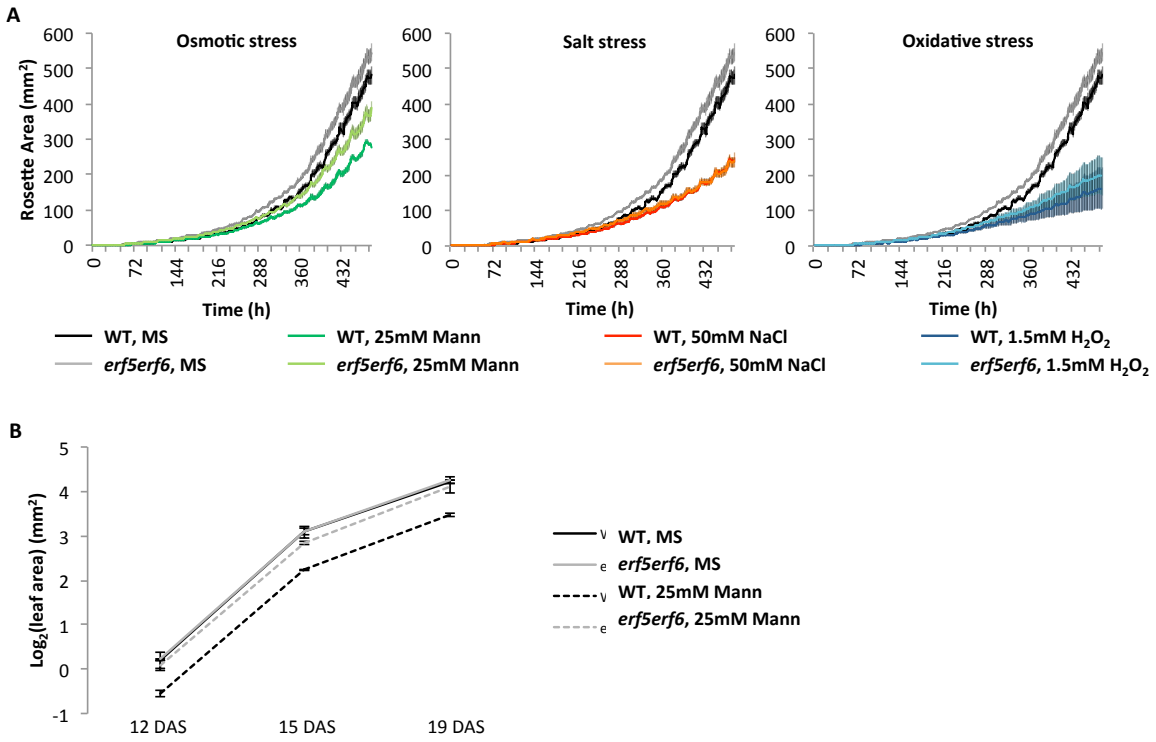

Figure 3.1. The *erf5erf6* double mutant is more tolerant to mild osmotic stress conditions. (A) Rosette area over time of wild-type plants (WT) and *erf5erf6* double mutants under standard MS medium and different stress conditions. The *erf5erf6* mutant shows significant tolerance to osmotic stress (MS medium supplemented with 25 mM mannitol) only. Colored shadows indicate standard error. Three biological repeats were performed with at least 12 seedlings per line per treatment. (B) Leaf area measurements (third leaf) of the *erf5erf6* mutant and the wild type upon transfer at 9 DAS to standard or mild osmotic stress conditions. On osmotic stress, the *erf5erf6* mutant is always about 50% larger than the wild type (for detailed measurements, see Supplemental Table S2). Error bars indicate standard error. Three biological repeats were performed with 16 leaves per repeat.

ERF6 represses leaf growth by inhibiting cell division and cell expansion

To investigate the cellular basis of ERF6-mediated growth inhibition, inducible gain-of-function ERF6 lines were analyzed. To this end, the ERF6 sequence was C-terminally fused to that of a glucocorticoid receptor (GR) domain and expressed in transgenic plants under the control of the cauliflower mosaic virus 35S promoter (p35S). This chimeric ERF6-GR protein is expected to stay in the cytoplasm, but after addition of the steroid hormone dexamethasone (DEX), it undergoes conformational changes and migrates to the nucleus, where it becomes functional as a transcription factor (Corrado and Karali, 2009). Two glucocorticoid-inducible overexpression (IOE) lines were used for further analysis: a strong ERF6-overexpressing line referred to as ERF6^{IOE}-S (fold change = 7,000 as compared with the p35S-GFP-GR line, measured in young seedlings) and a weaker line denominated ERF6^{IOE}-W (fold change = 220). As a control, a DEX-inducible 35S::GFP-GR (GFP:IOE) line was used. To examine the effect of *ERF6* overexpression specifically on actively growing leaves, plants were grown on a nylon mesh overlaying MS medium and transferred to medium containing 5 µm DEX at 9 DAS, when the third leaf is fully proliferating. ERF6 activation from 9 DAS onward drastically reduced the growth of this leaf: at 16 DAS, leaf area reductions of 83% and 55% were measured for ERF6^{IOE}-S and ERF6^{IOE}-W, respectively, and significant reductions were already observed 48 and 72 h after DEX treatment of ERF6^{IOE}-S and ERF6^{IOE}-W, respectively (Figure 3.2A). At the cellular level, the severe growth reduction of ERF6^{IOE}-S at 16 DAS was caused by both smaller (57%) and fewer (59%) leaf cells (Supplemental Figure S5). As expected, this cellular phenotype was less pronounced in the weaker ERF6^{IOE}-W line, in which mainly cell area was affected (Supplemental Figure S5). Flow cytometry showed an increase in endoreduplication upon strong *ERF6* overexpression, suggesting that ERF6 pushes cells from mitosis into endoreduplication and differentiation (Supplemental Figure S6). When left on DEX for longer times (until 22 DAS), ERF6-overexpressing plants remained dwarfed and dark green, with stunted rosettes (Figure 3.2B). Similar phenotypes were observed for soil-grown plants sprayed daily with a 5 µm DEX solution from 9 DAS onward (Figure 3.2B). Taken together, these data show that *ERF6* expression levels inversely correlate with leaf growth.

To further investigate the role of ERF6 in stress-mediated growth inhibition, we exposed the ERF6^{IOE}-W line to short-term osmotic stress. We only used the ERF6^{IOE}-W line, as the ERF6^{IOE}-S line shows a very severe phenotype making the accurate measurement of subtle growth changes rather difficult. The ERF6^{IOE}-W line was grown on MS medium until 9 DAS and then transferred to medium with or without 25 mM mannitol, in combination with or without DEX. In the presence of DEX, the ERF6^{IOE}-W line was found to be hypersensitive to osmotic stress as compared with the wild type (Figure 3.2C). When first germinated on MS medium and then transferred to

either DEX or mannitol, ERF6^{IOE}-W plants showed a reduction in growth but were still able to develop normally. However, when transferred to mannitol + DEX, the plants failed to develop correctly and were extremely dwarfed. Together, our data confirm that ERF6 plays an important role in modulating leaf growth under stress.

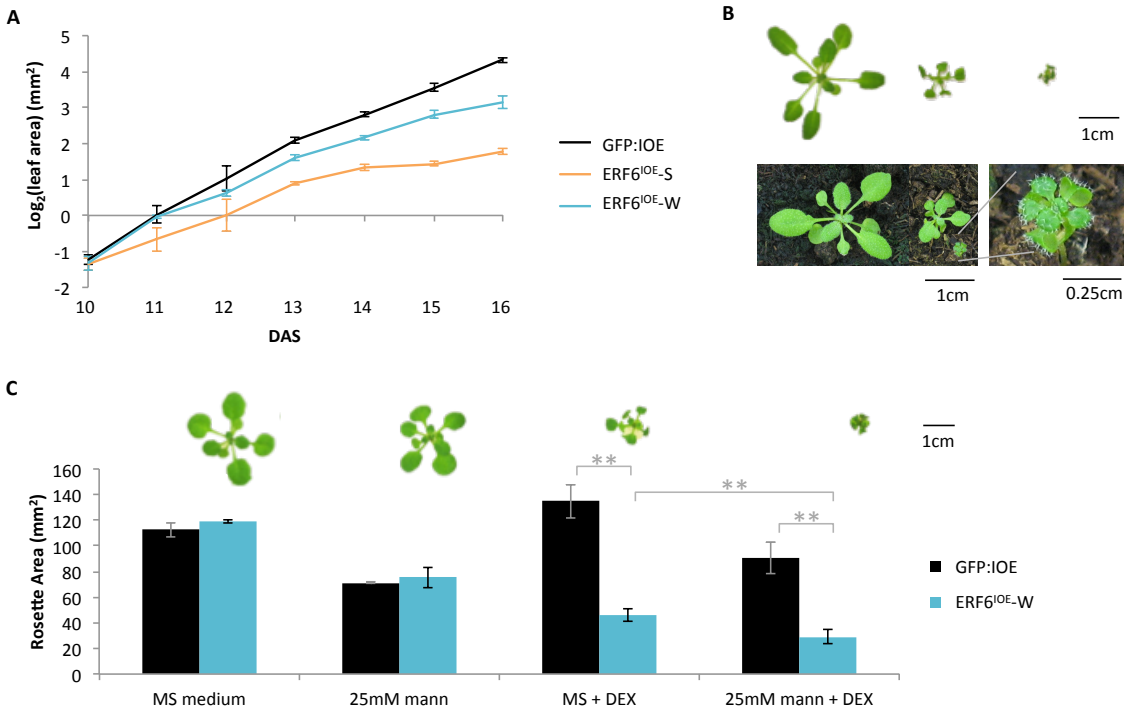

Figure 3.2. ERF6 negatively regulate leaf growth. (A) Growth measurements of the third leaf of inducible *ERF6* overexpression plants transferred to DEX at 9 DAS to induce *ERF6* overexpression. Leaf size becomes significantly smaller than that of the control at 11 DAS for ERF6^{IOE}-S and at 12 DAS for ERF6^{IOE}-W. (B) Rosettes of *ERF6*-overexpressing plants *in vitro* (growth medium supplied with DEX; top panel) and in soil (plants sprayed daily with DEX; bottom panel). From left to right: GFP:IOE control line, ERF6^{IOE}-W, and ERF6^{IOE}-S. Plants are 22 d old. (C) Nineteen-day-old rosettes of ERF6^{IOE}-W lines upon *ERF6* overexpression with DEX at 9 DAS, exposure to osmotic stress (25 mM mannitol), or the combination of mannitol and DEX. ***P* < 0.01. For (A) and (C), error bars indicate standard error of three repeats with 16 plants per repeat.

ERF6 inhibits growth through a GA/DELLA-dependent mechanism

To elucidate how ERF6 reduces leaf growth, we performed a genome-wide analysis of genes rapidly induced by the activation of *ERF6* overexpression. To this end, 9-d-old ERF6^{IOE}-S plants were transferred for 4 h to DEX, and subsequently, third leaf primordia (which are then smaller than 0.1 mm^2 in size) were microdissected and subjected to AGRONOMICS1 tiling arrays (Rehrauer et al., 2010). Already 4 h after DEX treatment, 344 genes were differentially expressed (false discovery rate-corrected $P < 0.05$), of which 332 were induced (Supplemental Table S3), suggesting that ERF6 acts as an activator of gene expression. Gene Ontology annotation analysis of the 332 up-regulated genes using BiNGO (Maere et al., 2005) revealed that the putative ERF6 targets are highly enriched in several stress-related and biological signaling process categories, such as "response to water stress," "response to chemical stimulus," "response to biotic stimulus," and "response to ethylene" (Supplemental Figure S7), again strongly suggesting a role for ERF6 in early stress response. Importantly, when comparing the putative ERF6 target genes with the previously identified list of genes specifically induced in leaf initials within 3 h of exposure to osmotic stress (Skirycz et al., 2011a), we observed a highly significant overlap (19 times higher than expected by chance; Figure 3.3). Out of the 332 putative ERF6 targets, 55 were found to be induced within 3 h of mannitol treatment (Supplemental Table S4). Interestingly, 14 of the 27 genes induced after 1.5 h of mannitol treatment are differentially expressed upon ERF6 induction (62 times more than expected by chance), again underlining the central role for ERF6 in early stress response. An additional 56 ERF6-induced genes are also found to be induced 12 and 24 h following mannitol treatment in proliferating leaves.

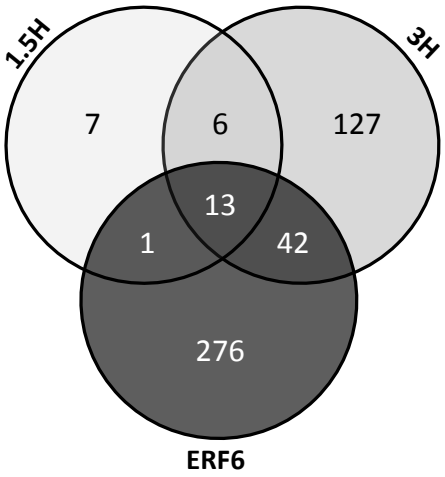

Figure 3.3. Overlap between ERF6 targets and genes rapidly induced by 25 mM mannitol. Comparison was performed of the 332 putative ERF6 targets with the previously identified list of genes specifically induced in leaf initials within hours upon exposure to osmotic stress (Skirycz et al., 2011a). Values indicated in the Venn diagram represent the number of genes induced upon 1.5- and 3-h mannitol treatment and the genes induced in leaf initials 4 h following DEX application in ERF6^{IOE}-S.

Genes that are rapidly induced by DEX-mediated activation of ERF6 are putative target genes. One of these genes, *GA2-OX6*, encoding an oxidase involved in GA inactivation, deserves particular attention because the ERF6^{IOE} dwarf phenotype phenocopies that of plants insensitive to GAs (Peng et al., 1997; Thomas and Sun, 2004). Moreover, from our previously established list of osmotic stress-responsive genes (Skirycz et al., 2011a), we observed that *GA2-OX6* is the only GA2-oxidase activated by mild osmotic stress (Supplemental Figure S8). We subsequently tested whether the ERF6-mediated activation of *GA2-OX6* expression could explain the growth retardation caused by ERF6 activation. Time-course quantitative PCR analysis confirmed the induction of *GA2-OX6* expression within 2 h after the activation of strong *ERF6* overexpression (Figure 3.4A). Consistently, there is a correlation between the timing and level of *GA2-OX6* induction and the observed growth inhibition, as seen in the ERF6^{IOE}-W line, where upon DEX treatment the growth is less affected and the *GA2-OX6* induction by ERF6 is slower and less pronounced (Supplemental Figure S9). Importantly, in the *erf5erf6* mutant, the growth of which is less affected by osmotic stress, the induction of *GA2-OX6* following stress exposure is delayed (Supplemental Figure S10).

Our data support a model in which ERF6 is able to activate *GA2-OX6* expression, triggering GA breakdown and consequently stabilizing DELLA proteins, which are known to negatively affect growth. To further confirm this model, we investigated whether DELLAs were stabilized after ERF6 activation by crossing the ERF6^{IOE} lines with a GFP-tagged DELLA reporter line (pRGA::GFP-RGA; Silverstone et al., 2001). Stabilization of RGA, the major DELLA expressed in developing leaves (Dill et al., 2001), following ERF6 activation can be followed by measuring GFP protein levels. Western-blot analysis using a primary antibody against GFP demonstrated the stabilization of RGA between 12 and 24 h after ERF6 activation (Figure 3.4B). Finally, to confirm the involvement of GA in the ERF6-mediated growth arrest, we tested whether the growth inhibition activated by ERF6 could be abolished by crossing the ERF6^{IOE}-W line with a transgenic line overexpressing the rate-limiting GA biosynthetic enzyme GA20-OXIDASE1 (35S::GA20-OX1; Coles et al., 1999; Gonzalez et al., 2010). When grown on DEX, the resulting plants (ERF6^{IOE}-W × 35S::GA20-OX1), in contrast to ERF6^{IOE}-W plants, did not show any growth retardation (Figure 3.4C), and the final size (at 21 DAS) of the third leaf was similar to that of control GFP:IOE plants (Figure 3.4D). A similar, albeit more partial, restoration of growth was obtained for ERF6^{IOE}-S × 35S::GA20-OX1 plants (Figure 3.4C). Together, these data confirm that, under osmotic stress, ERF6 induces the expression of the gene encoding the GA-inactivating enzyme GA2-OX6, thereby reducing the bioactive GA levels and stabilizing the DELLA proteins.

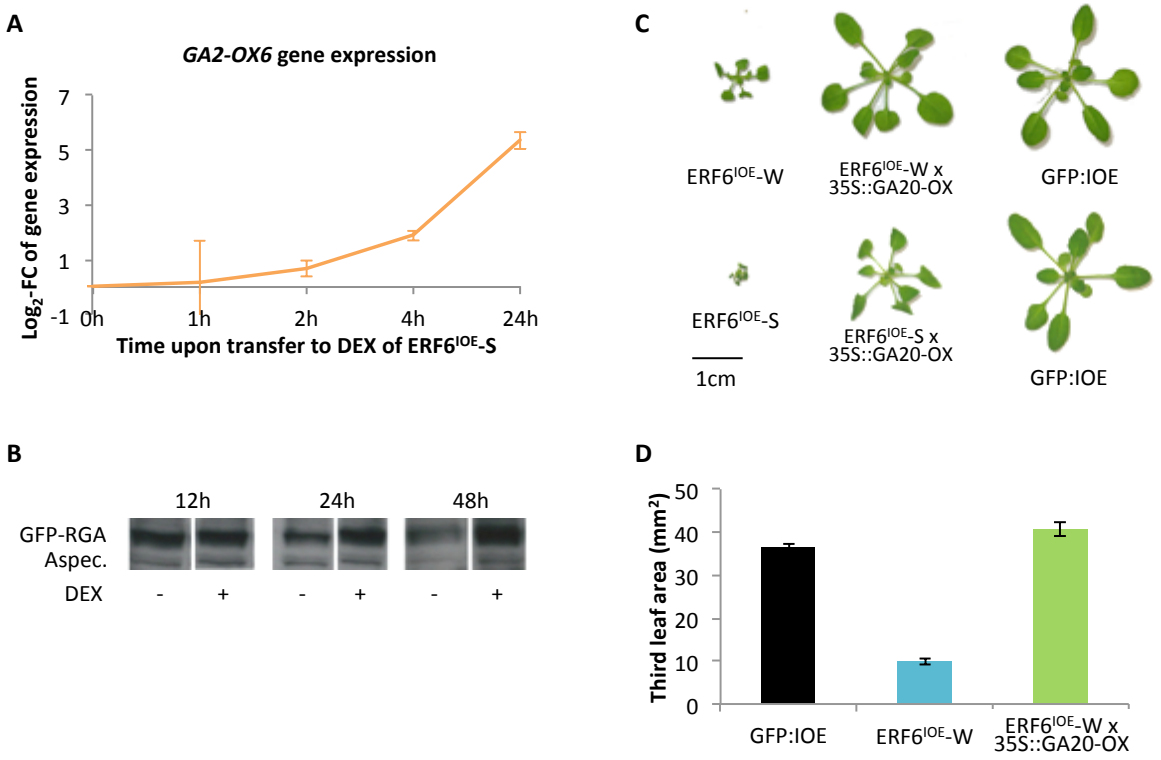

Figure 3.4. ERF6 affects the GA/DELLA pathway through transcriptional control of the *GA2-OX6* gene. (A) Induction of *GA2-OX6* following the activation of *ERF6* overexpression. Two hours after transfer to DEX of ERF6^{IOE}-S, *GA2-OX6* is significantly induced. Expression was measured in proliferating third leaves, and values are normalized to their expression in the GFP:IOE control line exposed to the same treatment. Error bars indicate standard error of three repeats with 64 young third leaves per repeat. (B) Stabilization of the DELLA protein RGA upon the activation of *ERF6* overexpression shown by western blot, targeting the GFP domain of the RGA-GFP fusion protein in pRGA::GFP-RGA × ERF6^{IOE}-S seedlings. DELLA stabilization first clearly appears 24 h after ERF6 activation. Three biological replicates were performed. (C) Growth complementation assay. By crossing the two independent ERF6:IOE lines with a 35S::GA*20-OX* line (ectopic GA overproduction), the dwarfed phenotype could be partially and fully complemented in ERF6^{IOE}-S and ERF6^{IOE}-W lines, respectively. Treatment with DEX was applied at 9 DAS, and photographs were taken at 21 DAS. (D) Measurements of third leaves at 21 DAS of GFP:IOE, ERF6^{IOE}-W, and ERF6^{IOE}-W × 35S::GA*20-OX* upon treatment with DEX at 9 DAS. Error bars indicate standard error of three repeats with 12 leaves per repeat.

ERF6 activates a plethora of stress-responsive genes

We subsequently further explored the ERF6 regulon of 332 putative target genes, which is enriched for stress-responsive genes, suggesting that ERF6 plays a role in orchestrating, besides growth, also early stress-induced gene expression. Multiple genes encoding stress-related transcription factors were identified within the overlap of putative ERF6 target genes and genes transcriptionally induced within 24 h after osmotic stress exposure (Skirycz et al., 2011a). To further uncover the link between ERF6 and this stress-related transcription factor network, we chose three

representative genes, *STZ*, *WRKY33*, and *MYB51*, as these were previously shown to have a role in biotic and abiotic stress signaling (Sakamoto et al., 2000, 2004; Gigolashvili et al., 2007; Jiang and Deyholos, 2009; Birkenbihl et al., 2012; Li et al., 2012; Niu et al., 2012). Additional quantitative PCR analysis confirmed the induction of these genes within 2 h after DEX-mediated ERF6 activation using the ERF6^{IOE}-S (Figure 3.5A) and ERF6^{IOE}-W (Supplemental Figure S9) transgenic lines, thereby rendering them primary candidates for being direct ERF6 targets. This is supported using a protoplast activation assay with promoter-luciferase reporter constructs (pSTZ:fLUC, pWRKY33:fLUC, and pMYB51:fLUC), in which the respective promoters were cloned upstream of the fLUC gene (encoding the firefly luciferase enzyme) and expressed together with a 35S-ERF6 or 35S-ERF5 construct in tobacco (*Nicotiana tabacum*) Bright Yellow-2 (BY-2) protoplasts. Binding of ERF6 or ERF5 to the promoter of interest triggers the expression of the fLUC gene and the production of the luciferase enzyme. A significant increase in luciferase activity shows the activation of pSTZ, pWRKY33, and pMYB51 by both ERF5 and ERF6 (Figure 3.5B). In summary, these data strongly suggest that ERF5 and ERF6 directly activate the expression of the stress-related transcription factor genes *STZ*, *WRKY33*, and *MYB51*.

Finally, we investigated whether the two functions of ERF6, being on the one hand leaf growth regulation and on the other hand the activation of a stress defense transcriptional cascade, are interdependent. For this purpose, we used the ERF6^{IOE}-W × 35S::GA20-OX1 and ERF6^{IOE}-S × 35S::GA20-OX1 lines, in which the growth inhibition is entirely and partially abolished, respectively. Importantly, when *ERF6* overexpression was activated at 9 DAS by DEX treatment for 8 h, the stress defense transcriptional cascade (represented here by the expression of *STZ*, *WRKY33*, and *MYB51*) was still activated at least as highly as in the positive control lines (Figure 3.5C). The expression of *STZ* and *WRKY33* was even considerably higher in the ERF6^{IOE}-W × 35S::GA20-OX1 plants (without growth reduction) as compared with that in ERF6^{IOE}-W × 35S::GFP^{IOE} plants. Thus, although the growth inhibition by ERF6 was suppressed, the stress-related transcription network was still active. These results are of significant importance, as they demonstrate that growth reduction caused by mild stress can be uncoupled from the stress defense response.

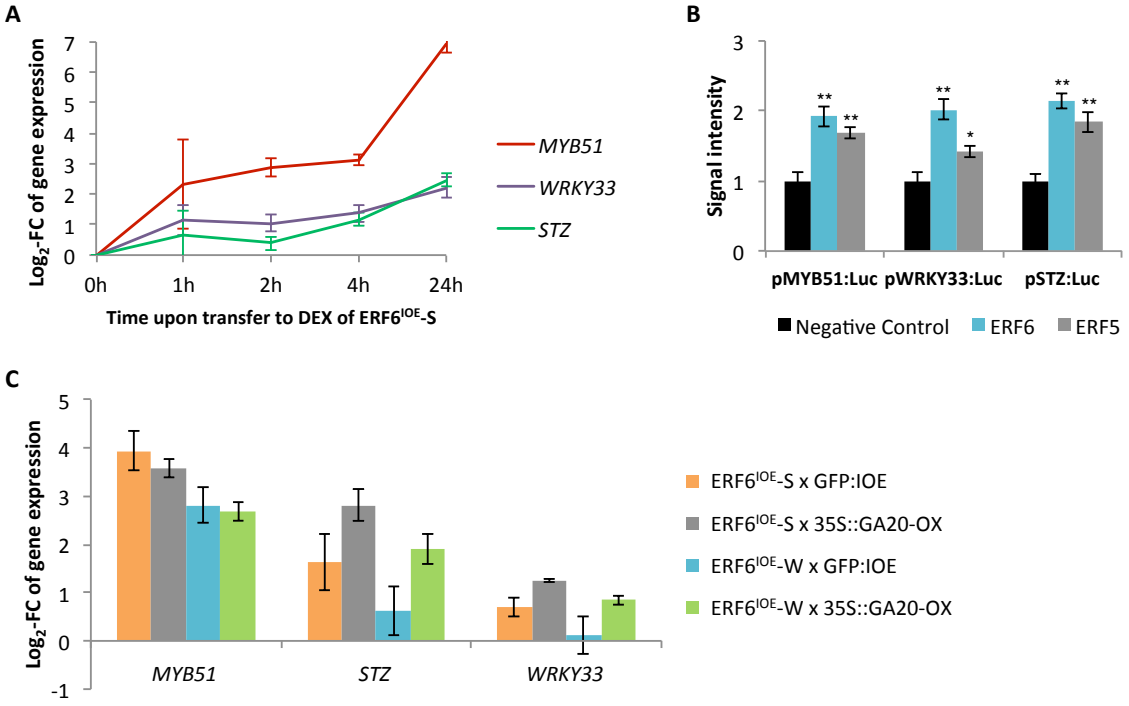

Figure 3.5. ERF6 regulates the stress-related transcription factors *STZ*, *MYB51*, and *WRKY33*. (A) Induction of *STZ*, *MYB51*, and *WRKY33* following the activation of *ERF6* overexpression. Within 2 h of the transfer of ERF6^{IOE}-S to DEX, *STZ*, *WRKY33*, and *MYB51* are significantly induced. Expression was measured in proliferating third leaves, and values are normalized to their expression in the GFP:IOE control line exposed to the same treatment. Error bars indicate standard error of three repeats with 64 young third leaves per repeat. (B) ERF5/ERF6-dependent activation of the promoters of *MYB51*, *WRKY33*, and *STZ* by protoplast activation assay. Indicated values are luciferine detection levels normalized to the negative control. Asterisks indicate significantly different values from the control at the 1% (**) and 5% (*) significance levels. Error bars indicate standard, and eight biological repeats were performed. (C) Induction of *STZ*, *MYB51*, and *WRKY33* expression 8 h after the activation of *ERF6* overexpression in ERF6^{IOE} × 35S::GA20-OX plants. Although the dwarfed growth phenotype is partially and completely rescued in ERF6^{IOE}-S × 35S::GA20-OX and ERF6^{IOE}-W × 35S::GA20-OX plants, respectively (Figure 3.4B), the stress-related transcription factors are still induced to the same extent as in the positive control lines (ERF6^{IOE}-S × GFP:IOE and ERF6^{IOE}-W × GFP:IOE, respectively). Expression values are normalized to their expression in the control line (GFP:IOE). Error bars indicate se of three repeats with 64 young third leaves per repeat.

DISCUSSION

ERFs are rapidly induced by osmotic stress

Osmotic stress was previously demonstrated to induce the expression of a large number of genes in actively growing leaves (more than 1,500 genes). Within 1.5 and 3 h of stress exposure, only a small number (27 and 193, respectively) were rapidly induced (Skirycz et al., 2011a). This suggests that stress signaling occurs through cascades in which, in a

simplified view, a few rapidly activated transcription factors orchestrate other transcription factors, which in turn switch on their own targets. In this context, ERF5 and ERF6, two transcription factors that are transcriptionally induced within 1 h of osmotic stress, belong to a very confined group of early stress-responsive genes. Intriguingly, the expression of the ERF6 targets (*STZ*, *WRKY33*, and *MYB51*) is induced within 1 h of osmotic stress as well, suggesting that there is yet another mechanism than ERF6 transcription that triggers *STZ*, *WRKY33*, and *MYB51* expression. A possible explanation for the fast induction of *STZ*, *WRKY33*, and *MYB51* could be that *ERF6* is expressed at basal levels under standard conditions (Andriankaja et al., 2012; Wang et al., 2013) and that ERF6 is posttranscriptionally activated by osmotic stress. A similar mechanism was recently shown to occur during oxidative stress, where ERF6 is phosphorylated by two mitogen-activated protein kinases (MPK3 and MPK6; Wang et al., 2013). Both kinases act downstream of ACC and independently of the EIN2 signaling pathway (Yoo and Sheen, 2008), and we have previously demonstrated their presence during very early osmotic stress (Skirycz et al., 2011a). Importantly, MPK3 and MPK6 were recently shown to physically interact with ERF5 and ERF6, and phosphorylation of ERF5 and ERF6 by MPK3 and MPK6 could be demonstrated (Popescu et al., 2009; Son et al., 2012; Wang et al., 2013). The very rapid transcriptional induction of ERF6 following stress exposure results from an autoactivation loop in which phosphorylated ERF6 activates its own expression, independent from induction by the upstream EIN3 and EIL1 transcription factors (Supplemental Figure S11). Therefore, we propose the hypothesis that ERF5 and ERF6, present at the basal level prior to stress exposure, are upon stress treatment rapidly phosphorylated through MPK3 and MPK6 and thereby converted into active transcription factors, able to rapidly regulate their own expression and the expression of *STZ*, *MYB51*, and *WRKY33*.

ERF5 and ERF6 form the connection between ACC accumulation and the GA/DELLA response in leaves subjected to mild osmotic stress

Recently, we have shown that growth inhibition by mild osmotic stress response occurs in two steps: first, a pause step, in which the cell cycle is temporally arrested in an ACC-dependent manner by inhibition of CDKA; and later, if stress is maintained, a stop mechanism, which pushes cells irreversibly out of the cell cycle and into cell differentiation (Skirycz et al., 2011a). The last step was shown to be mediated by DELLAs, driving cells into early endoreduplication and thus mitotic exit (Claeys et al., 2012). However, it was not yet clear how the early ACC accumulation causes DELLA stabilization. Here, we propose that ERF5 and ERF6 form the connection between stress sensing and GA/DELLA signaling (Figure 3.6A). The presence of *GA2-OX6* among the putative ERF6 targets strongly supported this hypothesis. The *GA2-OX6* gene encodes a

GA-inactivating enzyme and its induction thus decreases the levels of bioactive GA, thereby stabilizing the DELLAs (Figure 3.6A). An analysis of various transgenic lines with altered ERF6 levels and exposure of these lines to standard and mild osmotic stress conditions revealed a remarkable correlation between the levels of ERF6 expression and the severity of growth inhibition (Figure 3.6B). ERF6^{IOE}-S seedlings, which are characterized by very strong *ERF6* overexpression, are completely dwarfed. As osmotic stress transcriptionally induces *ERF6* expression and most likely triggers ERF6 activation, it is expected that osmotic stress would aggravate the growth phenotype. This is exactly what was observed for ERF6^{IOE}-W plants, which are smaller but still develop normally. Exposing these weak *ERF6* overexpression plants to mild osmotic stress (ERF6^{IOE}-W + DEX + mannitol) completely abolishes plant growth.

Interestingly, the phenotype of ERF6-overexpressing plants strongly resembles that of the 35S:gai-GR line, in which a mutant GA-insensitive version of the DELLA protein GAI is overexpressed (Claeys et al., 2012). Both lines show the same cellular phenotype in the presence of DEX, with less and smaller epidermal cells. Importantly, the cellular phenotype observed in ERF6-overexpressing plants matches that of the epidermal cells of plants exposed to mild osmotic stress (Skirycz et al., 2010). The reduced cell number, however, could only be obtained by strong *ERF6* overexpression and was not clear after weak *ERF6* overexpression, indicating that ERF6 mainly works on cell expansion and to a lesser extent on cell division, in accordance with how DELLAs inhibit root and probably shoot growth (Achard et al., 2009). Finally, in the ERF6-overexpressing plants, proliferating cells of young leaves are pushed faster into endoreduplication, a process mediated through GA/DELLA signaling that was also observed under osmotic stress (Skirycz et al., 2011a). In conclusion, several lines of evidence show that ERF5 and ERF6 provide a link between ACC accumulation and DELLA signaling in the pause-and-stop model.

The involvement of DELLA and/or ethylene signaling in growth and stress responses is not restricted to osmotic stress. A well-known example is the involvement of C-REPEAT/DROUGHT-RESPONSIVE ELEMENT BINDING FACTOR1 (CBF1) in freezing acclimation and growth inhibition under cold stress, upstream of several GA2-OXIDASES (GA2-OX3, GA2-OX6, and GA2-OX1), thereby causing DELLA accumulation (Achard et al., 2008). Another AP2 transcription factor, DDF1, was shown to play a similar function under salt stress by regulating the expression of the *GA2-OX7* gene (Magome et al., 2008). The data presented here demonstrated an analogous role for ERF6 in regulating growth under mild osmotic and oxidative stress. Moreover, whereas CBF1 acts upstream of several GA2-OXIDASES (GA2-OX3, GA2-OX6, and GA2-OX1), we provide evidence that osmotic stress specifically involves GA2-OX6 (Supplemental Figure S8). Thus, although hormonal interactions between ethylene and GA/DELLA might regulate

general growth mechanisms that are shared between different abiotic cues, the identity of the molecular players involved is highly condition and tissue specific. We speculate that, although these transcription factors all activate, on the one hand, the DELLA-mediated growth inhibition, they each activate, on the other hand, a specific cluster of stress tolerance genes according to the type of stress.

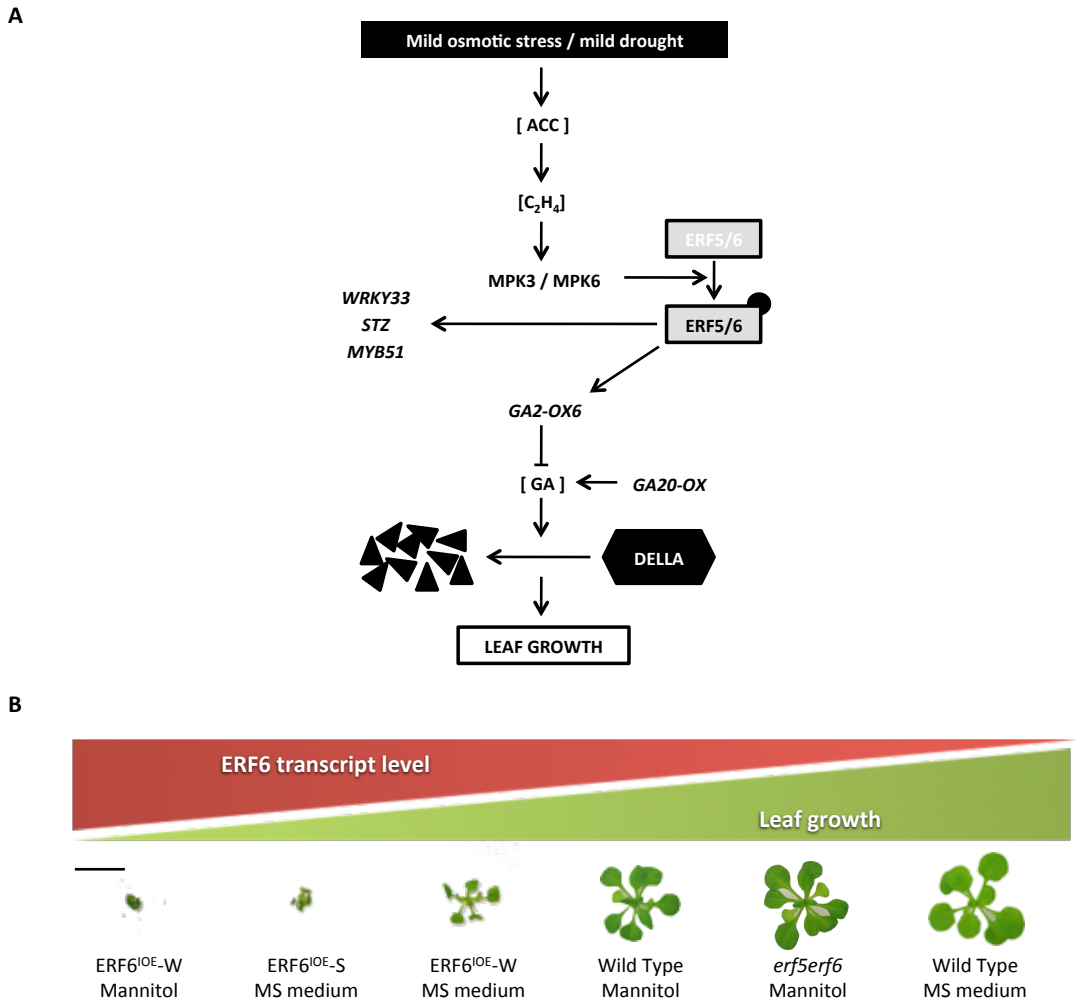

Figure 3.6. How ERF6 regulates leaf growth and stress defense under osmotic stress. (A) Immediately upon exposure to osmotic stress, ACC accumulates in the actively growing leaves, where it is converted to ethylene. Ethylene further activates the signaling pathway involving MPK3 and MPK6. These kinases phosphorylate the basal amount of ERF5 and ERF6 proteins present in the cell prior to stress exposure. The activated ERF5 and ERF6 then execute their dual functions: on the one hand, the activation of the stress defense transcriptional cascade with direct transcriptional activation of *WRKY33*, *STZ*, and *MYB51*, and on the other hand, the activation of leaf growth inhibition. This occurs through the transcriptional activation of the gene encoding the GA-inactivating enzyme GA2-OX6, thereby decreasing the bioactive GA concentration and stabilizing the DELLA proteins. (B) In accordance with the model presented in (A), *ERF6* transcript levels and stress-mediated activity inversely correlate with leaf growth (for discussion, see text). Bar = 1 cm.

ERFs regulate many stress resistance genes in a GA/DELLA-independent way

Genome-wide identification of putative ERF6 target genes provided a list of 332 genes highly enriched for genes involved in stress response and signaling. Among them were the well-known stress-related transcription factors *STZ*, *WRKY33*, and *MYB51*. Cotransfection of protoplasts with a promoter-luciferase reporter and 35S-ERF5 or 35S-ERF6 shows that *STZ*, *WRKY33*, and *MYB51* are most likely direct ERF5 and ERF6 target genes. STZ is a transcriptional repressor activated under severe salt stress to control survival mechanisms (Sakamoto et al., 2000, 2004; Mittler et al., 2006). MYB51 is a homeodomain-like transcription factor known to regulate the biosynthesis of indole-glucosinolates, a class of secondary metabolites involved in defense against herbivores (Gigolashvili et al., 2007). Finally, WRKY33 is a transcriptional activator involved in plant survival under high-salt, cold, and severe osmotic stress (Jiang and Deyholos, 2009). Furthermore, WRKY33 has a role in biotic stress defense, where it regulates the balance between necrotrophic and biotrophic pathogen responses (Lippok et al., 2007; Pandey and Somssich, 2009; Birkenbihl et al., 2012). In another recent study dealing with biotic stress, *WRKY33* also was found downstream of ERF5, but surprisingly, and in contrast to the data presented here, ERF5 overexpression appeared to down-regulate WRKY33 (Son et al., 2012). A possible reason for this discrepancy is that in the latter study, plants constitutively overexpressing *ERF5* were used, possibly activating negative feedback loops suppressing ERF5 activity. In contrast, using the inducible *ERF6* overexpression line, we could show that *WRKY33* expression increases gradually over time, demonstrating that under osmotic stress conditions, ERF6 works as a transcriptional activator to regulate *WRKY33* expression. Supporting our observations, ERF6 was recently shown to be necessary for *WRKY33* induction under oxidative stress (Wang et al., 2013). Consistent with the activation of stress tolerance genes by ERF5 and ERF6, overexpression of *SlERF5* in tomato (*Solanum lycopersicum*) plants was recently shown to confer tolerance to drought stress (Pan et al., 2012).

ERF6 regulates two diverse processes: on the one hand, the activation of the stress defense transcriptional cascade, and on the other hand, the regulation of growth inhibition. Our data show that both processes can be uncoupled. Overexpression of the gene encoding the GA biosynthetic enzyme *GA20-OX1* (Coles et al., 1999) in ERF6-overexpressing plants suppressed the growth reduction phenotype but left the ERF6-mediated induction of stress response genes intact. Thus, in plants in which the stress signaling pathway is activated through *ERF6* overexpression, the stress tolerance factors remain activated even when growth inhibition is completely suppressed. This is similar to CBF1, which regulates a cluster of cold-responsive genes in a DELLA-independent way (Achard et al., 2008). From an agricultural point of view, this means that it should

be possible to generate crops that are less affected by mild drought in terms of growth but are still able to activate their stress defense mechanisms.

ERF5 and ERF6 regulate growth under multiple, but not all, abiotic stresses

The *erf5erf6* double mutant is more tolerant to both short-term and long-term osmotic stress, most likely because *GA2-OX6* expression is no longer activated (Supplemental Figure S10). Although less clear due to experimental variability, a similar tendency is observed for plants exposed to long-term oxidative stress. Surprisingly, although salt stress is generally known to be closely related to osmotic stress, *erf5erf6* plants do not tolerate mild salt stress better than wild-type plants. This observation was supported by expression analysis demonstrating that ERF5 and ERF6 have no role in salt stress signaling in actively growing leaves. Consistently, in proliferating leaves, mild salt stress does not induce the expression of the *GA2-OX6* gene, in contrast to osmotic and oxidative stress. It is thus likely that growth inhibition induced by mild salt stress occurs independently of the ERF5/ERF6-centered growth regulatory pathway. Both mannitol-induced stress and salt stress are characterized by the reduced ability to take up water, causing cellular dehydration and wilting. In addition, since salt ions are taken up by plant cells, plants have to cope with toxic levels of Na^+. In the majority of species, NaCl concentrations above 40 mM cause toxicity (Munns and Tester, 2008). In this study, plants were exposed to 50 mM NaCl and the observed growth reduction was probably mainly caused by NaCl toxicity and thus less related to osmotic stress defense. Although salt and osmotic stress show similarities, genome-wide expression studies revealed that large sets of genes are specifically induced by only one of these stresses (Denby and Gehring, 2005). Depending on the duration and exact conditions by which the stresses were applied, the overlap of genes responding to both abiotic stresses varied on average between 10% and 40%. When comparing only expression analyses performed on shoot tissue, the overlap was reduced to 3%. Thus, early stress-sensing and signaling responses in Arabidopsis shoots are mainly specific to either salt or osmotic stress, and our data clearly support this notion in actively growing leaves. Both osmotic stress and salt stress implicate the ethylene precursor ACC as an early signal (Zhang et al., 2011), and the molecular mechanisms by which this difference between salt and osmotic stress response is established in actively growing leaves are far from resolved. We speculate that the intermediate regulator acting between ACC and ERF5/ERF6 in the cascade is active after either osmotic or salt stress and activates or inhibits ERF5/ERF6 specifically in this condition. A putative candidate for such a regulator is NEK6, a kinase transcriptionally induced by ACC and by salt stress (Skirycz et al., 2011a; Zhang et al., 2011) but not by osmotic stress (Skirycz et al., 2011a). We further speculate that upon

salt stress, the NEK6 kinase either rapidly phosphorylates and thereby inactivates ERF5/ERF6 or inhibits the ethylene biosynthesis pathway (Zhang et al., 2011), establishing a slower but stable ERF5/ERF6 inhibition. It is likely that CBF1 is the functional equivalent of ERF6 under salt stress conditions (Achard et al., 2008). This probably allows the activation of genes conferring tolerance to sodium toxicity, which are not activated by ERF6.

CONCLUSION

In this study, we provide a missing link between ACC accumulation and DELLA stabilization in the pause-and-stop mechanism by which Arabidopsis leaf growth is shut down under osmotic stress. We uncovered a dual regulatory role for the transcription factor ERF6 and propose it to be a central element in a signaling network summarized in Figure 3.6A. Mild osmotic stress triggers the accumulation of ACC and, most likely, initiates an ACC-dependent signaling cascade involving MPK3 and MPK6. These mitogen-activated protein kinases activate ERF6, which in turn initiates transcription of the *GA2-OX6* gene encoding a GA-degrading enzyme. GA breakdown stabilizes DELLA proteins and represses growth. In parallel, ERF6 activation triggers the expression of stress tolerance factor genes such as *STZ*, *WRKY33*, and *MYB51*. Interestingly, the ERF6-mediated growth inhibition and the activation of the stress-responsive network can be uncoupled. This uncoupling holds great potential for engineering crops that are less inhibited by mild stress while maintaining stress tolerance.

MATERIALS AND METHODS

Plant lines

The single *erf5* and *erf6* mutants of Arabidopsis (Arabidopsis thaliana) were obtained from the SALK collection, references SALK_076967 (erf5) and SALK_030723 (erf6). The pRGA:RGA-GFP line was a kind gift of Prof. Dr. Tai-ping Sun (Duke University). The 35S::GA20-OX1 line used was previously described by Gonzalez et al. (2010) and originally was a gift from P. Hedden (Coles et al., 1999). All lines used are in the Columbia background.

In vitro plant growth conditions

Seedlings were grown in vitro on one-half-strength MS medium (Murashige and Skoog, 1962) containing 1% Suc at 21°C under a 16-h-day (110 μmol m−2 s−1) and 8-h-night regime. For long-term experiments where no transfer was needed, 9 g L−1 agar was added to the medium. For short-term experiments involving transfer, 6.5 g L−1 agar was used, and the growth medium was overlaid with nylon mesh (Prosep) of 20-μm pore size to facilitate transfer. For expression analysis and growth experiments, 64 and 16 seeds, respectively, were equally distributed on a 14-cm-diameter petri dish. The different ERF6 gain- and loss-of-function lines were always grown together with the appropriate control on one plate to enable correct comparisons.

Exposure to short-term osmotic stress and/or glucocorticoid-induced activation of ERF6

Plants were grown on a nylon mesh covering control MS medium until the third leaf had completely emerged from the shoot apical meristem but was still in a fully proliferative stage, at 9 DAS. At this time point, the mesh was transferred to plates with one-half-strength MS medium containing 25 mm d-mannitol (plant culture tested; Sigma), 5 μm DEX (Sigma), or a combination of both. For expression analysis and growth experiments, all seedlings were transferred to DEX, including the GFP:IOE control lines, to account for the possible effects of DEX on growth or gene expression.

Growth analysis

Growth analysis was performed on the third true leaf harvested at different time points after transfer to DEX. After clearing with 70% ethanol, leaves were mounted in lactic acid on microscope slides. For each experiment, about 15 to 20 leaves were photographed with a binocular microscope, and abaxial epidermal cells (100–200) were drawn for three representative leaves with a DMLB microscope (Leica) fitted with a drawing tubus and a differential interference contrast objective. Photographs of leaves and drawings were used to measure leaf area and cell size, respectively, using ImageJ version 1.37o (http://rsb.info.nih.gov/ij/), and average cell numbers were calculated by dividing leaf area by cell area.

Sampling RNA for expression analysis

Samples were obtained from three independent experiments and from multiple plates within the experiment. Whole seedlings were harvested rapidly in an excess of RNAlater solution (Ambion) and, after overnight storage at 4°C, dissected using a binocular microscope on a cooling plate with precision microscissors. Dissected leaves were transferred to a new tube, frozen in liquid nitrogen, and ground with a Retsch machine

and 3-mm metal balls. RNA was extracted with Trizol (Invitrogen) and further purified with the RNeasy Mini Kit (Qiagen). DNA digestion was done on columns with RNase-free DNase I (Roche).

Genome-wide expression changes

For the identification of genome-wide expression changes, samples of the strong ERF6-overexpressing line ($ERF6^{IOE}$-S) and the control line (GFP:IOE) were harvested 4 h after transfer to DEX. Two micrograms of pure RNA samples was hybridized to AGRONOMICS1 Arabidopsis Tiling Arrays (Rehrauer et al., 2010) at the VIB Microarray Facility. Obtained expression data were processed with Robust Multichip Average (background correction, normalization, and summarization) as implemented in BioConductor (Irizarry et al., 2003a, 2003b; Gentleman et al., 2004). The Brainarray "agronomics1tair9genecdf" Chip Definition File was used to assign probes to genes (Brainarray). The BioConductor package Limma as well as the Rank Products method were used to identify differentially expressed genes (Breitling et al., 2004; Smyth, 2004). To compare gene expression with and without ERF6 induction (ERF6IOE-S × GFP:IOE), moderated Student's t test statistics were calculated using the eBayes function, and P values were corrected for multiple testing using topTable (Hochberg and Benjamini, 1990). False discovery rate-corrected $P < 0.05$ was used as a cutoff.

Flow cytometry

For flow cytometry analysis, 16 leaves were chopped with a razor blade in CyStain UV Precise P buffers (Partec) according to the manufacturer's instructions. The nuclei were analyzed with a CyFlow flow cytometer with FloMax Software (Partec).

Quantitative reverse transcription-PCR

For complementary DNA synthesis, the iScript cDNA Synthesis Kit (Bio-Rad) was used according to the manufacturer's instructions using 1 μg of RNA. Quantitative reverse transcription-PCR was done on a LightCycler 480 (Roche Diagnostics) on 384-well plates with LightCycler 480 SYBR Green I Master (Roche) according to the manufacturer's instructions. Melting curves were analyzed to check primer specificity. Normalization was done against the average of housekeeping genes AT1G13320, AT2G32170, and AT2G28390: ΔCt = Ct (gene) – Ct (mean [housekeeping genes]) and $\Delta\Delta Ct = \Delta Ct$ (control line) – ΔCt (line of interest). Ct refers to the number of cycles at which SYBR Green fluorescence reaches an arbitrary value during the exponential phase of amplification. Primers were designed with the QuantPrime Web site (Arvidsson et al., 2008; Skirycz et al., 2010). Primers used in this study are as follows:

ERF5, 5′-AAATTCGCGGCGGAGATTCGTG-3′ and 5′-TCAAACGTCCCAAGCCAAACGC-3′; ERF6, 5′-TCGAATCCTCCTCGCGTTACTG-3′ and 5′-TTCGGTGGTGCGATCTTCAACG-3′; GA2-OX6, 5′-TGGATCCCAATCCCATCTGACC-3′ and 5′-TCTCCCATTCGTCAATGCCTGAAG-3′; MYB51, 5′-GCCCTTCACGGCAACAAATG-3′ and 5′-GGTTATGCCCTTGTGTGTAACTGG-3′; STZ, 5′-TCACAAGGCAAGCCACCGTAAG-3′ and 5′-TTGTCGCCGACGAGGTTGAATG-3′; WRKY33, 5′-CTTCCACTTGTTTCAGTCCCTCTC-3′ and 5′-CTGTGGTTGGAGAAGCTAGAACG-3′.

RGA:GFP quantification

Amounts of RGA:GFP protein in either DEX-treated or nontreated ERF6IOE-S plants were quantified by western blotting. Complete seedlings were harvested in liquid nitrogen 48 h after transfer to DEX or control medium and ground with a Retsch machine. Protein extraction was done by adding extraction buffer (Van Leene et al., 2007) to ground samples, followed by two freeze-thaw steps and two centrifugation steps (20,817g, 10 min, 4°C), whereby the supernatant was collected each time. Western-blot analysis was performed with primary rabbit anti-GFP antibodies (Santa Cruz; diluted 1:200) and secondary horseradish peroxidase-conjugated donkey anti-rabbit antibodies (GE Healthcare; diluted 1:10,000). A chemiluminescence procedure (NEN Life Science Products) was used for detection.

Long-term stress exposure with IGIS

For long-term exposure to abiotic stress in combination with automated phenotypic analysis, plants were grown on the IGIS platform in the same conditions as described in "In Vitro Plant Growth Conditions." The one-half-strength MS medium contained 9 g L−1, and stresses were applied by adding 25 mm mannitol (osmotic stress), 50 mm NaCl (salt stress), or 1.5 mm hydrogen peroxide (oxidative stress). The platform allows for a detailed rosette growth analysis of in vitro-grown Arabidopsis plants and can hold up to 10 petri dishes. On each plate, the erf5erf6 mutant was grown next to the appropriate control (azygous for both transfer DNA constructs). Images were captured on an hourly basis, using near-infrared technology to visualize plants in the dark. Individual rosettes were extracted automatically by image analysis processing. A data analysis pipeline compiles the measurements and constructs rosette growth curves. Details about the IGIS platform will be published later.

Protoplast Activation Assay

The protoplast activation assay was performed as described previously (De Sutter et al., 2005; Pauwels et al., 2010). All transformation constructs were obtained using the Gateway cloning system, and all liquid handlings were done on the Tecan Genesis

automated platform (De Sutter et al., 2005). The protoplast activation assay was performed in a 3-d-old tobacco BY-2 cell culture, subcultured from a 6- to 10-d-old culture. BY-2 cells were protoplasted using a 1% cellulase (Kyowa Chemical Products) and 0.1% pectolyase (Kyowa Chemical Products) enzyme solution in a 0.4% mannitol (Sigma) buffer. Protoplasts were then washed, counted, and diluted to 500,000 mL−1. For every transcription factor-promoter combination, 100 µL (50,000 protoplasts) was used. To confirm direct binding of ERF5/ERF6 on the promoters of STZ, MYB51, and WRKY33, protoplasts were cotransfected with 35S-ERF5 or 35S-ERF6 (in p2GW7) and pSTZ-fLUC, pMYB51-fLUC, or pWRKY33-fLUC (in pM42GW7). Promoters were defined as the 2,000 bp upstream of the start codon. fLUC encodes the firefly luciferase enzyme. Every protoplast sample was transfected with 2 µg per construct as well as with 2 µg of normalization construct expressing the Renilla luciferase (rLUC) enzyme. Transformed protoplasts were further grown by gentle shaking overnight in BY-2 medium to allow expression of the constructs. The next day, the BY-2 medium was removed and protoplasts were lysed in Cell Culture Lysis Reagent (Promega). Protoplast content was transferred to Nunc plates (Thermo Scientific), and fLUC and rLUC activities were measured using the Dual Luciferase Assay (Promega) and the LumiStar Galaxy (De Sutter et al., 2005). Measured fLUC activities were then normalized to rLUC activities.

Microarray data from this article were deposited in the Gene Expression Omnibus database (GSE45830).

SUPPLEMENTAL DATA

All Supplemental Data is listed below. Supplemental Figures can be found at the end of this chapter. Supplemental tables S3 and S4 are available in the online version of this article.

Supplemental Figure S1. *ERF5* and *ERF6* are induced by abiotic stresses.
Supplemental Figure S2. *ERF5* and *ERF6* are homologous genes and share highly conserved functional domains.
Supplemental Figure S3. Gene structure and expression analysis of *erf5* and *erf6* mutants.
Supplemental Figure S4. Gene expression of *ERF5*, *ERF6*, and their targets under osmotic, salt, and oxidative stress.
Supplemental Figure S5. Cellular measurements of ERF6^{IOE}-S and ERF6^{IOE}-W.
Supplemental Figure S6. Endoreduplication index in third leaves of plants overexpressing ERF6.

Supplemental Figure S7. BiNGO analysis of the putative ERF6 target genes.
Supplemental Figure S8. Expression pattern of the multiple *GA2-OX* genes upon *ERF6* overexpression and under osmotic stress.
Supplemental Figure S9. Induction of the ERF6 targets upon *ERF6* overexpression in ERF6^{IOE}-S and ERF6^{IOE}-W.
Supplemental Figure S10. Induction of *GA2-OX6* in the *erf5erf6* double mutant following osmotic stress exposure.
Supplemental Figure S11. *ERF6* is transcriptionally induced by ERF6 itself and not by EIN3 and EIL1.
Supplemental Table S1. Measurements of *erf5erf6* rosettes under different long-term abiotic stress conditions.
Supplemental Table S2. Measurements of *erf5erf6* third leaves under control and osmotic stress conditions.
Supplemental Table S3. List of putative ERF6 target genes.
Supplemental Table S4. Genes induced within 3 h of osmotic stress exposure.

ACKNOWLEDGEMENTS

We thank the Systems Biology of Yield group for the stimulating scientific environment and fruitful discussions, Dr. Annick Bleys for help in preparing the manuscript, Prof. Dr. Tai-ping Sun for kindly providing RGA::GFP-RGA seeds, and Prof. Dr. Peter Hedden for the 35S::GA20-OX1 seeds. This work was supported by the Interuniversity Attraction Poles Program (grant no. P7/29 "MARS") initiated by the Belgian Science Policy Office, by Ghent University (Bijzonder Onderzoeksfonds Methusalem project no. BOF08/01M00408, Multidisciplinary Research Partnership Biotechnology for a Sustainable Economy project no. 01MRB510W, and Bijzonder Onderzoeksfonds van de Universiteit van Gent for a postdoctoral fellowship to S.D.), and by the Research Foundation Flanders (predoctoral fellowships to H.C. and S.D.B.).

REFERENCES

Achard P, Gong F, Cheminant S, Alioua M, Hedden P, Genschik P (2008) The cold-inducible CBF1 factor-dependent signaling pathway modulates the accumulation of the growth-repressing DELLA proteins via its effect on gibberellin metabolism. Plant Cell 20: 2117-2129

Achard P, Gusti A, Cheminant S, Alioua M, Dhondt S, Coppens F, Beemster GT, Genschik P (2009) Gibberellin signaling controls cell proliferation rate in Arabidopsis. Curr Biol 19: 1188-1193

Alonso JM, Stepanova AN, Leisse TJ, Kim CJ, Chen H, Shinn P, Stevenson DK, Zimmerman J, Barajas P, Cheuk R, Gadrinab C, Heller C, Jeske A, Koesema E, Meyers CC, Parker H, Prednis L, Ansari Y, Choy N, Deen H, Geralt M, Hazari N, Hom E, Karnes M, Mulholland C, Ndubaku R, Schmidt I, Guzman P, Aguilar-Henonin L, Schmid M, Weigel D, Carter DE, Marchand T, Risseeuw E, Brogden D, Zeko A, Crosby WL, Berry CC, Ecker JR (2003) Genome-wide insertional mutagenesis of Arabidopsis thaliana. Science 301: 653-657

Anastasiou E, Lenhard M (2007) Growing up to one's standard. Current Opinion in Plant Biology 10: 63-69

Anastasiou E, Lenhard M (2007) Growing up to one's standard. Curr Opin Plant Biol 10: 63-69

Andriankaja M, Dhondt S, De Bodt S, Vanhaeren H, Coppens F, De Milde L, Muhlenbock P, Skirycz A, Gonzalez N, Beemster GT, Inze D (2012) Exit from proliferation during leaf development in Arabidopsis thaliana: a not-so-gradual process. Dev Cell 22: 64-78

Andriankaja M, Dhondt S, De Bodt S, Vanhaeren H, Coppens F, De Milde L, Muhlenbock P, Skirycz A, Gonzalez N, Beemster GTS, Inze D (2012) Exit from Proliferation during Leaf Development in Arabidopsis thaliana: A Not-So-Gradual Process. Developmental Cell 22: 64-78

Arvidsson S, Kwasniewski M, Riano-Pachon DM, Mueller-Roeber B (2008) QuantPrime - a flexible tool for reliable high-throughput primer design for quantitative PCR. BMC Bioinformatics 9

Baerenfaller K, Massonnet C, Walsh S, Baginsky S, Buhlmann P, Hennig L, Hirsch-Hoffmann M, Howell KA, Kahlau S, Radziejwoski A, Russenberger D, Rutishauser D, Small I, Stekhoven D, Sulpice R, Svozil J, Wuyts N, Stitt M, Hilson P, Granier C, Gruissem W (2012) Systems-based analysis of Arabidopsis leaf growth reveals adaptation to water deficit. Molecular Systems Biology 8

Bailey-Serres J, Voesenek LA (2008) Flooding stress: acclimations and genetic diversity. Annu Rev Plant Biol 59: 313-339

Birkenbihl RP, Diezel C, Somssich IE (2012) Arabidopsis WRKY33 is a key transcriptional regulator of hormonal and metabolic responses toward Botrytis cinerea infection. Plant Physiol 159: 266-285

Boyer JS (1982) Plant productivity and environment. Science 218: 443-448

Cao WH, Liu J, He XJ, Mu RL, Zhou HL, Chen SY, Zhang JS (2007) Modulation of ethylene responses affects plant salt-stress responses. Plant Physiol 143: 707-719

Cao WH, Liu J, Zhou QY, Cao YR, Zheng SF, Du BX, Zhang JS, Chen SY (2006) Expression of tobacco ethylene receptor NTHK1 alters plant responses to salt stress. Plant Cell Environ 29: 1210-1219

Cao YR, Chen SY, Zhang JS (2008) Ethylene signaling regulates salt stress response: An overview. Plant Signal Behav 3: 761-763

Claeys H, Skirycz A, Maleux K, Inze D (2012) DELLA signaling mediates stress-induced cell differentiation in Arabidopsis leaves through modulation of anaphase-promoting complex/cyclosome activity. Plant Physiol 159: 739-747

Corrado G, Karali M (2009) Inducible gene expression systems and plant biotechnology. Biotechnol Adv 27: 733-743

De Smet I, Zhang H, Inze D, Beeckman T (2006) A novel role for abscisic acid emerges from underground. Trends Plant Sci 11: 434-439

Denby K, Gehring C (2005) Engineering drought and salinity tolerance in plants: lessons from genome-wide expression profiling in Arabidopsis. Trends Biotechnol 23: 547-552

Dill A, Jung HS, Sun TP (2001) The DELLA motif is essential for gibberellin-induced degradation of RGA. Proc Natl Acad Sci U S A 98: 14162-14167

Dinneny JR, Long TA, Wang JY, Jung JW, Mace D, Pointer S, Barron C, Brady SM, Schiefelbein J, Benfey PN (2008) Cell identity mediates the response of Arabidopsis roots to abiotic stress. Science 320: 942-945

Donnelly PM, Bonetta D, Tsukaya H, Dengler RE, Dengler NG (1999) Cell cycling and cell enlargement in developing leaves of Arabidopsis. Dev Biol 215: 407-419

Fujimoto SY, Ohta M, Usui A, Shinshi H, Ohme-Takagi M (2000) Arabidopsis ethylene-responsive element binding factors act as transcriptional activators or repressors of GCC box-mediated gene expression. Plant Cell 12: 393-404

Gentleman RC, Carey VJ, Bates DM, Bolstad B, Dettling M, Dudoit S, Ellis B, Gautier L, Ge Y, Gentry J, Hornik K, Hothorn T, Huber W, Iacus S, Irizarry R, Leisch F, Li C, Maechler M, Rossini AJ, Sawitzki G, Smith C, Smyth G, Tierney L, Yang JY, Zhang J (2004) Bioconductor: open software development for computational biology and bioinformatics. Genome Biol 5: R80

Gigolashvili T, Berger B, Mock HP, Muller C, Weisshaar B, Flugge UI (2007) The transcription factor HIG1/MYB51 regulates indolic glucosinolate biosynthesis in Arabidopsis thaliana. Plant J 50: 886-901

Gonzalez N, De Bodt S, Sulpice R, Jikumaru Y, Chae E, Dhondt S, Van Daele T, De Milde L, Weigel D, Kamiya Y, Stitt M, Beemster GT, Inze D (2010) Increased leaf size: different means to an end. Plant Physiol 153: 1261-1279

Gonzalez N, Vanhaeren H, Inze D (2012) Leaf size control: complex coordination of cell division and expansion. Trends in Plant Science 17: 332-340

Harb A, Krishnan A, Ambavaram MMR, Pereira A (2010) Molecular and Physiological Analysis of Drought Stress in Arabidopsis Reveals Early Responses Leading to Acclimation in Plant Growth. Plant Physiology 154: 1254-1271

Hernandez M, Fernandez-Garcia N, Diaz-Vivancos P, Olmos E (2010) A different role for hydrogen peroxide and the antioxidative system under short and long salt stress in Brassica oleracea roots. J Exp Bot 61: 521-535

Hochberg Y, Benjamini Y (1990) More Powerful Procedures for Multiple Significance Testing. Statistics in Medicine 9: 811-818

Hruz T, Laule O, Szabo G, Wessendorp F, Bleuler S, Oertle L, Widmayer P, Gruissem W, Zimmermann P (2008) Genevestigator v3: a reference expression database for the meta-analysis of transcriptomes. Adv Bioinformatics 2008: 420747

Huang D, Wu W, Abrams SR, Cutler AJ (2008) The relationship of drought-related gene expression in Arabidopsis thaliana to hormonal and environmental factors. J Exp Bot 59: 2991-3007

Irizarry RA, Bolstad BM, Collin F, Cope LM, Hobbs B, Speed TP (2003) Summaries of Affymetrix GeneChip probe level data. Nucleic Acids Res 31: e15

Irizarry RA, Hobbs B, Collin F, Beazer-Barclay YD, Antonellis KJ, Scherf U, Speed TP (2003) Exploration, normalization, and summaries of high density oligonucleotide array probe level data. Biostatistics 4: 249-264

Jackson MB (2008) Ethylene-promoted elongation: an adaptation to submergence stress. Ann Bot 101: 229-248

Jiang Y, Deyholos MK (2009) Functional characterization of Arabidopsis NaCl-inducible WRKY25 and WRKY33 transcription factors in abiotic stresses. Plant Mol Biol 69: 91-105

Kieber JJ (1997) The ethylene response pathway in Arabidopsis. Annu Rev Plant Physiol Plant Mol Biol 48: 277-296

Kieber JJ (1997) The ethylene signal transduction pathway in Arabidopsis. J Exp Bot 48: 211-218

Li G, Meng X, Wang R, Mao G, Han L, Liu Y, Zhang S (2012) Dual-level regulation of ACC synthase activity by MPK3/MPK6 cascade and its downstream WRKY transcription factor during ethylene induction in Arabidopsis. PLoS Genet 8: e1002767

Lippok B, Birkenbihl RP, Rivory G, Brummer J, Schmelzer E, Logemann E, Somssich IE (2007) Expression of AtWRKY33 encoding a pathogen- or PAMP-responsive WRKY transcription factor is regulated by a composite DNA motif containing W box elements. Mol Plant Microbe Interact 20: 420-429

Ma Z, Baskin TI, Brown KM, Lynch JP (2003) Regulation of root elongation under phosphorus stress involves changes in ethylene responsiveness. Plant Physiol 131: 1381-1390

Maere S, Heymans K, Kuiper M (2005) BiNGO: a Cytoscape plugin to assess overrepresentation of gene ontology categories in biological networks. Bioinformatics 21: 3448-3449

Magome H, Yamaguchi S, Hanada A, Kamiya Y, Oda K (2008) The DDF1 transcriptional activator upregulates expression of a gibberellin-deactivating gene, GA2ox7, under high-salinity stress in Arabidopsis. Plant Journal 56: 613-626

Mao G, Meng X, Liu Y, Zheng Z, Chen Z, Zhang S (2011) Phosphorylation of a WRKY transcription factor by two pathogen-responsive MAPKs drives phytoalexin biosynthesis in Arabidopsis. Plant Cell 23: 1639-1653

Mittler R, Kim Y, Song L, Coutu J, Coutu A, Ciftci-Yilmaz S, Lee H, Stevenson B, Zhu JK (2006) Gain- and loss-of-function mutations in Zat10 enhance the tolerance of plants to abiotic stress. FEBS Lett 580: 6537-6542

Moffat CS, Ingle RA, Wathugala DL, Saunders NJ, Knight H, Knight MR (2012) ERF5 and ERF6 play redundant roles as positive regulators of JA/Et-mediated defense against Botrytis cinerea in Arabidopsis. PLoS One 7: e35995

Munns R, Tester M (2008) Mechanisms of salinity tolerance. Annual Review of Plant Biology 59: 651-681

Murashige T, Skoog F (1962) A Revised Medium for Rapid Growth and Bio Assays with Tobacco Tissue Cultures. Physiologia Plantarum 15: 473-&

Nakano T, Suzuki K, Fujimura T, Shinshi H (2006) Genome-wide analysis of the ERF gene family in Arabidopsis and rice. Plant Physiol 140: 411-432

Neill S, Barros R, Bright J, Desikan R, Hancock J, Harrison J, Morris P, Ribeiro D, Wilson I (2008) Nitric oxide, stomatal closure, and abiotic stress. J Exp Bot 59: 165-176

Niu CF, Wei W, Zhou QY, Tian AG, Hao YJ, Zhang WK, Ma B, Lin Q, Zhang ZB, Zhang JS, Chen SY (2012) Wheat WRKY genes TaWRKY2 and TaWRKY19 regulate abiotic stress tolerance in transgenic Arabidopsis plants. Plant Cell Environ 35: 1156-1170

Pandey SP, Somssich IE (2009) The role of WRKY transcription factors in plant immunity. Plant Physiol 150: 1648-1655

Pauwels L, Barbero GF, Geerinck J, Tilleman S, Grunewald W, Perez AC, Chico JM, Vanden Bossche R, Sewell J, Gil E, Garcia-Casado G, Witters E, Inze D, Long JA, De Jaeger G, Solano R, Goossens A (2010) NINJA connects the co-repressor TOPLESS to jasmonate signalling. Nature 464: 788-U169

Peng JR, Carol P, Richards DE, King KE, Cowling RJ, Murphy GP, Harberd NP (1997) The Arabidopsis GAI gene defines a signaling pathway that negatively regulates gibberellin responses. Genes & Development 11: 3194-3205

Perez-Alfocea F, Ghanem ME, Gomez-Cadenas A, Dodd IC (2011) Omics of Root-to-Shoot Signaling Under Salt Stress and Water Deficit. Omics-a Journal of Integrative Biology 15: 893-901

Pierik R, de Wit M, Voesenek LACJ (2011) Growth-mediated stress escape: convergence of signal transduction pathways activated upon exposure to two different environmental stresses. New Phytologist 189: 122-134

Pierik R, Sasidharan R, Voesenek LACJ (2007) Growth control by ethylene: Adjusting phenotypes to the environment. Journal of Plant Growth Regulation 26: 188-200

Pierik R, Tholen D, Poorter H, Visser EJ, Voesenek LA (2006) The Janus face of ethylene: growth inhibition and stimulation. Trends Plant Sci 11: 176-183

Popescu SC, Popescu GV, Bachan S, Zhang Z, Gerstein M, Snyder M, Dinesh-Kumar SP (2009) MAPK target networks in Arabidopsis thaliana revealed using functional protein microarrays. Genes Dev 23: 80-92

Rehrauer H, Aquino C, Gruissem W, Henz SR, Hilson P, Laubinger S, Naouar N, Patrignani A, Rombauts S, Shu H, Van de Peer Y, Vuylsteke M, Weigel D, Zeller G, Hennig L (2010) AGRONOMICS1: a new resource for Arabidopsis transcriptome profiling. Plant Physiol 152: 487-499

Roman G, Lubarsky B, Kieber JJ, Rothenberg M, Ecker JR (1995) Genetic analysis of ethylene signal transduction in Arabidopsis thaliana: five novel mutant loci integrated into a stress response pathway. Genetics 139: 1393-1409

Sakamoto H, Araki T, Meshi T, Iwabuchi M (2000) Expression of a subset of the Arabidopsis Cys(2)/His(2)-type zinc-finger protein gene family under water stress. Gene 248: 23-32

Sakamoto H, Maruyama K, Sakuma Y, Meshi T, Iwabuchi M, Shinozaki K, Yamaguchi-Shinozaki K (2004) Arabidopsis Cys2/His2-type zinc-finger proteins function as transcription repressors under drought, cold, and high-salinity stress conditions. Plant Physiol 136: 2734-2746

Schachtman DP, Goodger JQ (2008) Chemical root to shoot signaling under drought. Trends Plant Sci 13: 281-287

Seki M, Umezawa T, Urano K, Shinozaki K (2007) Regulatory metabolic networks in drought stress responses. Curr Opin Plant Biol 10: 296-302

Silverstone AL, Jung HS, Dill A, Kawaide H, Kamiya Y, Sun TP (2001) Repressing a repressor: gibberellin-induced rapid reduction of the RGA protein in Arabidopsis. Plant Cell 13: 1555-1566

Skirycz A, Claeys H, De Bodt S, Oikawa A, Shinoda S, Andriankaja M, Maleux K, Eloy NB, Coppens F, Yoo SD, Saito K, Inze D (2011) Pause-and-stop: the effects of osmotic stress on cell proliferation during early leaf development in Arabidopsis and a role for ethylene signaling in cell cycle arrest. Plant Cell 23: 1876-1888

Skirycz A, De Bodt S, Obata T, De Clercq I, Claeys H, De Rycke R, Andriankaja M, Van Aken O, Van Breusegem F, Fernie AR, Inze D (2010) Developmental stage specificity and the role of mitochondrial metabolism in the response of Arabidopsis leaves to prolonged mild osmotic stress. Plant Physiol 152: 226-244

Skirycz A, De Bodt S, Obata T, De Clercq I, Claeys H, De Rycke R, Andriankaja M, Van Aken O, Van Breusegem F, Fernie AR, Inze D (2010) Developmental Stage Specificity and the Role of Mitochondrial Metabolism in the Response of Arabidopsis Leaves to Prolonged Mild Osmotic Stress. Plant Physiology 152: 226-244

Skirycz A, Inze D (2010) More from less: plant growth under limited water. Curr Opin Biotechnol 21: 197-203

Skirycz A, Vandenbroucke K, Clauw P, Maleux K, De Meyer B, Dhondt S, Pucci A, Gonzalez N, Hoeberichts F, Tognetti VB, Galbiati M, Tonelli C, Van Breusegem F, Vuylsteke M, Inze D (2011) Survival and growth of Arabidopsis plants given limited water are not equal. Nat Biotechnol 29: 212-214

Smyth GK (2004) Linear models and empirical bayes methods for assessing differential expression in microarray experiments. Stat Appl Genet Mol Biol 3: Article3

Son GH, Wan J, Kim HJ, Nguyen XC, Chung WS, Hong JC, Stacey G (2012) Ethylene-responsive element-binding factor 5, ERF5, is involved in chitin-induced innate immunity response. Mol Plant Microbe Interact 25: 48-60

Tanaka Y, Sano T, Tamaoki M, Nakajima N, Kondo N, Hasezawa S (2005) Ethylene inhibits abscisic acid-induced stomatal closure in Arabidopsis. Plant Physiol 138: 2337-2343

Tardieu F, Granier C, Muller B (2011) Water deficit and growth. Co-ordinating processes without an orchestrator? Curr Opin Plant Biol 14: 283-289

Thomas SG, Sun TP (2004) Update on gibberellin signaling. A tale of the tall and the short. Plant Physiology 135: 668-676

Thompson JD, Higgins DG, Gibson TJ (1994) CLUSTAL W: improving the sensitivity of progressive multiple sequence alignment through sequence weighting, position-specific gap penalties and weight matrix choice. Nucleic Acids Res 22: 4673-4680

Verslues PE, Agarwal M, Katiyar-Agarwal S, Zhu J, Zhu JK (2006) Methods and concepts in quantifying resistance to drought, salt and freezing, abiotic stresses that affect plant water status. Plant J 45: 523-539

Vlieghe K, Boudolf V, Beemster GT, Maes S, Magyar Z, Atanassova A, de Almeida Engler J, De Groodt R, Inze D, De Veylder L (2005) The DP-E2F-like gene DEL1 controls the endocycle in Arabidopsis thaliana. Curr Biol 15: 59-63

Wuriyanghan H, Zhang B, Cao WH, Ma B, Lei G, Liu YF, Wei W, Wu HJ, Chen LJ, Chen HW, Cao YR, He SJ, Zhang WK, Wang XJ, Chen SY, Zhang JS (2009) The ethylene receptor ETR2 delays floral transition and affects starch accumulation in rice. Plant Cell 21: 1473-1494

Xiong L, Schumaker KS, Zhu JK (2002) Cell signaling during cold, drought, and salt stress. Plant Cell 14 Suppl: S165-183

Yang S, Vanderbeld B, Wan J, Huang Y (2010) Narrowing down the targets: towards successful genetic engineering of drought-tolerant crops. Mol Plant 3: 469-490

Yoo SD, Cho Y, Sheen J (2009) Emerging connections in the ethylene signaling network. Trends Plant Sci 14: 270-279

Zhang B, Chen HW, Mu RL, Zhang WK, Zhao MY, Wei W, Wang F, Yu H, Lei G, Zou HF, Ma B, Chen SY, Zhang JS (2011) NIMA-related kinase NEK6 affects plant growth and stress response in Arabidopsis. Plant Journal 68: 830-843

Supplemental Figure S1. *ERF5* and *ERF6* are induced by abiotic stresses. (A) *ERF5* and *ERF6* are induced specifically in growing leaves within 1h of mild osmotic stress exposure. Their expression remains higher than under control conditions in very small (<1mm²) leaves, but not in fully grown leaves. (B) *ERF5* and *ERF6* are induced by several abiotic stresses (Genevestigator, latest release – Hruz et al., 2008). Log2-FC are shown only for significantly differentially expressed genes (p<0.05).

A

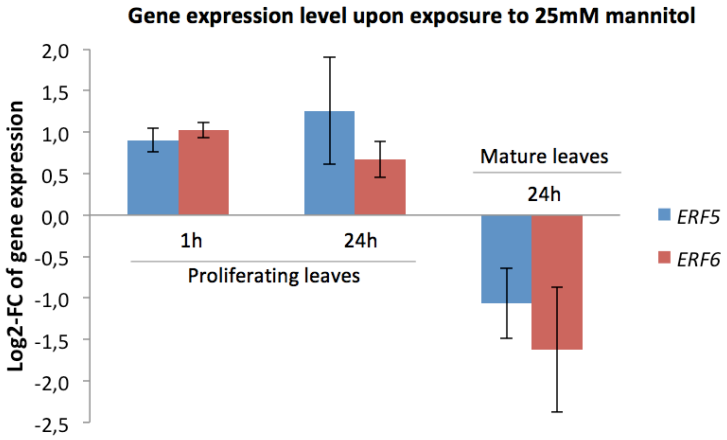

B

	ERF6	ERF5
Hypoxia (Study 6, Col-0)	4.82	1.97
Salt (Study 2, late samples)	4.53	1.9
Salt (Study 4, Col-0)	4.03	2.68
Cold (Study 10, 1h, in soil)	3.67	2.4
Drought (Study 6, Col-0)	3.67	1.87
Cold (early samples)	2.84	2.2
Hypoxia (Study 9, Col-0)	2.82	0.71
Cold (Study 2, late root samples)	2.65	2.72
Drought (Study 7, Col-0)	2.53	1.81
Drought (Study 5, aerial tissue)	2.5	2.5
Salt (Study 2, early root samples)	2.45	1.45
Cold (late, aerial tissue)	2.19	3.05
Osmotic (early, aerial tissue)	2.09	2.24
Hypoxia (Study 7, Col-0)	1.82	0.7
Oxidative (late, aerial tissue)	1.36	0.6
Cold (Study 2, early root samples)	1.07	1.42
Genotoxic (Study 2, late root samples)	1.03	0.89
Submergence (Study 2, 7h rosettes)	0.95	1.02
High Light (Study 4, exposed)	0.94	0.6
Osmotic (Study 2, late root samples)	0.92	1.14
Heat (Study 9)	-0.78	-0.96

Supplemental Figure S2. *ERF5* and *ERF6* are homologous genes and share highly-conserved functional domains. The homologs *ERF5* and *ERF6* belong to group IXb within the classification of ERF/AP2 transcription factors (Nakano et al., 2006). They share 2 Conserved Motifs of group IXb on top of the AP2/ERF domain conserved in all ERFs.

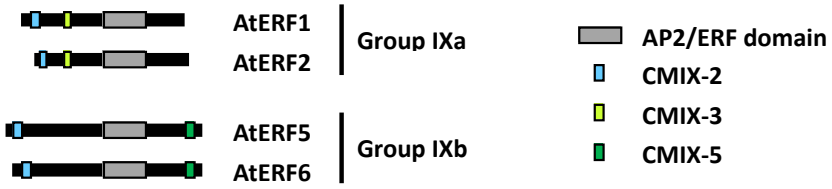

Supplemental Figure S3. Gene structure and expression analysis of *erf5* and *erf6* mutants. (A) Both mutants were obtained through insertional mutagenesis with insertion of the T-DNA in the 3'UTR and 5'UTR respectively (Alonso et al., 2003). Indicated values represent the coordinates, the white box represents the respective *ERF*-gene, the black box the T-DNA, the arrows represent the primers used for quantitative PCR. (B) Expression level of the *ERF5* and *ERF6* genes in the *erf5erf6* double knock-out relative to WT under control conditions (=100%). Expression levels were measured in the 3rd leaf at 10DAS under control conditions (MS medium) and mild osmotic stress (8h and 24h of stress exposure).

A

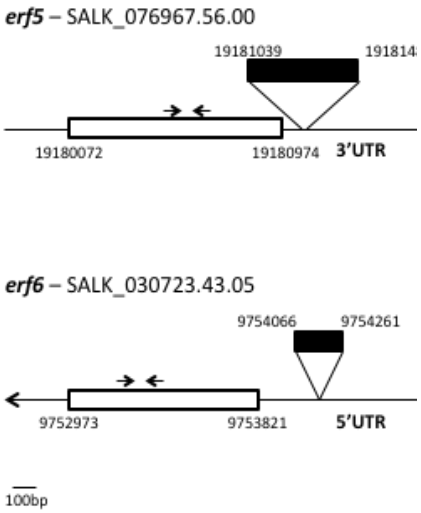

B

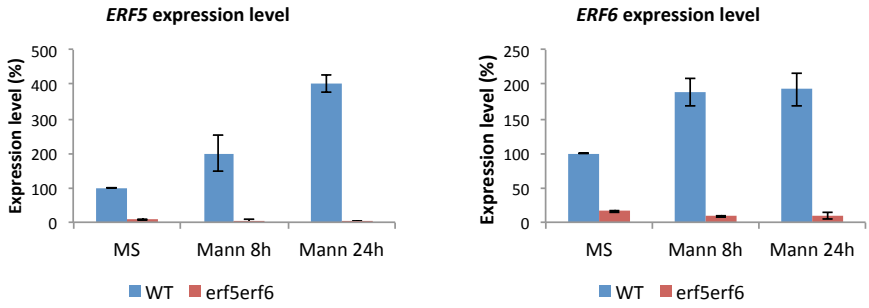

Supplemental Figure S4. Gene expression of *ERF5*, *ERF6* and their targets under osmotic, salt and oxidative stress. The *ERF5*, *ERF6* and the *GA2-OX6* gene are induced in young actively growing leaves 24h upon exposure to 25mM mannitol (Mann) and to 1.5mM H_2O_2. None of those genes is induced by mild salt stress (50mM) in actively growing leaves. Gene expression was measured specifically in Arabidopsis 3rd leaves at 9DAS + 24h, when the leaf is fully proliferating and thus actively growing.

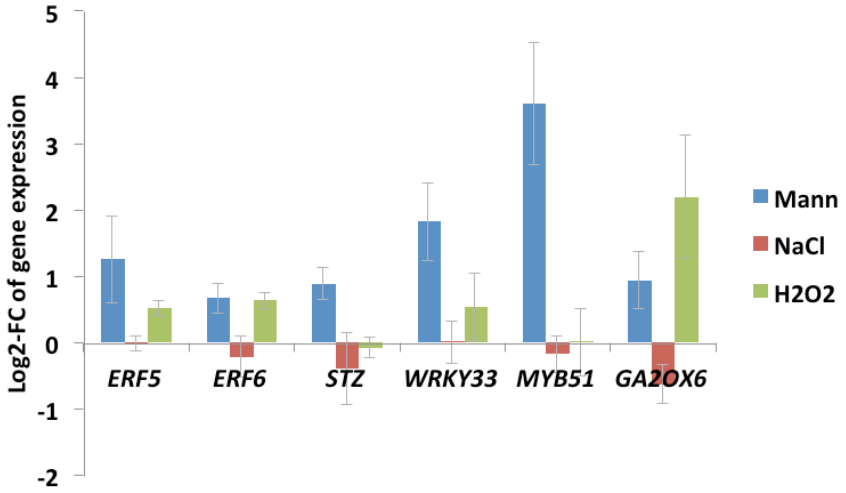

Supplemental Figure S5. Cellular measurements of ERF6^{IOE}-S and ERF6^{IOE}-W. Size and number of abaxial epidermal cells of harvested third leaves (n=3) at 12, 14 and 16DAS. Both strong as well as weak *ERF6* overexpression cause a decrease in cell area and strong *ERF6* overexpression reduces cell number by 59%.

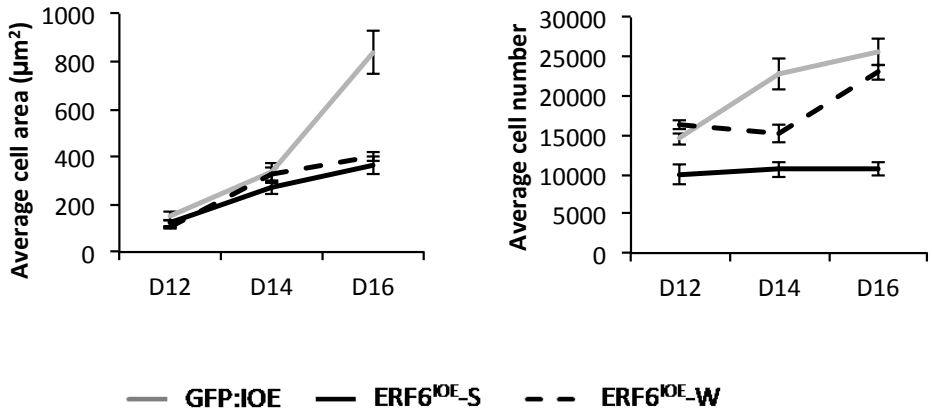

Supplemental Figure S6. Endoreduplication index in third leaves of plants overexpressing *ERF6*. Upon transfer to DEX at 9 days after stratification (DAS), plants strongly overexpressing *ERF6* show an increase in relative amount of cells undergoing endoreduplication, suggesting that ERF6 pushes cells toward differentiation. The endoreduplication index represents the number of endoreduplication cycles an average cell has gone through and was calculated as %4C + 2 × %8C + 3 × %16C.

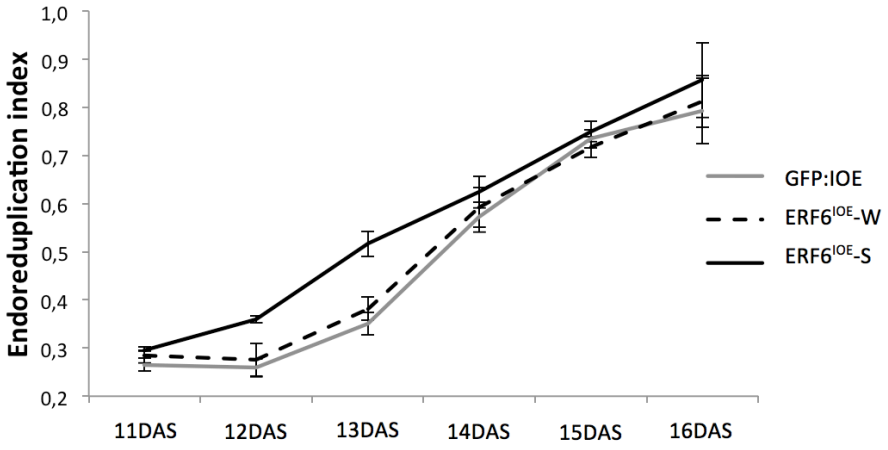

Supplemental Figure S7. BinGO analysis of the putative ERF6 target genes.

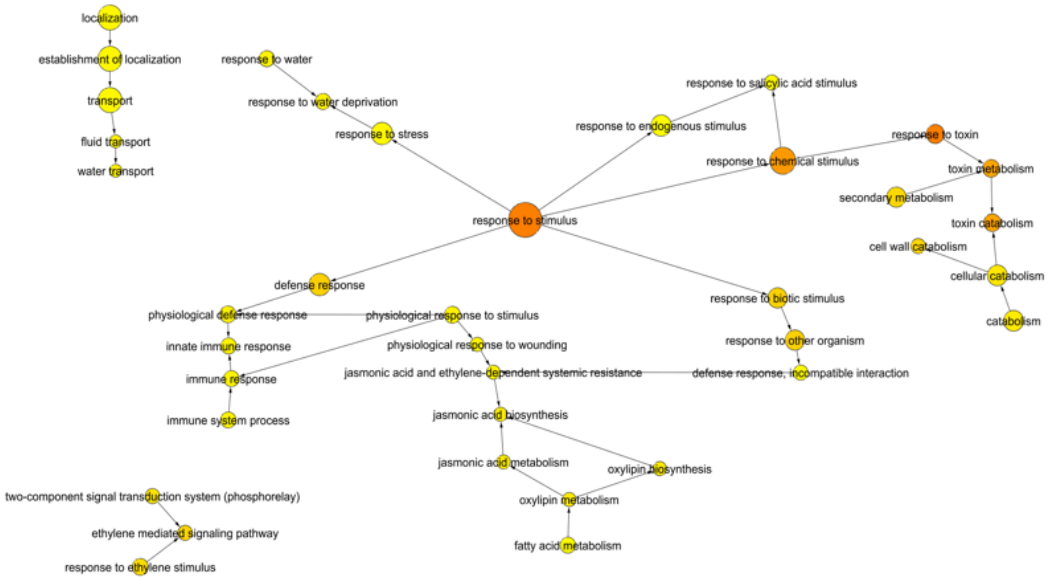

Supplemental Figure S8. Expression pattern of the multiple *GA2-OX* genes upon *ERF6* overexpression and under osmotic stress. The *GA2-OX6* gene is the only *GA2-OX* transcriptionally induced by *ERF6* overexpression and by mild osmotic stress treatments (osmotic stress dataset published in Skirycz et al., 2011a). Expression was measured with ATH1 microarrays (*) or with AGRONOMICS tiling arrays (**).

Gene Name	Log2-FC values upon					
	ERF6^{IOE}-S + Dex (4h)**	25mM mannitol (1,5h)*	25mM mannitol (3h)*	25mM mannitol (12h)*	25mM mannitol (24h)*	25mM mannitol (24h)**
GA2-OX1	-0,11	-0,06	-0,03	0,07	-0,10	-0,65
GA2-OX2	-0,13	0,30	0,02	0,01	-0,30	-0,13
GA2-OX3	-0,29	0,00	-0,07	0,00	0,02	0,28
GA2-OX4	-0,22	0,13	-0,10	-0,07	-0,14	-0,22
GA2-OX6	**2,03**	-0,12	0,37	0,76	0,89	**2,03**
GA2-OX7	-0,15	-0,04	-0,18	0,00	-0,07	-0,21
GA2-OX8	0,02	0,08	-0,04	-0,04	0,24	-0,33

Supplemental Figure S9. Induction of the ERF6 targets upon *ERF6* overexpression in ERF6^{IOE}-S and ERF6^{IOE}-W. Expression was measured in proliferating 3rd leaves and values are normalized to their expression in the GFP:IOE control line exposed to the same treatment. Error bars indicate standard errors.

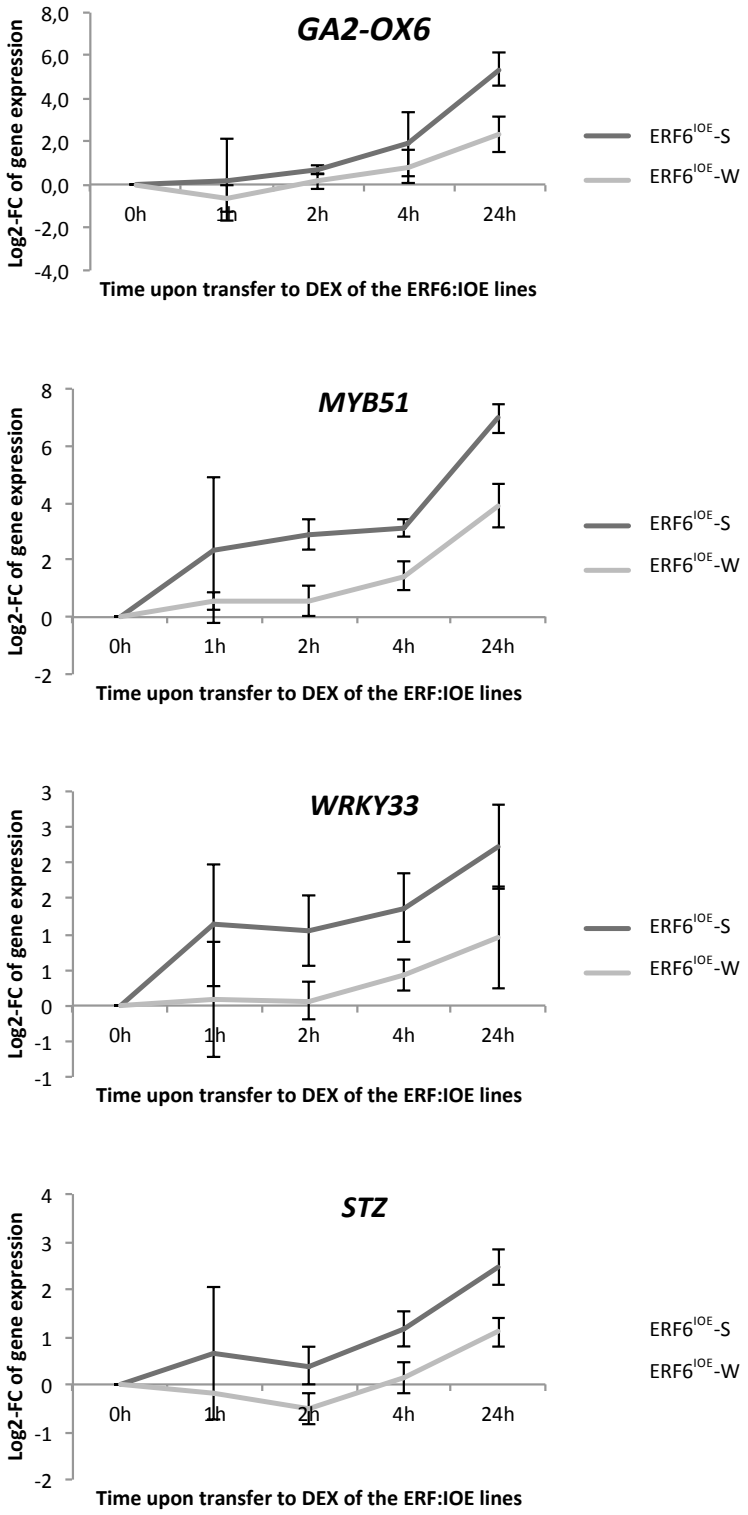

Supplemental Figure S10. Induction of *GA2-OX6* in the *erf5erf6* double mutant following osmotic stress exposure. Expression level of the *GA2-OX6* gene in the *erf5erf6* double mutant relative to WT under control conditions (=100%). Expression levels were measured in the 3rd leaf at 10 DAS under standard conditions (Murashige and Skoog medium) and 8 and 24 h upon mild osmotic stress exposure (MS medium supplemented with 25 mM mannitol). Error bars indicate standard errors. Three biological replicates were performed.

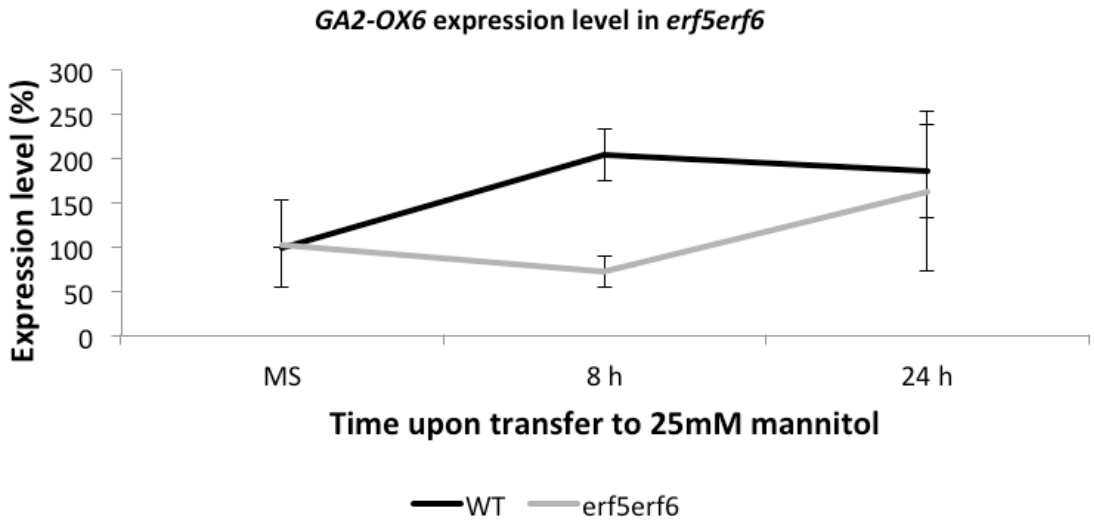

Supplemental Figure S11. *ERF6* is transcriptionally induced by ERF6 itself and not by EIN3 and EIL1. (A) ERF6-dependent activation of the promoters of *ERF6* itself by the protoplast activation assay. Indicated values are luciferine detection levels normalized to the negative control. ** = significantly different from control at respectively 1% significance level. Error bars indicate standard errors, 8 biological repeats were performed. (B) Expression level of the *ERF6* gene in the *ein3eil1* double mutant relative to WT under control conditions (=100%). Expression levels were measured in the 3rd leaf at 10 DAS under standard conditions (Murashige and Skoog medium) and 8 and 24 h upon mild osmotic stress exposure (MS medium supplemented with 25 mM mannitol). Error bars indicate standard errors. Two biological replicates were performed.

A

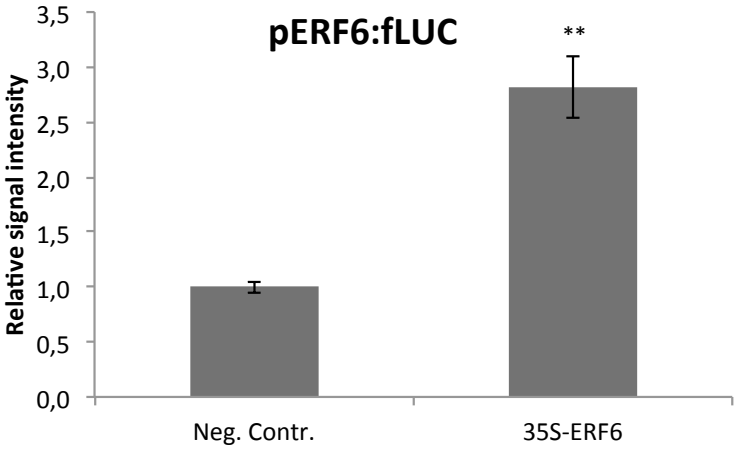

B

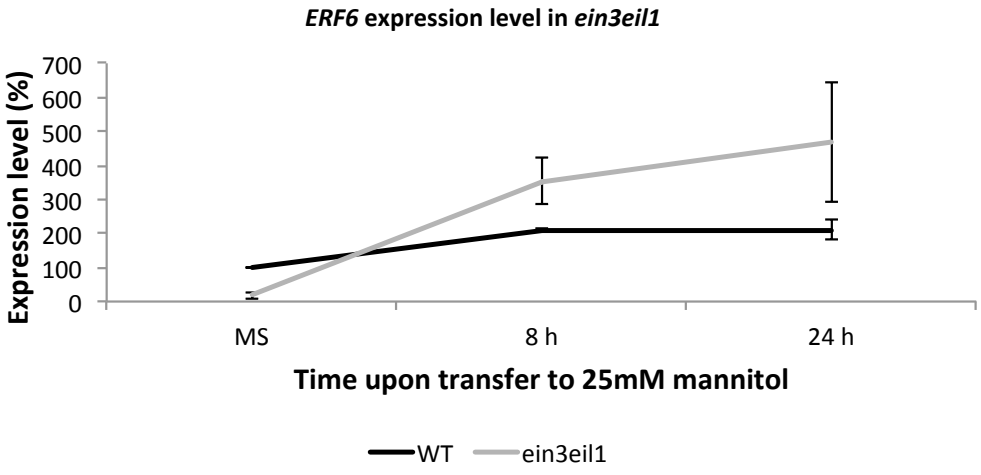

Supp. Table S1. Measurements of *erf5erf6* rosettes under different long term abiotic stress conditions. Stresses were applied by adding resp. 25mM Mannitol, 1.5mM H_2O_2, and 50mM NaCl to the growth medium. Pictures of the rosettes were taken every hour by the IGIS platform to measure rosette growth. Rosettes areas (mm^2) here were measured at final timepoint (=20 days after stratification).

MS	exp.1	exp.2	exp.3	Average	% increase	p
WT	530	441	473	481		
erf5erf6	569	571	497	546	13%	0.15

mannitol	exp.1	exp.2	exp.3	Average	% increase	p
WT	261	280	279	274		
erf5erf6	410	314	369	364	33%	0.03

H_2O_2	exp.1	exp.2	exp.3	Average	% increase	p
WT	164	262	59	162		
erf5erf6	226	267	93	195	21%	0.69

NaCl	exp.1	exp.2	exp.3	Average	% increase	p
WT	257	241	230	243		
erf5erf6	285	228	213	242	0%	0.97

Supp. Table S2. Measurements of *erf5erf6* third leaves under control and osmotic stress conditions.

A. Leaf area third leaf on control medium (mm²)				
	WT	*erf5erf6*	*erf5erf6* vs. WT	p
12DAS	1,2	1,2	0%	0,975
15DAS	8,6	8,6	0%	0,984
19DAS	18,6	19,2	+3%	0,659

B. Leaf area third leaf on 25mM Mannitol (mm²)				
	WT	*erf5erf6*	*erf5erf6* vs. WT	p
12DAS	0,7	1,1	+56%	0,015
15DAS	4,7	7,2	+51%	0,0001
19DAS	11,0	17,5	+59%	0,025

C. Leaf area third leaf of WT (mm²)				
	MS	25mM Mannitol	MS vs. Mann	p
12DAS	1,2	0,7	-42%	0,038
15DAS	8,6	4,7	-45%	0,009
19DAS	18,6	11,0	-41%	0,0003
Average % reduction by Mannitol			-42%*	

D. Leaf area third leaf of *erf5erf6* (mm²)				
	MS	25mM Mannitol	MS vs. Mann	p
12DAS	1,2	1,1	-9%	0,333
15DAS	8,6	7,2	-17%	0,048
19DAS	19,2	17,5	-9%	0,4679
Average % reduction by Mannitol			-11%*	p* = 0.0004

Chapter 4

THE ETHYLENE RESPONSE FACTORS ERF6 AND ERF11 ANTAGONISTICALLY REGULATE MANNITOL-INDUCED GROWTH INHIBITION

Marieke Dubois [a,b], Lisa Van den Broeck [a,b], Hannes Claeys [a,b], Kaatje Van Vlierberghe [a,b], Minami Matsui [c] and Dirk Inzé [a,b]

[a] Department of Plant Systems Biology, VIB, Ghent, Belgium
[b] Department of Plant Biotechnology and Bioinformatics, Ghent University, Belgium
[c] RIKEN Plant Science Center, Tsurumi-ku, Yokohama, Kanagawa 230–0045, Japan

This chapter is based on a research article published in:
Plant Physiology, 2015, 166(1): 166-179

Contributions: M.D. designed and performed most experiments, and was the main author of the manuscript. L.V.d.B. performed experiments, was involved in the discussions throughout the project and contributed to the writing of the manuscript. H.C. was involved in the discussions throughout the project and contributed to the writing of the manuscript. K.V.V. performed experiments. M.M. provided plant material. D.I. supervised the project and contributed to the writing of the manuscript.

Leaf growth is a tightly regulated and complex process, which responds in a dynamic manner to changing environmental conditions, but the mechanisms that reduce growth under adverse conditions are rather poorly understood. We previously identified a growth-inhibitory pathway regulating leaf growth upon exposure to a low concentration of mannitol, and characterized the ERF/AP2 transcription factor ERF6 as a central activator of both leaf growth inhibition and induction of stress tolerance genes. Here, we describe the role of the transcriptional repressor ERF11 in relation to the ERF6-mediated stress response in Arabidopsis. Using inducible overexpression lines, we show that ERF6 induces the expression of *ERF11*. ERF11 in turn molecularly counteracts the action of ERF6 and represses at least some of the ERF6-induced genes by directly competing for the target gene promoters. As a phenotypical consequence of the ERF6-ERF11 antagonism, the extreme dwarfism caused by *ERF6* overexpression is suppressed by overexpression of *ERF11*. Together, our data demonstrate that dynamic mechanisms exist to fine-tune the stress response and that ERF11 counteracts ERF6 to maintain a balance between plant growth and stress defense.

INTRODUCTION

Plants are constantly challenged to survive and maintain growth in changing environments. In natural environments, as well as in laboratories, growth conditions are rarely optimal, generating a weak but continuous stress. In such suboptimal conditions, the equilibrium between sustained plant growth and activation of stress defense mechanisms is defied and needs to be continuously re-balanced and fine-tuned (Claeys and Inzé, 2013).

To unravel these growth- and defense-related mechanisms in Arabidopsis thaliana, researchers commonly use in vitro setups in which different growth-inhibitory compounds are added to the growth medium (Verslues et al., 2006; Lawlor, 2013; Claeys et al., 2014). Mannitol, for example, is a frequently applied compound to induce mild stress, since it results in both inhibition of leaf growth as well as activation of stress-responsive genes (Kreps et al., 2002; Skirycz et al., 2010; Skirycz et al., 2011; Dubois et al., 2013; Claeys et al., 2014; Trontin et al., 2014). Two putative receptor-like kinases, EGM1 and EGM2 (for ENHANCED GROWTH on MANNITOL), are presumably involved in the detection of mannitol and further downstream activation of the growth and tolerance responses (Trontin et al., 2014). Previously, we have shown that mannitol-induced responses are specific to the different stages of Arabidopsis leaf development (Skirycz et al., 2010). In very young Arabidopsis leaves, in which cells are

not yet expanding but still actively dividing, exposure to mannitol triggers the accumulation of the ethylene precursor 1-aminocyclopropane-1-carboxylic acid (ACC) and the transcriptional induction of ethylene-related genes. Interestingly, these responses are extremely fast, with several ETHYLENE RESPONSE FACTORs (*ERF1*, *ERF2*, *ERF5*, *ERF6*, *ERF11*) being induced in growing leaves within hours upon sudden exposure of roots to mannitol (Skirycz et al., 2011).

The ERFs are transcription factors belonging to the large AP2/ERF family of plant-specific transcription factors (Riechmann and Meyerowitz, 1998; Nakano et al., 2006). They all possess a single repeat of the well-conserved AP2 domain, which is important for DNA binding. Additionally, other small domains are conserved between several but not all ERFs, enabling a detailed classification in 12 ERF subgroups (Sakuma et al., 2002; Nakano et al., 2006). For example, the mannitol-induced ERF11 belongs to subgroup VIIIa, the members of which contain a C-terminal ERF amphiphilic repression (EAR) motif enabling transcriptional repression of the downstream targets (Ohta et al., 2001; Yang et al., 2005; Nakano et al., 2006; Li et al., 2011). The other mannitol-induced ERFs are members of the subgroups IXa (ERF1 – ERF2) or IXb (ERF5 – ERF6). These contain an N-terminally located conserved stretch of acidic amino acids (called the 2nd Conserved Motif of group IX – CMIX-2), which might function as a transcriptional activator domain. The transcriptional activators ERF5 and ERF6 additionally harbor a conserved C-terminal motif (CMIX-5) identified as a putative phosphorylation site by mitogen-activated protein kinases (MAPKs/MPKs), which distinguishes group IXa from group IXb (Fujimoto et al., 2000; Nakano et al., 2006).

ERF6 is an activating transcription factor with documented roles in the response to various abiotic and biotic stress conditions, such as oxidative stress (Sewelam et al., 2013; Wang et al., 2013; Vermeirssen et al., 2014), high light (Vogel et al., 2014), cold (Lee et al., 2005; Xin et al., 2007), and biotic stress induced by biotrophic and necrotrophic pathogens (AbuQamar et al., 2006; Dombrecht et al., 2007; Hu et al., 2008; Moffat et al., 2012; Son et al., 2012; Meng et al., 2013). We have previously unraveled the molecular and biological function of ERF6 in the mannitol-induced stress response, specifically in actively growing young Arabidopsis leaves (Dubois et al., 2013). We propose the following model: upon sudden exposure to mannitol, MPK3 and MPK6 could posttranslationally activate ERF6 and its close homolog ERF5 through phosphorylation, as has previously been reported under ROS-mediated oxidative stress (Popescu et al., 2009; Son et al., 2012; Wang et al., 2013). Active ERF6 proteins transcriptionally induce *ERF6* gene expression and act as early and central regulators of the mannitol-induced stress response. On the one hand, ERF6 transcriptionally activates the *GA2-OXIDASE6* gene, encoding an enzyme degrading bioactive gibberellins (GAs), and thus reducing cellular GA levels (Rieu et al., 2008). Through activation of GA

degradation, ERF5/ERF6 stimulate the stabilization of DELLA proteins, which in turn inhibit growth of young leaves by pushing dividing cells out of the mitotic cell cycle (Claeys et al., 2012). Under mannitol stress, ERF5/ERF6 thus induce leaf growth inhibition, and consequently, plants overexpressing *ERF6* show extreme dwarfism. On the other hand, ERF6 was found to rapidly activate 332 putative target genes, highly enriched for stress-responsive genes and for genes involved in transcriptional regulation, suggesting that ERF6 is situated upstream of a stress-related network of transcription factors. ERF6 was for example shown to directly activate the expression of genes encoding the stress tolerance-related transcription factors MYB DOMAIN PROTEIN 51 (*MYB51*), Salt Tolerance Zinc Finger (*STZ*) and *WRKY33*. Thus, on top of inhibiting Arabidopsis leaf growth, ERF6 also induces, independently of the GA/DELLA-pathway, genes involved in stress tolerance (Dubois et al., 2013).

The transcriptional repressor ERF11 has been much less studied but has been identified in several gene expression studies following different kinds of stresses. For example, *ERF11* expression is altered upon several abiotic stresses such as K^+ depletion (Hampton et al., 2004), cold exposure (Lee et al., 2005; Vergnolle et al., 2005), H_2O_2 treatment (Wang et al., 2006), and to 3-(3,4-dichlorophenyl)-1,1-dimethylurea, an inhibitor of photosynthetic electron transport (Vogel et al., 2012). *ERF11* is also known to be responsive to several hormones, especially jasmonic acid (JA) and abscisic acid (ABA), and to infection with the oomycete *Phytophthora parasitica* and with *Alternaria brassicicola* (McGrath et al., 2005; Dombrecht et al., 2007; Eulgem and Somssich, 2007; Libault et al., 2007). ERF11 is further known to be a negative regulator of ethylene biosynthesis upon increased ABA levels by directly repressing the expression of the ACC synthases *ACS2* and *ACS5*, explaining the known ABA – ethylene antagonism (Li et al., 2011). However, despite its induction by various and numerous stresses, the biological and molecular role of ERF11 in biotic and abiotic stress responses is still poorly understood.

In this study, we demonstrate that the transcriptional repressor ERF11 antagonizes the activator ERF6, providing a mechanism to maintain the balance between plant growth and stress tolerance upon stress exposure.

RESULTS

ERF6 and ERF11 are induced simultaneously by mannitol-mediated stress as well as by ACC

Previously, we have developed a mild stress assay in which young Arabidopsis seedlings were exposed to a low concentration of mannitol (25 mM), which induces a rapid leaf growth inhibition without affecting developmental timing. Using this assay, the transcription factors ERF6 and ERF11 have been shown to be transcriptionally induced by mannitol within hours upon exposure, specifically in actively growing Arabidopsis leaves (Skirycz et al., 2011). To get a better time-resolution on this expression pattern, we performed a detailed time-course experiment and measured the expression of *ERF6* and *ERF11* within minutes upon exposure to mannitol using the following experimental setup: Arabidopsis seedlings are grown in vitro on half-strength Murashige and Skoog (MS) medium overlaid with a nylon mesh until 9 days after stratification (DAS). At this moment, the third true leaf is still mainly composed of proliferating cells. The mesh with plants is subsequently transferred to growth medium supplemented with 25 mM mannitol, and the young Arabidopsis seedlings are harvested on mRNA-stabilizing solution after 5, 10, 15, 30, 45, 60, 120 and 180 min of stress exposure, followed by microdissection of the third true leaf (less than 0.1mm^2 in size). By measuring *ERF6* and *ERF11* expression levels by qRT-PCR, we show that in young Arabidopsis leaves both genes were induced simultaneously by mannitol stress already after 60 min (P_{ERF6}=0.003 and P_{ERF11}=0.002, ANOVA; Figure 4.1A). Consistent with our previous observation that mannitol rapidly induces ACC accumulation (Skirycz et al., 2011), transfer of young seedlings to 5 µM ACC-containing growth medium triggered a simultaneous up-regulation of *ERF6* and *ERF11* within 45 min of exposure (p_{ERF6}=0.002 and p_{ERF11}=0.037, ANOVA; Figure 4.1B). We also measured the expression level of *STZ*, *MYB51* and *GA2-OX6*, which are target genes of ERF6 (Dubois et al., 2013). Interestingly, the increased expression of these genes upon mannitol treatment occured simultaneously with the *ERF6* and *ERF11* induction (Supplemental Figure S1). The transcriptional induction of *ERF6* at the same time as its own target genes is consistent with our previous observations that stress-activated ERF6 proteins are able to induce both their own expression as well as that of *STZ*, *MYB51* and *GA2-OX6*. Thus, *ERF11*, *ERF6* and its target genes are induced at the same time upon treatment with mannitol in actively growing Arabidopsis leaves.

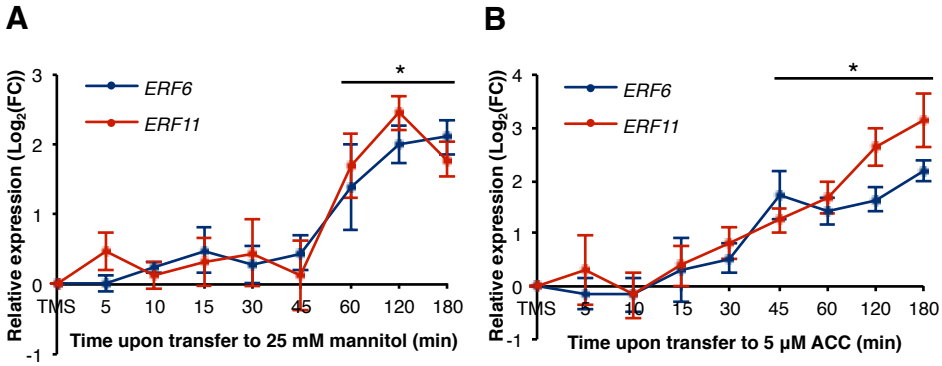

Figure 4.1. Transcriptional induction of *ERF6* and *ERF11* upon short-term exposure to mannitol or ACC. Expression levels of *ERF6* and *ERF11* in proliferating leaf tissue measured by qRT-PCR upon exposure to mild mannitol-induced stress (25 mM) (A) or 5 µM ACC (B). Represented values are means of three biological repeats with their standard error relative to the expression value upon transfer to MS (TMS) medium as a control. * = P< 0.05 (ANOVA) for both genes.

ERF6 is an activator of ERF11 expression under mannitol-mediated stress

The expression pattern of *ERF11* upon mannitol exposure is similar to that of known ERF6 target genes, raising the question whether *ERF11* is an ERF6 target gene as well. To further investigate this possibility, we first determined whether ERF6 is able to activate *ERF11* expression. To this end, 35S:ERF6-GR (ERF6-GR) line, containing a fusion between ERF6 and the glucocorticoid receptor (GR) in wild type *Col-0* background, was used (Dubois et al., 2013). If *ERF11* is a target gene of ERF6, up-regulation of *ERF11* transcripts is expected to occur rapidly upon induction of ERF6. We therefore transferred ERF6-GR plants to dexamethasone-containing growth medium (see "Material and Methods"), and measured *ERF11* transcript levels by qRT-PCR at multiple time points following induction (Figure 4.2A). *ERF11* transcript levels gradually increased within 4 h upon dexamethasone treatment to up to 2-fold (P = 0.02, ANOVA), suggesting that *ERF11* is a direct target of ERF6.

Next, activation of the ERF11 promoter (pERF11) by ERF6 was analyzed using a luciferase transactivation assay in tobacco (*Nicotiana tabacum*) protoplasts by co-transformation of 35S:ERF6 and pERF11:fLUC (firefly luciferase) constructs. The observed increase in light signal emitted by fLUC suggests that ERF6 is able to activate the promoter of *ERF11* (P<2E-16; Figure 4.2B). To further confirm this, the mannitol-mediated induction of *ERF11* was analyzed in an *erf5erf6* double mutant background (Dubois et al., 2013), as compared to wild-type plants. After 4h of exposure to mannitol, *ERF11* was 11.3-fold higher expressed in mannitol-treated wild-type plants compared to

the controls transferred to MS medium (Figure 4.2C). This clear induction of *ERF11* expression was less pronounced (P = 0.07) in *erf5erf6* mutants, where the induction by mannitol was 4.9-fold (Figure 4.2C). Together, these data show that ERF5/ERF6 are involved in the rapid induction of *ERF11* upon exposure to low concentrations of mannitol.

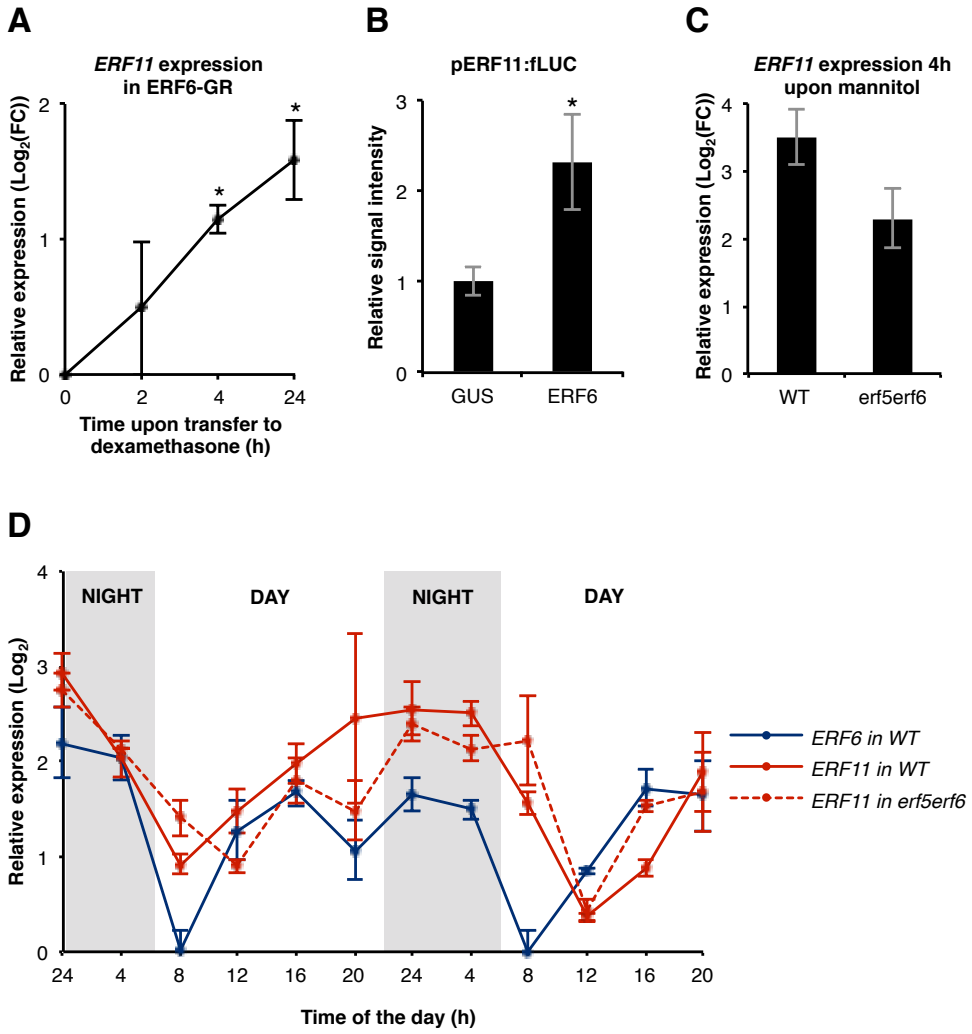

Figure 4.2. Transcriptional activation of *ERF11* by ERF6 under mannitol-induced stress. (A) Expression levels of *ERF11* in the growing third leaf (15 DAS) of ERF6-GR plants, relative to wild type, measured by qRT-PCR at several time points (h) upon transfer to dexamethasone-containing medium. * = P<0.05 (ANOVA). (B) Luciferase transactivation assay with co-transformation of 35S:ERF6 and pERF11:fLUC showing the activation of the *ERF11* promoter by ERF6. Values are signal intensities normalized to the co-transformed normalization plasmid rLUC and relative to the negative control (35S:GUS + pERF11:fLUC). * = P <0.05. (C) Expression levels of *ERF11* in wild-type plants (WT) and *erf5erf6* mutants 4 h upon exposure to mannitol. (D) Expression levels of *ERF6* and *ERF11* at different times of the day in actively growing leaves (15 DAS) of wild-type and *erf5erf6* plants grown in soil. For all graphs the represented values are the means of three biological repeats with their standard error.

The expression of the mannitol-induced ERFs was previously thought to be low under control conditions (Andriankaja et al., 2012; Dubois et al., 2013; Meng et al., 2013). However, in growing Arabidopsis leaves of plants grown in soil, we observed that this is not the case throughout the entire day, but that instead *ERF6* and *ERF11* transcript profiles show a similar, diurnal pattern (Figure 4.2D), suggesting co-regulation of both genes. *ERF6* and *ERF11* transcript levels were low in the morning and gradually accumulated until the evening. During the night, transcript levels remain stable and abruptly decreased again in the early morning. To test if the regulation of *ERF11* expression throughout the day is mediated by ERF6, the diurnal *ERF11* pattern was measured in *erf5erf6* mutants under non-stress conditions, showing a similar *ERF11* expression pattern as in wild type (Figure 4.2D). We thus conclude that ERF6 is an activator of *ERF11* under mannitol-induced stress, but that it is not responsible for the diurnal expression pattern of *ERF11* expression under control conditions.

Overexpression of ERF11 negatively affects leaf growth

Because under growth-repressive conditions, *ERF11* is induced in actively growing leaves of plants, we speculated that ERF11 might be involved in the regulation of leaf growth. To test this hypothesis, we first measured rosette growth of the homozygous line *erf11* (SALK_116053) (Alonso et al., 2003), knocked out for *ERF11* due to a T-DNA insertion in the 5' untranslated region of *ERF11*, and showing clearly reduced *ERF11* expression levels (residual *ERF11* expression on average 5%) (Supplemental Figure S2). At 22 DAS, the rosettes of *erf11* mutants were indistinguishable from wild-type rosettes (P = 0.96, ANOVA) (Figure 4.3A). Because the absence of a phenotype in the knock-out line might be due to low ERF11 activity under control conditions, we also phenotyped transgenic plants overexpressing the dexamethasone-inducible ERF11-GR construct. Rosettes of ERF11-GR plants grown *in vitro* on dexamethasone-containing medium were significantly smaller than wild-type plants (Figure 4.3A), with an average size reduction of 21% (P = 2E-5, ANOVA; Figure 4.3, A and B). The ERF11-mediated growth reduction was also visible on every individual leaf of the rosette of soil-grown plants watered with a dexamethasone solution (P = 2E-5, ANOVA; Figure 4.3C and Supplemental Figure S3A).

To investigate the effect of overexpressing *ERF11* on leaf development in more detail, 35S:ERF11-GR and WT plants were grown on MS medium and dexamethasone-treatment was started at 9 DAS, when all cells of the third leaf are actively proliferating, and the size of the third leaf was measured every day until 20 DAS. Leaf growth inhibition started to be visible at 18 DAS, i.e. after 9 days of overexpression of *ERF11* (Figure 4.3B). To unravel the cellular mechanism behind this growth reduction, cell number and cell area of the harvested leaves were measured at 20 DAS. Leaves of plants overexpressing *ERF11* showed a 16% decrease in cell area (P = 0.01, ANOVA) and a 18%

reduction in cell number (P = 0.01, ANOVA; Figure 4.3D). Together, these data show that ERF11 has the capacity to repress leaf growth by negatively affecting cell area and number.

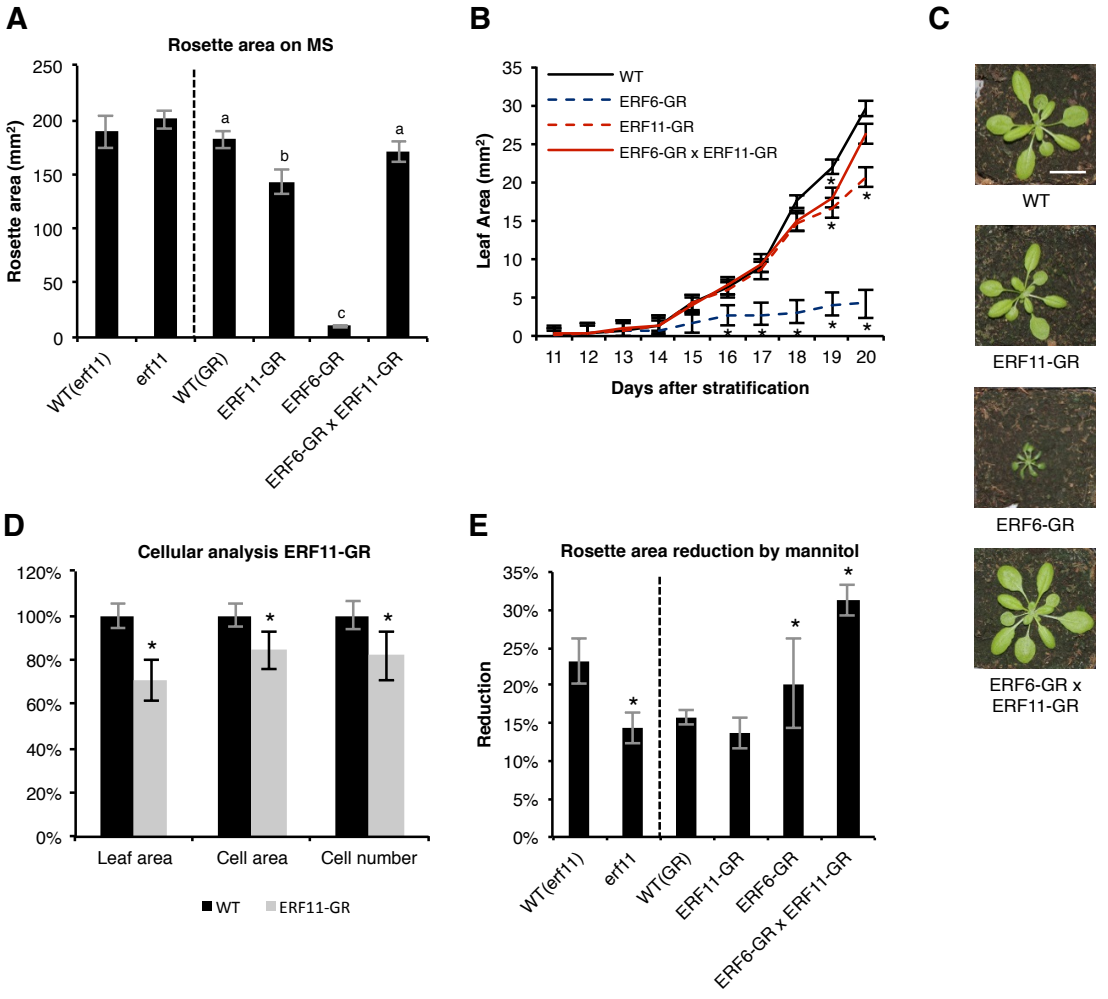

Figure 4.3. ERF11 regulates Arabidopsis leaf growth under mannitol-induced stress conditions. (A) Projected rosette area at 22 DAS of the *erf11* mutant and the dexamethasone-inducible overexpression lines of *ERF6* (ERF6-GR), *ERF11* (ERF11-GR) and of both in ERF6-GR x ERF11-GR double homozygous plants, grown under control conditions (medium supplemented with dexamethasone for the GR-lines). Represented values are the means of three biological repeats with their standard error. * = P <0.05 compared with WT. (B) Size of the third true leaf over time of the GR-lines described in (A) upon exposure to dexamethasone from 9 DAS onward. * = P <0.05 (ANOVA) compared with WT. (C) Rosettes of the GR-lines described in (A) grown in soil for 22 days and watered with a dexamethasone-containing solution. Scalebar = 2 cm. (D) Cellular measurements of the abaxial side of the third leaf of WT and ERF11-GR at 20 DAS from the plants shown in (B). * = P <0.05 compared with WT. (E) Reduction in rosette area caused by growth for 22 days on medium supplemented with 25 mM mannitol, compared with the rosette area of the same line grown under control conditions. Error bars represent the standard error of three biological repeats. * = P <0.05 (ANOVA) compared with WT.

Finally, since *ERF6* and *ERF11* are co-regulated and since the ERF6-GR line has previously been reported to inhibit leaf growth as well (Dubois et al., 2013), we further explored whether both transcription factors could act together to regulate leaf growth. We therefore crossed the 35S:ERF6-GR line with the 35S:ERF11-GR line and selected plants that were homozygous for both constructs and that expressed the respective constructs as high as the single homozygous lines (Figure 4.4A). Although both individual lines showed respectively strong and mild growth inhibition when grown on dexamethasone, surprisingly, when both *ERF6* and *ERF11* are overexpressed simultaneously, the extreme dwarfism induced by ERF6 is almost completely abolished and the rosette area is again comparable with wild type (Figure 4.3A). This rescue of the phenotype was observed both in experiments conducted *in vitro* (Figure 4.3A) and in soil (Figure 4.3C), under long-term (Figure 4.3A) and short-term (Figure 4.3B) dexamethasone treatment, and holds for all rosette leaves (Supplemental Figure S3B). Taken together, these results demonstrate that ERF6 and ERF11 are able to negatively affect leaf growth individually, while simultaneous overexpression of both transcription factors releases this growth inhibition.

ERF11 is involved in the regulation of leaf growth under mild stress

To explore whether ERF11 is involved in leaf growth inhibition under stress, we phenotyped ERF11 loss- and gain-of-function lines under growth-limiting conditions mediated by low concentrations of mannitol. After 22 days of growth, the rosette size on mannitol was reduced by 14% in erf11 and by 23% in wild type as compared with the rosette area of the corresponding line on control conditions (Figure 4.3E). Thus, erf11 mutants are more tolerant to mannitol ($P = 0.02$; ANOVA), indicating that ERF11 plays a role in leaf growth regulation under mannitol-induced growth-limiting conditions. For the ERF11-overexpressing plants, however, exposure to mild stress caused a growth inhibition comparable with the mannitol-induced growth reduction observed in wild-type plants (14% and 16% respectively; $P = 0.7$; ANOVA) (Figure 4.3E). This shows that ERF11-overexpressing plants are equally sensitive to mannitol-induced stress and that overexpression of ERF11 does not mimick mannitol-induced growth inhibition. In contrast, ERF6-overexpressing plants were previously shown, using a weaker ERF6-overexpression line with a milder phenotype, to be hypersensitive to mannitol (Dubois et al., 2013). Interestingly, when 35S:ERF6-GR x 35S:ERF11-GR plants were grown on medium supplemented with mannitol, the reduction in leaf growth was also more pronounced than in WT plants (31% versus 16% for WT; $P = 0.02$; ANOVA). Taken together, these data demonstrate that ERF11 and ERF6 are both involved in the regulation of leaf growth inhibition under stress.

At the molecular level, ERF6 and ERF11 compete for common target genes

Since ERF6 is a transcriptional activator and ERF11 a transcriptional repressor, we reasoned that simultaneous induction of both transcription factors by stress could generate a possible antagonism and competition for common target genes. We therefore transferred the double homozygous ERF6-GR x ERF11-GR line and the appropriate controls to dexamethasone-containing medium and measured in the actively growing third leaf the expression level of the ERF6 target genes: *GA2-OX6*, *MYB51*, *WRKY33* and *STZ* (Dubois et al., 2013). In the ERF6-GR line, these target genes were induced within 4 h upon dexamethasone treatment ($P < 0.05$) (Figure 4.4A). In contrast, overexpression of only *ERF11* (ERF11-GR) did not affect the expression of these genes. Interestingly, when ERF11 was co-overexpressed with *ERF6* (ERF6-GR x ERF11-GR), the expression of the target genes was not induced by dexamethasone, and thus, these genes were no longer induced by ERF6 within the measured time frame (Figure 4.4A).

Multiple molecular models can explain this antagonistic relationship between ERF6 and ERF11. First, ERF11 could directly repress the expression of *ERF6* and thereby indirectly repress the induction of the ERF6 target genes. However, neither expression analyses of ERF6 in the ERF11-GR line upon dexamethasone treatment, nor promoter-binding assays of 35S:ERF11 on pERF6:fLUC support this hypothesis (Supplemental Figure S4). Second, ERF6 and ERF11 could form heterodimers, which would be responsible for the repressive function on the promoters of the genes targeted by ERF6. Third, ERF11 could physically withhold ERF6 proteins from their targets, indirectly inhibiting their induction. Both hypotheses imply physical interaction at the protein level between ERF6 and ERF11. However, despite successive attempts using quantitative yeast 2-hybrid (Y2H) assays to measure putative interactions between ERF6 and ERF11, no protein-protein interactions between both transcription factors could be detected (Supplemental Figure S5). Finally, ERF11 could directly compete with ERF6 for binding on the promoter of target genes. To test this hypothesis, we first performed multiple protoplast activation assays using fusions of the promoters of the known ERF6 target genes with the gene encoding fLUC (pSTZ:fLUC, pMYB51:fLUC and pWRKY33:fLUC) and co-transformed each of them with either 35S:ERF6, or 35S:ERF11, or a combination of both in a 1:1 ratio. As expected, transformation with ERF6 alone caused an increase in signal intensity, strongly suggesting activation of the promoters of the three target genes. In contrast, upon transformation with ERF11 alone, the signal intensity did not increase and even showed a weak, but significant and reproducible, reduction for pMYB51 and pWRKY33 (Figure 4.4B). Upon co-transformation with both transcription factors, only a slight activation of the three reporter constructs was observed.

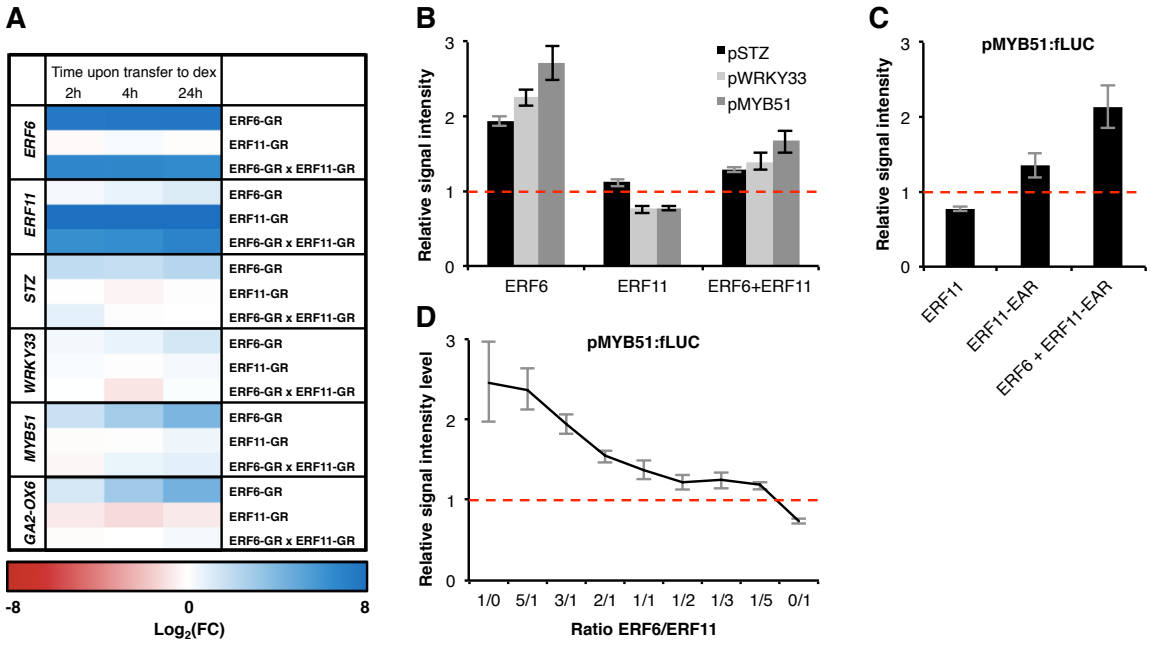

Figure 4.4. ERF6 and ERF11 antagonistically regulate common target genes. (**A)** Expression levels of ERF6, ERF11 and the ERF6 target genes in dexamethasone-inducible overexpression lines of *ERF6* (ERF6-GR), *ERF11* (ERF11-GR) and of both in ERF6-GR x ERF11-GR double homozygous plants. Expression values are the average of at least three biological repeats. Values are relative to the expression level in WT plants subjected to the same treatment. (**B)** Protoplast activation assay with pSTZ:fLUC, pWRKY33:fLUC and pMYB51:fLUC for binding and effect of ERF6, ERF11 and a combination of both in a 1:1 ratio. (**C)** Protoplast activation assay on the promoter of *MYB51* for the native ERF11 protein, a truncated ERF11 in which the repressive EAR-domain has been removed, and a combination in a 1:1 ratio of ERF6 and the truncated ERF11. (**D)** Titration protoplast activation assay on the promoter of *MYB51* with multiple concentrations of ERF6 and ERF11. For B, C, and D, values are signal intensities normalized to the co-transformed normalization plasmid rLUC and relative to the negative control (35S:GUS + pTARGET:fLUC, horizontal line). Values represent the average of at least two biological repeats with their standard error.

To further confirm these indications that ERF11 would bind and repress the promoters of the ERF6 target genes rather than withholding ERF6 from activating the targets, we generated a truncated variant of ERF11 in which the EAR-domain was removed. The signal intensities using ERF11-EAR were always higher than the signal obtained with native ERF11, and the truncated ERF11 was unable to inhibit the activation by ERF6 when co-transformed in a 1:1 ratio (Figure 4.4C). Finally, to further quantify the strength of the transcriptional activation and repression by ERF6 and ERF11, respectively, we performed a titration assay using pMYB51:fLUC (the promoter on which ERF6 and ERF11 had the most pronounced effect) in combination with multiple ERF6/ERF11 ratios (Figure 4.4D). The ability of ERF6 to activate the expression of pMYB51:fLUC gradually decreased with rising ERF11 concentrations. The decrease holds until a 1:1 ratio was reached, when protoplasts were transfected with an equal

concentration of 35S:ERF6 and 35S:ERF11. Further increase in ERF11 concentration did then no longer dramatically decrease the ability of ERF6 to activate the pMYB51:fLUC signal, which reached a plateau. Only when no ERF6 was present did become visible the absolute repression of the pMYB51 by ERF11. Based on these experiments, we conclude that ERF11 antagonizes ERF6 function most likely through direct competition for the same promoters and plausibly the same cis-regulatory elements. The resulting effect on target gene expression depends on the abundance of each of the transcription factors, and the activation by ERF6 appears to be stronger than the repression by ERF11, which occurs through the presence of the EAR-domain.

At least two parallel pathways are upstream of ERF6 and ERF11

Recently, two receptor-like kinases, EGM1 and EGM2, were shown to be involved in the mannitol-induced growth inhibition and were suggested to act upstream of the ERF5/ERF6 pathway (Trontin et al., 2014). The latter study analyzed *egm1* and *egm2* mutants on higher concentrations of mannitol (60 mM), which not only restrict plant growth, but also induce clear stress symptoms (narrow and curling leaves). Therefore, we first phenotypically characterized the *egm1* and *egm2* mutant on 25 mM mannitol. Since EGM1 and EGM2 are tandem-duplicated genes, no double *egm1egm2* mutant is available, but both genes are not fully redundant (Trontin et al., 2014). Surprisingly, although *egm1* and *egm2* did, as reported, tolerate high mannitol concentrations (60 mM; respectively 43% and 39% larger rosettes than the wild type; $P < 0.05$) significantly better, they were not significantly more tolerant to the mild mannitol concentration (25 mM) (Supplemental Figure S6A). In contrast, the *erf5erf6* mutant grew significantly better than the wild type under low mannitol stress conditions ($P < 0.05$, ANOVA) (Dubois et al., 2013), but not on higher mannitol concentrations (Supplemental Figure S6B). These differential growth responses to mannitol suggest that the EGMs and ERF5/ERF6 are not directly involved in the same linear pathway. The observation that both *egm* mutants show a growth reduction of on average 21% and 49% under 25 mM and 60 mM mannitol stress, respectively, as compared with growth on MS, further indicates that EGM1 and EGM2 are not solely responsible for leaf growth reduction by mannitol, but that instead, multiple pathways are controlling the mannitol-induced leaf growth inhibition.

EGM1 is known to be transcriptionally induced by 60 mM mannitol in growing leaves (Trontin et al., 2014), thus in the same tissue as in which *ERF5*, *ERF6*, and *ERF11* are induced. Therefore, we further explored the exact timing of the induction of *EGM1* upon mannitol stress and measured the *EGM1* transcript levels upon short-term exposure to 25 mM mannitol (as above). Surprisingly, the short-term mild mannitol treatment did not increase the *EGM1* transcript level within the measured time frame (from 5 min to

180 min) (Supplemental Figure S7A). This is consistent with the short-term expression data from Skirycz et al. (2011), where the *EGM* transcript is only significantly induced 12 h upon mannitol (2-fold induction at 24 h), but not at 1.5 h nor at 3 h (Supplemental Figure S7B). Thus, these results demonstrate that *EGM* genes are not transcriptionally induced by mannitol in actively growing leaves within the same time frame as *ERF6* and *ERF11*.

Finally, we analyzed whether *ERF5*, *ERF6* or *ERF11* expression was modified in the *egm1* and *egm2* mutant backgrounds. To this end, *egm1* and *egm2* mutants were exposed to long-term mannitol (25 mM and 60 mM) treatment, and *ERF5*, *ERF6* and *ERF11* transcript levels were measured by qRT-PCR. Under long term severe mannitol stress, the expression level of the selected *ERF* genes was significantly lower (on average 40%) in the *egm1* mutant than in the wild type, and the same tendency was found for the *egm2* mutant (Supplemental Figure S8C). Surprisingly, under control conditions, the *ERF6* expression level in the *egm1* mutant was slightly, but significantly, higher (34%) than in the wild type (Supplemental Figure S8A). Moreover, the expression of *ERF6* and *ERF11* in the *egm1* mutant under low mannitol concentrations were down-regulated to levels lower than under control conditions (25% and 66%, respectively; $P < 0.05$), whereas levels similar to control conditions would be expected in the case of a simple linear, activating EGM/ERF pathway (Supplemental Figure S8B). Thus, although these results indeed suggest that EGMs are involved in the regulation of *ERF* expression under severe mannitol stress, the EGM/ERF pathway is not linear and might act in parallel with other pathways.

DISCUSSION

As demonstrated before, low concentrations of mannitol trigger a dual response in young Arabidopsis leaves. Mannitol induces, on the one hand, a rapid inhibition of leaf growth and, on the other hand, the transcriptional activation of a plethora of stress-responsive genes (Skirycz et al., 2010; Skirycz et al., 2011; Dubois et al., 2013; Trontin et al., 2014). This transcriptional response, involving more than 1,500 genes in growing leaves, is thought to be established through transcriptional cascades. In a simplified view, one or a few early transcription factors activate multiple other regulators, which in turn activate their own target genes. To unravel the sequential steps of these cascades and to distinguish the early players from late-induced stress-responsive genes, we opted in our previous research and in the presented manuscript for time-course experiments following sudden exposure to mannitol (Skirycz et al., 2011; Claeys et al., 2012). As described previously, ERF5 and ERF6 are among the few early regulators induced by

mannitol and regulate more than half of the early mannitol-induced genes (Skirycz et al., 2011; Dubois et al., 2013). Here, we show that *ERF11* is induced in growing leaves at the same timing as *ERF6*, within one hour upon sudden exposure to mannitol.

ERF6 induces ERF11 under mannitol stress in growing leaves

Although the mechanisms that activate the ERF6 protein under stress start to be unraveled (Son et al., 2012; Dubois et al., 2013; Wang et al., 2013), much less is known about how *ERF11* is induced by mannitol. Since *ERF11* and the known ERF6 target genes are induced simultaneously by mannitol, we tested the hypothesis that *ERF11* could be a target gene of ERF6 by expression analysis with qRT-PCR and a luciferase assay, and indeed confirmed the induction of ERF11 by ERF6. Because it is rather counterintuitive that the activator (ERF6) and its targets are induced simultaneously, it is important to emphasize that ERF6 is first activated posttranslationally upon stress and subsequently activates its downstream target genes, as well as its own expression. Thus, in growing leaves of plants exposed to mannitol, *ERF11* and *ERF6* are induced simultaneously, since both transcripts are activated by ERF6. We further used this co-expression as a characteristic to explore whether ERF6 could activate *ERF11* under other stress conditions. A clear co-expression (Pearson correlation coefficient = 0.73) was observed between ERF6 and ERF11 under numerous biotic and abiotic stress conditions (Supplemental Figure S9) (Dombrecht et al., 2007; Hruz et al., 2008). Interestingly, a fast and simultaneous induction of *ERF6* and *ERF11*, similarly to our findings upon mannitol-induced stress, has been reported during short-term cold treatment, where ERF6 and ERF11 were identified among the very few early (74 genes after 3 h treatment) cold-responsive genes (Lee et al., 2005), and after 15-min treatment with the chitin-mimicking compound chito-octaose (Libault et al., 2007). In general, a meta-analysis of available stress datasets showed that *ERF5*, *ERF6*, *ERF11*, as well as *STZ* and *WRKY33* all belong to a confined group of 197 genes differentially expressed in more than 80% of the stress-related datasets, suggesting that they belong to a core set of general stress-responsive genes (Ma and Bohnert, 2007).

The regulators upstream of ERF11 are diverse and context-dependent

Several other transcription factors have been proposed to transcriptionally regulate ERF11 in different developmental contexts. The MULTIPROTEIN BRIDGE FACTOR 1c (MBF1c), a transcriptional co-activator, has been suggested to act upstream of ERF11 expression, since *ERF11* transcript levels were increased in MBF1c overexpression lines, although no evidence of direct regulation was provided (Suzuki et al., 2005). Among the genes induced upon MBF1c overexpression (steady state), *ERF6* and several ERF6 target

genes, such as *GA2-OX6* and *WRKY33*, were found, so it cannot be excluded that ERF6 also induced these genes as a secondary effect of MBF1c overexpression. Another identified candidate for transcriptional activation of *ERF11* is the ELONGATED HYPOCOTYL5 (HY5), a bZIP transcriptional activator involved in hypocotyl growth (Lee et al., 2007; Song et al., 2008; Li et al., 2011). HY5 has been shown to bind the *ERF11* promoter *in vivo* through its preferential CACGTG binding sequence, present in the 1 kb region upstream of the ERF11 coding sequence. The *ERF11* transcript levels have also been shown to be decreased in the *hy5* mutant, which might indeed be consistent with the more pronounced hypocotyl growth of this mutant, since ERF11 is able to negatively affect growth. Hypocotyl growth is primarily driven by cell expansion (Boron and Vissenberg, 2014; Ragni and Hardtke, 2014), a process that ERF11 is able to control. Finally, the MYC2/JIN1 bHLH transcriptional repressor has been proposed to be a negative regulator of *ERF11* expression during the jasmonic acid-mediated response by binding the same CACGTG box in the *ERF11* promoter (Dombrecht et al., 2007). Thus, multiple transcription factors have been proposed as regulators of *ERF11* expression in different developmental or environmental contexts, and for HY5, MYC2/JIN1 and ERF6, direct regulation has been found. In contrast to *ERF6*, neither *MYC2/JIN1* or *HY5* are induced in growing leaves by low concentrations of mannitol, and under stress, *ERF11* is less co-expressed with these regulators than with ERF6 (Supplemental Figure S9). Therefore, we conclude that *ERF11* is transcriptionally regulated by different transcription factors depending on the context, and that ERF6 might be one of the activators of *ERF11* under several stresses and particularly under mannitol-induced stress.

Competition for the same promoters at the molecular basis of the ERF6-ERF11 antagonism

ERF11 is known as a transcriptional repressor, since it possesses an EAR domain (Ohta et al., 2001; Yang et al., 2005; Nakano et al., 2006; Li et al., 2011). The simultaneous induction of a transcriptional activator and repressor suggests the presence of a regulatory network in which the repressor could attenuate the response induced by the activator. Our experimental data support this hypothesis: in a transgenic line overexpressing both transcription factors, ERF11 is able to suppress the ERF6-mediated activation of the downstream genes. In a transactivation assay, competition for the promoter of common target genes was shown to occur, resulting in either activation by ERF6 or repression by ERF11 in a concentration-dependent way. Furthermore, the growth-inhibitory pathway induced by ERF6 was no longer activated when both *ERF6* and *ERF11* were overexpressed and the plants overexpressing both transcription factors did no longer show the ERF6-induced dwarfism. Similar antagonistic relationships

between two or more regulatory proteins controlling growth and stress defense have been described in relation to both biotic and abiotic stress. Generally, the activator and repressor are both transcriptionally induced by the stress, and this also holds true for *ERF6* and *ERF11*. For example, upon infection with *Pseudomonas syringae*, effector-triggered immunity mechanisms induce both activators of defensive mechanisms, i.e. rps4-RLD1 and several TCP transcription factors, as well as the repressor SRFR1 (Kim et al., 2014). In a similar way, exposure to UV-B-induced stress induces both *HY5* and *UVR8* as activators and *RUP1* and *RUP2* to antagonize UVR8, although it should be noted that in this example, RUP1 and RUP2 are not transcription factors (Gruber et al., 2010). In both examples, however, the antagonism was established through heterodimerization of the activating and repressing regulatory proteins, resulting in a repressive complex which blocks further stress response. Despite several attempts, we did not detect heterodimerization between ERF6 and ERF11. Moreover, our data showed that ERF11 uses its EAR domain to repress gene expression, and that the truncated ERF11 without EAR is unable to counteract the activation by ERF6, demonstrating that ERF6 sequestration by ERF11 is unlikely to be at the basis of the competition. Heterodimerization between ERFs is however known to exist and has previously been reported for ERF5 and ERF6 (Son et al., 2012). This interaction was therefore included as a positive control in our assays, but could not be validated. Thus, antagonistic relationships between an activating and a repressing transcription factor occur both under biotic and abiotic stress to temper the stress response and can be conferred at the molecular level both through protein-protein interaction and through competition for shared target genes.

Multiple players act upstream of the ERF6-ERF11 regulon

Upstream of the ERFs, multiple pathways have previously been identified in different contexts and might therefore induce the transcriptional cascade under mannitol stress. First, a phosphorylation cascade working downstream of the ethylene receptors and mediated through MPK3 and MPK6 has been shown to phosphorylate and thereby activate ERF6 in other abiotic stress contexts (Popescu et al., 2009; Son et al., 2012; Wang et al., 2013). Supporting the involvement of this ethylene-mediated pathway in actively growing leaves of plants exposed to mannitol, the time-course experiments showed that ACC induced *ERF6* and *ERF11* more rapidly than mannitol, which is consistent with our previously proposed model, in which mannitol first triggers the accumulation of ACC, which in turn activates several ERFs (Skirycz et al., 2011). However, a recent study identified two putative receptor-like kinases, EGM1 and EGM2, as possible activators upstream of the mannitol-induced ERFs (Trontin et al., 2014). If so, our results suggest that their activation by mannitol should occur at the

posttranscriptional level, since it was shown that their transcriptional induction was much slower than the up-regulation of the ERFs. Furthermore, phenotypic analysis of *egm1*, *egm2* and *erf5erf6* mutants under control conditions and mild and severe mannitol stress demonstrated that the *egm* mutants did not phenocopy the *erf5erf6* mutant under stress: the *egm* mutants were more tolerant to severe stress, the *erf5erf6* mutant more to mild stress. Based on these results, we speculate that *ERF5* and *ERF6* are induced by low mannitol concentrations and regulate growth under these conditions, while EGM proteins are more likely to be involved in tolerance against more severe stress levels. Thus, although EGM proteins and ERF5 and ERF6 are all involved in mannitol-induced stress response, it is unlikely that they act in a same linear pathway. The reduced *ERF5*, *ERF6* and *ERF11* expression levels in *egm* mutants grown on high mannitol concentrations nonetheless indicate that the EGM proteins are involved in the activation of these ERFs. Thus, although the way how EGMs might regulate ERF expression under mannitol stress still remains highly elusive, our experiments demonstrate that several pathways interact at multiple levels, probably in a concentration-dependent manner, rendering the stress response extremely complex.

A model for the antagonism between ERF6 and ERF11 in the regulation of leaf growth under stress

Based on our results, we propose the following model for the role of ERF6 and ERF11 in the regulation of leaf growth under stress (Figure 4.5). Prior to stress, *ERF11* and *ERF6* are lowly expressed and their expression varies throughout the day. ERF11, which to our knowledge does not possess any putative phosphorylation site for posttranslational regulation (Nakano et al., 2006), is likely to be active and restricts the expression of *GA2-OX6* and the stress-responsive genes such as *MYB51*. ERF6, in contrast, is known to need activation through phosphorylation by MPK3 and MPK6 in order to activate downstream targets (Son et al., 2012; Meng et al., 2013; Wang et al., 2013). However, since growth conditions are never optimal, low levels of ERF6 proteins are probably sporadically phosphorylated. In this low-level of stress context, the sporadically activated ERF6 proteins cannot compete with the ERF11 repressive proteins. Plant growth is sustained, since the ERF6/ERF11 balance is equilibrated. Disturbing this balance by, for example, overexpressing only ERF6 or ERF11 clearly affects leaf growth, while overexpression of both restores the balance and thereby growth. When plants gradually perceive stress, rising but still mild stress levels cause phosphorylation of ERF6 and the ratio of active ERF6 is likely to dramatically increase, resulting in out-competition of ERF11 by ERF6 on the promoters of their target genes, and in a net activation of the targets by ERF6. Indeed, as demonstrated by luciferase assays, activation of targets by ERF6 was stronger than repression by ERF11 when ERF6 levels

exceeded ERF11 levels. Thereby, growth is blocked and defense mechanisms are activated to safeguard plant survival. However, higher amounts of active ERF6 proteins also generate the production of more ERF11 proteins. When stress levels are again declining, this relatively high amount of ERF11 proteins is able to rapidly block the stress response when ERF6 activity levels are decreasing, in order to rapidly switch off the stress response when it becomes unnecessary.

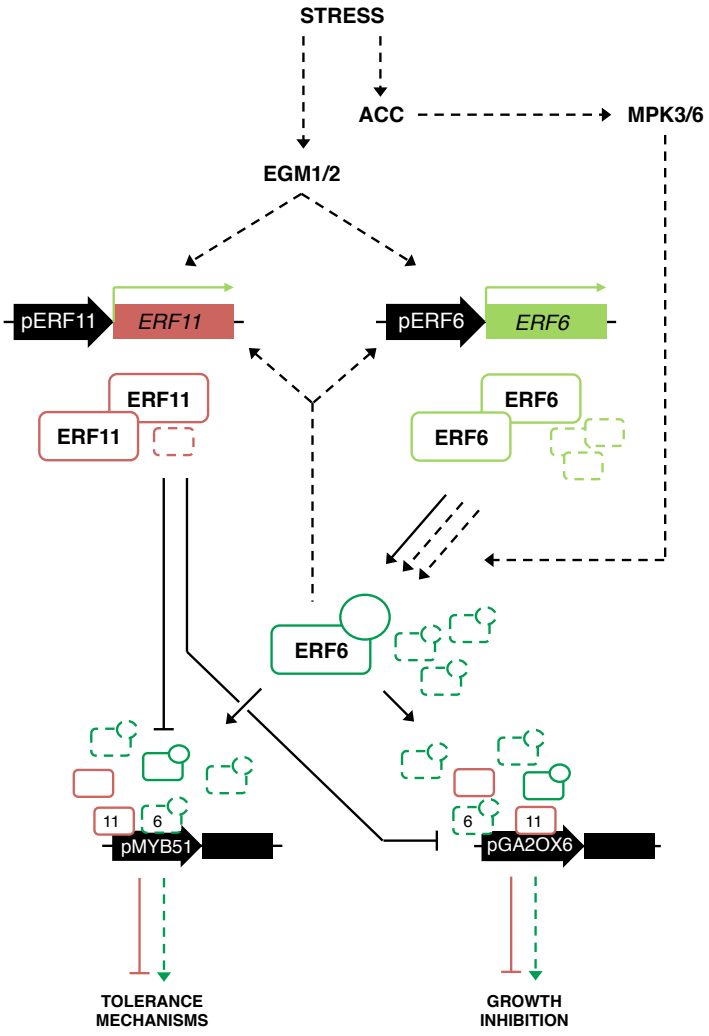

Figure 4.5. Schematic overview of the putative roles of ERF6 and ERF11 under stress. Under basal levels of stress (plain arrows and proteins), *ERF11* and *ERF6* are lowly expressed. Low levels of ERF11 proteins are sufficient to repress the activation of the stress response mechanisms as they are likely more abundant than the active, phosphorylated ERF6 proteins. Under higher stress levels (dotted arrows and proteins), ACC accumulates and MPK3/6 phosphorylate and thereby activate ERF6. ERF6 now outcompetes ERF11 proteins on the promoter of the target genes, activating tolerance mechanisms and growth inhibition. However, ERF6 also transcriptionally activates *ERF11*, increasing ERF11 protein levels which enables a rapid inhibition of the stress response when the stress levels decrease. P, phosphorylation residue.

The ERF6-ERF11 loop may be a general module to fine-tune stress responses

The literature also contains many examples of studies, mainly biotic stress-related, in which *ERF6* and *ERF11* were found among the differentially expressed genes, although the experiments were not conducted on growing leaves, but rather on mature leaf tissue or complete seedlings (McGrath et al., 2005; AbuQamar et al., 2006; Dombrecht et al., 2007; Eulgem and Somssich, 2007; Libault et al., 2007; Ma and Bohnert, 2007; Hu et al., 2008; Moffat et al., 2012; Son et al., 2012; Meng et al., 2013; Vermeirssen et al., 2014). In brief, ethylene and the described ERFs are generally induced in response to necrotrophic pathogens such as *Botrytis cinerea* and control the expression of the plant defensive proteins *PDF1.1* and *PDF1.2*. Moreover, the described target genes of ERF6 and ERF11, i.e. *STZ*, *WRKY33* and *MYB51*, were reported to be involved in tolerance against biotic stress as well. This suggests that the presented regulatory network might be active in a broader context than growing leaf tissue. Thus, we speculate that the described balance might also be involved in mature leaves to avoid uncontrolled activation of the defensive response upon biotic stress exposure. Because mannitol is a molecule secreted by fungal pathogens during the infection process (Trontin et al., 2014), it might mimick such a biotic stress response in vitro. At low concentrations, mannitol was found to induce the presented regulatory network only in actively growing leaves, but at higher concentrations, the ERFs were also induced in complete seedlings. Thus, the presented ERF-centered network might be functional during different developmental stages of leaf growth, depending on the severity of the stress. For this reason, future studies to elucidate the role of ERF6 and ERF11 in different stress contexts and different tissue should take development, stress levels and timing into account, not confounding growing leaves and in seedlings, low stress levels and severe stress, and the short-term stress response and the long-term adaptive response, since it is likely that the subtle balance between plant growth and stress defense is regulated in a specific way in these different contexts.

CONCLUSIONS

In this study, we uncovered the presence of a negative feedback mechanism to balance growth and defense upon exposure to mild mannitol-induced stress. We demonstrated that the transcriptional repressor ERF11 is able to counteract the action of the activator ERF6 by inhibiting their common target genes in a dose-dependent manner. Further investigations are, however, necessary to elucidate the exact mechanism occurring in leaves and should include analysis for competition on the same cis-regulatory elements

and *in planta* protein-protein interaction studies. We speculated that inhibition of the downstream responses by ERF11 ensures sustained growth under low-stress conditions. Upon sudden exposure to mannitol, the expression of both transcription factors is induced simultaneously in growing Arabidopsis leaves, activated upstream by both an ethylene-mediated cascade and through a mannitol receptor-mediated pathway. In these stress conditions, the balance is shifted toward extensive activation of ERF6, the levels of which increase exponentially through an auto-activation loop, causing the activation of the growth-inhibitory pathway and the induction of downstream tolerance-related transcription factors. In parallel, the activation of the repressive factor ERF11 functions as a brake to counteract the ERF6-driven activation and to ensure proper restoration of the balance when the stress levels are again decreasing. Consistently, the generation of transgenic plants in which the balance is disturbed in one or the other direction generates plants with pronounced growth penalties, while plants overexpressing both the activator and the repressor have a re-equilibrated balance and therefore normal growth phenotypes. The described balance likely occurs in all shoot tissues and conditions where *ERF6* and *ERF11* are expressed, but might fulfil different functions and therefore result in a specific outcome depending on the exact context. In actively growing Arabidopsis leaves, it provides a tightly regulated, but flexible, system to control leaf growth in a dynamic way upon continuously changing environmental stress conditions.

MATERIALS AND METHODS

Plant lines

The single *erf5*, *erf6* and *erf11* mutants were obtained from the SALK collection, references SALK_076967 (*erf5*), SALK_030723 (*erf6*) and SALK_116053 (*erf11*). The *egm1* and *egm2* mutants were described by Trontin et al. (2014) and were kindly provided by Prof. Olivier Loudet. All lines used are in Col-0 background.

Soil plant growth conditions and individual leaf area measurements

Plants were grown in Gottinger pots (8x8x8.5cm) filled with soil (Saniflor, without osmocot) at 21˚C under a 16-h day (110 µmol m-2 s-1) and 8-h night regime. Pots were covered with transparent plastic foil for 4 days to stimulate germination. Watering with 15 mL of water was applied at 9, 13, 16 and 20 DAS. In experiments in which GR-lines were used, plants were watered with 15 mL of a 15 µM dexamethasone-containing solution. For leaf size measurements, twelve plants were grown per line and the transgenic lines were always grown together with the appropriate control on the same

tray and randomization was done between the genotypes. At 22 DAS, plants were harvested and leaf series were made by cutting each individual leaf of the rosette and ranking them from old to young on a square agar plate. Plates were photographed and pictures were subsequently analyzed using ImageJ v1.45 (NIH; http://rsb.info.nih.gov/ij/) to measure the size of each individual leaf.

In vitro plant growth conditions and experiments

Seedlings were grown in vitro on half-strength MS medium (Murashige and Skoog, 1962) containing 1% sucrose at 21˚C under a 16-h day (110 µmol m-2 s 1) and 8-h night regime. For long-term experiments without transfer, 9 g/L agar was added to the medium. To facilitate transfer for the short-term experiments, 6.5 g/L agar was used and the growth medium was overlaid with a nylon mesh (Prosep, Zaventem, Belgium) of 20 µm pore size. For leaf growth experiments and expression analyses, 32 and 64 seeds, respectively, were distributed equally on a 14 cm diameter petri dish. To enable correct comparisons, the different lines were always grown together on one plate with the appropriate control.

Exposure to long-term mannitol stress and rosette growth analysis

For long-term exposure to mannitol stress, plants were grown on half-strength MS medium containing 9 g/L agar and 25 mM or 60 mM mannitol and plates were photographed at 22 DAS. The pictures were subsequently analyzed using ImageJ v1.45 (NIH; http://rsb.info.nih.gov/ij/) to measure the size of each individual rosette.

Exposure to short-term mannitol stress or ACC- and DEX-induced expression of ERF6 and/or ERF11

Arabidopsis seedlings were grown in vitro on half-strength MS medium overlaid with a nylon mesh until the third leaf had completely emerged from the shoot apical meristem but was still in a fully proliferative stage, at 9 DAS (except for the experiments performed for Figure 4.4A, where the transfer was done at 15 DAS). At this time point, the mesh with plants was transferred to plates with half-strength MS medium containing 25 mM mannitol (plant culture tested, Sigma), 5 µM ACC (Sigma), or 5 µM dexamethasone (Sigma).

For expression analysis performed for Figure 4.1, the young Arabidopsis seedlings were harvested in after 5, 10, 15, 30, 45, 60, 120 and 180 min of stress exposure, followed by microdissection of the third true leaf for leaf growth analysis (<0.1 mm2 in size).

Leaf growth analysis

Leaf growth analysis over time was performed on the third true leaf harvested at different time points after transfer to Dexamethasone. After clearing with 70% ethanol, leaves were mounted in lactic acid on microscopic slides. For each time point, about 15-20 leaves per genotype were photographed with a binocular, and abaxial epidermal cells (100-200) were drawn for three representative leaves with a DMLB microscope (Leica) fitted with a drawing tube and a differential interference contrast objective. Photographs of leaves and drawings were used to measure leaf area and cell size, respectively, using ImageJ v1.45, and average cell numbers were calculated by dividing the leaf area by the drawn area followed by multiplication of this factor with the number of drawn pavement cells. Calculated cell areas were ln-transformed prior to all subsequent analyses.

Expression analysis (qRT-PCR)

RNA samples were obtained from three independent experiments and from multiple plates within each experiment. For the experiments depicted in Figure 4.1, whole seedlings were harvested rapidly and submerged in 6 mL of the mRNA-stabilizing RNAlater® solution (Ambion) and, after overnight storage at 4˚C, dissected under a binocular microscope on a cooling plate with precision micro-scissors. Dissected leaves were transferred to a new tube, frozen in liquid nitrogen, and ground with a Retsch machine and 3-mm metal balls. For the experiments depicted in Figures 4.2D and 4.4A, the third true leaf was harvested and frozen immediately in liquid nitrogen and grinded. The harvesting of samples during the night was performed under green light. RNA was subsequently extracted with TriZol (Invitrogen) and further purified with the RNeasy Mini Kit (Qiagen). DNA digestion was done on columns with RNase-free DNase I (Invitrogen).

For cDNA synthesis, the iScript cDNA Synthesis Kit (Biorad) was used according to the manufacturer's instructions using 1 µg of RNA. qRT-PCR was done on a LightCycler 480 (Roche Diagnostics) in 384-well plates with LightCycler 480 SYBR Green I Master Mix (Roche) according to the manufacturer's instructions. Melting curves were analyzed to check primer specificity. Normalization was done against the average of housekeeping genes AT1G13320, AT2G32170, AT2G28390; ΔCt = Ct (gene) – Ct (mean (housekeeping genes)) and ΔΔCt = ΔCt(control line)- ΔCt(line of interest). Ct refers to the number of cycles at which SYBR Green fluorescence reaches an arbitrary value during the exponential phase of amplification. Primers were designed with the QuantPrime website (Arvidsson et al., 2008; Skirycz et al., 2010). Primers used in this study are:

ERF5: AAATTCGCGGCGGAGATTCGTG and TCAAACGTCCCAAGCCAAACGC,
ERF6: TCGAATCCTCCTCGCGTTACTG and TTCGGTGGTGCGATCTTCAACG,
ERF11: ATGGCACCGACAGTTAAAAC and TCAGTTCTCAGGTGGAGGA,
EGM: TGGCTCATGTGTGGTCAATCTGG and TCATTAGCAGCGTCTTGCACAC
GA2-OX6: TGGATCCCAATCCCATCTGACC and TCTCCCATTCGTCAATGCCTGAAG,
MYB51: GCCCTTCACGGCAACAAATG and GGTTATGCCCTTGTGTGTAACTGG,
STZ: TCACAAGGCAAGCCACCGTAAG and TTGTCGCCGACGAGGTTGAATG,
WRKY33: CTTCCACTTGTTTCAGTCCCTCTC and CTGTGGTTGGAGAAGCTAGAACG

Protoplast activation assay

The protoplast activation assay was performed as previously described (De Sutter et al., 2005; Pauwels et al., 2010). All transformation constructs were obtained using the Gateway cloning system and all liquid handlings were done on the Tecan Genesis automated platform (De Sutter et al., 2005). The protoplast activation assay was performed in a 3-d-old Bright Yellow-2 tobacco (BY-2) cell culture, sub-cultured from a 6- to 10-d-old culture. BY-2 cells were protoplasted using a 1% Cellulase (Kyowa Chemical Products) and 0.1% Pectolyase (Kyowa Chemical Products) enzyme solution in a 0.4% mannitol (Sigma) buffer. Protoplasts were then washed, counted and diluted to 500.000 mL-1. For every transcription factor – promoter combination, 100 µL (50.000 protoplasts) was used. To confirm the activating and repressing regulatory effect of ERF6 or ERF11, respectively, on the promoters of ERF6, ERF11, STZ, MYB51 and WRKY33, protoplasts were co-transfected with 35S:ERF6 or/and 35S:ERF11 (in p2GW7) and pERF6:fLUC, pERF11:fLUC, pSTZ:fLUC, pMYB51:fLUC or pWRKY33:fLUC (in pM42GW7). Promoters were defined as the 2000 bp upstream of the start codon. fLUC encodes the firefly luciferase enzyme. Every protoplast sample was transfected with 2 µg per construct as well as with 2 µg normalization construct expressing the Renilla luciferase (rLUC) enzyme. For the experiments depicted in Figure 4.5C, the used amount of 35S:ERF6 and 35S:ERF11 constructs was respectively: 4 µg and 0 µg (1/0 ratio), 3 µg and 1 µg (3/1), 2.68 µg and 1.32 µg (2/1), 2 µg and 2 µg (1/1), 1.32 µg and 2.68 µg (1/2), 1 µg and 3 µg (1/3) and 0 µg and 4 µg (0/1). Transformed protoplasts were further grown by gentle shaking overnight in the dark in BY-2 medium to allow expression of the constructs. The next day, the BY-2 medium was removed and protoplasts were lysed in Cell Culture Lysis Reagent (Promega). Protoplast content was transferred to Nunc plates (Thermo Scientific) and fLUC and rLUC activities were measured using the Dual Luciferase Assay (Promega) and the LumiStar Galaxy (De Sutter et al., 2005). Measured fLUC activities were then normalized to rLUC activities.

Quantitative Y2H

For the protein-protein interaction analysis with quantitative Y2H, the ERF6 or ERF11 coding sequence was fused N-terminally to either the GAL4BD (DNA-binding domain of GAL4, "bait") or to the GAL4AD (Activation Domain, "prey"). Each transcription factor was used both as a bait and as a prey, generating 4 possible construct combinations. For each combination, the 2 constructs were co-transformed in competent yeast cells of the PJ69-4A strain using poly-ethylene glycol lithium acetate-mediated transformation. As a control, each construct was also co-transformed with an empty vector to detect auto-activation. For the quantitative assay, yeast cultures were grown overnight in liquid Synthetic Defined (SD, Clontech) minimal medium supplemented with an amino acid mix without Leucine and Tryptophan (-L-W DO supplement, Clontech). The next day, the OD600 was determined and used to start new cultures with equal amounts of yeast cells, either in non-selective medium (SD –L-W) or in selective medium (-L-W-H, Clontech). The selective cultures were supplemented with 5 mM, 25 mM or 50 mM 3-Amino-1,2,4-triazole (Sigma) to distinguish auto-activation from protein-protein interaction. Upon 24 h of growth, the OD600 was measured to quantify the growth, and the non-selective cultures were measured as a control.

SUPPLEMENTAL DATA

All Supplemental Data is listed below. Supplemental Figures can be found at the end of this chapter.

Supplemental Figure S1. Transcriptional induction of ERF6 target genes upon short-term exposure to mannitol.
Supplemental Figure S2. Expression levels of *ERF11* in the *erf11* (SALK_116053) line.
Supplemental Figure S3. Rosette phenotype of ERF11-GR line grown in soil.
Supplemental Figure S4. Effect of ERF11 on ERF6 expression.
Supplemental Figure S5. Quantitative Y2H assay with ERF6 and ERF11.
Supplemental Figure S6. Growth measurements of *egm1*, *egm2* and *erf5erf6* mutants on mild and severe mannitol stress.
Supplemental Figure S7. Expression analysis of *EGM* in young Arabidopsis leaves upon short-term mannitol treatment.
Supplemental Figure S8. Expression levels of *ERF5*, *ERF6* and *ERF11* in *egm1* and *egm2* mutants.
Supplemental Figure S9. Co-expression analysis of ERF11 and its putative regulators under multiple stress-related conditions.

ACKNOWLEDGEMENTS

We thank the whole Systems Biology of Yield group for the stimulating environment and constructive scientific discussions. Special thanks to Katrien Maleux for the practical help and to Dr. Annick Bleys for help with improving the manuscript. This work was supported by the Interuniversity Attraction Poles Program (IUAP P7/29 "MARS") initiated by the Belgian Science Policy Office, by Ghent University ('Bijzonder Onderzoeksfonds Methusalem Project' no. BOF08/01M00408, Multidisciplinary Research Partnership "Biotechnology for a Sustainable Economy" Project no. 01MRB510W), by the Agency for Innovation by Science and Technology (IWT) (predoctoral fellowship to L.V.d.B.), and by the Research Foundation Flanders (FWO) (predoctoral fellowship to H.C.).

REFERENCES

AbuQamar S, Chen X, Dhawan R, Bluhm B, Salmeron J, Lam S, Dietrich RA, Mengiste T (2006) Expression profiling and mutant analysis reveals complex regulatory networks involved in Arabidopsis response to Botrytis infection. Plant J 48: 28-44

Alonso JM, Stepanova AN, Leisse TJ, Kim CJ, Chen H, Shinn P, Stevenson DK, Zimmerman J, Barajas P, Cheuk R, et al (2003) Genome-wide insertional mutagenesis of Arabidopsis thaliana. Science 301: 653-657

Andriankaja M, Dhondt S, De Bodt S, Vanhaeren H, Coppens F, De Milde L, Mühlenbock P, Skirycz A, Gonzalez N, Beemster GTS, et al (2012) Exit from proliferation during leaf development in Arabidopsis thaliana: a not-so-gradual process. Dev Cell 22: 64-78

Arvidsson S, Kwasniewski M, Riaño-Pachón DM, Mueller-Roeber B (2008) QuantPrime - a flexible tool for reliable high-throughput primer design for quantitative PCR. BMC Bioinformatics 9: 465

Boron AK, Vissenberg K (2014) The Arabidopsis thaliana hypocotyl, a model to identify and study control mechanisms of cellular expansion. Plant Cell Rep 33: 697-706

Claeys H, Inzé D (2013) The agony of choice: how plants balance growth and survival under water-limiting conditions. Plant Physiol 162: 1768-1779

Claeys H, Skirycz A, Maleux K, Inzé D (2012) DELLA signaling mediates stress-induced cell differentiation in Arabidopsis leaves through modulation of anaphase-promoting complex/cyclosome activity. Plant Physiol 159: 739-747

Claeys H, Van Landeghem S, Dubois M, Maleux K, Inzé D (2014) What is stress? Dose-response effects in commonly used in vitro stress assays. Plant Physiol 165: 519-527

De Sutter V, Vanderhaeghen R, Tilleman S, Lammertyn F, Vanhoutte I, Karimi M, Inzé D, Goossens A, Hilson P (2005) Exploration of jasmonate signalling via automated and standardized transient expression assays in tobacco cells. Plant J 44: 1065-1076

Dombrecht B, Xue GP, Sprague SJ, Kirkegaard JA, Ross JJ, Reid JB, Fitt GP, Sewelam N, Schenk PM, Manners JM, et al (2007) MYC2 differentially modulates diverse jasmonate-dependent functions in Arabidopsis. Plant Cell 19: 2225-2245

Dubois M, Skirycz A, Claeys H, Maleux K, Dhondt S, De Bodt S, Vanden Bossche R, De Milde L, Yoshizumi T, Matsui M, et al (2013) ETHYLENE RESPONSE FACTOR6 acts as a central regulator of leaf growth under water-limiting conditions in Arabidopsis. Plant Physiol 162: 319-332

Eulgem T, Somssich IE (2007) Networks of WRKY transcription factors in defense signaling. Curr Opin Plant Biol 10: 366-371

Fujimoto SY, Ohta M, Usui A, Shinshi H, Ohme-Takagi M (2000) Arabidopsis ethylene-responsive element binding factors act as transcriptional activators or repressors of GCC box-mediated gene expression. Plant Cell 12: 393-404

Gruber H, Heijde M, Heller W, Albert A, Seidlitz HK, Ulm R (2010) Negative feedback regulation of UV-B-induced photomorphogenesis and stress acclimation in Arabidopsis. Proc Natl Acad Sci USA 107: 20132-20137

Hampton CR, Bowen HC, Broadley MR, Hammond JP, Mead A, Payne KA, Pritchard J, White PJ (2004) Cesium toxicity in Arabidopsis. Plant Physiol 136: 3824-3837

Hectors K, Prinsen E, De Coen W, Jansen MAK, Guisez Y (2007) Arabidopsis thaliana plants acclimated to low dose rates of ultraviolet B radiation show specific changes in morphology and gene expression in the absence of stress symptoms. New Phytol 175: 255-270

Hruz T, Laule O, Szabo G, Wessendorp F, Bleuler S, Oertle L, Widmayer P, Gruissem W, Zimmermann P (2008) Genevestigator v3: a reference expression database for the meta-analysis of transcriptomes. Adv Bioinformatics 2008: 420747

Hu J, Barlet X, Deslandes L, Hirsch J, Feng DX, Somssich I, Marco Y (2008) Transcriptional responses of Arabidopsis thaliana during wilt disease caused by the soil-borne phytopathogenic bacterium, Ralstonia solanacearum. PLoS ONE 3: e2589

Kim SH, Son GH, Bhattacharjee S, Kim HJ, Nam JC, Nguyen PDT, Hong JC, Gassmann W (2014) The Arabidopsis immune adaptor SRFR1 interacts with TCP transcription factors that redundantly contribute to effector-triggered immunity. Plant J 78: 978-989

Kreps JA, Wu Y, Chang H-S, Zhu T, Wang X, Harper JF (2002) Transcriptome changes for Arabidopsis in response to salt, osmotic, and cold stress. Plant Physiol 130: 2129-2141

Lawlor DW (2013) Genetic engineering to improve plant performance under drought: physiological evaluation of achievements, limitations, and possibilities. J Exp Bot 64: 83-108

Lee B-h, Henderson DA, Zhu J-K (2005) The Arabidopsis cold-responsive transcriptome and its regulation by ICE1. Plant Cell 17: 3155-3175

Lee J, He K, Stolc V, Lee H, Figueroa P, Gao Y, Tongprasit W, Zhao H, Lee I, Deng XW (2007) Analysis of transcription factor HY5 genomic binding sites revealed its hierarchical role in light regulation of development. Plant Cell 19: 731-749

Li Z, Zhang L, Yu Y, Quan R, Zhang Z, Zhang H, Huang RF (2011) The ethylene response factor AtERF11 that is transcriptionally modulated by the bZIP transcription factor HY5 is a crucial repressor for ethylene biosynthesis in Arabidopsis. Plant J 68: 88-99

Libault M, Wan J, Czechowski T, Udvardi M, Stacey G (2007) Identification of 118 Arabidopsis transcription factor and 30 ubiquitin-ligase genes responding to chitin, a plant-defense elicitor. Mol Plant-Microbe Interact 20: 900-911

Ma S, Bohnert HJ (2007) Integration of Arabidopsis thaliana stress-related transcript profiles, promoter structures, and cell-specific expression. Genome Biol 8: R49

McGrath KC, Dombrecht B, Manners JM, Schenk PM, Edgar CI, Maclean DJ, Scheible W-R, Udvardi MK, Kazan K (2005) Repressor- and activator-type ethylene response factors functioning in jasmonate signaling and disease resistance identified via a genome-wide screen of Arabidopsis transcription factor gene expression. Plant Physiol 139: 949-959

Meng X, Xu J, He Y, Yang K-Y, Mordorski B, Liu Y, Zhang S (2013) Phosphorylation of an ERF transcription factor by Arabidopsis MPK3/MPK6 regulates plant defense gene induction and fungal resistance. Plant Cell 25: 1126-1142

Moffat CS, Ingle RA, Wathugala DL, Saunders NJ, Knight H, Knight MR (2012) ERF5 and ERF6 play redundant roles as positive regulators of JA/Et-mediated defense against Botrytis cinerea in Arabidopsis. PLoS ONE 7: e35995

Murashige T, Skoog F (1962) A revised medium for rapid growth and bio assays with tobacco tissue cultures. Physiol Plant 15: 473-497

Nakano T, Suzuki K, Fujimura T, Shinshi H (2006) Genome-wide analysis of the ERF gene family in Arabidopsis and rice. Plant Physiol 140: 411-432

Ohta M, Matsui K, Hiratsu K, Shinshi H, Ohme-Takagi M (2001) Repression domains of class II ERF transcriptional repressors share an essential motif for active repression. Plant Cell 13: 1959-1968

Pauwels L, Barbero GF, Geerinck J, Tilleman S, Grunewald W, Cuéllar Pérez A, Chico JM, Vanden Bossche R, Sewell J, Gil E, et al (2010) NINJA connects the co-repressor TOPLESS to jasmonate signalling. Nature 464: 788-791

Popescu SC, Popescu GV, Bachan S, Zhang Z, Gerstein M, Snyder M, Dinesh-Kumar SP (2009) MAPK target networks in Arabidopsis thaliana revealed using functional protein microarrays. Genes Dev 23: 80-92

Ragni L, Hardtke CS (2014) Small but thick enough – the Arabidopsis hypocotyl as a model to study secondary growth. Physiol Plant 151: 164-171

Riechmann JL, Meyerowitz EM (1998) The AP2/EREBP family of plant transcription factors. Biol Chem 379: 633-646

Rieu I, Eriksson S, Powers SJ, Gong F, Griffiths J, Woolley L, Benlloch R, Nilsson O, Thomas SG, Hedden P, et al (2008) Genetic analysis reveals that C19-GA 2-oxidation is a major gibberellin inactivation pathway in Arabidopsis. Plant Cell 20: 2420-2436

Sakuma Y, Liu Q, Dubouzet JG, Abe H, Shinozaki K, Yamaguchi-Shinozaki K (2002) DNA-binding specificity of the ERF/AP2 domain of Arabidopsis DREBs, transcription factors involved in dehydration- and cold-inducible gene expression. Biochem Biophys Res Commun 290: 998-1009

Sewelam N, Kazan K, Thomas-Hall SR, Kidd BN, Manners JM, Schenk PM (2013) Ethylene response factor 6 is a regulator of reactive oxygen species signaling in Arabidopsis. PLoS ONE 8: e70289

Skirycz A, Claeys H, De Bodt S, Oikawa A, Shinoda S, Andriankaja M, Maleux K, Eloy NB, Coppens F, Yoo S-D, et al (2011) Pause-and-stop: the effects of osmotic stress on cell proliferation during early leaf development in Arabidopsis and a role for ethylene signaling in cell cycle arrest. Plant Cell 23: 1876-1888

Skirycz A, De Bodt S, Obata T, De Clercq I, Claeys H, De Rycke R, Andriankaja M, Van Aken O, Van Breusegem F, Fernie AR, et al (2010) Developmental stage specificity and the role of mitochondrial metabolism in the response of Arabidopsis leaves to prolonged mild osmotic stress. Plant Physiol 152: 226-244

Son GH, Wan J, Kim HJ, Nguyen XC, Chung WS, Hong JC, Stacey G (2012) Ethylene-responsive element-binding factor 5, ERF5, is involved in chitin-induced innate immunity response. Mol Plant-Microbe Interact 25: 48-60

Song YH, Yoo CM, Hong AP, Kim SH, Jeong HJ, Shin SY, Kim HJ, Yun D-J, Lim CO, Bahk JD, et al (2008) DNA-binding study identifies C-box and hybrid C/G-box or C/A-box motifs as high-affinity binding sites for STF1 and LONG HYPOCOTYL5 proteins. Plant Physiol 146: 1862-1877

Suzuki N, Rizhsky L, Liang H, Shuman J, Shulaev V, Mittler R (2005) Enhanced tolerance to environmental stress in transgenic plants expressing the transcriptional coactivator multiprotein bridging factor 1c. Plant Physiol 139: 1313-1322

Trontin C, Kiani S, Corwin JA, Hématy K, Yansouni J, Kliebenstein DJ, Loudet O (2014) A pair of receptor-like kinases is responsible for natural variation in shoot growth response to mannitol treatment in Arabidopsis thaliana. Plant J 78: 121-133

Vergnolle C, Vaultier M-N, Taconnat L, Renou J-P, Kader J-C, Zachowski A, Ruelland E (2005) The cold-induced early activation of phospholipase C and D pathways determines the response of two distinct clusters of genes in Arabidopsis cell suspensions. Plant Physiol 139: 1217-1233

Vermeirssen V, De Clercq I, Van Parys T, Van Breusegem F, Van de Peer Y (2014) Arabidopsis ensemble reverse-engineered gene regulatory network discloses interconnected transcription factors in oxidative stress. Plant Cell 26: 4656-4679

Verslues PE, Agarwal M, Katiyar-Agarwal S, Zhu J, Zhu J-K (2006) Methods and concepts in quantifying resistance to drought, salt and freezing, abiotic stresses that affect plant water status. Plant J 45: 523-539

Vogel MO, Gomez-Perez D, Probst N, Dietz K-J (2012) Combinatorial signal integration by APETALA2/ethylene response factor (ERF)-transcription factors and the involvement of AP2-2 in starvation response. Int J Mol Sci 13: 5933-5951

Vogel MO, Moore M, König K, Pecher P, Alsharafa K, Lee J, Dietz K-J (2014) Fast retrograde signaling in response to high light involves metabolite export, MITOGEN-ACTIVATED PROTEIN KINASE6, and AP2/ERF transcription factors in Arabidopsis. Plant Cell 26: 1151-1165

Wang P-C, Du Y-Y, An G-Y, Zhou Y, Miao C, Song C-P (2006) Analysis of global expression profiles of Arabidopsis genes under abscisic acid and H2O2 applications. J Integr Plant Biol 48: 62-74

Wang P, Du Y, Zhao X, Miao Y, Song C-P (2013) The MPK6-ERF6-ROS-responsive cis-acting element7/GCC box complex modulates oxidative gene transcription and the oxidative response in Arabidopsis. Plant Physiol 161: 1392-1408

Xin Z, Mandaokar A, Chen J, Last RL, Browse J (2007) Arabidopsis ESK1 encodes a novel regulator of freezing tolerance. Plant J 49: 786-799

Yang Z, Tian L, Latoszek-Green M, Brown D, Wu K (2005) Arabidopsis ERF4 is a transcriptional repressor capable of modulating ethylene and abscisic acid responses. Plant Mol Biol 58: 585-596

Supplemental Figure S1. Transcriptional induction of ERF6 target genes upon short-term exposure to mannitol. Expression levels of *STZ, MYB51* and *GA2-OX6* in proliferating leaf tissue measured by qRT-PCR upon exposure to mild mannitol-induced stress (25 mM). Represented values are means of three biological repeats with their standard error relative to the expression value upon transfer to MS (TMS) medium as a control. * = p< 0.05 (ANOVA) for all genes.

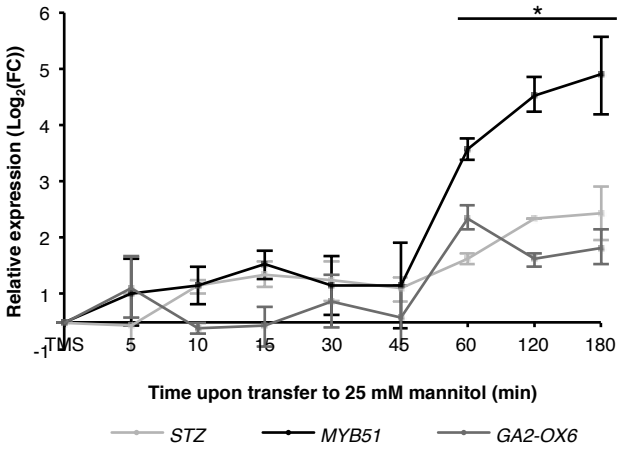

Supplemental Figure S2. Expression levels of *ERF11* in the *erf11* (SALK_116053) line. Expression levels of *ERF11* measured at different time points during the 15th day after stratification in the growing Arabidopsis leaves. Represented values are means of three biological repeats with their standard error.

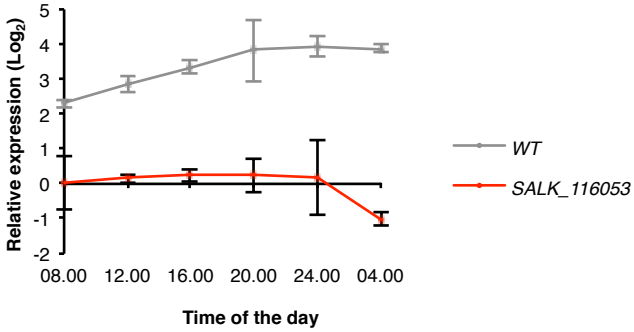

Supplemental Figure S3. Rosette phenotype of *ERF11*-overexpressing plants grown in soil. Leaf series at 22 DAS of soil-grown WT, ERF11-GR **(A)** and ERF6-GR x ERF11-GR **(B)** plants watered with a 15 µM dexamethasone solution. Represented values are means of three biological repeats with their standard error. * = p< 0.05 (mixed models).

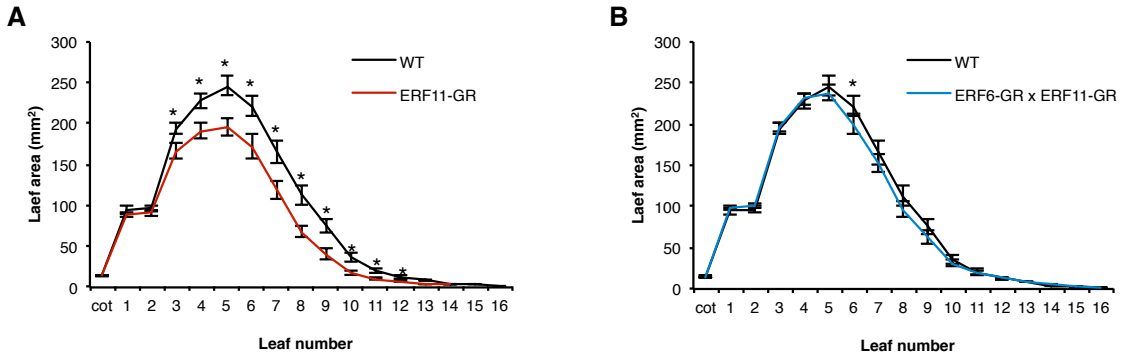

Supplemental Figure S4. Effect of ERF11 on *ERF6* expression. (**A)** Expression levels of *ERF6* in WT and ERF11-GR, 24 h upon induction of *ERF11* overexpression in growing Arabidopsis leaves (15 DAS). Represented values are means of five biological repeats with their standard error. (**B)** Luciferase activation assay upon co-transformation of 35S:ERF11 and pERF6:fLUC in protoplasts. Represented values are means of two biological repeats with their standard error. * = p<0.05 (Student's t-test)

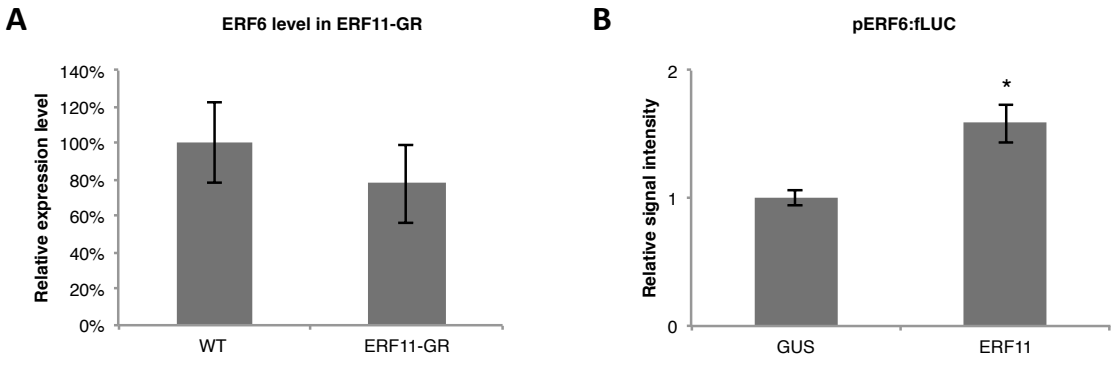

Supplemental Figure S5. Quantitative yeast 2-hybrid assay with ERF6 and ERF11. Yeast cultures transformed with the indicated bait/prey constructs were grown in liquid SD cultures on either non-selective medium depleted with Leucine and Tryptophan (-L-W) or selective medium depleted with Leucine, Tryptophan and Histidine (-L-W-H). Since ERF6 as a bait shows auto-activation, increasing concentrations of the 3'-amino-triazol were added to the selective cultures to distinguish between auto-activation and interactions with ERF6 as bait. Optical density of the cultures were measured upon overnight growth. Represented values are means of three biological repeats with their standard error.

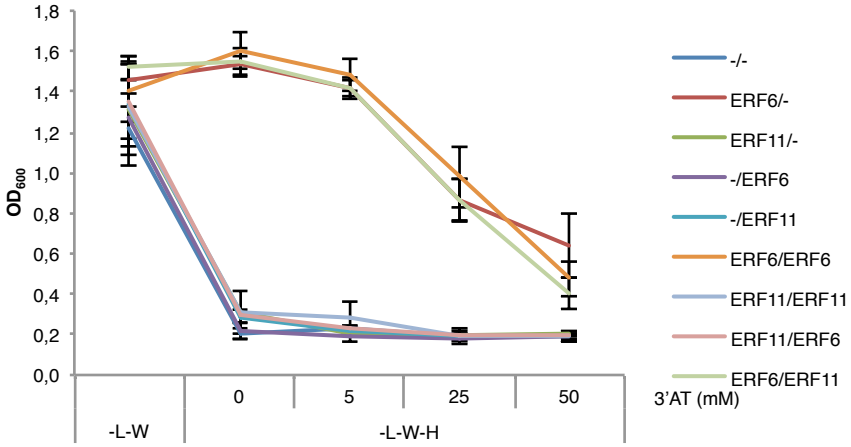

Supplemental Figure S6. Growth measurements of *egm1*, *egm2* and *erf5erf6* mutants on mild and severe mannitol stress. Projected rosette areas were measured at 22 DAS upon growth of *egm1* and *egm2* mutants and their respective wild type **(A)** or *erf5erf6* mutants and the wild type **(B)** on MS, mild (25 mM; Mann25) and severe (60 mM; Mann60) mannitol stress. Represented values are the means of at least two biological repeats with their standard error. * = p< 0.05 compared to WT.

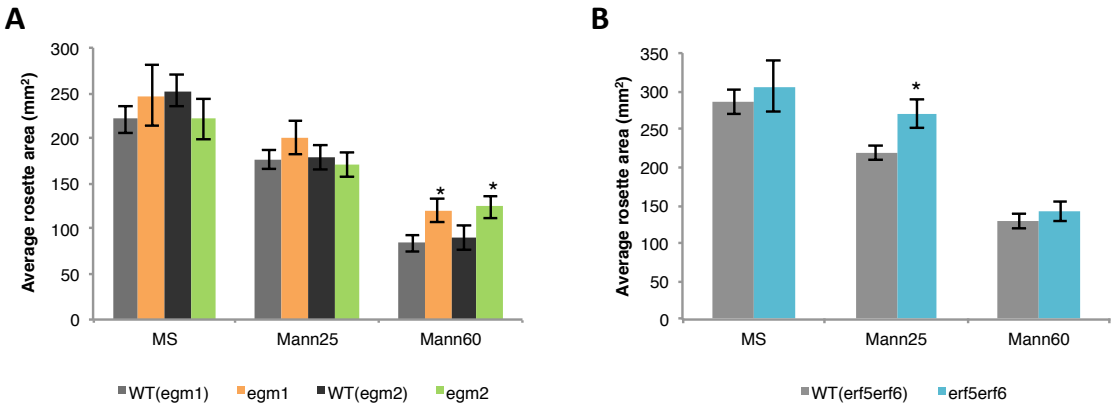

Supplemental Figure S7. Expression analysis of EGM in young Arabidopsis leaves upon short-term mannitol treatment. (**A)** Expression analysis of *EGM1* in proliferating leaf tissue measured by qRT-PCR upon exposure to mild mannitol-induced stress. Represented values are means of three biological repeats with their standard error relative to the expression value upon transfer to MS medium as a control (TMS). (**B)** *EGM* expression in the Skirycz et al. (2011) dataset. Only one *EGM* transcript is represented since performed micro-arrays did not distinguish between *EGM1* and *EGM2*. * = p< 0.05 (ANOVA)

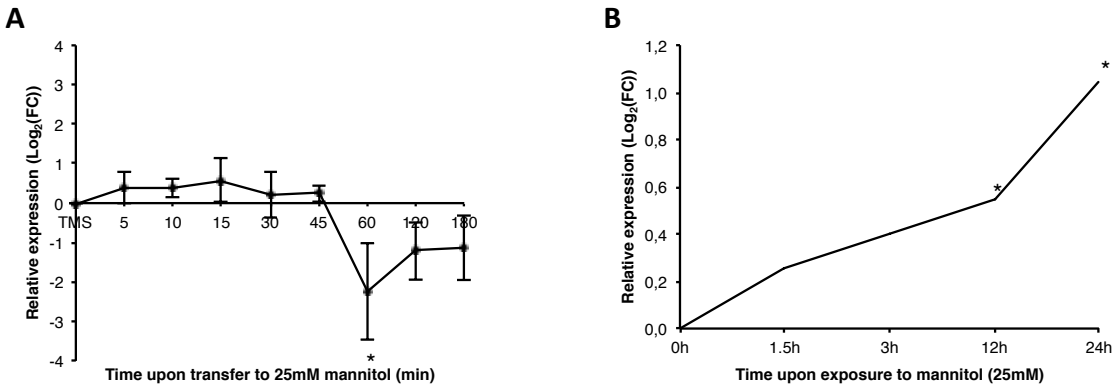

Supplemental Figure S8. Expression levels of *ERF5*, *ERF6* and *ERF11* in *egm1* and *egm2* mutants. Expression levels of *ERF5, ERF6* and *ERF11* in 12 days old seedlings (setup of Trontin et al., 2014) grown from germination onward on either MS **(A)**, 25 mM **(B)**, or 60 mM **(C)** mannitol. For all graphs, represented values are means of three biological repeats with their standard error relative to the expression value upon transfer to MS medium as a control. * = p< 0.05 compared to WT.

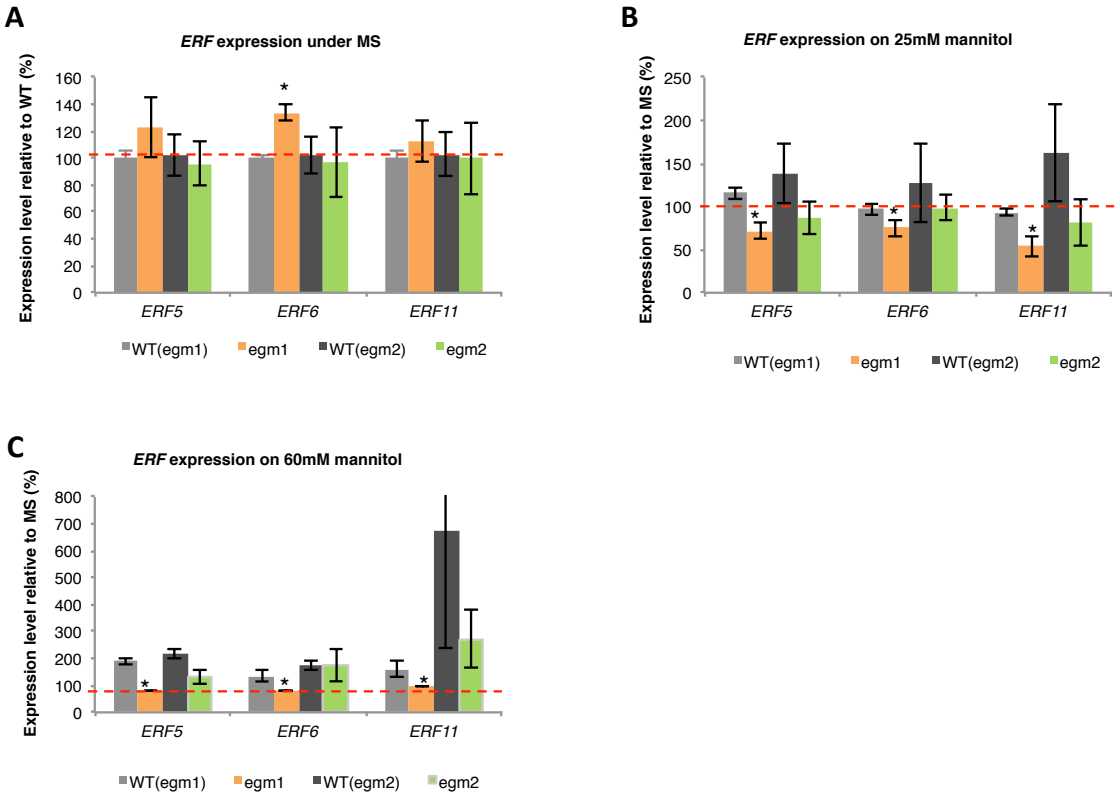

Supplemental Figure S9. Co-expression analysis of ERF11 and its putative regulators under multiple stress-related conditions. Study performed with Genevestigator (Hruz et al., 2008) using all available ATH1 datasets related to perturbations. Only datasets in which *ERF11* was induced with $Log_2(FC) > 2$ or < -2 were included. Values are Log_2FC as compared with mock-treated samples. Hierarchical tree depicts correlations between the transcripts calculated using the complete perturbation dataset (no FC filter).

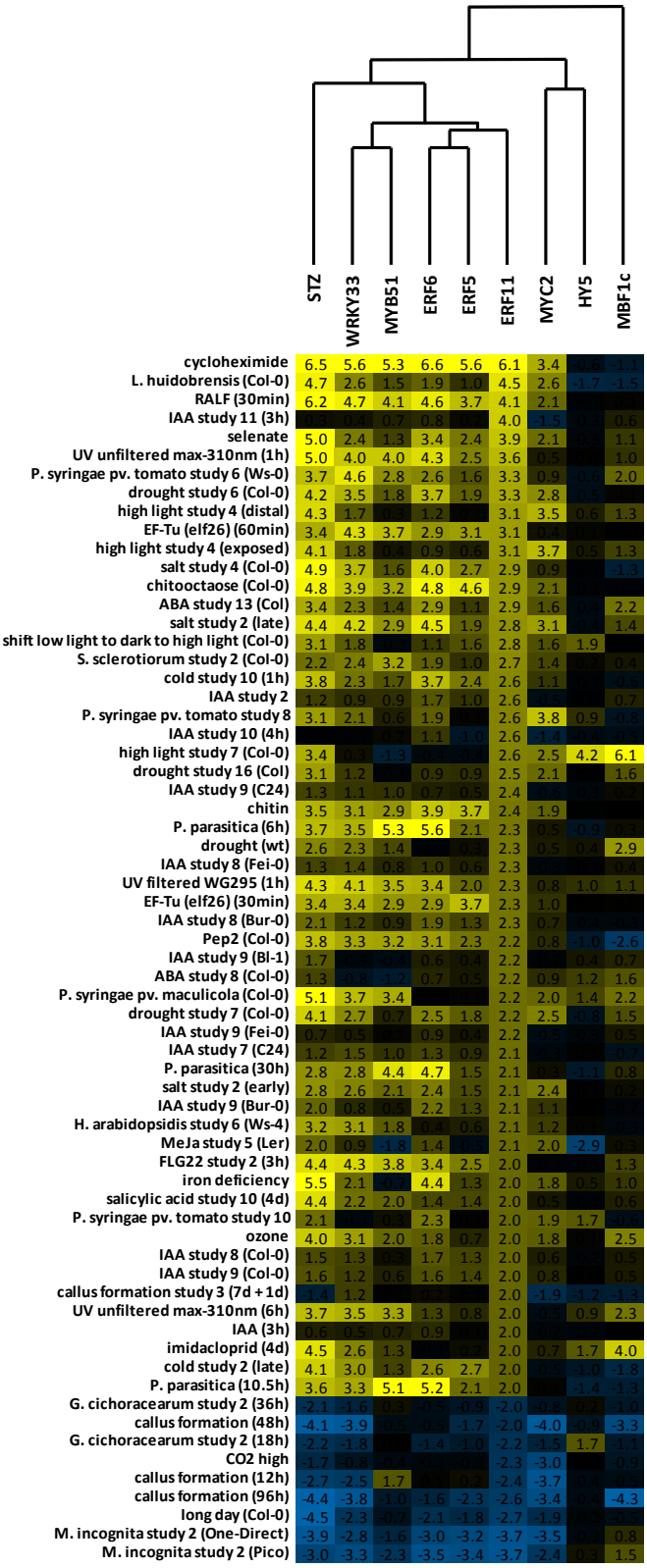

Chapter 5

EXTENDING THE NETWORK: IDENTIFICATION OF NEW GENES INVOLVED IN ERF6-MEDIATED GROWTH REGULATION

Marieke Dubois [a,b], Twiggy Van Daele [a,b], Stijn Dhondt [a,b], Nathalie Wuyts [a,b], Ting Li [a,b], and Dirk Inzé [a,b]

[a] Department of Plant Systems Biology, VIB, Ghent, Belgium
[b] Department of Plant Biotechnology and Bioinformatics, Ghent University, Belgium

Contributions: M.D. performed most of the experiments and wrote the manuscript, T.V.D. provided practical help, S.D. and N.W. developed the phenotyping platform for the experiment presented in Figure 5.4D, T.L. performed the experimental validation of the mutations, D.I. supervised the project and contributed to the writing of the manuscript.

This Chapter is unpublished but provides an overview of the first results of a project currently being continued by a beginning PhD student.

Leaf growth is a complex and highly regulated process continuously fine-tuned in response to changing environmental conditions. Under environmental stress conditions, leaf growth is actively shut down, mainly as a mechanism to save water and energy. Our previous studies report the identification of an ETHYLENE RESPONSE FACTOR 6 (ERF6)-centered growth-regulatory pathway inhibiting leaf growth in young leaves. To identify additional players of this growth-regulatory network without imposing restrictions on molecular function or hormonal pathway, we performed a forward genetic screen based on the severe dwarfism induced by *ERF6* overexpression. Here, we report the selection of 7 mutants suppressing the ERF6-induced dwarfism and the identification of the corresponding causal genes. We mainly focus on a mutant that, on top of suppressing the ERF6-induced dwarfism, showed a pronounced increase in rosette leaf size under control conditions and was more tolerant to mild drought stress. This mutant was found to be mutated in the ethylene-signalling gene *EIN5/XRN4* (ETHYLENE INSENSITIVE5/EXORIBONUCLEASE4). Several new alleles of *EIN5* were identified and we show that the allelic mutants have different growth phenotypes. Together, these data show that multiple additional genes are involved in growth regulation around the ERF6-pathway, and that some of these genes might be important for growth under control conditions as well.

INTRODUCTION

Leaf growth is a complex process, integrating genetically programmed developmental processes and environmental signals. Under stress conditions, these environmental signals can trigger inhibition of leaf growth, which is part of an active mechanism to redirect the energy and, in case of drought stress for example, to limit water evaporation from the leaf surface. During the past decades, extensive research has been performed on *Arabidopsis thaliana* to study plant behaviour under extreme environmental conditions, either in soil under severe drought or *in vitro*, with osmotic stress as a proxy (Xiong et al., 2002; Verslues et al., 2006; Seki et al., 2007; Schachtman and Goodger, 2008). These studies mainly scored plant survival or used final rosette area as a measure for plant tolerance to stress (Umezawa et al., 2006; Claeys et al., 2014). However, it became clear that the often rather harsh conditions used in these studies are not very representative for natural conditions, in which the stress is generally milder and does not always threaten survival (Skirycz and Inzé, 2010). Moreover, it was shown that tolerance to severe drought stress and the ability of plants to continue to grow under mild stress conditions are very different traits mediated by different

molecular processes (Skirycz et al., 2011a; Claeys and Inzé, 2013). Furthermore, recent studies pointed out the importance of evaluating stress responses at organ or tissue level, as the response to abiotic stress is highly dependent on the organ and its developmental stage (Dinneny, 2008; Harb et al., 2010; Skirycz et al., 2010; Baerenfaller et al., 2012; Verelst et al., 2013). Thus, in order to understand the specific mechanisms involved in growth inhibition under stress, it is important to study growth response specifically in actively growing leaves.

Leaf growth in Arabidopsis consists of three major developmental phases (Anastasiou and Lenhard, 2007; Andriankaja et al., 2012; Gonzalez et al., 2012). First, growth of very young leaves emerging from the shoot apical meristem is driven exclusively by cell proliferation. Next, cell division starts to cease at the tip of the leaf and gradually all cells in the leaf exit the mitotic cell cycle and start to expand (Donnelly et al., 1999; Andriankaja et al., 2012; Gonzalez et al., 2012). Finally, cell division in the developing leaves stops and further leaf growth mainly occurs by cell expansion (Vlieghe et al., 2005). Under mild drought conditions, or mild *in vitro* osmotic stress, both cell proliferation and cell expansion are affected resulting in a final leaf size reduction of on average 50% (Skirycz et al., 2010; Skirycz et al., 2011b; Claeys et al., 2012).

When mild stress occurs during the proliferation phase of early leaf development (leaves <0.1mm^2 in size), cell cycle progression is affected in a two-step process denominated the "Pause-and-Stop" mechanism, involving crosstalk between the plant hormones ethylene and gibberellic acid (GA) (Skirycz et al., 2011b; Claeys et al., 2012). In the first step of mild stress response, the ethylene precursor 1-aminocyclopropane-1-carboxylic acid (ACC) accumulates and inactivates the Cyclin Dependent Kinase A (CDKA), thereby transiently blocking further cell cycle progression ("Pause"). In parallel, the accumulation of ACC induces, specifically in growing leaves, the expression of the downstream *ETHYLENE RESPONSE FACTOR 6* (*ERF6*). This transcription factor occupies a central role in this pathway, as on the one hand it activates the stress tolerance mechanisms, while on the other hand it further converts the paused cell cycle into a definitive cell cycle exit ("Stop") (Dubois et al., 2013). Molecularly, the latter occurs through transcriptional activation of the *GA2-OX6* gene, which stimulates breakdown of GAs. Decreased GA levels further result in stabilization of DELLA proteins, which push cells into cell expansion and endoreduplication (Claeys et al., 2012; Achard et al., 2008).

It is however very unlikely that this rather simple linear pathway on its own is the sole regulator of leaf growth under stress. Considering the complexity of regulation of leaf growth under normal conditions (Gonzalez et al., 2012), and the numerous pathways that are responding to changing environments (Skirycz an Inzé, 2010), it is likely that the integration of environmental signals into leaf growth adaptation is an extremely

complex response involving different molecular processes such as, but not limited to, signal detection, post-transcriptional regulation and protein complex formation. To identify new genes involved in leaf growth regulation under adverse conditions without bias for certain molecular processes or biological functions, we performed a forward genetic screen. As a starting point, we used the easily screenable severe dwarfed phenotype of an inducible *ERF6* overexpression line, mutagenized it with 1-methylsulfonyloxyethane (EMS), and screened for suppressor mutants. Here, we report the selection of seven suppressor mutants accompanied by the identification of seven genes involved in leaf growth regulation under stress.

RESULTS

Screen for mutants suppressing ERF6-induced dwarfism

As ERF6 is a negative regulator of leaf growth, plants highly overexpressing the transcription factor *ERF6* are extremely dwarfed, and show dark green, down curling leaves (Figure 5.1A). We used this easily detectable phenotype as a starting point for a forward genetics screen and subjected 10,000 seeds of an ERF6-GR line to treatment with the mutagen EMS, generating an M1 population. This commonly used mutagen introduces random and stable point mutations in the genome (Weigel and Glazebrook, 2006). Mutagenized plants were selfed to obtain M2 mutants homozygous for both the ERF6-GR construct and for the introduced mutations, enabling the identification of recessive mutations.

To screen for mutants suppressing the ERF6-induced phenotype 40,000 M2 seeds were grown *in vitro* on medium containing dexamethasone (DEX) to induce the ERF6-overexpression, and kanamycin (Km, 1mg/L) to ensure selection of plants containing the ERF6-GR construct, and limit false positives. In the presence of the inducing compound DEX, the non-mutated plants and those that were mutated in genes which do not influence the ERF6 function grew normally (Figure 5.1B). In contrast, twelve plants able to repress the ERF6-phenotype, presumably because they were mutated in a gene related to ERF6-mediated growth regulation, grew normally (Supp. Figure 1). These were selected and selfed to obtain large amounts of non-segregating M3 seeds. Next, the mutants were crossed and the seeds directly produced from the cross were sown on medium supplemented with DEX and Km. If both parental mutants were mutated in the same gene, the cross product is able to suppress ERF6-induced dwarfism similarly as the parents. On the contrary, if the parental mutants were mutated in different genes,

the progeny is heterozygous for each mutation, and won't be able to suppress ERF6-induced dwarfism. These crosses thus enabled the identification of allelic groups. In total, the twelve mutants were classified in seven different allelic groups: six groups containing each only one mutant, and one group containing six allelic mutants. For this last group, one representative mutant was chosen for further analysis. The seven non-allelic mutants were named *sgi1 – sgi7* (*suppressor of ERF6-mediated growth inhibition*).

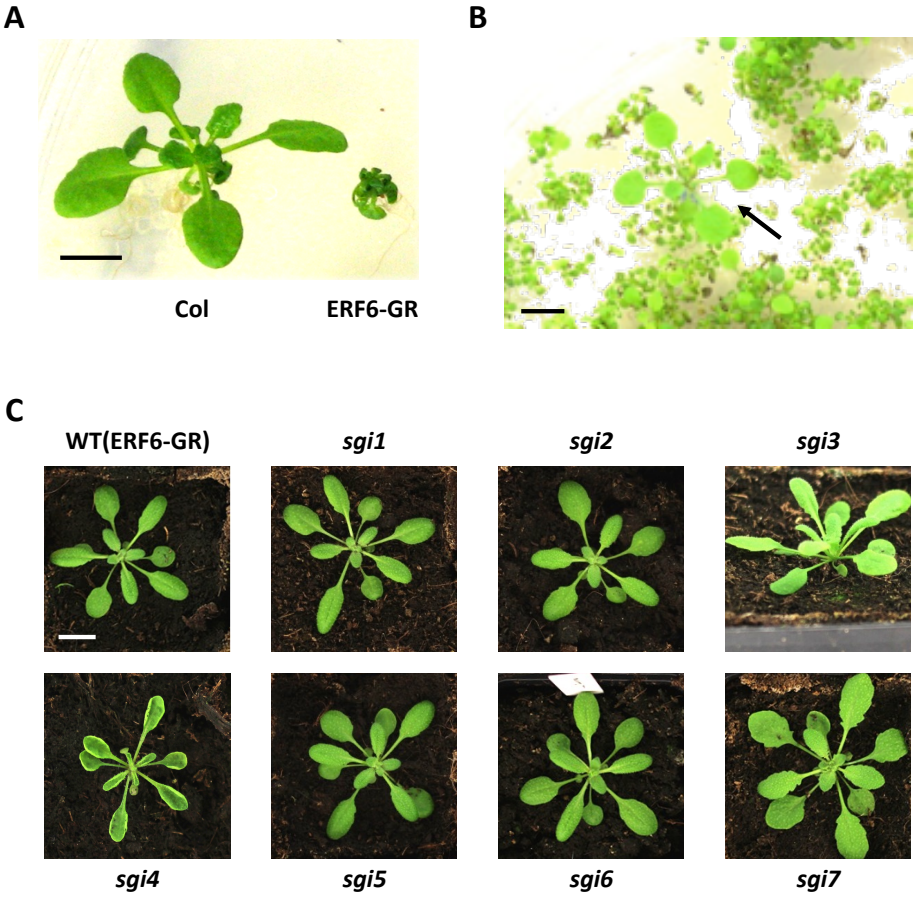

Figure 5.1. A forward genetics screen based on the ERF6-induced dwarfism identified 7 suppressor mutants. (A) Growth of the ERF6-GR line on dexamethasone (DEX)-containing medium results in extreme dwarfism. (B) In the forwards genetics screen, the large majority of the plants show dwarfism (on DEX-containing medium), but some mutants suppress the ERF6-induced growth inhibition and show a wild type phenotype (arrow). (C) Phenotype of the selected suppressor-mutants when grown in soil, in the absence of DEX. Scale bar: 5 mm.

To validate the mutants, we first checked by PCR and sequencing for the presence of an intact ERF6-GR construct, and confirmed by qRT-PCR that the ERF6-GR construct was still overexpressed to levels similar as the original ERF6-GR line (Supp. Figure 2). Two mutants, named *sgi1* and *sgi2* were found to be mutated in the ERF6-domain of the ERF6-GR construct. These resulted in missense mutations, respectively A270T and R285Q, which are situated in the DNA-binding AP2-domain of the ERF6 protein. To determine whether this mutation in ERF6 was causal for the suppression of the phenotype, we crossed these mutants with a wild-type and allowed selfing of the progeny. When grown on DEX and Km containing medium, a segregating ratio according to the 2nd Mendelian law for 2 independent alleles for the suppression of the ERF6-induced dwarfism is expected if a second mutation is responsible for the suppression of the phenotype. On the contrary, 100% of the progeny are expected to show the wild-type phenotype if the mutation in ERF6 itself is causal. Since we observed, for both mutants, a segregating F2 population when grown on DEX and Km (Supp. Figure 3), we concluded that the mutations in *ERF6* are not responsible for the suppression of the ERF6-induced dwarfism.

Some selected mutants show additional phenotypes, on top of ERF6-suppression

Interestingly, when growing the seven different mutants (M3) in soil, under non-DEX conditions, we observed that several mutants show additional phenotypes, on top of the capacity to suppress the ERF6-GR phenotype (Figure 5.1C). For example, the *sgi3* mutant exhibits a clear hyponastic phenotype accompanied by early flowering. The *sgi4* mutant also shows hyponasty with up-curling leaves, and has trichomes at both sides of the rosette leaves, while these are generally only observed on the adaxial leaf size. This mutant also shows defective formation of siliques, which often remain very small and contain only few seeds. The same silique phenotype was observed for *sgi7*, and seed quantification showed a significant reduction in seed number and total seed weight, but compensated by a slight increase in seed size (Supp. Figure 4). Importantly, this *sgi7* mutant showed a visible increase in rosette size (see further). We thus concluded that the seven non-allelic mutants are able to suppress ERF6-induced dwarfism and that some of these mutants show interesting rosette phenotypes on top of the capacity to suppress the ERF6 phenotype.

Identification of the causal genes

To identify the gene mutated in each of the seven mutants, each mutant (in *Col-0* background) was outcrossed with the Arabidopsis *Ler-1* accession. About 3,000

segregating F2 seeds were screened *in vitro* on growth medium containing both Km and DEX. Between 400 and 500 mutants showing a normal growth phenotype, thus containing at least a single copy of the ERF6-GR and being homozygous for the causal mutation, were selected and pooled for whole genome DNAseq (as illustrated in Supp. Figure 5). Illumina sequencing was performed with 100bp reads and a 40x coverage of the genome. Rough sequencing data was analysed with SHORE followed by peak calling using SHOREmap (Schneeberger et al., 2009). Based on the principle that in the F2 population *Col-0* and *Ler-1* SNPs should be equally distributed, except in the chromosomal region linked to the phenotype (where exclusively *Col-0* is expected), a candidate region can be mapped (Supp. Figure 6). The numerous predicted mutations within the candidate region were further prioritized based on their location (priority to coding sequence or 5' untranslated region), their effect (introducing an amino acid change or premature stop codon), and the available litterature about the candidate genes (Supp. Table S1). Experimental validation of the predicted mutations is work in progress, but candidate genes carrying the causal mutation are provided in Table 5.1.

Table 5.1. Identification of the mutations in the 7 non-allelic EMS-mutants.

Mutant	Mutated gene(s)	Gene name	Predicted effect on protein
sgi1	AT2G36350, AT2G38220, AT2G42480	*To be identified*	
sgi2	*To be identified*		
sgi3	AT2G31810, AT2G32620, **AT2G33540**, AT2G38220	*CPL3*	Substitution
sgi4	AT3G05040	*HASTY*	Truncation
sgi5	AT3G44670, AT3G45560	*To be identified*	
sgi6	AT3G27670	*RST1*	Frameshift
sgi7	AT1G54490	*EIN5*	See Table 2

Three mutants, *sgi1*, *sgi2*, and *sgi5*, contained more than one mutation within the predicted region, are currently investigated to identify the causal mutation, and are thus no longer discussed here. Also in the *sgi3* mutant, several mutations occurred in the region of interest, requiring further experimental validation. However, one of the candidate genes encodes the CPL3 protein, a phosphatase regulating RNA polymerase II, and *cpl3* mutants were reported to show decreased rosette size (Li et al., 2014). As this gene thus appears to have a function in leaf growth, it might be the causal mutation suppressing the ERF6-GR phenotype. The mutant *sgi4* was found to be mutated in AT3G05040, a gene encoding the HASTY protein. The G-to-A mutation in this gene generates a premature stop codon and probably a truncated protein. In the mutant *sgi6*,

the mutated gene, AT3G27670, encodes the transmembrane receptor-like protein *RESURRECTION1 (RST1)*. The mutation in the splice acceptor site of the first intron generates a postponed splicing engendering a frameshift, which has been confirmed on cDNA (Supp. Figure 7). This thus likely results in loss-of-function of *RST1*. Finally, the *sgi7* mutant carried a mutation in the gene encoding EIN5/XRN4, encoding an RNA-exoribonuclease involved in the ethylene signalling pathway. The *sgi7* mutant looked particularly interesting as it showed a visible increase in leaf size and as it was the representative mutant of the group of six allelic mutants, further called *sgi7-1* – *sgi7-6*. We therefore chose to characterize these mutants in more detail.

Multiple mutations identified in conserved domains of EIN5

As the promising *sgi7* mutant (from now on named *sgi7-1*) was the representative of an allelic group of six mutants, we also identified the exact mutation in each of the 5 other mutants (Table 5.2; Figure 5.2). The mutations mapped on 6 different sites on the coding sequence of EIN5 and had different predicted effects on the protein sequence: in *sgi7-1*, *sgi7-2* and *sgi7-4*, the point mutation results in a amino acid substitution, while in *sgi7-3* and *sgi7-5*, the mutation is likely to generate a nonsense mutation. Finally, in *sgi7-6*, the mutation was situated in the splice acceptor site of the 14th intron, which could generate incorrect splicing and finally result in a frameshift.

The EIN5/XRN4 protein is a rather large protein of 947 amino acids with relatively well-conserved orthologs in Drosophila and yeast (Nagarajan et al., 2013). The protein structure of the yeast XRN1 has recently been described, and the N-terminal half of the protein, containing the most important functional domains, is thought to be conserved between the orthologs. At its N-terminal, the exoribonuclease EIN5 contains several small well-conserved domains, such as a steric barrier to prevent penetrance of dsRNA, a basic pocket for substrate stabilisation and a RNA binding motif (Figure 5.2). Next to this, the N-terminal side contains several extremely well-conserved amino acids which are thought to be crucial for proper functionality of the active site and which are situated in short stretches of very well-conserved amino acids. Interestingly, several of the identified mutations are localized within these very conserved and thus potentially important motifs (Figure 5.2).

Table 5.2. Position of the mutations in the EMS-mutants for EIN5 and their effect. Six mutations were identified on different positions of the EIN5 coding sequence. Based on the validated mutations, the effect on protein level was predicted: three of them generate a missense mutation, two a nonsense mutation and one generates an incorrect splicing variant probably resulting in a frameshift. Nt = nucleotide, AA = amino acid.

Mutant	Nt position	Mutation Nt	AA position	Mutation AA
sgi7-1	314	G -> A	105	G -> E
sgi7-2	329	C -> T	110	A -> V
sgi7-3	343	C -> T	115	Q -> STOP
sgi7-4	706	G -> A	236	D -> N
sgi7-5	1476	C -> T	526	Q -> STOP
sgi7-6	1603	G -> A	Splice acceptor site mutated	

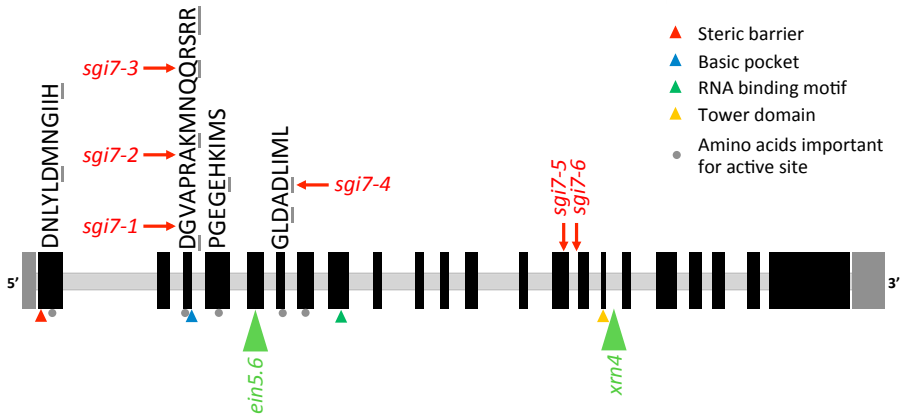

Figure 5.2. Structure of the EIN5/XRN4 protein with location of the identified mutations. Based on structure predicted by PLAZA (Proost et al., 2009) and on the observations of Nagarajan et al. (2013). Underlined residues indicate key residues for active site function surrounded by conserved stretches of amino acids. Mutants obtained with the EMS-screen are indicated in red, mutants used in previous studies in green (Potuschak et al., 2006). Small arrows indicate point mutants, large triangles indicate T-DNA insertions.

The different alleles have diverse effects on leaf growth

When grown under in soil conditions without addition of DEX, *sgi7* mutants showed visibly larger rosettes (Figure 5.1C). To investigate whether all identified mutations in *EIN5* had a similar effect on Arabidopsis leaf growth, all mutants were simultaneously grown in soil for 22 days (without DEX) and rosette size was measured by making leaf series. Interestingly, the six *sgi7* alleles showed different levels of increase in leaf size (Figure 5.3A). The most pronounced increase in leaf size was observed for the *sgi7-1* mutant, with an average increase of 49% (P = 2E-9). The mutants *sgi7-5* and *sgi7-2* also showed a significant increase in final rosette area of respectively 26% and 15%. In contrast, the mutants *sgi7-3*, *sgi7-4* and *sgi7-6* were not larger than the WT.

To further evaluate these growth phenotypes, two independent previously used mutants of *EIN5* (*ein5.6* and *xrn4*) were phenotyped in a similar way. These three mutants are confirmed loss-of-function mutants as they carry a T-DNA insertion in the fifth exon, and in an intron, respectively (Figure 5.2) (Olmedo et al., 2006). Although these mutants have been extensively studied, their leaf growth has never been characterized in detail. At 22 days after stratification (DAS), the final rosette area was unaltered as compared to wild-type rosette size (Figure 5.3B). The observation that in these loss-of-function mutants the leaf size is not increased suggests that the point mutations found in the *sgi7-1*, *sgi7-2* and *sgi7-5* mutants, with increased rosettes size, likely do not generate EIN5 loss-of-function alleles, but rather alter some activity of this protein.

Additional phenotypes observed in the by EMS-generated *ein5* mutants as well as in the loss-of-function *ein5* mutants are the pronounced leaf serration (Olmedo et al., 2006), as well as the typical ethylene-insensitive phenotype; the suppression of the triple response of etiolated seedlings germinated on ACC (Van Der Straeten et al., 1993) (Supp. Figure 8). These phenotypes were equally present in all *sgi7* mutants, which would suggest that the different alleles of *EIN5* do not differently affect the expression of this particular leaf phenotype and this general ethylene response.

The EIN5^{G105E} mutation increases leaf size under control conditions and drought

To unravel the mechanisms behind the stimulation of leaf growth in the *sgi7* mutants, we further focused on the mutant with the largest rosette area, *sgi7-1*. Detailed analysis showed that this mutant is on average 49% larger resulting from an increased size of all leaves (Figure 5.3A, 5.4A and 5.4B). To uncover the cellular mechanism behind it, cellular drawings of the abaxial epidermal layer were made to determine whether

increased leaf growth results from more and/or larger cells. We observed a pronounced increase in cell area, with an average increase of 36% (Figure 5.4C). The increase in cell area was however not sufficient to explain the increased leaf size (51% for the third leaf), but the cell number was only slightly and not significantly increased in all biological repeats. We thus conclude that the leaf size increase in the *sgi7-1* mutant mainly results from an increase in cell area.

Because the growth-inhibitory pathway on which the forward genetics screen is based is mainly active under adverse environmental conditions reducing rosette growth, we exposed the *sgi7-1* mutant to mild drought stress. The mutant and wild type were grown on the Weighing Imaging and Watering Machine xyz (WIWAMxyz) under a well-watered regime for 10 days and then exposed to a mild drought stress regime reducing wild-type rosette size by about 30-40% (Skirycz et al., 2011). Rosette size was measured at 22 DAS. Interestingly, the drought-induced growth inhibition was less pronounced in the *sgi7-1* mutant (-23% in *sgi7-1* compared to -33% in WT) (Figure 5.4D). As this mutant already shows a growth advantage under normal conditions, this resulted in *sgi7-1* mutants being under mild drought equally large as wild type under control conditions. We thus conclude that the EIN5^{G105E} allele not only positively affects growth under control conditions, but also under mild drought stress.

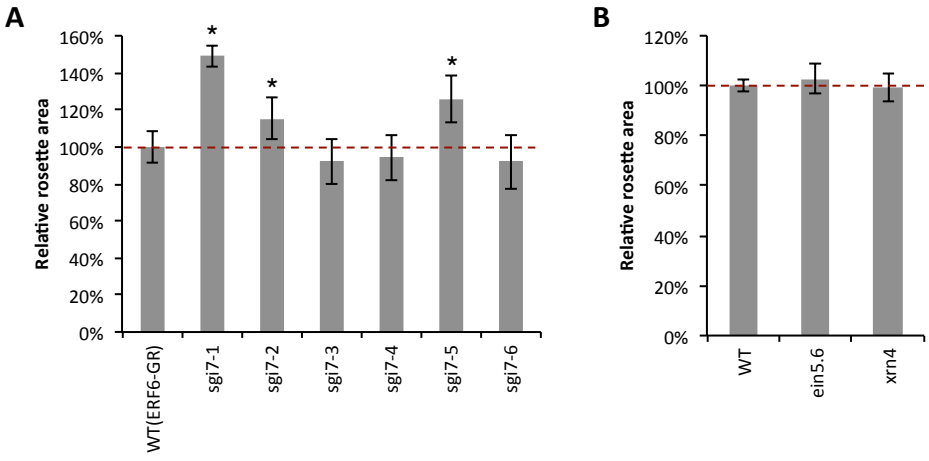

Figure 5.3. Rosette size of the EMS-mutants and the previously described *ein5* mutants. (A) Rosette size of the EMS-mutants at 22 days after stratification (DAS) upon growth in soil without DEX. (B) Rosette size of the previously characterized *ein5* mutants at 22 days after stratification (DAS) upon growth in soil. Values were normalized to the size of the wild type. Error bars represent standard error.

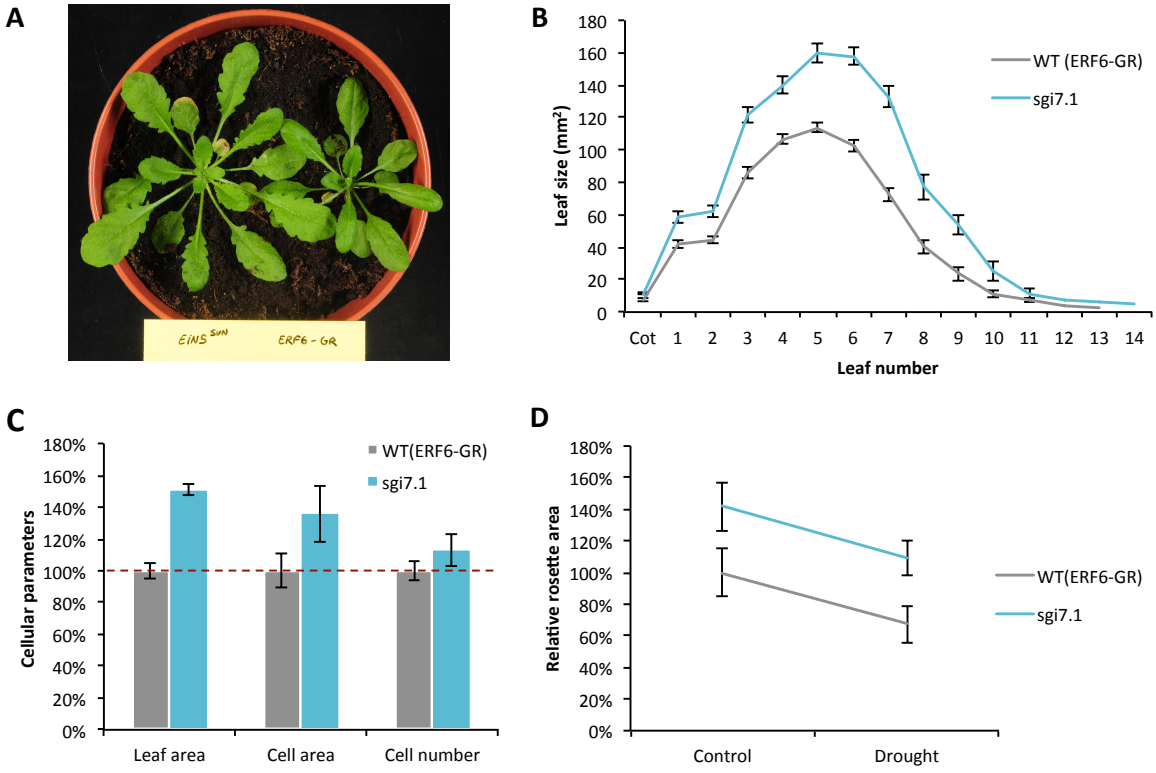

Figure 5.4. Rosette phenotype and cellular measurements of *sgi7-1*. (A) Picture of a representative *sgi7-1* rosette (left) and appropriate WT (ERF6-GR) (right) after 25 days of growth in soil. (B) Size per leaf of the *sgi7-1* mutant and wild type at 22 days after stratification (DAS) upon growth in soil. Error bars represent standard deviation of four biological repeats. (C) Cellular measurements of the abaxial epidermal cell layer of the third leaves from the plants in (B), relative to WT. Error bars represent standard error. (D) Rosette size of the *sgi7-1* mutant at 22 days after stratification (DAS) when grown on the WIWAMxyz under either well-watered conditions or mild drought stress.

DISCUSSION

Loss-of-function of EIN5 suppresses ERF6 function

Amongst the mutated genes, *EIN5* was an interesting candidate to further characterize in detail, since it was directly linked to ethylene signaling. The EIN5 gene encodes an exoribonuclease, the activity of which is induced by ethylene. It negatively regulates the stability of the transcripts of two F-box proteins, EBF1 and EBF2 (Olmedo et al., 2006; Potuschak et al., 2006), which trigger the degradation of the central ethylene response-mediating transcription factors EIN3 and EIL1 (Guo and Ecker, 2003; Potuschak et al., 2003). At the molecular level, EIN5 is a large protein of close to 1,000 amino acids with several highly conserved functional domains, mainly at the N-terminus, which also contains the 5' -> 3' exoribonuclease domain (Figure 5.2) (Nagarajan et al., 2013). EIN5

does not randomly degrade unstable mRNA and is not involved in the general silencing mechanisms, but instead recognizes target mRNA through defined motifs (Souret et al., 2004; Potuschak et al., 2006; Rymarquis et al., 2011). Candidate EIN5 target transcripts were identified in etiolated seedlings, and a computational study for motif enrichement in these targets identified 27 specific hexamer-motifs (Souret et al., 2004; Olmedo et al., 2006).

As mutations in *EIN5* trigger stabilization of *EBF1* and *EBF2* transcripts, and as a consequence constitutive degradation of EIN3 and EIL1, *ein5* mutants no longer show the typical triple response of ethylene-treated seedlings grown in the dark (Van der Straeten et al., 1993; Roman et al., 1995). This insensitivity to ethylene has also clearly been observed in all the *sgi7* mutants. Thus, all alleles of *EIN5* generated by the mutagenesis trigger loss of the ethylene signaling-related function of EIN5. It is, however, unlikely that a general reduction in ethylene signaling is responsible for the suppression of the ERF6-induced dwarfism, as ERF6 has previously been shown to be induced by a parallel MPK3/MPK6 branch of the pathway, instead of being controlled by the EIN3-mediated ethylene signaling (Skirycz et al., 2011; Dubois et al., 2013). Besides ethylene insensitivity, *ein5* loss-of-function mutants generated through reverse genetics are also known to show serration of the rosette leaves (Olmedo et al., 2006), and this phenotype was observed for all mutants of the *sgi7* allelic group as well.

New EIN5 alleles for improved leaf growth?

ein5 loss-of-function mutants grown under control conditions in soil do not show an altered rosette size. In this respect, the *sgi7-3*, *sgi7-4* and *sgi7-6* mutants phenocopy the *ein5* loss-of-function mutants regarding suppression of triple response, leaf serration, and leaf growth. This can be explained through the nature of the mutations: a premature stopcodon in the first exon of *EIN5*, a mutation of a crucial amino acid in a conserved domain or a frame shift mutation, as observed in respectively *sgi7-3*, *sgi7-4* and *sgi7-6*, which all likely result in complete loss-of-function EIN5 alleles.

Three other mutants, *sgi7-1*, *sgi7-2* and *sgi7-5*, phenocopied *ein5* loss-of-function mutants regarding leaf serration and suppression of triple response, but additionally showed increased rosette size, which was for *sgi7-1* shown to be a result of increased cell expansion. EIN5 has previously already been linked to leaf growth, as upon treatment of plants with the growth-stimulating Harpin peptide, EIN5 is necessary to confer the increased rosette size phenotype (Dong et al., 2004). Importantly, this function of EIN5 occurs independently of the EIN2-mediated ethylene signaling. Here, we additionally showed that the ethylene insensitive trait observed in *ein5* can be uncoupled from the role of EIN5 in leaf growth regulation.

The mutations in *sgi7-1* and *sgi7-2* caused amino acid substitutions within a very conserved domain, but not on crucial residues. It can be speculated that these substitutions slightly affect the physical conformation of the conserved active site of the exoribonuclease, affecting the recognition of target motifs, but not the catalytic activity. We thus speculate that the mutations in *sgi7-1* and *sgi7-2* alter the specificity to certain but not all motifs, resulting in the loss of certain EIN5-mediated functions, but also in growth increase. *sgi7-1* and *sgi7-2* alleles of *EIN5* might, for example, recognize new motifs and thus degrade new mRNA targets. None of the genes known to be involved in the ERF6-related network are amongst the EIN5 target genes, and growth-related putative targets of EIN5 are still to be identified.

We believe that the identification of the transcripts targetted in growing leaves by the different alleles of EIN5 will provide the key to understand the precise role of EIN5 in leaf growth. As the EIN5 protein binds RNA, a suitable approach could be to use RNA Immuno Precipitation, a technique in which RNA and proteins are crosslinked, RNA:protein complexes are immunoprecipitated, and RNA is subsequently identified upon decrosslinking. In an attempt to complete this part of the project, we generated 35S:EIN5^{WT}:GFP and 35S:EIN5^{G105E}:GFP lines. As we hereby induce over-activation of the ethylene signaling pathway, we expected these lines (at least 35S:EIN5^{WT}:GFP) to show a smaller phenotype, similar to what was reported for *EIN2*-overexpression lines (Feng et al., 2015). However, we did not observe any phenotype resulting from the overexpression, and although the *EIN5* gene was strongly overexpressed in all lines, we also did not detect accumulation of the protein. As the regulatory mechanisms upstream of EIN5 are still elusive, it is very challenging to produce lines overexpressing a stable EIN5 protein, and unfortunately we and other groups did not succeed thus far (Thomas Potuschak, personal communication). A new attempt with similar constructs driven by the endogenous EIN5-promotor in the *ein5* mutant background might be more successful and might provide the key to new insights in the role of EIN5 in leaf growth.

Future perspectives for a network combining diverse molecular functions

We show here that our forward genetics screen, which was set up to expand the network around ERF6, is a powerful tool to identify genes involved in leaf growth and stress response, and holds great promise for the future. Several causal genes still remain to be identified or validated, and it will be very exciting to connect the already identified genes to the ERF6 protein and its function in leaf growth at the molecular level. However, based on the preliminary identification of mutated genes in several mutants, we can already speculate about how the mutants affect ERF6 function.

The HASTY gene, which is the most likely candidate underlying the *sgi4* phenotype, encodes a karyopherin of the importin family, regulating nucleocytoplasmic transport of proteins and miRNAs to the nucleus (Telfer and Poethig, 1998; Bollman et al., 2003). Importantly, the HASTY gene has already been identified in several EMS screens and might thus have pleiotrophic functions (Allen et al., 2013; Pascal Genschik, personal communication). As the functionality of GR lines relies on proper transport of the constitutively overexpressed fusion protein to the nucleus, it can be speculated that HASTY is involved in this translocation, and that truncated HASTY proteins fail in this process. The molecular question to be answered is thus whether the suppression of the phenotype is due to inhibition of the ERF6 function, or due to a more general suppression of the GR translocation-based system. This is currently being investigated by crossing 35S:ERF6 lines with high ERF6-overexpression level and smaller rosettes with the *sgi4* mutant. If the phenotype is still rescued, this would indicate that the suppression mechanism acts specifically on ERF6, for example by regulating its import into the nucleus. In that case, it will be valuable to continue to unravel this molecular connection between HASTY and ERF6, by investigating whether ERF6 import is perturbed in *hasty* mutants, and by demonstrating physical binding between ERF6 and HASTY, as protein interaction is known to be detectable upon import of a transcription factor by HASTY (Ciftci-Yilmaz et al., 2007).

The *CPL3* gene encodes a biotic and abiotic stress-inducible phosphatase likely negative regulating stress defense responses (Koiwa et al., 2002; Li et al., 2014). CPL3 and other members of the CPL family are known to affect rosette growth, and *cpl3* mutants grow slower than wild type plants but show early flowering (Koiwa et al., 2002), a phenotype that has also been observed in the *sgi3* mutant (Ting Li and Dirk Inzé, personal communication). With its clear effect on leaf size when mutated, and emerging roles in the regulation of biotic stress response downstream of a MAPK-signaling cascade (Li et al., 2014), CPL3 forms a good candidate to mediate suppression of the ERF6 function. At the molecular level, CPL3 was found to have a phosphatase function that acts on RNA polymerase II, thereby blocking transcription (Li et al., 2014). It can be speculated that loss-of-function of CPL3 alters the transcriptional control of Arabidopsis genes involved in growth, or of ERF6 target genes, thereby suppressing part of the ERF6 function. Here, transcriptome analysis of *cpl3* mutants can shed light on the growth-related target genes whose expression is altered when CPL3 is mutated.

The *RST1* gene has been identified in a screen for mutants with altered cuticular waxes (Chen et al., 2005). While the molecular function of the protein is still unknown as it has no known domains, it is thought to be involved in acyl-CoA reduction to aldehydes in the long chain fatty acid biosynthesis. Because *rst1* leaves have elevated levels of cuticular waxes, mutants are more tolerant to necrotrophic fungal pathogens such as *Botrytis*

cinerea (Mang et al., 2009). Interestingly, *erf5erf6* mutants were also found to be more tolerant to this necrotroph (Moffat et al., 2012), although contradictory results exist about the function of ERF6 in biotic stress response (Son et al., 2012). As *rst1* mutants produce 70% of shrunken seeds that are unviable, which was also observed for the *sgi6* mutant, the *RST1* gene is also thought to play a role in embryo development (Chen et al., 2005). Unraveling the molecular link between ERF6 and RST1 might be even more challenging, as it would, for example necessitate metabolic profiling of *erf5erf6* plants for comparison, and nothing is known about possible effects of ERF6 on fatty acid metabolism. As RST1 has already been described to be possibly involved in biotic stress response and in ethylene response (Mang et al., 2009), two fields to which ERF6 is also directly linked, the mechanistic link between ERF6, RST1, and leaf growth undoubtedly deserves particular attention.

Together, the different genes that were up to now identified as (potential) suppressors of the ERF6 phenotype when mutated have clearly divergent molecular functions. This shows that the network around ERF6 possibly involves regulation on transcriptional (CPL3), posttranscriptional (EIN5), metabolic (RST1), and localisation (HASTY) level. This forward genetics screen thus offered a unique approach to capture this diversity, and the unraveling of the network around ERF6 will be of high value to gain new insights in the molecular functions of this important growth regulator.

MATERIALS AND METHODS

Plant Lines

The mutagenesis was performed on the ERF6^{IOE}-S line described in Chapter 3.

Mutagenesis

The mutagenesis was performed by treatment of the seeds with EMS as described in Schneeberger et al., 2009. Mutagenized seeds were upscaled to M2 in greenhouse conditions.

Forward Genetics Screen

The screen was performed in vitro on ½ MS plates supplemented with 5µM DEX and 1mg/L Kanamycine. On such medium, only seedlings suppressing the ERF6-mediated growth inhibition are able to grow normally. Seedlings suppressing the ERF6-induced dwarfism were selected and transplanted to soil for upscale. About 40,000 seedlings were screened. The selected mutants were checked by Sanger sequencing for the

presence of an intact 35S:ERF6-GR construct. qRT-PCR was performed to measure the ERF6-overexpression level. For this purpose, RNA extraction, cDNA synthesis and qRT-PCR were performed as described previously (Chapter 4).

Identification of the Mutation

The causal mutation was identified as explained in Schneeberger et al., 2009. In short, the selected mutants were crossed with the Landsberg Erecta ecotype and upscaled to F2 generation. The segregating population was sown in vitro on ½ MS medium supplemented with 5µM DEX and Kanamycine. 400 to 500 seedlings with normal growth in these conditions (indicative for the presence of at least one copy of the ERF6-GR domain and the homozygous causal mutation) were pooled. DNA was extracted with the CTAB method and RNA was removed with an on column RNase treatment. Whole genome DNA was sequenced using Illumina sequencing, 100nt paired end, performed at the nucleomics facility (VIB). Raw DNA sequences were processed using SHORE and peak calling was further performed with SHOREmap, as explained in Schneeberger et al., 2009. Identified putative mutations were further validated experimentally by PCR and sequencing the genes of interest in the mutant and in the non-mutagenized ERF6-GR plants.

Soil Plant Growth Conditions and Leaf Size Measurements

Plants were grown in Gottinger pots (8x8x8.5cm) filled with soil (Saniflor, without osmocot) at 21˚C under a 16-h day (110 µmol m-2 s-1) and 8-h night regime. Pots were covered with transparent plastic foil for 4 days to stimulate germination. Watering with 15 mL of water was applied at 9, 13, 16 and 20 DAS. For leaf size measurements, twelve plants were grown per line and the transgenic lines were always grown together with the appropriate control on the same tray and randomization was done between the genotypes. At 22 DAS, plants were harvested and leaf series were made by cutting each individual leaf of the rosette and ranking them from old to young on a square agar plate. Plates were photographed and pictures were subsequently analysed using ImageJ v1.45 (NIH; http://rsb.info.nih.gov/ij/) to measure the size of each individual leaf.

***In Vitro* Plant Growth Conditions**

Seedlings were grown *in vitro* on half-strength MS medium (Murashige and Skoog, 1962) containing 1% sucrose at 21˚C under a 16-h day (110 µmol m-2 s 1) and 8-h night regime. 9 g/L agar was added to the medium.

Drought stress experiments with the Weighing, Imaging, and Watering Machine xyz

Plants were grown under a long-day regime (16h light / 8h dark), at 21°C and a light intensity of 110-120 µmol m-2 s-1, on a automated platform called the WIWAMxyz. The WIWAMxyz is an automated platform for 392 Arabidopsis plants, with a robotic arm bringing each pot once a day to a weighing and watering unit, with a scale to weigh the pots, calculate and add the required amount of water, and subsequently to an imaging platform (not used in these experiments). Plants were grown in polypropylene pots (Skirycz et al., 2011) filled with 85g +- 1g of Saniflor compost (Van Isreal N.V., Geraardsbergen, Belgium). The initial absolute water content was determined at the beginning of each experiment and used to calculate the target weight of pots for well-watered regime (2.2 g_{water}/g_{soil}) and mild drought (1.2 g_{water}/g_{soil}). The pots were randomized daily to homogenously mix the mutants and the wild type plants. All plants were watered daily from 5 DAS until 10 DAS with a well-watered regime. At 11 DAS, half of the pots were maintained at the well-watered regime until the end of the experiment, while the other half of the pots were not watered until the relative humidity dropped to 1.2 g_{water}/g_{soil} (on average 6 days after the water was first withheld). All experiments lasted until 21 DAS.

SUPPLEMENTAL DATA

All Supplemental Data is listed below. Supplemental Figures can be found at the end of this chapter. Supplemental Table S1. can be downloaded from:
http://www.psb.ugent.be/~madub/Supp_Table_S1.xlsx

Supplemental Figure S1. Phenotype of the selected mutants.

Supplemental Figure S2. Expression level of ERF6 in the selected mutants.

Supplemental Figure S3. Overview of the phenotypes of F2 seedlings of *sgi1* x *Col-0* and *sgi2* x *Col-0* crosses.

Supplemental Figure S4. Seed yield phenotype of the *sgi7* mutant.

Supplemental Figure S5. Illustation of the selection of the seedlings for bulk segregant analysis.

Supplemental Figure S6. Output of the SHOREmap analysis per mutant.

Supplemental Figure S7. cDNA sequences of *RST1* in *sgi6* and wild type.

Supplemental Figure S8. Suppression of the triple response in the sgi7 mutants grown in darkness on 5 µM ACC.

ACKNOWLEDGEMENTS

We thank Dr. Hannes Claeys for the fruitful scientific discussions along the project and the help to improve the manuscript, as well as the whole Systems Biology of Yield group for the stimulating environment and constructive scientific discussions. Special thanks to Jordi Denecker for the precious help to get started with SHORE and SHOREmap and to Michiel Rydant for the practical help during his thesis. This work was supported by the Interuniversity Attraction Poles Program (IUAP P7/29 "MARS") initiated by the Belgian Science Policy Office, by Ghent University ('Bijzonder Onderzoeksfonds Methusalem Project' no. BOF08/01M00408, Multidisciplinary Research Partnership "Biotechnology for a Sustainable Economy" Project no. 01MRB510W).

REFERENCES

Achard, P., F. Gong, S. Cheminant, M. Alioua, P. Hedden and P. Genschik (2008). "The cold-inducible CBF1 factor-dependent signaling pathway modulates the accumulation of the growth-repressing DELLA proteins via its effect on gibberellin metabolism." Plant Cell 20(8): 2117-2129.

Allen, R. S., K. Nakasugi, R. L. Doran, A. A. Millar and P. M. Waterhouse (2013). "Facile mutant identification via a single parental backcross method and application of whole genome sequencing based mapping pipelines." Frontiers in Plant Science 4.

Anastasiou, E. and M. Lenhard (2007). "Growing up to one's standard." Current Opinion in Plant Biology 10(1): 63-69.

Andriankaja, M., S. Dhondt, S. De Bodt, H. Vanhaeren, F. Coppens, L. De Milde, P. Muhlenbock, A. Skirycz, N. Gonzalez, G. T. S. Beemster and D. Inze (2012). "Exit from Proliferation during Leaf Development in Arabidopsis thaliana: A Not-So-Gradual Process." Developmental Cell 22(1): 64-78.

Ascencio-Ibanez, J. T., R. Sozzani, T. J. Lee, T. M. Chu, R. D. Wolfinger, R. Cella and L. Hanley-Bowdoin (2008). "Global analysis of Arabidopsis gene expression uncovers a complex array of changes impacting pathogen response and cell cycle during geminivirus infection." Plant Physiology 148(1): 436-454.

Baerenfaller, K., C. Massonnet, S. Walsh, S. Baginsky, P. Buhlmann, L. Hennig, M. Hirsch-Hoffmann, K. A. Howell, S. Kahlau, A. Radziejwoski, D. Russenberger, D. Rutishauser, I. Small, D. Stekhoven, R. Sulpice, J. Svozil, N. Wuyts, M. Stitt, P. Hilson, C. Granier and W.

Gruissem (2012). "Systems-based analysis of Arabidopsis leaf growth reveals adaptation to water deficit." Molecular Systems Biology 8.

Birkenbihl, R. P., C. Diezel and I. E. Somssich (2012). "Arabidopsis WRKY33 Is a Key Transcriptional Regulator of Hormonal and Metabolic Responses toward Botrytis cinerea Infection." Plant Physiology 159(1): 266-285.

Bollman, K. M., M. J. Aukerman, M. Y. Park, C. Hunter, T. Z. Berardini and R. S. Poethig (2003). "HASTY, the Arabidopsis ortholog of exportin 5/MSN5, regulates phase change and morphogenesis." Development 130(8): 1493-1504.

Chen, X. B., S. M. Goodwin, X. L. Liu, X. L. Chen, R. A. Bressan and M. A. Jenks (2005). "Mutation of the RESURRECTION1 locus of Arabidopsis reveals an association of cuticular wax with embryo development." Plant Physiology 139(2): 909-919.

Ciftci-Yilmaz S, Morsy MR, Song L, Coutu A, Krizek BA, Lewis MW, Warren D, Cushman J, Connolly EL, Mittler R (2007) The EAR-motif of the Cys2/His2-type zinc finger protein Zat7 plays a key role in the defense response of Arabidopsis to salinity stress. J Biol Chem 282: 9260-9268

Claeys, H. and D. Inze (2013). "The Agony of Choice: How Plants Balance Growth and Survival under Water-Limiting Conditions." Plant Physiology 162(4): 1768-1779.

Claeys, H., A. Skirycz, K. Maleux and D. Inze (2012). "DELLA Signaling Mediates Stress-Induced Cell Differentiation in Arabidopsis Leaves through Modulation of Anaphase-Promoting Complex/Cyclosome Activity." Plant Physiology 159(2): 739-+.

Dinneny, J. R. (2008). "Cell identity mediates the response of Arabidopsis roots to abiotic stress (vol 320, pg 942, 2008)." Science 322(5898): 44-44.

Dong HP, Peng J, Bao Z, Meng X, Bonasera JM, Chen G, Beer SV, Dong H (2004) Downstream divergence of the ethylene signaling pathway for harpin-stimulated Arabidopsis growth and insect defense. Plant Physiol 136: 3628-3638

Donnelly, P. M., D. Bonetta, H. Tsukaya, R. E. Dengler and N. G. Dengler (1999). "Cell cycling and cell enlargement in developing leaves of Arabidopsis." Developmental Biology 215(2): 407-419.

Dubois, M., A. Skirycz, H. Claeys, K. Maleux, S. Dhondt, S. De Bodt, R. Vanden Bossche, L. De Milde, T. Yoshizumi, M. Matsui and D. Inze (2013). "ETHYLENE RESPONSE FACTOR6 Acts as a Central Regulator of Leaf Growth under Water-Limiting Conditions in Arabidopsis." Plant Physiology 162(1): 319-332.

Feng G, Liu G, Xiao J (2015) The Arabidopsis EIN2 restricts organ growth by retarding cell expansion. Plant Signal Behav 10: e1017169

Gigolashvili, T., B. Berger, H. P. Mock, C. Muller, B. Weisshaar and U. I. Fluegge (2007). "The transcription factor HIG1/MYB51 regulates indolic glucosinolate biosynthesis in Arabidopsis thaliana." Plant Journal 50(5): 886-901.

Gonzalez, N., H. Vanhaeren and D. Inze (2012). "Leaf size control: complex coordination of cell division and expansion." Trends in Plant Science 17(6): 332-340.

Guo H, Ecker JR (2003) Plant responses to ethylene gas are mediated by SCF(EBF1/EBF2)-dependent proteolysis of EIN3 transcription factor. Cell 115: 667-677

Harb, A., A. Krishnan, M. M. R. Ambavaram and A. Pereira (2010). "Molecular and Physiological Analysis of Drought Stress in Arabidopsis Reveals Early Responses Leading to Acclimation in Plant Growth." Plant Physiology 154(3): 1254-1271.

Jiang, Y. Q. and M. K. Deyholos (2009). "Functional characterization of Arabidopsis NaCl-inducible WRKY25 and WRKY33 transcription factors in abiotic stresses." Plant Molecular Biology 69(1-2): 91-105.

Li, G. J., X. Z. Meng, R. G. Wang, G. H. Mao, L. Han, Y. D. Liu and S. Q. Zhang (2012). "Dual-Level Regulation of ACC Synthase Activity by MPK3/MPK6 Cascade and Its Downstream WRKY Transcription Factor during Ethylene Induction in Arabidopsis." Plos Genetics 8(6).

Li F, Cheng C, Cui F, de Oliveira MV, Yu X, Meng X, Intorne AC, Babilonia K, Li M, Li B, Chen S, Ma X, Xiao S, Zheng Y, Fei Z, Metz RP, Johnson CD, Koiwa H, Sun W, Li Z, de Souza Filho GA, Shan L, He P (2014) Modulation of RNA polymerase II phosphorylation downstream of pathogen perception orchestrates plant immunity. Cell Host Microbe 16: 748-758

Mang, H. G., K. A. Laluk, E. P. Parsons, D. K. Kosma, B. R. Cooper, H. C. Park, S. AbuQamar, C. Boccongelli, S. Miyazaki, F. Consiglio, G. Chilosi, H. J. Bohnert, R. A. Bressan, T. Mengiste and M. A. Jenks (2009). "The Arabidopsis RESURRECTION1 Gene Regulates a Novel Antagonistic Interaction in Plant Defense to Biotrophs and Necrotrophs." Plant Physiology 151(1): 290-305.

Meng, X. Z., J. Xu, Y. X. He, K. Y. Yang, B. Mordorski, Y. D. Liu and S. Q. Zhang (2013). "Phosphorylation of an ERF Transcription Factor by Arabidopsis MPK3/MPK6 Regulates Plant Defense Gene Induction and Fungal Resistance." Plant Cell 25(3): 1126-1142.

Moffat CS, Ingle RA, Wathugala DL, Saunders NJ, Knight H, Knight MR (2012) ERF5 and ERF6 play redundant roles as positive regulators of JA/Et-mediated defense against *Botrytis cinerea* in Arabidopsis. PLoS ONE 7: e35995

Nagarajan, V. K., C. I. Jones, S. F. Newbury and P. J. Green (2013). "XRN 5 ' -> 3 ' exoribonucleases: Structure, mechanisms and functions." Biochimica Et Biophysica Acta-Gene Regulatory Mechanisms 1829(6-7): 590-603.

Nakano, T., K. Suzuki, T. Fujimura and H. Shinshi (2006). "Genome-wide analysis of the ERF gene family in Arabidopsis and rice." Plant Physiology 140(2): 411-432.

Niu, C. F., W. Wei, Q. Y. Zhou, A. G. Tian, Y. J. Hao, W. K. Zhang, B. A. Ma, Q. Lin, Z. B. Zhang, J. S. Zhang and S. Y. Chen (2012). "Wheat WRKY genes TaWRKY2 and TaWRKY19

regulate abiotic stress tolerance in transgenic Arabidopsis plants." Plant Cell and Environment 35(6): 1156-1170.

Olmedo, G., H. W. Guo, B. D. Gregory, S. D. Nourizadeh, L. Aguilar-Henonin, H. J. Li, F. Y. An, P. Guzman and J. R. Ecker (2006). "ETHYLENE-INSENSITIVE5 encodes a 5 '-> 3 ' exoribonuclease required for regulation of the EIN3-targeting F-box proteins EBF1/2." Proceedings of the National Academy of Sciences of the United States of America 103(36): 13286-13293.

Potuschak T, Lechner E, Parmentier Y, Yanagisawa S, Grava S, Koncz C, Genschik P (2003) EIN3-dependent regulation of plant ethylene hormone signaling by two arabidopsis F box proteins: EBF1 and EBF2. Cell 115: 679-689

Potuschak, T., A. Vansiri, B. M. Binder, E. Lechner, R. D. Vierstra and P. Genschik (2006). "The exoribonuclease XRN4 is a component of the ethylene response pathway in Arabidopsis." Plant Cell 18(11): 3047-3057.

Roman, G., B. Lubarsky, J. J. Kieber, M. Rothenberg and J. R. Ecker (1995). "Genetic-Analysis of Ethylene Signal-Transduction in Arabidopsis-Thaliana - 5 Novel Mutant Loci Integrated into a Stress-Response Pathway." Genetics 139(3): 1393-1409.

Rymarquis, L. A., F. F. Souret and P. J. Green (2011). "Evidence that XRN4, an Arabidopsis homolog of exoribonuclease XRN1, preferentially impacts transcripts with certain sequences or in particular functional categories." Rna-a Publication of the Rna Society 17(3): 501-511.

Sakamoto, H., T. Araki, T. Meshi and M. Iwabuchi (2000). "Expression of a subset of the Arabidopsis Cys(2)/His(2)-type zinc-finger protein gene family under water stress." Gene 248(1-2): 23-32.

Sakamoto, H., K. Maruyama, Y. Sakuma, T. Meshi, M. Iwabuchi, K. Shinozaki and K. Yamaguchi-Shinozaki (2004). "Arabidopsis Cys2/His2-type zinc-finger proteins function as transcription repressors under drought, cold, and high-salinity stress conditions." Plant Physiology 136(1): 2734-2746.

Schachtman, D. P. and J. Q. D. Goodger (2008). "Chemical root to shoot signaling under drought." Trends in Plant Science 13(6): 281-287.

Schneeberger, K., S. Ossowski, C. Lanz, T. Juul, A. H. Petersen, K. L. Nielsen, J. E. Jorgensen, D. Weigel and S. U. Andersen (2009). "SHOREmap: simultaneous mapping and mutation identification by deep sequencing." Nature Methods 6(8): 550-551.

Seki, M., A. Matsui, J. M. Kim, J. Ishida, M. Nakajima, T. Morosawa, M. Kawashima, M. Satou, T. K. To, Y. Kurihara, E. Kaminuma, T. Endo, Y. Mochizuki, N. Kobayashi, T. Toyoda and K. Shinozaki (2007). "Arabidopsis whole-genome transcriptome analysis under drought, cold, high-salinity, and ABA treatment conditions using tiling array and 454 sequencing technology." Plant and Cell Physiology 48: S8-S8.

Skirycz, A., H. Claeys, S. De Bodt, A. Oikawa, S. Shinoda, M. Andriankaja, K. Maleux, N. B. Eloy, F. Coppens, S. D. Yoo, K. Saito and D. Inze (2011). "Pause-and-Stop: The Effects

of Osmotic Stress on Cell Proliferation during Early Leaf Development in Arabidopsis and a Role for Ethylene Signaling in Cell Cycle Arrest." Plant Cell 23(5): 1876-1888.

Skirycz, A., S. De Bodt, T. Obata, I. De Clercq, H. Claeys, R. De Rycke, M. Andriankaja, O. Van Aken, F. Van Breusegem, A. R. Fernie and D. Inze (2010). "Developmental Stage Specificity and the Role of Mitochondrial Metabolism in the Response of Arabidopsis Leaves to Prolonged Mild Osmotic Stress." Plant Physiology 152(1): 226-244.

Skirycz, A. and D. Inze (2010). "More from less: plant growth under limited water." Current Opinion in Biotechnology 21(2): 197-203.

Skirycz, A., K. Vandenbroucke, P. Clauw, K. Maleux, B. De Meyer, S. Dhondt, A. Pucci, N. Gonzalez, F. Hoeberichts, V. B. Tognetti, M. Galbiati, C. Tonelli, F. Van Breusegem, M. Vuylsteke and D. Inze (2011). "Survival and growth of Arabidopsis plants given limited water are not equal." Nature Biotechnology 29(3): 212-214.

Son GH, Wan J, Kim HJ, Nguyen XC, Chung WS, Hong JC, Stacey G (2012) Ethylene-responsive element-binding factor 5, ERF5, is involved in chitin-induced innate immunity response. Molecular Plant-Microbe Interactions 25: 48-60

Souret, F. F., J. P. Kastenmayer and P. J. Green (2004). "AtXRN4 degrades mRNA in Arabidopsis and its substrates include selected miRNA targets." Molecular Cell 15(2): 173-183.

Telfer, A. and R. S. Poethig (1998). "HASTY: a gene that regulates the timing of shoot maturation in Arabidopsis thaliana." Development 125(10): 1889-1898.

Tominaga R, Iwata M, Sano R, Inoue K, Okada K, Wada T (2008) Arabidopsis CAPRICE-LIKE MYB 3 (CPL3) controls endoreduplication and flowering development in addition to trichome and root hair formation. Development 135: 1335-1345

Umezawa, T., M. Fujita, Y. Fujita, K. Yamaguchi-Shinozaki and K. Shinozaki (2006). "Engineering drought tolerance in plants: discovering and tailoring genes to unlock the future." Current Opinion in Biotechnology 17(2): 113-122.

Vanderstraeten, D., A. Djudzman, W. Vancaeneghem, J. Smalle and M. Vanmontagu (1993). "Genetic and Physiological Analysis of a New Locus in Arabidopsis That Confers Resistance to 1-Aminocyclopropane-1-Carboxylic Acid and Ethylene and Specifically Affects the Ethylene Signal-Transduction Pathway." Plant Physiology 102(2): 401-408.

Verslues, P. E., M. Agarwal, S. Katiyar-Agarwal, J. Zhu and J. K. Zhu (2006). "Methods and concepts in quantifying resistance to drought, salt and freezing, abiotic stresses that affect plant water status. (vol 45, pg 523, 2006)." Plant Journal 46(6): 1092-1092.

Vlieghe, K., V. Boudolf, G. T. S. Beemster, S. Maes, Z. Magyar, A. Atanassova, J. D. Engler, R. De Groodt, D. Inze and L. De Veylder (2005). "The DP-E2F-like gene DEL1 controls the endocycle in Arabidopsis thaliana." Current Biology 15(1): 59-63.

Wang, P. C., Y. Y. Du, X. L. Zhao, Y. C. Miao and C. P. Song (2013). "The MPK6-ERF6-ROS-Responsive cis-Acting Element7/GCC Box Complex Modulates Oxidative Gene

Transcription and the Oxidative Response in Arabidopsis." Plant Physiology 161(3): 1392-1408.

Weigel, D., J., Glazebrook (2006). Adapted from "Obtaining Mutants," Chapter 2 in Arabidopsis by Detlef Weigel and Jane Glazebrook. Cold Spring Harbor Laboratory Press, Cold Spring Harbor, NY, USA, 2002.

Xiong, L. M., K. S. Schumaker and J. K. Zhu (2002). "Cell signaling during cold, drought, and salt stress." Plant Cell 14: S165-S183.

Supp. Figure S1. Phenotype of the selected mutants when grown on medium supplemented with Kanamycine (Km) or Dexamethasone (DEX). Seedlings grown on 1mg/L Km or 5 µM DEX until 19 days after stratification.

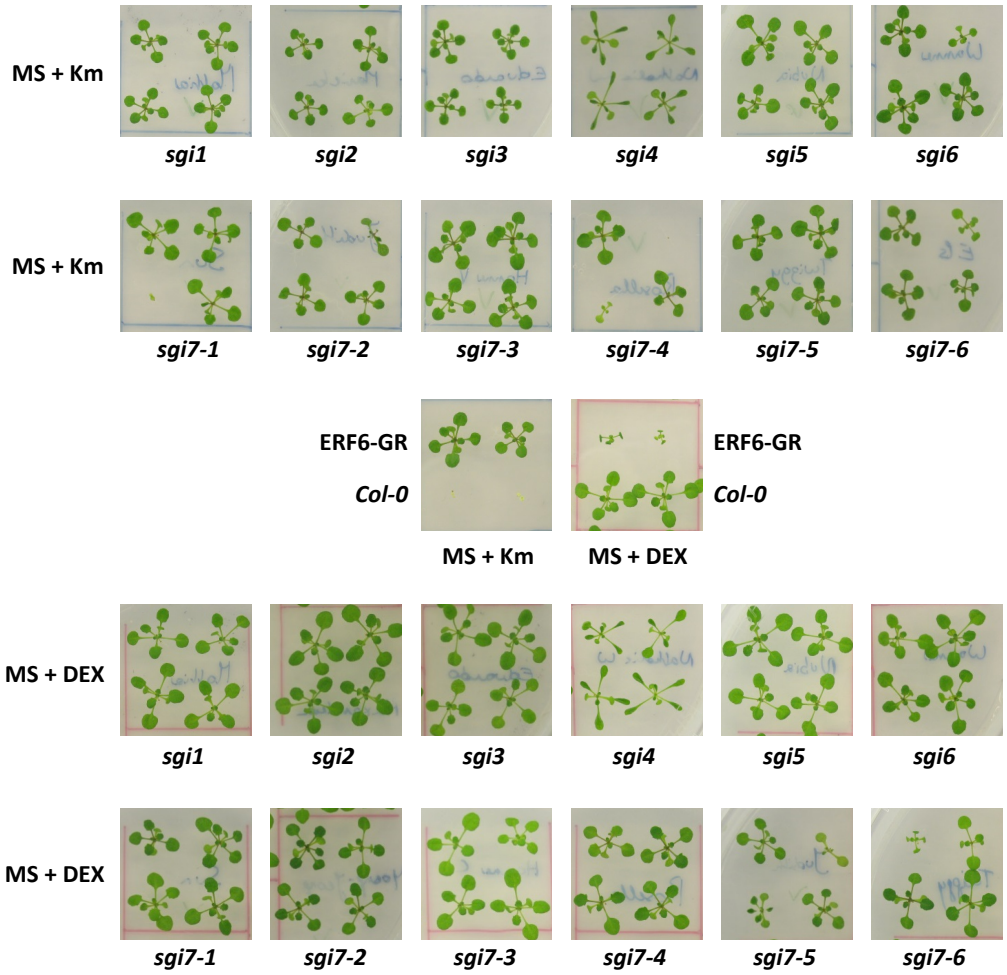

Supp. Figure S2. Expression level of ERF6 in the selected mutants. qRT-PCR measurements of the ERF6 level in the third true leaf of a 15-days-old plant grown *in vitro*. The indicated values are the Log_2(fold change) as compared to the ERF6 level in *Col-0*.

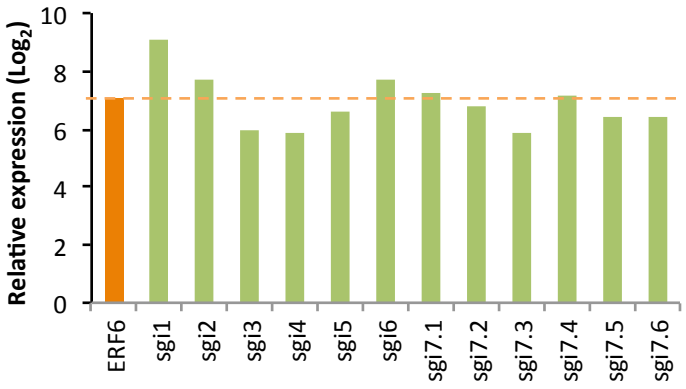

Supp. Figure S3. Overview of the phenotype of the F2 seedlings of *sgi1* x *Col-0* and *sgi2* x *Col-0* crosses. *sgi1* and *sgi2* mutants were crossed with *Col-0* and the F2 population was grown on medium supplemented with 1mg/L Km and 5 µM DEX. An F2 population in which seedlings exhibiting the ERF6-induced dwarfism are present in the segregating population (arrows) indicates that the mutation observed in ERF6-GR is not causative for the suppression of the ERF6-GR phenotype.

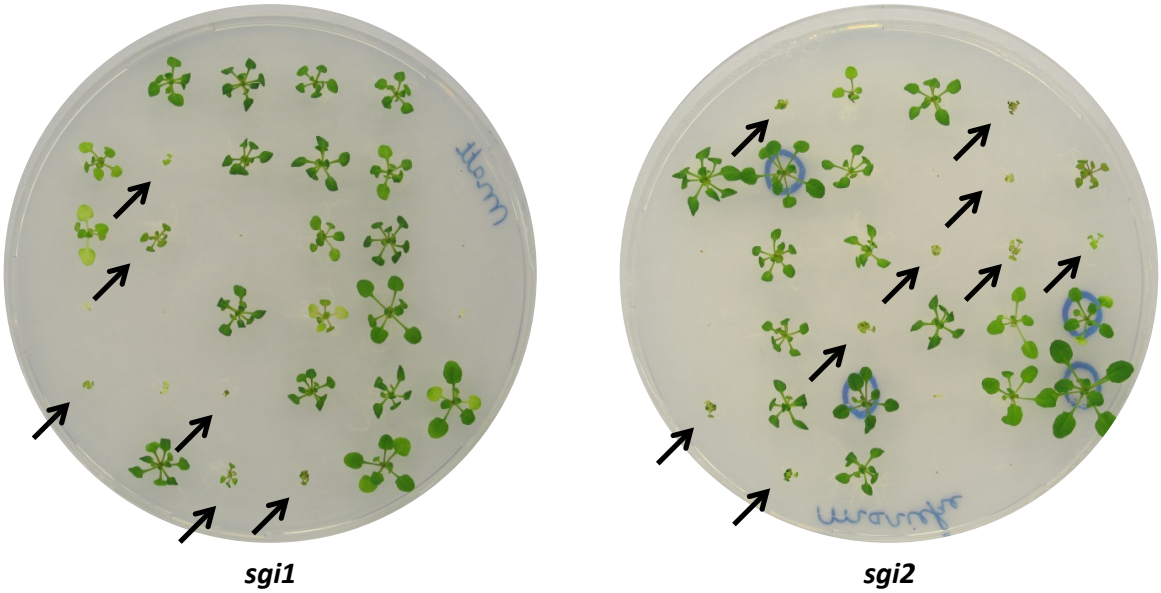

Supp. Figure S4. Seed yield phenotype of the *sgi7* mutant. (A) Average seed yield per plant. (B) Estimation of the number of seeds per plant, calculated by extrapolation from the weight of 500 seeds per plant. (C) Average projected seed size. * p<0.05

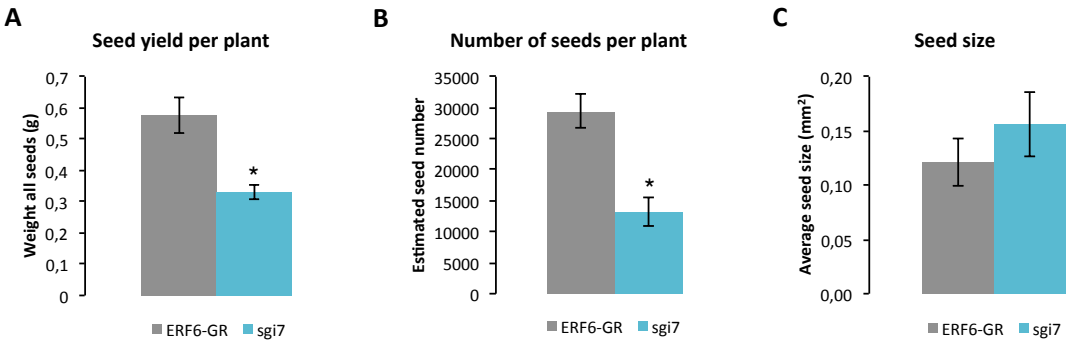

Supp. Figure S5. Illustation of the selection of the seedlings for bulk segregant analysis. (A) Overview of the expected distribution of the ERF6-GR and the causative EMS-mutation in the F2 population upon crossing of the mutants with *Col-0* and subsequent growth of the F2 population on medium supplemented with 1mg/L Km and 5 µM DEX. (B) From this segregating population, only seedlings clearly suppressing the ERF6-induced dwarfism were selected for DNAseq (red circle).

A

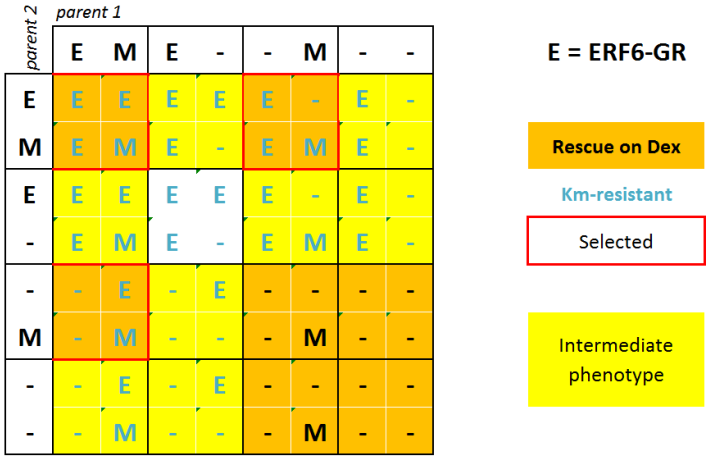

B

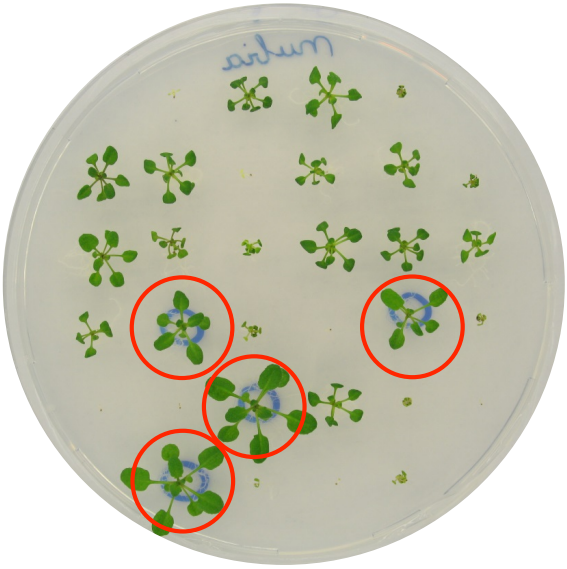

Supp. Figure S6. Output of the SHOREmap analysis per mutant. For each chromosome, the ratio of *Ler-1/Col-0* SNPs (y-axis) was calculated per position (x-axis) and is represented by a grey dot. Regions where this ratio is low likely harbour the causal mutations since they are highly enriched for Col-0 (mutant) DNA. Blue rectangles indicate these regions. Red rectangles indicate a *Col-0* enriched region which contains the ERF6-GR construct.

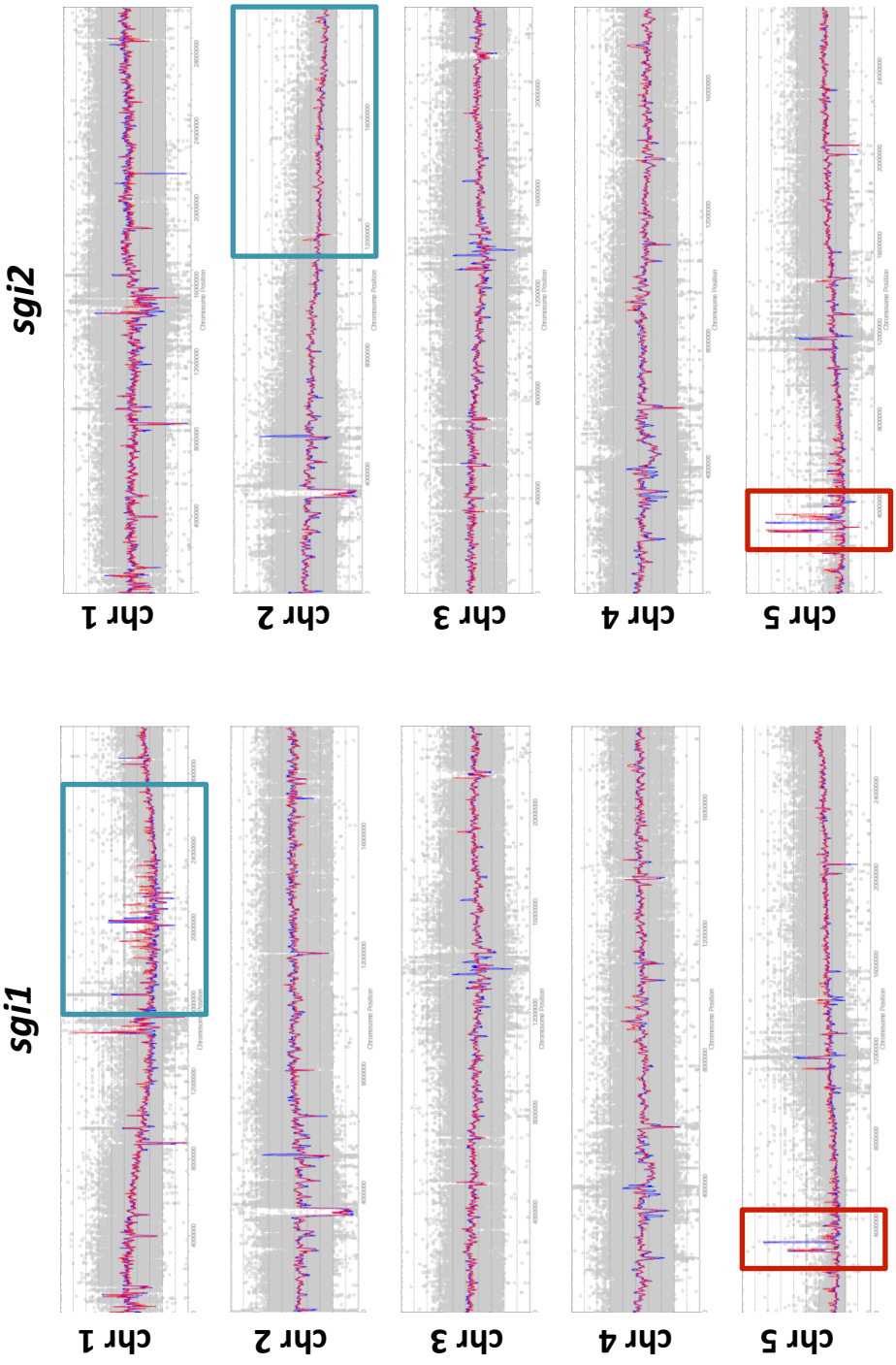

(Supp. Figure S6, continued)

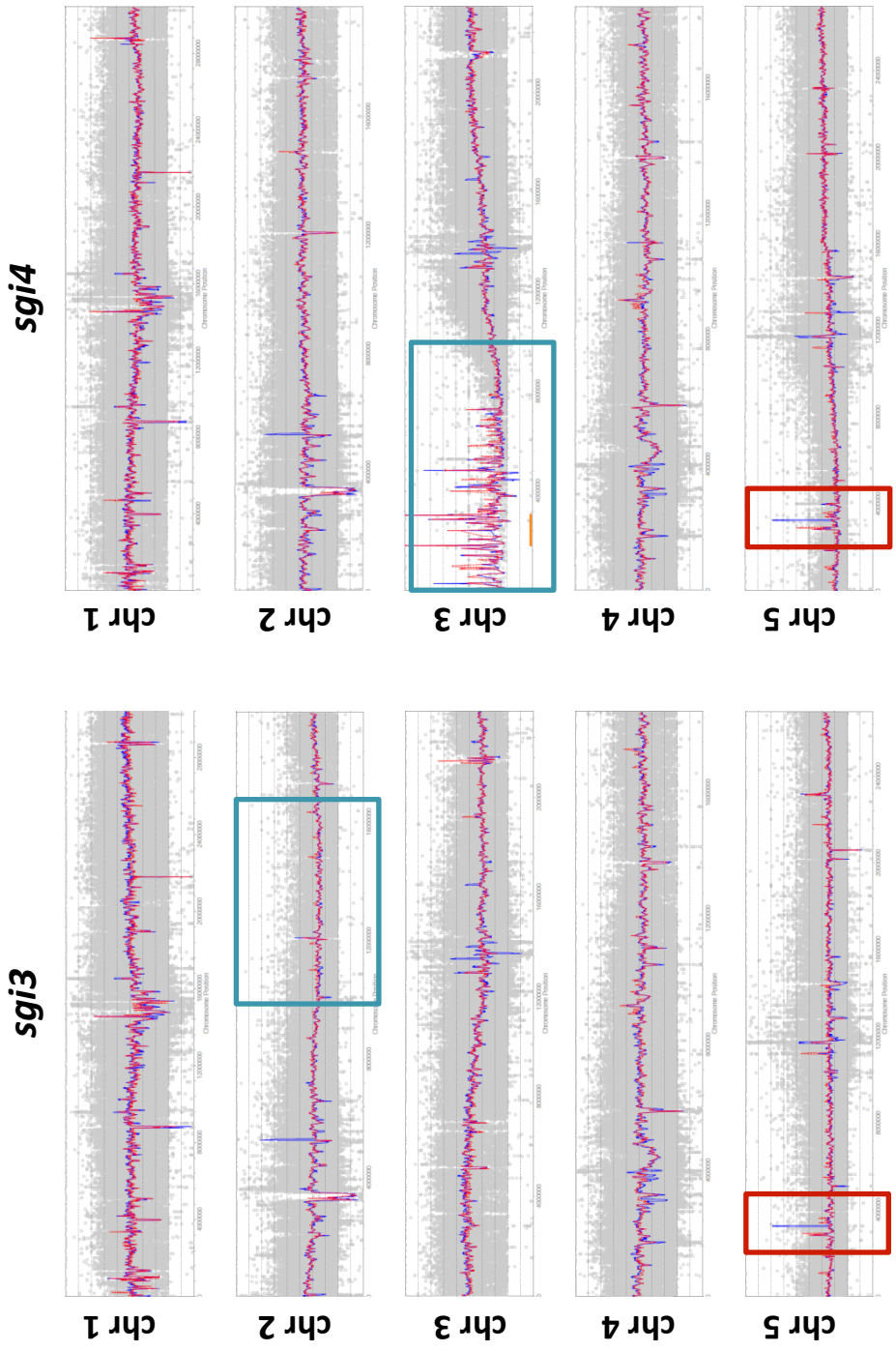

(Supp. Figure S6, continued)

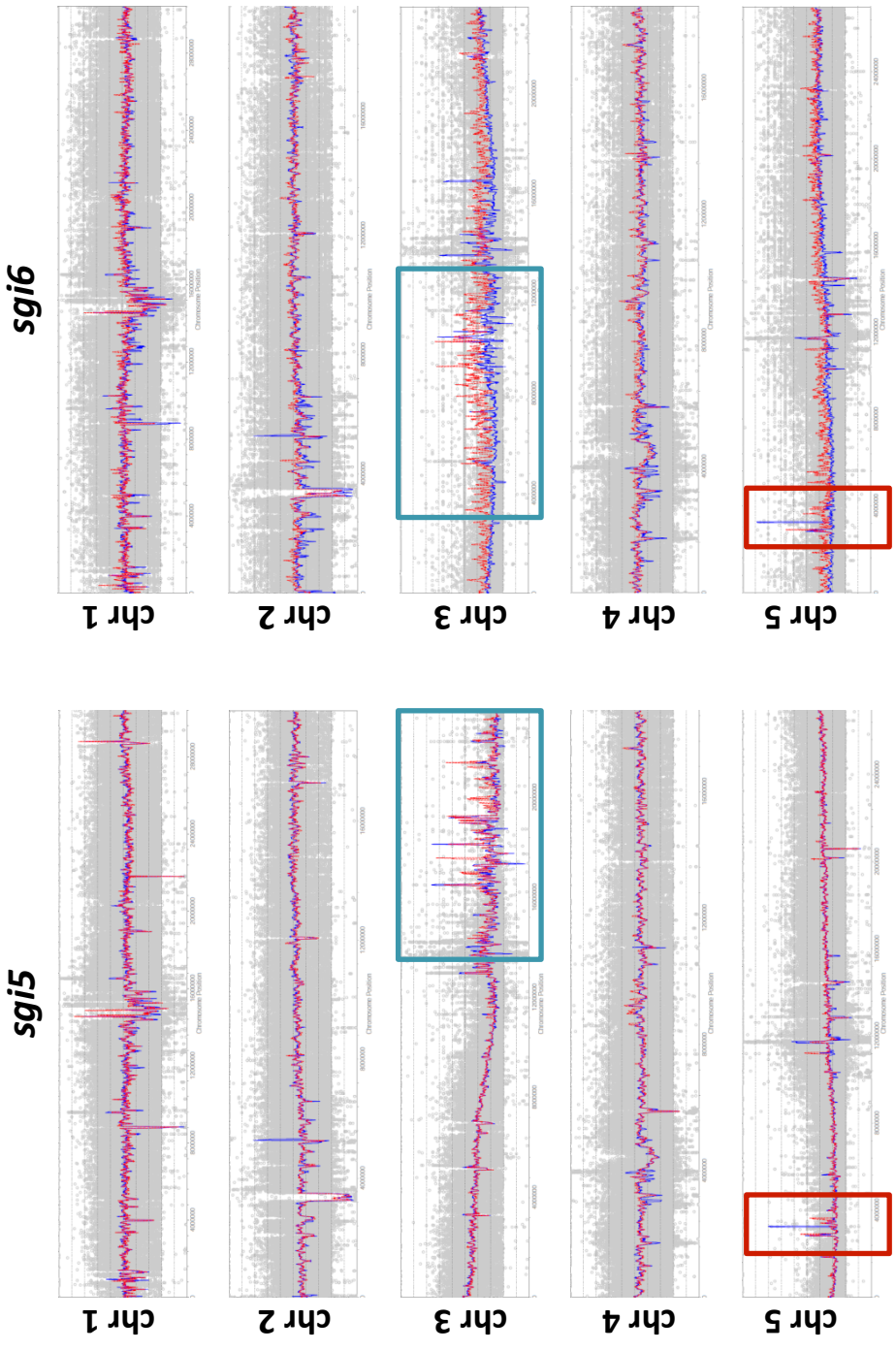

(Supp. Figure S6, continued)

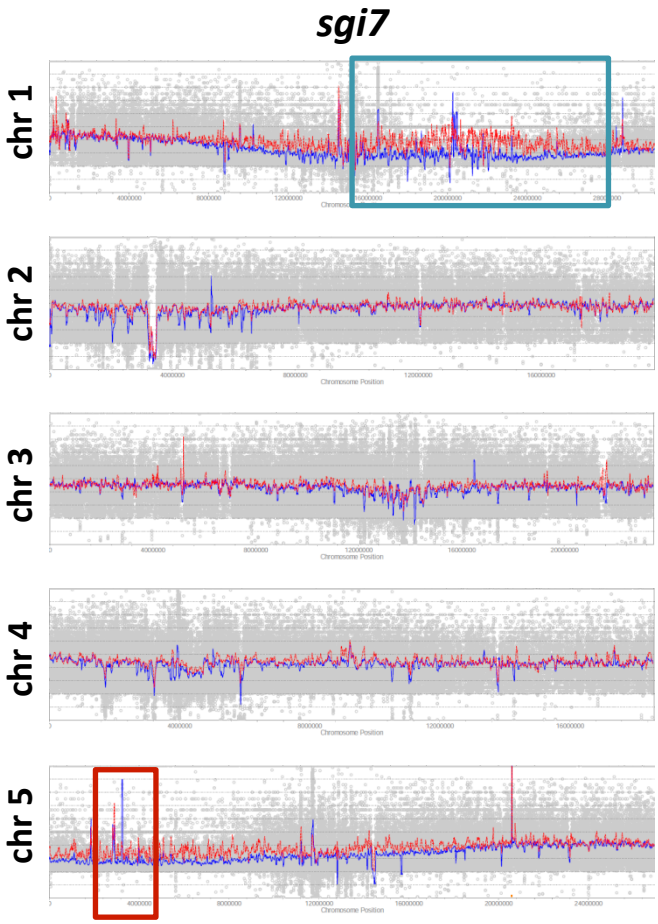

Supp. Figure S7. cDNA sequences of *RST1* in *sgi6* (RST1_EMS) and wild type (ERF6-GR). The splice acceptor of the *RST1* gene was mutated in the *sgi6* mutant. As a result, the splice acceptor site was skipped by the spliceosome and the next splice acceptor site, 10 nucleotides downstream was wrongly recognized. The missed splicing site generated an additional 10 bp in the exon sequence, which causes a frame shift at protein level.

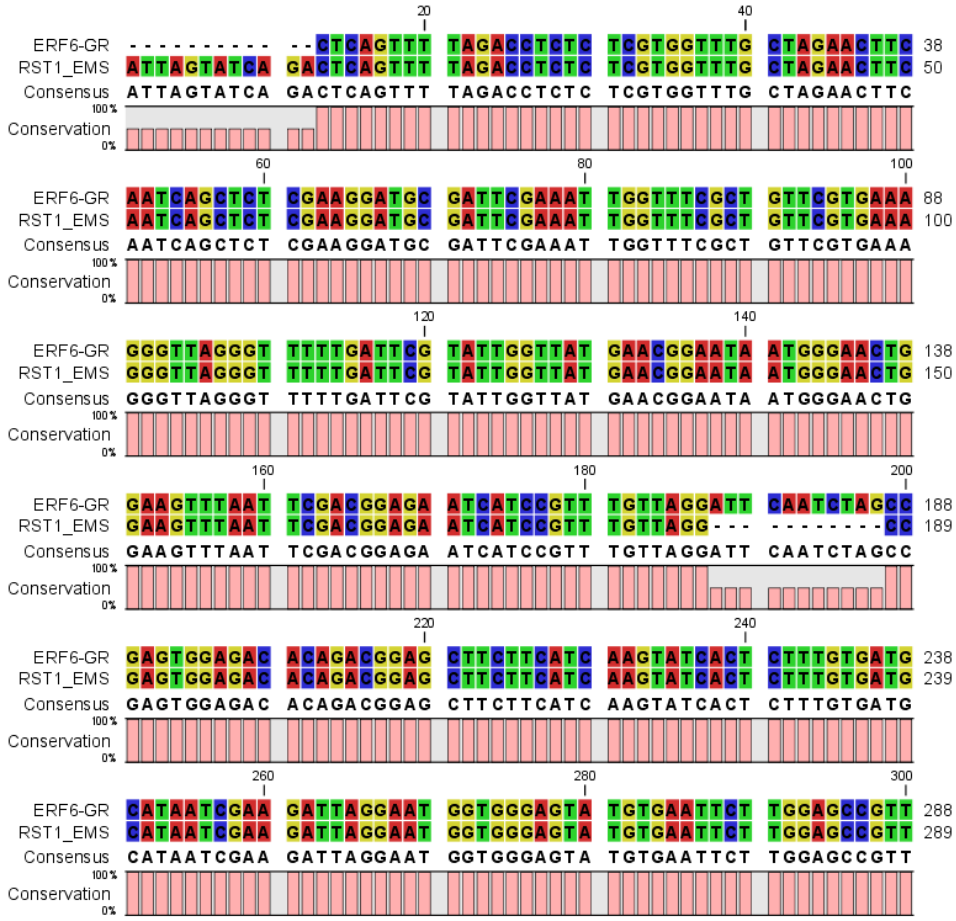

Supp. Figure S8. Suppression of the triple response in the *sgi7* mutants grown in darkness on 5 µM ACC.

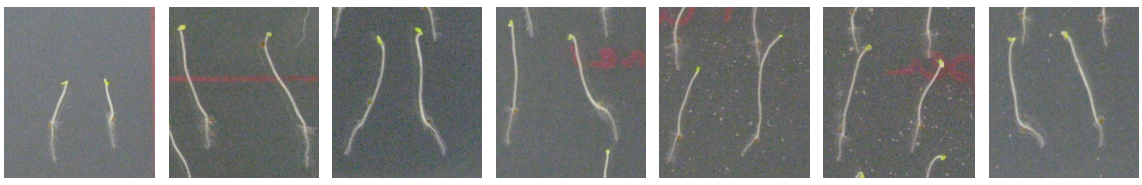

Col | ***sgi7-1*** | ***sgi7-2*** | ***sgi7-3*** | ***sgi7-4*** | ***sgi7-5*** | ***sgi7-6***

Chapter 6

UNRAVELING THE MOLECULAR MECHANISMS UNDERLYING LEAF GROWTH INHIBITION UNDER DROUGHT: IT'S ALL ABOUT TIMING

Marieke Dubois [a,b,*], Hannes Claeys [a,b,*] and Dirk Inzé [a,b]

[a] Department of Plant Systems Biology, VIB, Ghent, Belgium
[b] Department of Plant Biotechnology and Bioinformatics, Ghent University, Belgium
[*] These authors contributed equally to the work.

Contributions: M.D and H.C. designed and performed the experiments, and wrote the manuscript. D.I. supervised the project and contributed to the writing of the manuscript.

An adapted version of this Chapter has been submitted as a Letter to Nature Plants and is currently under review.

Leaf growth is a complex process that is very responsive to changing environmental conditions. Adverse conditions, such as drought, negatively affect leaf growth, but the molecular mechanisms and regulators governing this growth inhibition are largely unknown. Here, we construct a time line of the drought stress response in actively growing Arabidopsis leaves by combining transcriptomics and detailed growth measurements in order to identify regulators of leaf growth under drought. The Weighing Imaging and Watering Machine (WIWAM) was used to apply controlled mild drought stress, and leaf growth dynamics were measured with high resolution to track the speed and timing of growth inhibition. For transcriptomics, a detailed time course was obtained by sampling the growing leaf every 4 hours, day and night, during 4 days following drought. On the transcriptome level, the time of day largely determines the outcome of drought-induced changes, by affecting the extent, the specificity and the direction of the response. We demonstrate that matching these oscillating transcript patterns with growth dynamics holds great potential to identify new putative regulators of leaf growth under drought.

INTRODUCTION

Drought stress is a major problem for agriculture worldwide, causing tremendous yield losses (Boyer, 1982; Araus et al., 2002). Around 40% of global land area is already situated in arid or semiarid climates (Marris, 2008; Fedoroff et al., 2010) and, most likely, the problem will worsen in the next decades due to rising temperatures which will increase the duration of drought periods (Fedoroff, 2010). Drought can be of multiple levels of severity and can hit during all stages of plant development, requiring specific responses (Bray, 2004; Verslues et al., 2006; Claeys and Inzé, 2013; Langridge and Reynolds, 2015). When drought occurs during vegetative growth, plants react in a flexible way and reprogram growth (for reviews, see Claeys and Inzé (2013), and Pierik and Testerink (2014)). Repression of leaf growth is amongst the first responses to drought stress, and as this is one of the factors at the origin of the yield losses caused by drought (Dosio et al., 2011), efforts have been made during the last years to understand and eventually circumvent or delay this growth inhibition.

At the cellular level, leaf growth is mediated through two tightly spatio-temporally regulated processes: cell division and cell expansion. In *Arabidopsis thaliana*, growth of emerging leaves is first driven by cell proliferation, generating the pool of cells which subsequently enter cell expansion to drive so-called expansive leaf growth (Donnelly et al., 1999; Kawade et al., 2010; Andriankaja et al., 2012; Gonzalez et al., 2012). Drought

was found to negatively affect both cell proliferation and expansion in different natural variants of Arabidopsis and maize (Tardieu and Granier, 2000; Harb et al., 2010; Baerenfaller et al., 2012; Bonhomme et al., 2012; Claeys and Inzé, 2013; Clauw et al., 2015). From a physiological point of view, expansive leaf growth results from a combination of increase in volume and increase in dry mass, and is thus driven by the availability or absence of two crucial elements: water and carbon, respectively (Pantin et al., 2012; Tardieu et al., 2015). Under drought, the stomata are rapidly closed by ABA (Harb et al., 2010; Jarzyniak and Jasinski, 2014), limiting evaporation but also photosynthesis. Therefore, constraints in C-supply and energy metabolism have long been thought to be at the basis of leaf growth inhibition. However, starch metabolism, responsible for proper energy storage and consumption, is not negatively affected by drought (Hummel et al., 2010). In contrast, genes encoding aquaporins and cell wall remodeling enzymes (Harb et al., 2010; Bonhomme et al., 2012; Clauw et al., 2015), such as expansins, are induced by drought stress. Under lowered water potential, plants thus activate mechanisms to facilitate water uptake and sustain turgor pressure. Consequently, physiological studies concluded that water uptake is driving leaf growth and that therefore mainly constraints in leaf hydraulics underlie leaf growth inhibition under drought (Pantin et al., 2013; Caldeira et al., 2014; Tardieu et al., 2014).

However, although under severe or prolonged drought stress the lack of sustained turgor undoubtedly negatively affects leaf expansion, evidence exists that milder drought stress inhibits leaf growth even before leaf hydraulics are affected (Parent et al., 2010; Bonhomme et al., 2012). Moreover, mild drought stress also clearly affects cell division (Baerenfaller et al., 2012; Bonhomme et al., 2012; Clauw et al., 2015), a process which is, compared to cell expansion, less dependent on hydraulics. The hypothesis that leaf growth can be uncoupled from water shortage is further supported by the observation that growth is inhibited under drought even when the turgor pressure is maintained through osmotic adjustment (Tang and Boyer, 2002), or upon maintenance of the water potential in the xylem (Nonami et al., 1997). These findings suggest that there are active mechanisms inhibiting growth following drought stress.

Arabidopsis leaf growth rate, measured through the Relative Growth Rate (RGR; generated area per unit of existing area per unit of time) varies according to the developmental stage of the leaf and to the time of day: young leaves have higher growth rates during the day, while older leaves grow more during the night (Schurr et al., 2006; Wiese et al., 2007; Pantin et al., 2011; Pantin et al., 2012; Ruts et al., 2012). In dicot species particularly (Poire et al., 2010; Caldeira et al., 2014), disturbing environmental factors that are linked with day/night rhythms, such as light and temperature, does not alter the plants diurnal growth rhythm. In contrast, diurnal rhythms are disturbed in circadian clock mutants and mutants affected in starch metabolism, indicating that leaf

growth is endogenously controlled by a mechanism integrating metabolic signals and the circadian clock (Nozue and Maloof, 2006; Nozue et al., 2007; Poire et al., 2010; Ruts et al., 2012; Stitt and Zeeman, 2012). In Arabidopsis, this self-sustained endogenous mechanism, which is fine-tuned by environmental signals such as light and temperature, is known to trigger hypocotyl, leaf, and root growth rhythms (Dornbusch et al., 2014). The core circadian clock machinery is based on transcription-translation feedback loops between two major components: the LHY1/CCA1 (LATE ELONGATED HYPOCOTYL1 and CIRCADIAN CLOCK ASSOCIATED1) complex, highly expressed in the morning, which represses the expression of *TOC1* (TIMING OF CAB EXPRESSION1), which itself is an inducer of *LHY1* and *CCA1*. As a result, oscillating expression patterns of *LHY1/CCA1* and *TOC1* trigger the expression of morning and evening genes, respectively (reviewed in Hsu and Harmer, 2014). Although several studies focused on the molecular connection between the circadian clock and hypocotyl growth, little is known about the molecular players linking the clock to leaf growth (Arana et al., 2011; Ruts et al., 2012; Filo et al., 2015). Additionally, very little is known on how drought influences the effect of the clock on Arabidopsis leaf growth.

Numerous studies analyzed the molecular effects triggered by drought stress, often using either sudden dehydration by excision of leaves or prolonged moderate drought, followed by transcriptomics on full seedlings or mature leaves (Kilian et al., 2007; Wilkins et al., 2010). Responses to stress are, however, known to be dependent on the developmental stage of the organ or tissue, making for example mature plants unsuitable to study growth-related drought responses (Skirycz et al., 2010). Consequently, in numerous cases, dehydration-responsive genes were identified in mature plants, and plants with altered expression of these genes are occasionally more resilient to severe dehydration. However, in most cases, important growth penalties were found when grown under milder, sub-lethal drought stress (Kang et al., 2011; Skirycz et al., 2011; Westwood et al., 2013; Barboza-Barquero et al., 2015). This observation likely explains why so few transgenic crops with improved drought tolerance but without yield penalties in well-watered conditions are currently on the market, despite enormous efforts. A notable exception is the transgenic Droughtgard cultivar developed by Monsanto, which overexpresses a bacterial RNA chaperone (Cold Shock Protein B) of which the molecular function in plants is still poorly understood (Castiglioni et al., 2008; Nemali et al., 2015).

To identify genes involved in the active regulation of early growth responses to stress, research was performed *in vitro* using low concentrations of osmotic compounds, such as mannitol, to lower the water potential and induce growth repression of young leaves (Verslues et al., 2006; Skirycz et al., 2011; Claeys et al., 2012; Dubois et al., 2013; Claeys et al., 2014). By transferring young Arabidopsis plants suddenly to mild osmotic stress

conditions followed by transcriptomics within hours specifically in the actively growing leaf, multiple genes involved in early regulation of leaf growth inhibition were identified. In young leaves, growth inhibition upon mannitol was governed by an early ethylene response involving several Ethylene Response Factors (ERFs) which induce downstream inactivation of bioactive GAs through the induction of *GA2-OX6* (Skirycz et al., 2011; Dubois et al., 2013). As a consequence of decreased GA levels, DELLA proteins are stabilized in young leaves, where they inhibit further progression of the mitotic cell cycle and cell expansion (Achard et al., 2009; Claeys et al., 2012). Although this research demonstrated that identification of early players in molecular cascades are the key to understanding regulatory pathways governing leaf growth, it is entirely unclear how well these *in vitro* unraveled mechanisms translate to the drought response in soil. Transcriptome analysis of young developing leaves of plants exposed to long term drought treatments did previously not reveal any involvement of ethylene signaling in this response (Clauw et al., 2015).

Here, we present a different approach to explore the short term molecular mechanisms underlying leaf growth inhibition following drought. Using the Weighing, Imaging and Watering Automated Machine (WIWAM) to precisely control soil water content, we exposed young Arabidopsis seedlings to mild drought and tracked the growth and transcriptional responses over time specifically in actively growing Arabidopsis leaves. This allowed us to build a high-resolution time line of dynamic plant responses to drought and to identify novel genes putatively involved in the regulation of leaf growth under physiologically relevant mild drought conditions in soil.

RESULTS

Drought inhibits leaf growth within 3 days following stress onset, mainly during the day

To explore the dynamics of leaf growth under drought, we developed a mild drought stress assay, in soil, enabling to track the growth of young Arabidopsis leaves over time. We chose mild drought conditions that reproducibly reduce the size of the third true leaf, used as a model organ for all presented experiments, by 20% at the final harvesting time point (17 days after stratification, DAS) (Figure 6.1; Supp. Figure S1). Over 800 young Arabidopsis plants were grown in a single run on the automated phenotyping platform (WIWAM) (Skirycz et al., 2011; Clauw et al., 2015), and automatically watered every day under a well-watered (WW) regime until 12 DAS, when the third true leaf is

large enough to be easily harvested (±1mm^2) (Supp. Figure S1). At this developmental stage (stage 1.03), the third leaf is still actively growing and composed of both proliferating and expanding cells. Subsequently, half of the pots were kept under this WW-regime, while the other half were dried out progressively until they reached mild drought levels at 17 DAS, after 6 days since the last watering (DSLW) (Figure 6.1). Leaf size was accurately measured by harvesting the third leaf from multiple plants every morning (at dawn, 6AM) and evening (at dusk, 10PM) from before the water was first withheld (12 DAS, morning) until the area of the third leaf was visibly reduced (6DSLW)(Figure 6.1, Figure 6.2A, Supp. Figure S1).

Because leaf growth rates are known to be different during day and night (Nozue and Maloof, 2006; Dornbusch et al., 2014), relative growth rates (RGR) were calculated separately to quantify growth during the day and during the night (dRGR and nRGR, respectively). In our experimental setup and in WW conditions, dRGR was higher than nRGR, but gradually decreased, and reached levels similar to nRGR around 17 DAS (Figure 6.2B and Supp. Figure S2B). Under drought, the decrease in dRGR over time was much more pronounced than under control conditions, reaching nRGR levels much faster (Figure 6.2C). In contrast, nRGR was completely unaffected (Figure 6.2C). Thus, drought stress only affected leaf growth during the day.

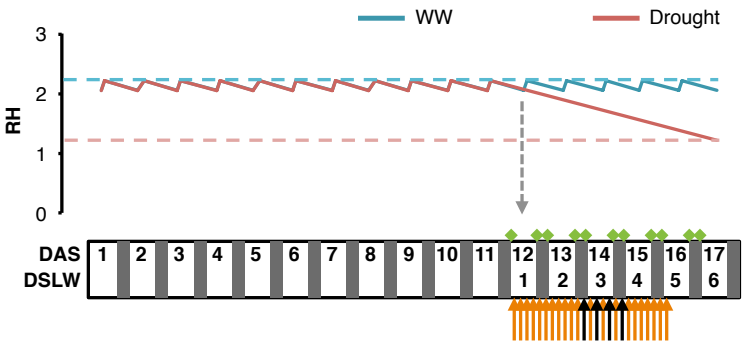

Figure 6.1. Experimental setup used to measure short term response to mild drought. Arabidopsis plants were grown under well-watered (WW) conditions (2.2 g_{water}/g_{soil}, blue line) until 12 days after stratification (DAS). Subsequently, half of the pots were exposed to a mild drought (Dr) treatment (1.2 g_{water}/g_{soil}, red line) while the other pots were kept under WW regime. Harvests were performed from before the stress onset until 6 days since the last watering (DSLW), every morning and every evening for the leaf growth measurements (green diamonds), and every 4h for expression analysis (orange arrows). Samples used for transcriptomics are indicated with black arrows. RH = targetted relative humidity of the soil (g_{water}/g_{soil}).

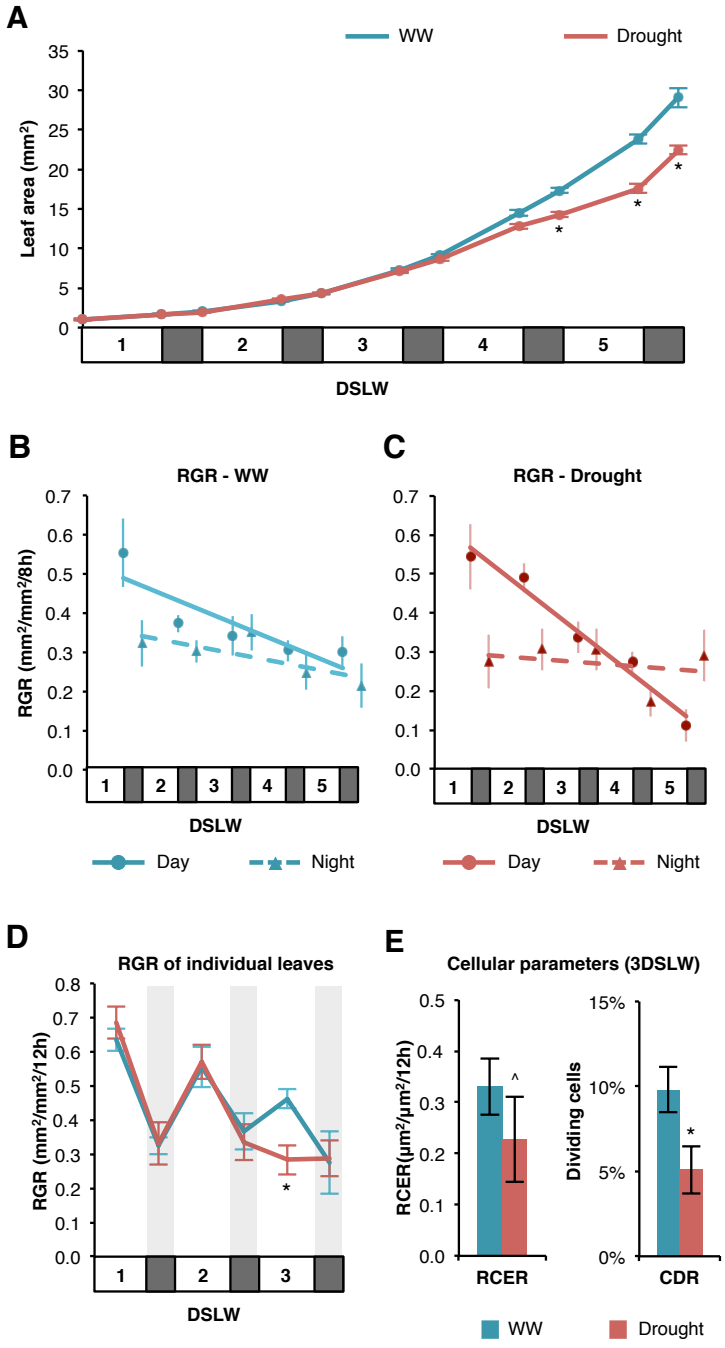

Figure 6.2. Leaf growth dynamics under well-watered (WW) and drought conditions. (A) Leaf area over time of the third Arabidopsis leaf under control and drought conditions during 5 days since the last watering (DSLW). (B) Relative growth rates (RGR) of the third leaf under control and drought conditions (C) during the day and during the night, showing the day-specific inhibition of leaf growth under drought. (D) Average RGR of individual third leaves (n=7 per repeat) followed using leaf imprints (see Material and Methods). (E) Cellular measurements during the third day since the last watering over a period of 12 hours. RCER = relative cell elongation rate, CDR = cell division rate. Four biological repeats were performed for (A), (B) and (C), and two for (D) and (E). Error bars represent standard error. Grey zones represent night periods, white zones represent day periods. * $p < 0.05$ ^ $p < 0.1$

To capture regulators underlying leaf growth inhibition, we first determined the earliest time point at which drought starts to affect leaf size. In the experimental setup described above, when third leaves of multiple plants were pooled at each time point, leaf size was first visibly affected by drought during the fourth day following stress onset (15 DAS) (Figure 6.2A). However, we speculated that subtle growth-inhibitory effects might be diluted when using the average of this pool of leaves as a measure, and we therefore measured growth of individual third leaves over time by taking non-destructive leaf imprints every morning and evening during the days following drought (Supp. Figure S3A). Interestingly, besides validating the previously observed day vs. night growth rhythms and the day-specific growth-inhibition by drought, this method enabled to capture drought-induced growth inhibition one day earlier, 3 DSLW (Figure 6.2D). Thus, although growth at the level of the rosette is generally only found to be reduced 10-11 days following mild drought (Harb et al., 2010; Clauw et al., 2015), much earlier effects can be observed at the level of individual leaves, especially when following growth of the same leaf over time.

Next, we explored the cellular mechanisms underlying diurnal leaf growth rhythms and drought-induced growth inhibition using the leaf imprints to visualize division and expansion of individual leaf cells over time (Supp. Figure S3B). At cellular level, leaf growth dynamics during the analyzed time frame highly correlated with both cell division and cell expansion rate (respectively PCC 0.93 and PCC 0.97; $p = 0.02$ and $p = 0.001$) (Supp. Figure S3C). Both processes also show diurnal rhythms, with highest levels during the day. Under drought stress, the growth inhibition observed during the third day following stress onset results from a negative effect on cell expansion rate (RCER) (–31%; $p = 0.06$), as well as a decrease in cell division rate (CDR) (-48%; $p = 0.001$) (Figure 6.2E). Together, these results show that young leaves of plants exposed to stress reduce their growth during the day only, from the third day following stress onward, through inhibition of both cell division and cell expansion.

Time of day determines the extent of the drought response

To identify the molecular players orchestrating the observed leaf growth inhibition, without knowing *a priori* how long upon drought stress signaling pathways are activated, we performed a very detailed time course analysis harvesting leaf samples every 4 hours during the 4 days since the last watering (Figure 6.1). As leaf growth is clearly inhibited in our setup during the third DSLW (14DAS), leaf samples (pools of four leaves of on average 5 mm^2) harvested during this day were selected for transcriptomics (Figure 6.1). Because drought affects growth differently during day and night, we profiled the transcriptome of WW and drought stress samples from two day and two night time points: 4AM in the night between the second and the third DSLW,

12PM and 8PM during the third DSLW, and 4AM between the third and the fourth DSLW (labeled hereafter as 4AM'). Principal component analysis showed that gene expression is mainly affected by the time of the day (Supp. Figure S4), separating the noon, evening and night samples but clustering both night samples together. Within each time point, expression is also clearly separated by the treatment, with as expected, a more pronounced effect at the latest time point compared to the first one.

Differential expression under drought vs. well-watered conditions was calculated with multifactorial ANOVA analysis using FDR <0.05 and $Log_2FC > |0.2|$ as a cutoff. Although mild, the drought stress significantly affected the expression of 5,659 genes in at least one time point. Strikingly, the extent of the drought response clearly depends on the time of the day, as shown by the amount of differentially expressed (DE) genes at each time point: 728 genes at 4AM, 459 at 12PM, 3,537 at 8PM and 2,538 at 4AM' (Figure 6.3A). The effect of progressive drought is clear from the increase between the two comparable night time points (4AM and 4AM'). Surprisingly, we observed that the amount of DE genes at noon is lower than at the earlier time point at night, and that the amount of DE genes in the evening is higher than at the later time point at night. Thus, time of day clearly affects the amount of drought-responsive genes.

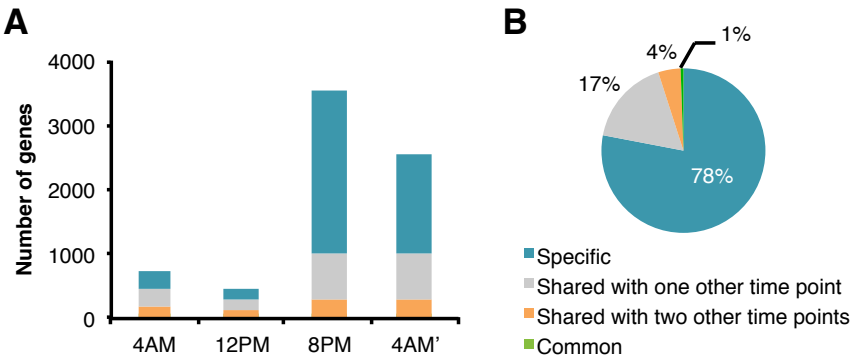

Figure 6.3. Gene expression analysis following mild drought stress. (A) Number of differentially expressed genes with FDR < 0.05 at 4AM, 12PM, 8PM during the third day since last watering (DSLW) and at 4AM during the fourth DSLW (labeled 4AM'). (B) Comparison of the differentially expressed genes between the time points.

Time of day determines the identity of the drought-responsive genes

Direct comparison of the DE genes between the time points shows that the large majority (78%) of the genes are specifically DE at one time point or are shared with only one other time point (17%)(Figure 6.3B, Supp. Figure S5). Surprisingly, only 29 genes are DE in the same direction along the whole time course (Supp. Table 1). Thus, not only the extent of the drought response varies according to the time of the day, but also the identity of the stress-responsive genes. Correlation analysis between the Log(fold change) of drought vs. control at each time point showed that the highest similarities are found between both night samples and the evening sample. In contrast, the evening and night datasets do not highly correlate with the 12PM dataset, showing again that the response at noon is clearly different from the drought-response during the evening/night. We further compared these datasets with 5 other publicly available and comparable datasets, including only transcriptomics on shoot tissue and excluding severe, desiccation stress experiments (Supp. Table 2). All datasets were re-analyzed similarly as our dataset, taking into account the multiple time points when available (Harb et al., 2010; Wilkins et al., 2010; Baerenfaller et al., 2012), separating the developmental stages when originally multiple were pooled (Baerenfaller et al., 2012), and extracting only the Col-0 dataset from the natural variants studies (Des Marais et al., 2012; Clauw et al., 2015). Comparison with the other datasets shows that overall the 8PM datasets correlates best with all other datasets, likely because this time point triggers the largest response. Interestingly, the 8PM dataset correlates best with the evening (6PM) dataset of Wilkins and colleagues, while again weak correlations are found with the other time points. No correlations are however found between the night time points of this study with the 12AM time point of Wilkins, likely due to the very weak drought response in the Wilkins night sample (Supp. Table 2). These comparisons thus demonstrate that timing clearly determines the specificity of the drought response at the transcriptome level, and that the response is very different during the day, the evening and the night.

Classical drought-responsive processes are amongst the core set of genes

In growing Arabidopsis leaves of plants exposed to mild drought stress, only 29 genes are differentially expressed along the four analyzed time points (Supp. Table 1). While 11 genes still have an unknown function, most of them encode genes involved in classical drought-responsive processes: cell wall loosening; proline accumulation; lipid and wax biosynthesis; and ABA signaling (reviewed in Fang and Xiong, 2015). 26 out of 29 of these drought-responsive genes also responded to drought in the same way in previous studies (Supp. Table 1). Importantly, as the different studies shown here were

conducted on leaves of developmental stages ranging from proliferation to maturity, these common drought genes are most likely involved in general drought-responsive processes rather than in growth-regulatory pathways.

As proline and ABA have widely accepted importance in the general drought response, we further detailed the expression pattern of *ERD5* (EARLY RESPONSE to DEHYDRATION5) and *PYL6* (PYRABACTIN-RESISTANCE-LIKE) along the whole time course (Figure 6.4). The *ERD5* gene, encoding a proline dehydrogenase, is consistently downregulated both during day and night, already from the first time point onwards. Thus, *ERD5* is an extremely sensitive marker and reacts as soon as plants are not re-watered. Consistently, the proline biosynthesis enzyme *P5CS1* is transcriptionally induced along all profiled time points (Supp. Table 1). Similarly, the expression of the ABA-receptor *PYL6* is robustly downregulated under drought. As compared to *ERD5*, *PYL6* is a less sensitive marker, as its downregulation only clearly starts during the second day following drought onset. Thus, the tested genes amongst the core set are strongly affected by the drought independently of the time of day. However, as drought stress does clearly not affect leaf growth equally throughout day and night, regulators of growth under stress are not expected to be amongst this general core set of genes. Accordingly, these classical drought-responsive processes, including proline synthesis and ABA signaling, likely do not regulate leaf growth inhibition under drought.

Time of day affects the direction of the drought-response

As illustrated above for *ERD5* and *PYL6*, expression levels under well-watered conditions clearly oscillate in a diurnal manner. In total, the expression of 62% of the genes present in this dataset was significant influenced by the time of day under well-watered conditions. To explore the general effect of drought on this diurnal expression patterns, we calculated drought-induced changes in amplitude of oscillations. We defined the amplitude as the difference in absolute expression level between the highest and the lowest observed expression within a treatment, and compared this value under well-watered conditions and under drought. 19% of the oscillating transcripts showed a clear (>10%) reduction in amplitude of oscillation under drought, but drought also increased the amplitude for 14% of the genes. Thus, drought can affect diurnal oscillations of gene expression, but in our experimental conditions does not systematically reduce the amplitude as has previously been reported (Baerenfaller et al., 2012).

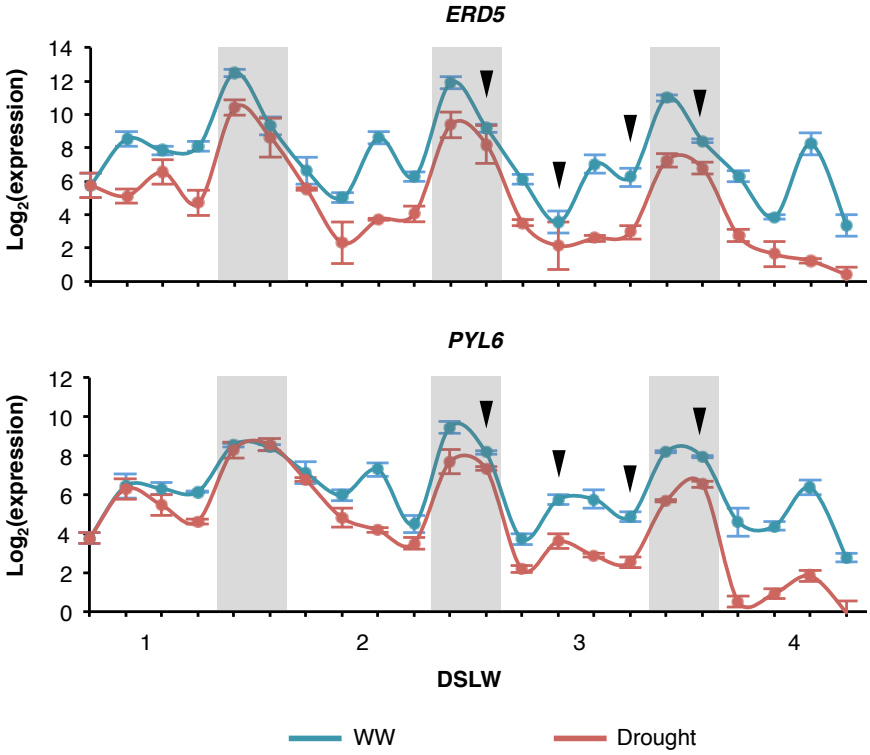

Figure 6.4. Expression pattern of *ERD5* and *PYL6* under well-watered (WW) and drought conditions. Expression level of the proline degradation enzyme *ERD5* and of the ABA-receptor *PYL6* during 4 days since the last watering (DSLW). Error bars represent standard error. Black arrowheads indicate time points used for RNAseq. Grey zones represent night periods, white zones represent day periods.

Intrinsically, changes in amplitude are expected to result from opposite effects of drought at different times of the day. As drought affects diurnally regulated physiological processes to different extent during the day and the night, we further explored whether gene expression could be differently affected by stress during the day and during the night. Amongst the 5,659 genes DE by drought, 166 are significantly affected by drought in opposite direction during day and night. GO enrichment analysis shows that these genes are highly (10-fold) enriched for genes involved in fatty acid biosynthesis. Upon clustering of the 166 genes based on fold change (Figure 6.5A), the genes involved in fatty acid biosynthesis all cluster into the groups of genes repressed by drought during the day but up-regulated under drought during the night. Clearly, multiple genes encoding enzymes involved in the elongation of very long chain fatty acids (VLCFA), *KSC1*, *KCS9*, *KCS12*, *KCS20*, and their regulator *MYB30*, which were previously found in drought-studies amongst the down-regulated genes, are all consistently up-regulated during the night (Figure 6.5B). We validated this for *KCS20* by qRT-PCR along the whole time course, where this clear pattern was first observed during the second night following drought onset (Figure 6.5C). Suprisingly, similar observations could be made for classical drought stress marker genes, such as the

DREB2A, whose expression was also induced by drought during the day, but downregulated under drought during the night (Supp. Figure S6). Together, these data show that drought can both positively and negatively affect the amplitude of oscillating transcript levels resulting in different effects depending on the time of day. Consequently, some drought-responsive processes are affected in opposite direction during day and night.

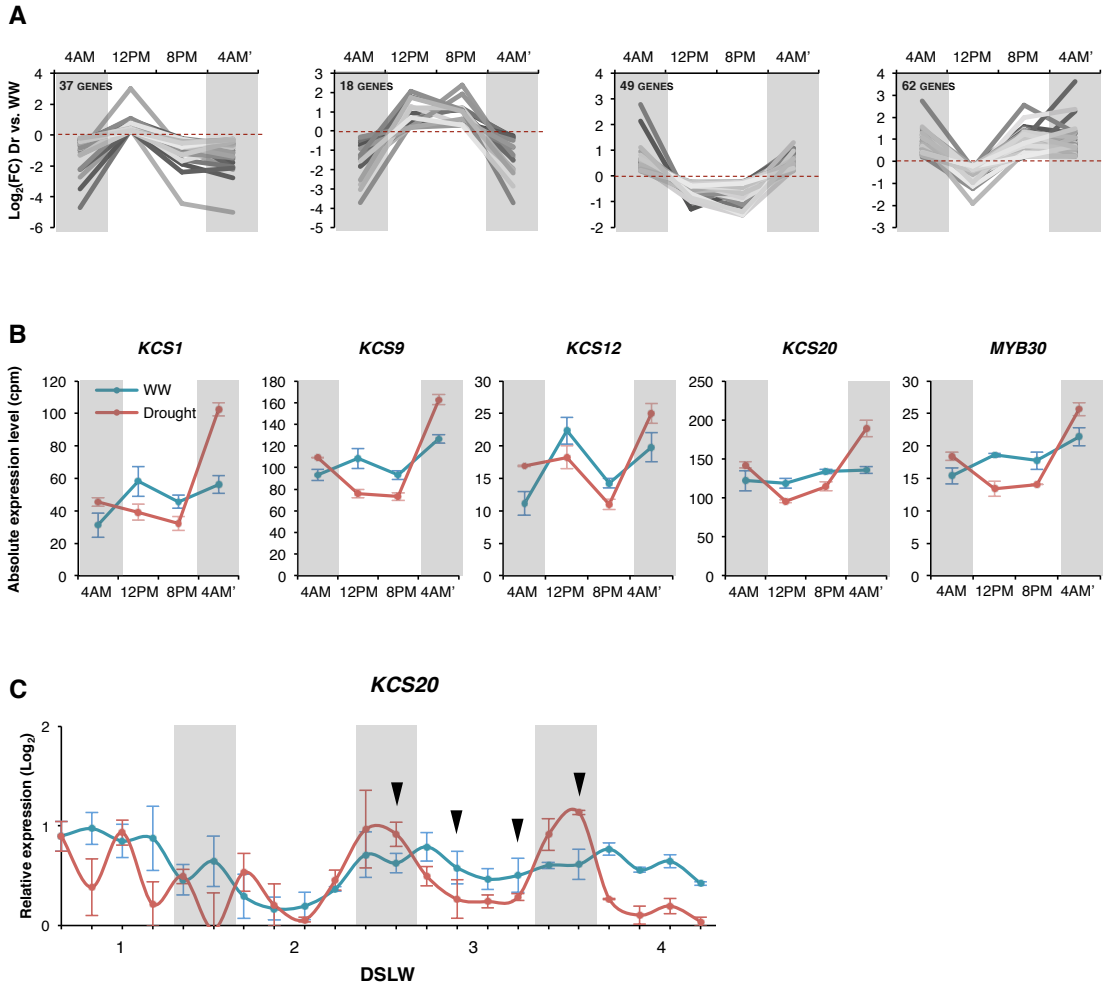

Figure 6.5. Genes affected by drought in opposite direction during the day and the night. (A) Clustering genes based on their Log_2(Fold-Change) under drought yields 4 clusters of genes which are significantly affected in opposite direction by drought stress depending on the time of day. Amongst the 49 genes within the 3rd cluster, multiple *KCS* genes encoding enzymes for Very Long Chain Fatty Acid elongation were found. (B) Expression level of the *KCS* genes significantly induced by drought during the night, but repressed by drought during the day. (C) Expression level of *KCS20* during 4 days since the last watering (DSLW). Error bars represent standard error. Grey zones represent night periods, white zones represent day periods.Dr = drought, WW = well-watered, cpm = read counts per million. Black arrowheads indicate time points used for RNAseq.

The circadian clock affects the drought response and vice versa

To further explore whether the changes in diurnal expression patterns result from altered circadian clock regulation under drought stress, we measured the expression of three central circadian clock genes along the complete time course. Although drought stress does not drastically affect the expression of *TOC1*, *LHY1* and *CCA1*, subtle but statistically significant effects could be observed, at specific times of the day, day after day (Figure 6.6). *CCA1* expression was on average 1.5-fold higher under drought stress when measured every evening at 20.00 from the 2nd day following stress onward (Figure 6.6A). As 20.00 is the time of the day with the lowest *CCA1* expression under WW conditions, this weak induction in the evening causes a slight reduction in the amplitude of *CCA1* oscillation. The opposite effect is observed for *TOC1*, of which the expression is generally at its lowest point at 8.00, and reduced even more in plants exposed to drought stress, on average 2.1-fold from the 2nd day following stress onward (Figure 6.6). Finally, *LHY1* expression is most clearly affected by drought, with significant down-regulations of *LHY1* expression in the afternoon, from the beginning of the stress onward (Figure 6.6).

To further unravel a putative connection between drought and the Arabidopsis core circadian clock, we exposed loss-of-function lines for each of these clock components to mild drought stress on the WIWAM in the setup described above and measured the area of the third leaf at 17 DAS. The *cca1* mutant had smaller leaves than the wild type, both under WW and drought conditions (Figure 6.6B). When comparing the relative leaf area reduction caused by drought in the different lines, the *cca1* and *lhy1* mutants were affected by drought to the same extent as wild type plants (Figure 6.6C). In contrast, the *toc1* mutant was hypersensitive to drought, as evidenced by a leaf area reduction of on average 32.2% under drought, as compared to 20.8% in the wild type ($P_{genotype*treatment}$ = 0.007) (Figure 6.6C). Moreover, *toc1* seedlings were also found to be 18% smaller than wild type when grown under WW conditions over a longer time frame ($P < 0.001$) (Supp. Figure S7). To get more insight in this hypersensitive phenotype of *toc1* mutants, the growth of individual *toc1* leaves was followed over time using the leaf imprints as described above. On top of being affected by drought during the day to the same extent as wild type plants, *toc1* leaf growth was also reduced by drought stress during the night, when wild type leaf growth is unaffected (Supp. Figure S7). Thus, the diel period of drought-induced growth inhibition is extended when the *TOC1* gene is mutated, resulting at the end of the experiment in a drought-hypersensitive phenotype of *toc1* seedlings.

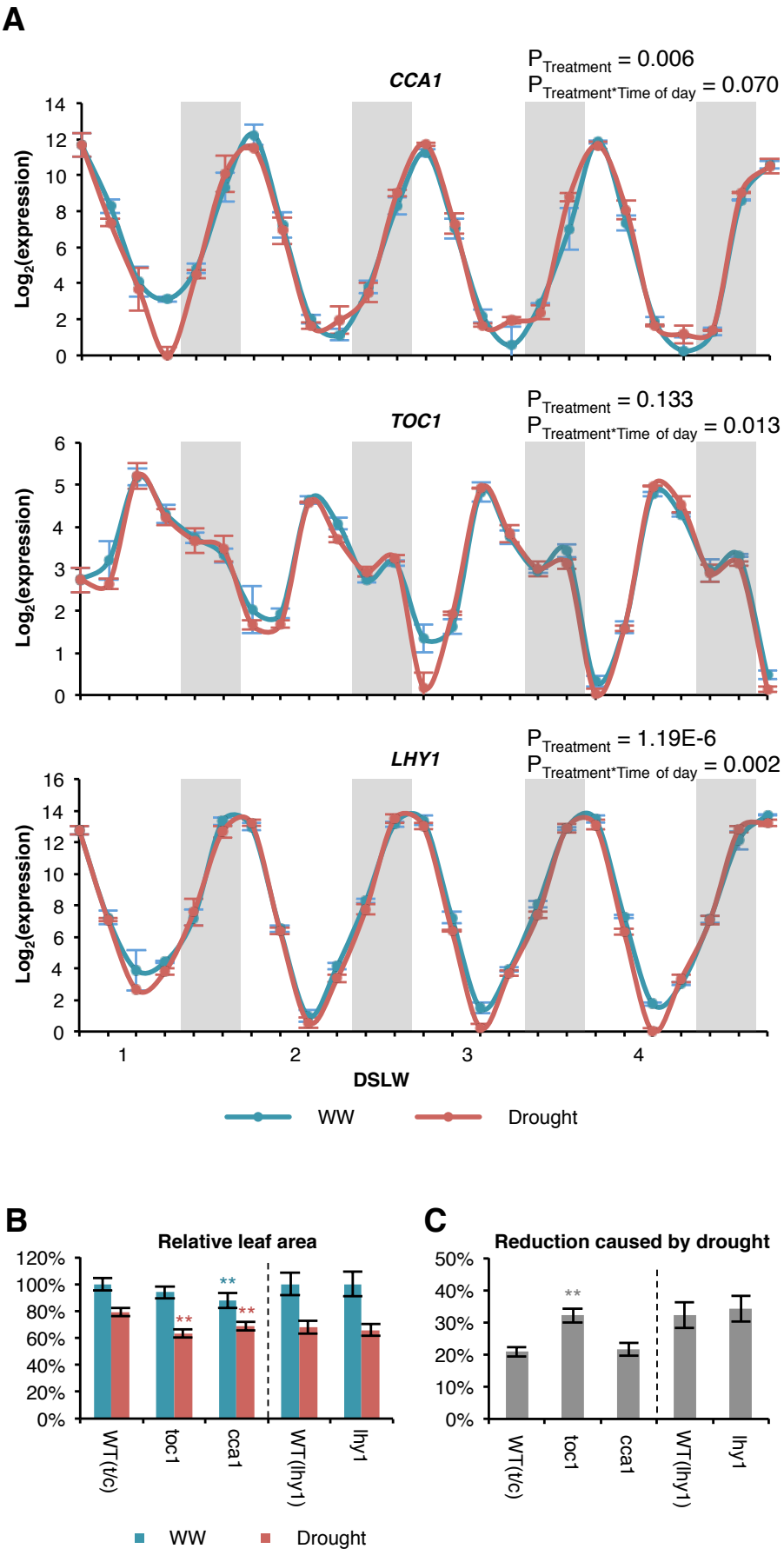
A
CCA1
P Treatment = 0.006
P Treatment*Time of day = 0.070
TOC1
P Treatment = 0.133
P Treatment*Time of day = 0.013
LHY1
P Treatment = 1.19E-6
P Treatment*Time of day = 0.002
Log2(expression)
DSLW
WW
Drought
B
Relative leaf area
120%
100%
80%
60%
40%
20%
0%
WT(t/c)
toc1
cca1
WT(lhy1)
lhy1
WW
Drought
C
Reduction caused by drought
50%
40%
30%
20%
10%
0%

Figure 6.6. Analysis of core circadian clock genes and mutants under drought. (A) Expression of the core circadian clock regulators *CCA1*, *TOC1* and *LHY1* at different times of the day during four days following drought onset. $P_{treatment}$ and $P_{Treatment*Time\ of\ day}$ represent p-values for the effect of drought and the interaction between drought and time of day, respectively (ANOVA). DSLW = days since last watering, WW = well-watered. (B) Average area of the third leaf of the respective circadian clock mutants measured at 6 DSLW, relative to the respective wild type under WW conditions. ** P < 0.001 (ANOVA), compared with the respective wild type under the same condition. (C) Relative reduction in average leaf area caused by drought in each line at 6 DSLW. ** P < 0.001 (ANOVA), compared with the respective wild type. Grey zones represent night periods, white zones represent day periods. For all panels, error bars represent standard error of three biological repeats.

Matching growth and transcript dynamics to identify novel regulators

As growth is differently affected by drought stress during the day and the night, regulators orchestrating this process are not expected to be amongst the genes in the overlap but instead vary in expression throughout the day. To identify additional growth-related mechanisms under drought, the 5,659 genes that were DE in at least one of the selected time points were clustered based on their absolute normalized expression under WW and on their fold change under drought conditions. Next, clusters with profiles correlating or anti-correlating with growth dynamics were selected. For example, negative regulators of leaf growth are expected to have low absolute expression during the day, but to be induced by drought during the day and less during the night. As such, six clusters were selected with putative negative regulators, and the opposite reasoning was made to select seven clusters with putative positive regulators of leaf growth under drought. Interestingly, the selected clusters are enriched for ontology terms that are different from the general processes identified from the full drought-responsive dataset. Particularly, GO classes related to three phytohormones are over-represented in the clusters matching the growth dynamics and are thus potentially involved in growth regulation: ethylene, jasmonic acid (JA), and gibberellins (GA). In total, 228 genes are present in these clusters (Supp. Table 3). As an additional filter, we further selected transcription factors (81 genes), as previous experiments conducted *in vitro* have shown that they are central regulators of the growth-inhibitory response to stress. Finally, we also curated the gene list manually by removing the genes that were wrongly assigned to the cluster as their expression did not clearly show the desired pattern (7 genes), and discarded the genes of which the transcript could not be amplified by qPCR for validation (7 genes). In total, 67 transcription factors were selected and 49 of them (73%) could be validated by qPCR in two additional biological repeats, yielding only putative regulators with a very robust expression pattern (Supp. Figures S8-S10).

Finally, we further selected several genes with functions related to the overrepresented hormones for functional characterization under drought stress (*ALC*, *K11J9.4*, *ERF11*, *WRKY28*, *ERF8* and *ERF2*) (Supp. Figure S11). Loss-of-function lines were grown on the WIWAM to expose them to mild drought as described above and the size of the third leaf was measured at 6 DSLW. Interestingly, two mutant lines showed reproducible phenotypes: *erf2* and *erf8* (Figure 6.7). The *erf2* mutants do not have a phenotype different from wild type under well-watered conditions, but are more sensitive to stress since *erf2* leaves are 18% smaller than wild type under drought ($P < 0.001$) (Figure 6.7A). *ERF8* in contrast negatively affects leaf growth already under control conditions and mutants are 27% larger than wild type ($P < 0.001$) (Figure 6.7A). Also under drought, *erf8* mutants have leaves that are 20% larger than wild type ($P < 0.001$), but *erf8* was thus relatively more affected by the drought ($P < 0.05$) (Figure 6.7B). This data thus shows that by combining the dynamics of a phenotype with the dynamics of the gene expression, promising candidates putatively regulating the phenotype of interest can be identified.

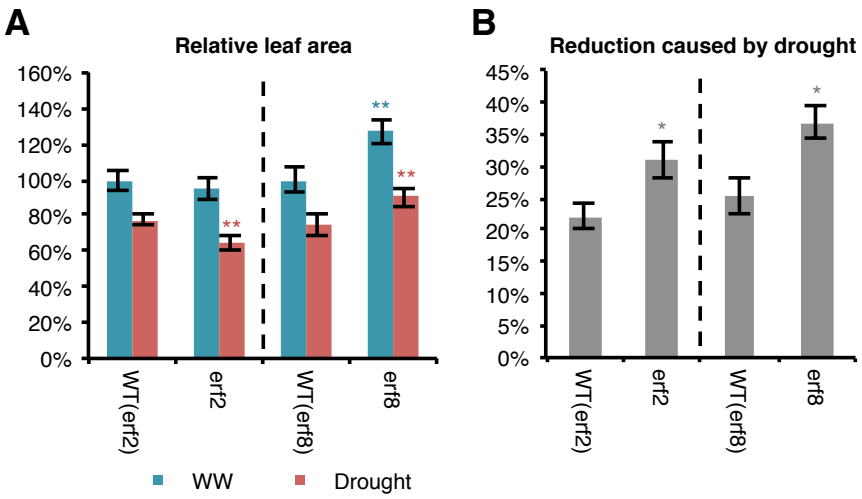

Figure 6.7. Leaf area measurements of *erf2* and *erf8* mutants exposed to drought. (A) Average area of the third leaf of *erf2* and *erf8* mutants measured after 6 days since last watering (DSLW), relative to the wild type under well-watered (WW) conditions. ** $P < 0.001$ (ANOVA), compared with the wild type under the same condition. (B) Relative reduction in average leaf area caused by drought in each line at 6 DSLW. * $P < 0.05$ (ANOVA), compared with the wild type. For all panels, error bars represent standard error of three biological repeats.

DISCUSSION

Fast and day-specific inhibition of leaf growth under drought

Mild drought stress has often been reported to cause a negative effect on Arabidopsis rosette or leaf growth (Harb et al., 2010; Baerenfaller et al., 2012). In Arabidopsis, it is very challenging to track the growth dynamics of these small, actively growing leaves. Generally, the growth is approximated using top-view imaging, which is either perturbed by the diel leaf movements (Granier et al., 2006; Harb et al., 2010; Skirycz et al., 2011; Tisne et al., 2013; Clauw et al., 2015), or obtained from immobilized growing leaves (Wiese et al., 2007). Here, we opted for both an accurate but destructive method (cutting and pooling leaves of different plants) and a more labor-intensive but non-destructive imprint-based approach, which is less suitable to track leaf growth over a longer period but enables detection of more subtle differences between two conditions over a short period of time. Whereas measurements of the rosette size over time have shown drought-triggered growth inhibition from 10 days following drought onset (Clauw et al., 2015), our method showed that, using progressive soil drying, the growth rate of Arabidopsis leaves significantly slows down already three days following the watering arrest. Growth is repressed specifically during the day, when the young leaves grow most under well-watered conditions, which is likely an active decision of the plant to save resources when they are most scarce. Non-destructive accurate measurements are also often performed in crop species (Matt et al., 1998; Tardieu and Granier, 2000; Poire et al., 2010; Tardieu et al., 2014), particularly in maize, where time-course leaf growth measurements following drought showed much faster growth inhibitory responses, within hours upon water withholding (Caldeira et al., 2014). Neither leaf size analysis nor cellular measurements of a single leaf over time pointed towards such early effects in Arabidopsis. Although we cannot fully exclude that technical limitations of our setup explain part of this important difference in timing, this fits with the observations that growth of maize leaves appears to be less controlled by the circadian clock (Poire et al., 2010), but is instead very dependent on hydraulics (Caldeira et al., 2014). Maize leaves may therefore react much earlier to water deficits than Arabidopsis, where growth in changing conditions is known to be mainly regulated by clock-regulated mechanisms.

Transcriptomics at multiple time points is crucial

We have shown that over the course of one day of progressive soil drying, the extent of the drought response on transcriptome level did not increase gradually. We expected a small set of differentially expressed genes at the first time point, that would increase in

the subsequent time points the more the stress became severe. Instead, we observed that the time of day clearly determined the extent of the drought response, as well as the identity of the genes altered at that specific time point. Even more surprisingly, we found examples of genes down-regulated at one time point, but up-regulated at all the other time points, and *vice versa*. Some of these genes we identified here encode enzymes contributing to the subsequent steps of Very Long Chain Fatty Acid elongation, *KCS20*, *KCS9* and *KCS1* (Todd et al., 1999; Lee et al., 2009; Kim et al., 2013), and their regulator, *MYB30* (Kim et al., 2013). All are present amongst the genes that are generally identified as down-regulated under drought, as this is the case during the day, but that are in fact, at the night time points, significantly up-regulated. It is possible that VLCFA, which are building blocks for cuticular wax, are mostly synthesized during the night to thicken the cuticula at night and prevent extensive evaporation from dawn onward (Seo and Park, 2011). Alternatively, recent advances suggest new emerging roles for VLCFA in signaling, although it is not yet understood how the VCLFA biosynthesis is regulated in different environmental contexts (Li-Beisson et al., 2013). We might speculate that differences in VLCFA levels during day and night under drought might contribute to different diurnal growth dynamics under drought, as decreases in VLCFA were reported to stimulate division of vasculature cells but inhibit leaf growth in both Arabidopsis and rice (Tresch et al., 2012; Nobusawa et al., 2013). While the biological meaning of the time-specific drought effect on VLCFA biosynthesis still deserves some further exploration, this expression analysis showed that transcriptomics at only one time point can cause serious underestimation of the response, or even lead to misinterpretations, as drought affects different genes, to a different extent, and sometimes also in a different direction depending on the time of the day.

Very mild stress triggers large transcriptional and phenotypic effects

In this study, the effect of drought on the phenotype was already visible when pots lost only about 25% of their water content (for comparison, mild drought studies are generally performed using around 50% water loss; (Granier et al., 2006; Clauw et al., 2015). Transcriptomics performed around this time identified thousands of genes affected by this mild level of drought. Considering the relative high number of genes (>700) differentially expressed at our earliest profiled time point, even earlier time points might be useful to uncover more upstream regulators, rather than downstream effectors of the phenotypic response. Still many studies perform transcriptomics after week(s) of drought, thereby missing parts of the signaling that might include the regulators orchestrating this whole drought response. A recent study tracking transcriptome changes in flowers of plants exposed for 3 or 10 days to mild or severe drought stress demonstrated that 277 genes were only differentially expressed under

the mild stress, and that, interestingly this set comprised genes involved in the repression of plant growth, such as genes encoding DELLA proteins (Ma et al., 2014). Generally, in the stress studies in which multiple time points were taken into account, on average about ¼ of the genes that were affected by the early mild stress were no longer differentially expressed at later time points (Kreps et al., 2002; Matsui et al., 2008; Zeller et al., 2009; Skirycz et al., 2011). In our opinion, performing transcriptomics at more early time points following drought holds huge potential to uncover a new set of rapid drought responses orchestrating the now already well-characterized later stress responses.

The circadian clock is necessary for proper drought stress response

As the time of day appeared to be crucial for the stress response and might even influence the direction of the expression changes, we explored the connection between the drought response and the circadian clock. The tightly interconnected core clock loop consists of two morning-phased transcription factors, CCA1 and LHY1, repressing the expression of an evening-phased component, *TOC1*. Under biotic stress, down-regulation of this evening-complex gene has been shown to generate a reinforcement of the circadian clock. In our expression analysis under mild drought, *TOC1* expression was also down-regulated, pointing towards similar stress-response mechanisms (Zhou et al., 2015). Under biotic stress, *LHY* expression was up-regulated, while in our dataset it is down-regulated, but the other morning gene *CCA1* is up-regulated. Another similarity is found in the phenotype of the mutants: under biotic stress as well as in our mild drought stress setup the *toc1* mutant was hypersensitive to the applied stress. Together, several similitudes point towards shared mechanisms connecting the circadian clock with environmental stress, both of biotic and abiotic origin (Espinoza et al., 2008). Under biotic stress the defense response is known to be gated by the circadian clock, enabling expression of the defense genes during the day, but restricting the defense during the night in order to use the resources for growth (Wang et al., 2011; Zhang et al., 2013). A similar mechanism could function under mild drought conditions, where growth is also preserved during the night, while it is shut down during the day, when other defense responses might be activated.

Ethylene, JA, and GA as putative regulators of leaf growth under drought

When selecting genes whose expression pattern matched with the dynamics of the leaf growth under drought, we observed that this gene set was enriched for genes involved in ethylene, JA, and GA biosynthesis and signaling. These processes were not clearly overrepresented within the genes of the complete dataset, highlighting the power of

transcriptomics over time coupled to time course phenotyping. JA has previously already been shown to be involved in drought stress response, and some mutants in jasmonate signaling (*coi1* and *jin1*) are known to have a less pronounced decrease in biomass upon long term moderate drought (Harb et al., 2010).

Ethylene and gibberellins are generally not associated with drought stress response in growing Arabidopsis leaves, or if they are, they are underrepresented or enriched amongst the downregulated genes (Baerenfaller et al., 2012; Clauw et al., 2015). In contrast, both hormones were previously described as central regulators of leaf growth inhibition of plants exposed to *in vitro* osmotic stress. Specifically in actively growing Arabidopsis leaves, ethylene and multiple genes encoding ETHYLENE RESPONSE FACTORs are induced by short term osmotic stress treatments, followed by a growth-regulatory cascade involving gibberellins and the DELLA proteins as final regulators of the pathway to inhibit cell division and cell expansion (Skirycz et al., 2011; Claeys et al., 2012; Dubois et al., 2013). Our data suggests that similar mechanisms might exist under mild drought stress in soil. Amongst the genes specifically induced during the day but not during the night the gene encoding ACC-SYNTHASE 8 (ACS8) is present (Supp. Table 3). ACC-synthases catalyze the rate-limiting step in ethylene biosynthesis. Interestingly, amongst the 12 ACS enzymes, ACS8 was previously identified as the ACC-synthase enzyme of which the expression correlates best with the ethylene levels when it comes to diurnal fluctuations (Thain et al., 2004). Clearly, ACS8 forms a good candidate to increase ethylene levels during the day, but not during the night. We hypothesize that the induction of ethylene triggers the activation of ERFs, such as ERF2 and ERF8, of which we showed that they are likely involved in the early stress response to mild drought. Also in maize ethylene signaling was found to regulate growth responses to mild drought stress. Maize plants with decreased ACS activity (Habben et al., 2014) or reduced ethylene sensitivity resulting from overexpression of *ARGOS* have an increased yield under well-watered and drought stress conditions (Shi et al., 2015). Finally, we also identified three genes encoding DELLA proteins amongst the genes upregulated in actively growing leaves upon drought. As these genes were not identified in previous similar datasets obtained later upon drought, we speculate that this induction of growth-inhibitors might be specific to the early drought response, similar to what has been observed in flowers (Ma et al., 2014). We conclude that this unique approach combining high-resolution phenotyping and transcriptomics enabled the identification of putative regulators underlying leaf growth inhibition under drought and that these mechanisms might be similar to was has previously been observed under osmotic stress.

CONCLUSION

In this study, we combined time course phenotyping and transcriptomics in young Arabidopsis plants exposed to mild drought in order to identify putative genes regulating leaf growth inhibition under stress. We showed that mild drought stress affects leaf growth already three days following the onset of progressive soil drying by inhibiting cell division and cell expansion. Importantly, this inhibition is a day-specific process, and leaf growth during the night remains unaffected by drought. In accordance with this observation that physiological processes such as growth can react to drought to different extents depending on the time of day, we demonstrated that also the transcriptional responses to drought are time-specific. By performing transcriptomics on multiple time points during the third day after stress, we showed that time of day determines the extent and the specificity of the drought response. Only 0.5% of the genes whose expression is affected under drought, are equally responsive to drought independently of the time of day. This core dataset represents well-known drought-responsive processes such as ABA and proline accumulation, which are sensitive drought markers, but likely not linked to the inhibition of leaf growth, since the latter is clearly time-dependent. More surprisingly, we also observed that time of day can influence the direction of drought-induced expression changes. This was illustrated for the genes involved in very long chain fatty acid biosynthesis; these genes are down-regulated by drought during the day, but upregulated during the night. Also genes potentially involved in the regulation of leaf growth under drought are expected to be affected by drought in opposite direction during day and night. By matching the dynamics in gene expression with the dynamics of leaf growth inhibition, we could select 228 genes potentially involved in leaf growth under mild drought, and observed enrichment for genes related to the phytohormones ethylene, GA and JA. We show that, amongst these genes, *ERF8* is a good candidate regulator since mutations in it result in increased leaf growth under both well-watered and control conditions. Additional investigations, including hormone measurements in actively growing leaves, are essential to fully unravel these time-dependent mechanisms orchestrating leaf growth regulation under drought.

MATERIALS AND METHODS

Plant lines

All experiments in which the growth and the gene expression were measured on wild type plant, were performed with a same batch of Col-0 seeds. N531092 (*lhy1*), N513233

(*cca1*) mutant lines were obtained from the SALK collection and the *toc1-101* mutant was a kind gift from Dr. Marcelo Yanovsky. FLAG_314D04 (*erf2*), FLAG_157D10 (*erf8*) mutants were obtained from the ATRC (IJBP, Versailles) collection and were upscaled and grown with the FLAG wild type.

Plant growth conditions

Plants were grown under a long-day regime (16h light / 8h dark), at 21°C and a light intensity of 110-120 µmol m-2 s-1. All reported experiments were performed on the Weighing, Imaging and Watering Machine (WIWAM)(Skirycz et al., 2011). Briefly, the WIWAM is an automated platform with a robotic arm, bringing each pot once a day to subsequently an imaging platform, a scale to weigh the pots and calculate the required amount of water, and a watering platform. In our experimental setup, 4 seedlings were grown per pot (polypropylene pots, Skirycz et al., 2011). In total, 864 seedlings were grown simultaneously on the platform.

The seeds were sown in 85g +- 1g of Saniflor compost (Van Israel N.V., Geraardsbergen, Belgium) of approximately 70% absolute water content. The seeds were covered with plastic foil until 5 days after stratification (DAS) and upon removal of the foil, the automated watering was started the same day. When runs with mutants were performed, the pots were randomized to homogenously mix the mutants and the wild type plants. All plants were watered daily from 5 DAS until 11 DAS with a well-watered regime of 2.2 g_{water}/g_{soil}. At 12 DAS, half of the pots (random positions) were maintained at the well-watered regime until the end of the experiment, while the other half of the pots were not watered until the relative humidity dropped to 1.2 g_{water}/g_{soil} (which was generally not reached before the end of an experiment). All experiments lasted until 17 DAS.

Leaf size measurements

All described measurements were performed on the third true leaves of the rosettes.

For the growth experiments represented in Figures 6.2A, 6.2B, and 6.2C, third true leaves of 20 plants per time point per condition were cut from the rosette, cleared in 100% ethanol and mounted on microscopic slides in lactic acid. Leaves were photographed with the Leica binocular and the area was measured based on the pictures, using ImageJ v1.45 (NIH; https://rsb.info.nih.gov/ij/). The harvesting of the leaves was done at 6AM and at 10PM. Leaf size measurements were performed in four biological repeats. Relative Growth Rates were calculated as the increase in leaf area over a defined period divided by the leaf area at the start of this period.

For the growth experiments performed on a same leaf over time, as represented in Figure 6.2D, an imprint of the abaxial surface of the leaf was taken with dental resin (Kagan et al., 1992) every morning and evening. The imprints on the resin were subsequently photographed and measured as described above. Approximately seven leaves were analyzed per condition per experiment.

For the leaf size measurements to compare mutant and wild type phenotypes, as shown in Figures 6.6D, 6.6E, and 6.7, the third true leaf of 30 – 50 plants was harvested only at the end of the experiment, at 17 DAS. Leaf area was measured as described above.

Cellular analysis over time

Imprints of the abaxial surface of the leaves were made with dental resin (Kagan et al., 1992) every morning and evening and subsequently overlaid with a thin layer of nail polish. The nail polish copy of the imprint was analyzed by scanning electron microscopy. A region of approximately 200 cells was followed over time and the number of cells that divided within that region between two consecutive time points was counted. The expansion of the selected zone of cells was calculated using ImageJ. The absolute expansion rate of the zone was divided by the number of cells (taking into account the newly formed cells) to estimate the cell expansion rate.

Sampling for expression analysis

All described measurements were performed on the third true leaves of the rosettes. Per treatment and per time point, 4 leaves were harvested at 04.00, 08.00, 12.00, 16.00, 20.00, 24.00 on 12 DAS (except 04.00), 13 DAS, 14 DAS, 15 DAS and 16 DAS (until 08.00). The leaves were pooled and flash frozen on liquid nitrogen immediately upon harvest. For the harvests during the night, a low-intensity green light was used to enable harvesting without perturbing the plants light rhythms.

RNA extraction

RNA was extracted using Trizol (Invitrogen) according to the manufacturer's instructions. DNase treatment was performed on-column with the RNase-free DNase kit (Promega). The samples were further purified on column with the RNeasy Mini Kit (Qiagen) according to the manufacturer's instructions. Samples were eluted in RNase-free water.

Expression analysis by qRT-PCR

cDNA was synthesized from 200 - 500 ng RNA using the iScript cDNA Synthesis Kit (Biorad) according to the manufacturer's instruction. The cDNA was diluted 5 times.

qRT-PCR was done on a LightCycler 480 (Roche Diagnostics) in 384-well plates with LightCycler 480 SYBR Green I Master Mix (Roche) according to the manufacturer's instructions. All samples of the same time point were always assayed together on the same plate. Melting curves were analyzed to check primer specificity. Normalization was done against the average of housekeeping genes AT1G13320, AT2G32170, AT2G28390; ΔCt = Ct(gene) – Ct(mean(housekeeping genes)). Ct refers to the number of cycles at which SYBR Green fluorescence reaches an arbitrary value during the exponential phase of amplification. For the graphs represented in Figures 6.4 and 6.6, the –ΔCt values were plot relative to the lowest –ΔCt of this gene, in order to set the lowest observed expression value to 0. Primers were designed with the QuantPrime website (Arvidsson et al., 2008). Primers used in this study are:

LHY1: GAGCTTGGCAACGAATTGAAGAAC and AAAGCTTGGCAAACAGGGATGC
CCA1: TCGAAAGACGGGAAGTGGAACG and GTCGATCTTCATTGGCCATCTCAG
TOC1: TTAGGTCCACCAACCCACAGAGAG and AGGAGCAGTAGCAACAGACCACTC
KCS20: CTCGCTAAACAGATGCTTCAGGTG and GCATTGATCGGTCGTTGCCTAAG
PYL6: AAAGCTGCCACGTGGTTATCGG and AGAGACGACTCTGACCTCTCTCAC

RNA sequencing

The sequencing was performed at the Nucleomics Core Facility (VIB, Leuven, Belgium). Library preparation was done with the TruSeq RNA Sample Preparation Kit (Illumina). The quality was checked with the 2100 Bioanalyzer (Agilant), and clusters were generated through amplification using the TruSeq PE Cluster Kit (Illumina). Samples were sequenced on a HiSeq 2000 in paired-end mode with reads of 50 bp in length.

The quality of the received sequences was verified with FASTQC (http://bioinformatics.babraham.ac.uk/projects/fastqc/), and filtering of the adaptor and other overrepresented sequences was done with the fastx-Toolkit (http://hannonlab.cshl.edu/fastx_toolkit/). The remaining reads were mapped to the Arabidopsis reference genome according to TAIR10 (TAIR10_chr_all.fas; ftp.arabidopsis.org). Reads that did not map to a unique position were removed using samtools (v0.1.18; Li et al., 2009). The final read count per gene for all samples will be available upon publication of this chapter.

Differential expression analysis

Differential expression analysis was performed with multifactorial ANOVA using the EdgeR and ggplot2 libraries in R 3.0.1 (https://www.r-project.org). Rough counts were normalized to the library size. Very lowly expressed genes were removed by filtering for

genes with counts >5 in at least 3 samples. The new libraries were normalized by TMM. A Generalized Linear Model was applied with Time and Treatment as factors using the glmFit function. This model allowed taking into account the time-course aspect of this dataset, in which a Treatment effect in one time point for a certain gene is strengthened if a similar Treatment effect is observed for that same gene at another time point. Significant interactions were extracted using the glmLRT function and the interaction term as a coefficient. This represents the genes that are differently affected by the Treatment at different Times. Differentially expressed genes in drought vs. well-watered at each time point were calculated using predefined contrasts for each group (each time point). The cut-off was set on FDR<0.05 and Log_2 Fold Change of >0.2. The "core set" of drought-responsive genes as presented in Supp. Table S1 was obtained by selecting genes with FDR<0.5 at each of the 4 sequenced time points. Clustering was performed in TMEV (www.tm4.org) using K-means clustering with 50 clusters and 200 iterations. GO enrichment analysis was performed using the PLAZA Workbench (http://bioinformatics.psb.ugent.be/plaza).

SUPPLEMENTAL DATA

All Supplemental Data is listed below. Supplemental Figures can be found at the end of this chapter. Supplemental Table 3. can be downloaded from:
http://www.psb.ugent.be/~madub/Supp_Table_S3.xlsx

Supplemental Figure S1. Experimental setup used to measure short term response to mild drought.

Supplemental Figure S2. Relative growth rates (RGR) day and night during the development of the third Arabidopsis leaf.

Supplemental Figure S3. Imprint setup to measure (cellular) leaf growth over time.

Supplemental Figure S4. Principal component analysis of RNAseq data.

Supplemental Figure S5. Overlaps between the datasets of drought-responsive genes.

Supplemental Figure S6. Expression analysis of the *DREB2A* gene.

Supplemental Figure S7. Phenotypical analysis of *toc1* mutants.

Supplemental Figure S8. Confirmation by qPCR of putative positive regulators of leaf growth under drought.

Supplemental Figure S9. Confirmation by qPCR of putative negative regulators of leaf growth under drought.

Supplemental Figure S10. Genes that were removed from the qPCR validation experiments.

Supplemental Figure S11. Phenotype of the not-retained knock-outs of the screen.

Supplemental Table 1. Overview of the 29 genes differentially expressed at all time points from this study.

Supplemental Table 2 . Overview of the datasets used for comparison.

Supplemental Table 3. Genes differently affected by drought during day and night.

ACKNOWLEDGEMENTS

We thank the whole Systems Biology of Yield group for the fruitful discussions and the stimulating scientific environment. We are particularly grateful to Lisa Van den Broeck, Alexandra Baekelandt, and Andres Ritter for kindly sharing seeds for the mutant screen, as well as to Twiggy Van Daele and Vanessa Goncalves for the practical help. This work was supported by the Interuniversity Attraction Poles Program (IUAP P7/29 "MARS") initiated by the Belgian Science Policy Office, by Ghent University ('Bijzonder Onderzoeksfonds Methusalem Project' no. BOF08/01M00408, Multidisciplinary Research Partnership "Biotechnology for a Sustainable Economy" Project no. 01MRB510W), and by the Research Foundation Flanders (FWO) (predoctoral fellowship to H.C.).

REFERENCES

Achard P, Gusti A, Cheminant S, Alioua M, Dhondt S, Coppens F, Beemster GT, Genschik P (2009) Gibberellin signaling controls cell proliferation rate in Arabidopsis. Curr Biol 19: 1188-1193

Andriankaja M, Dhondt S, De Bodt S, Vanhaeren H, Coppens F, De Milde L, Mühlenbock P, Skirycz A, Gonzalez N, Beemster GTS, Inzé D (2012) Exit from proliferation during leaf development in *Arabidopsis thaliana*: a not-so-gradual process. Developmental Cell 22: 64-78

Arana MV, Marin-de la Rosa N, Maloof JN, Blazquez MA, Alabadi D (2011) Circadian oscillation of gibberellin signaling in Arabidopsis. Proc Natl Acad Sci U S A 108: 9292-9297

Araus JL, Slafer GA, Reynolds MP, Royo C (2002) Plant breeding and drought in C3 cereals: what should we breed for? Ann Bot 89 Spec No: 925-940

Baerenfaller K, Massonnet C, Walsh S, Baginsky S, Buhlmann P, Hennig L, Hirsch-Hoffmann M, Howell KA, Kahlau S, Radziejwoski A, Russenberger D, Rutishauser D, Small I, Stekhoven D, Sulpice R, Svozil J, Wuyts N, Stitt M, Hilson P, Granier C, Gruissem W (2012) Systems-based analysis of Arabidopsis leaf growth reveals adaptation to water deficit. Mol Syst Biol 8: 606

Barboza-Barquero L, Nagel KA, Jansen M, Klasen JR, Kastenholz B, Braun S, Bleise B, Brehm T, Koornneef M, Fiorani F (2015) Phenotype of Arabidopsis thaliana semi-dwarfs with deep roots and high growth rates under water-limiting conditions is independent of the GA5 loss-of-function alleles. Ann Bot

Bonhomme L, Valot B, Tardieu F, Zivy M (2012) Phosphoproteome dynamics upon changes in plant water status reveal early events associated with rapid growth adjustment in maize leaves. Mol Cell Proteomics 11: 957-972

Boyer JS (1982) Plant productivity and environment. Science 218: 443-448

Bray EA (2004) Genes commonly regulated by water-deficit stress in Arabidopsis thaliana. J Exp Bot 55: 2331-2341

Caldeira CF, Jeanguenin L, Chaumont F, Tardieu F (2014) Circadian rhythms of hydraulic conductance and growth are enhanced by drought and improve plant performance. Nat Commun 5: 5365

Castiglioni P, Warner D, Bensen RJ, Anstrom DC, Harrison J, Stoecker M, Abad M, Kumar G, Salvador S, D'Ordine R, Navarro S, Back S, Fernandes M, Targolli J, Dasgupta S, Bonin C, Luethy MH, Heard JE (2008) Bacterial RNA chaperones confer abiotic stress tolerance in plants and improved grain yield in maize under water-limited conditions. Plant Physiol 147: 446-455

Claeys H, Inzé D (2013) The agony of choice: how plants balance growth and survival under water-limiting conditions. Plant Physiology 162: 1768-1779

Claeys H, Skirycz A, Maleux K, Inzé D (2012) DELLA signaling mediates stress-induced cell differentiation in Arabidopsis leaves through modulation of anaphase-promoting complex/cyclosome activity. Plant Physiology 159: 739-747

Claeys H, Van Landeghem S, Dubois M, Maleux K, Inzé D (2014) What is stress? Dose-response effects in commonly used in vitro stress assays. Plant Physiology 165: 519-527

Clauw P, Coppens F, De Beuf K, Dhondt S, Van Daele T, Maleux K, Storme V, Clement L, Gonzalez N, Inze D (2015) Leaf responses to mild drought stress in natural variants of Arabidopsis. Plant Physiol 167: 800-816

Des Marais DL, McKay JK, Richards JH, Sen S, Wayne T, Juenger TE (2012) Physiological genomics of response to soil drying in diverse Arabidopsis accessions. Plant Cell 24: 893-914

Donnelly PM, Bonetta D, Tsukaya H, Dengler RE, Dengler NG (1999) Cell cycling and cell enlargement in developing leaves of Arabidopsis. Dev Biol 215: 407-419

Dornbusch T, Michaud O, Xenarios I, Fankhauser C (2014) Differentially phased leaf growth and movements in Arabidopsis depend on coordinated circadian and light regulation. Plant Cell 26: 3911-3921

Dosio GA, Tardieu F, Turc O (2011) Floret initiation, tissue expansion and carbon availability at the meristem of the sunflower capitulum as affected by water or light deficits. New Phytol 189: 94-105

Dubois M, Skirycz A, Claeys H, Maleux K, Dhondt S, De Bodt S, Vanden Bossche R, De Milde L, Yoshizumi T, Matsui M, Inzé D (2013) ETHYLENE RESPONSE FACTOR6 acts as a central regulator of leaf growth under water-limiting conditions in Arabidopsis. Plant Physiology 162: 319-332

Espinoza C, Bieniawska Z, Hincha DK, Hannah MA (2008) Interactions between the circadian clock and cold-response in Arabidopsis. Plant Signal Behav 3: 593-594

Fang Y, Xiong L (2015) General mechanisms of drought response and their application in drought resistance improvement in plants. Cell Mol Life Sci 72: 673-689

Fedoroff NV (2010) The past, present and future of crop genetic modification. N Biotechnol 27: 461-465

Fedoroff NV, Battisti DS, Beachy RN, Cooper PJ, Fischhoff DA, Hodges CN, Knauf VC, Lobell D, Mazur BJ, Molden D, Reynolds MP, Ronald PC, Rosegrant MW, Sanchez PA, Vonshak A, Zhu JK (2010) Radically rethinking agriculture for the 21st century. Science 327: 833-834

Filo J, Wu A, Eliason E, Richardson T, Thines BC, Harmon FG (2015) Gibberellin driven growth in elf3 mutants requires PIF4 and PIF5. Plant Signal Behav 10: e992707

Gonzalez N, Vanhaeren H, Inze D (2012) Leaf size control: complex coordination of cell division and expansion. Trends Plant Sci 17: 332-340

Granier C, Aguirrezabal L, Chenu K, Cookson SJ, Dauzat M, Hamard P, Thioux JJ, Rolland G, Bouchier-Combaud S, Lebaudy A, Muller B, Simonneau T, Tardieu F (2006) PHENOPSIS, an automated platform for reproducible phenotyping of plant responses to soil water deficit in Arabidopsis thaliana permitted the identification of an accession with low sensitivity to soil water deficit. New Phytol 169: 623-635

Habben JE, Bao X, Bate NJ, DeBruin JL, Dolan D, Hasegawa D, Helentjaris TG, Lafitte RH, Lovan N, Mo H, Reimann K, Schussler JR (2014) Transgenic alteration of ethylene biosynthesis increases grain yield in maize under field drought-stress conditions. Plant Biotechnol J 12: 685-693

Harb A, Krishnan A, Ambavaram MM, Pereira A (2010) Molecular and physiological analysis of drought stress in Arabidopsis reveals early responses leading to acclimation in plant growth. Plant Physiol 154: 1254-1271

Hsu PY, Harmer SL (2014) Wheels within wheels: the plant circadian system. Trends Plant Sci 19: 240-249

Hummel I, Pantin F, Sulpice R, Piques M, Rolland G, Dauzat M, Christophe A, Pervent M, Bouteille M, Stitt M, Gibon Y, Muller B (2010) Arabidopsis plants acclimate to water deficit at low cost through changes of carbon usage: an integrated perspective using growth, metabolite, enzyme, and gene expression analysis. Plant Physiol 154: 357-372

Jarzyniak KM, Jasinski M (2014) Membrane transporters and drought resistance - a complex issue. Front Plant Sci 5: 687

Kang HG, Kim J, Kim B, Jeong H, Choi SH, Kim EK, Lee HY, Lim PO (2011) Overexpression of FTL1/DDF1, an AP2 transcription factor, enhances tolerance to cold, drought, and heat stresses in Arabidopsis thaliana. Plant Sci 180: 634-641

Kawade K, Horiguchi G, Tsukaya H (2010) Non-cell-autonomously coordinated organ size regulation in leaf development. Development 137: 4221-4227

Kilian J, Whitehead D, Horak J, Wanke D, Weinl S, Batistic O, D'Angelo C, Bornberg-Bauer E, Kudla J, Harter K (2007) The AtGenExpress global stress expression data set: protocols, evaluation and model data analysis of UV-B light, drought and cold stress responses. Plant J 50: 347-363

Kim J, Jung JH, Lee SB, Go YS, Kim HJ, Cahoon R, Markham JE, Cahoon EB, Suh MC (2013) Arabidopsis 3-ketoacyl-coenzyme a synthase9 is involved in the synthesis of tetracosanoic acids as precursors of cuticular waxes, suberins, sphingolipids, and phospholipids. Plant Physiol 162: 567-580

Kreps JA, Wu Y, Chang H-S, Zhu T, Wang X, Harper JF (2002) Transcriptome changes for Arabidopsis in response to salt, osmotic, and cold stress. Plant Physiology 130: 2129-2141

Langridge P, Reynolds MP (2015) Genomic tools to assist breeding for drought tolerance. Curr Opin Biotechnol 32: 130-135

Lee SB, Jung SJ, Go YS, Kim HU, Kim JK, Cho HJ, Park OK, Suh MC (2009) Two Arabidopsis 3-ketoacyl CoA synthase genes, KCS20 and KCS2/DAISY, are functionally redundant in cuticular wax and root suberin biosynthesis, but differentially controlled by osmotic stress. Plant J 60: 462-475

Li-Beisson Y, Shorrosh B, Beisson F, Andersson MX, Arondel V, Bates PD, Baud S, Bird D, Debono A, Durrett TP, Franke RB, Graham IA, Katayama K, Kelly AA, Larson T, Markham JE, Miquel M, Molina I, Nishida I, Rowland O, Samuels L, Schmid KM, Wada H, Welti R, Xu C, Zallot R, Ohlrogge J (2013) Acyl-lipid metabolism. Arabidopsis Book 11: e0161

Ma T, Li ML, Zhao AG, Xu X, Liu GS, Cheng LQ (2014) LcWRKY5: an unknown function gene from sheepgrass improves drought tolerance in transgenic Arabidopsis. Plant Cell Reports 33: 1507-1518

Marris E (2008) Water: more crop per drop. Nature 452: 273-277

Matsui A, Ishida J, Morosawa T, Mochizuki Y, Kaminuma E, Endo TA, Okamoto M, Nambara E, Nakajima M, Kawashima M, Satou M, Kim JM, Kobayashi N, Toyoda T, Shinozaki K, Seki M (2008) Arabidopsis transcriptome analysis under drought, cold, high-salinity and ABA treatment conditions using a tiling array. Plant Cell Physiol 49: 1135-1149

Matt P, Schurr U, Klein D, Krapp A, Stitt M (1998) Growth of tobacco in short-day conditions leads to high starch, low sugars, altered diurnal changes in the Nia transcript and low nitrate reductase activity, and inhibition of amino acid synthesis. Planta 207: 27-41

Nemali KS, Bonin C, Dohleman FG, Stephens M, Reeves WR, Nelson DE, Castiglioni P, Whitsel JE, Sammons B, Silady RA, Anstrom D, Sharp RE, Patharkar OR, Clay D, Coffin M, Nemeth MA, Leibman ME, Luethy M, Lawson M (2015) Physiological responses related to increased grain yield under drought in the first biotechnology-derived drought-tolerant maize. Plant Cell Environ 38: 1866-1880

Nobusawa T, Okushima Y, Nagata N, Kojima M, Sakakibara H, Umeda M (2013) Restriction of cell proliferation in internal tissues via the synthesis of very-long-chain fatty acids in the epidermis. Plant Signal Behav 8

Nonami H, Wu Y, Boyer JS (1997) Decreased Growth-Induced Water Potential (A Primary Cause of Growth Inhibition at Low Water Potentials). Plant Physiol 114: 501-509

Nozue K, Covington MF, Duek PD, Lorrain S, Fankhauser C, Harmer SL, Maloof JN (2007) Rhythmic growth explained by coincidence between internal and external cues. Nature 448: 358-361

Nozue K, Maloof JN (2006) Diurnal regulation of plant growth. Plant Cell Environ 29: 396-408

Pantin F, Fanciullino AL, Massonnet C, Dauzat M, Simonneau T, Muller B (2013) Buffering growth variations against water deficits through timely carbon usage. Front Plant Sci 4: 483

Pantin F, Simonneau T, Muller B (2012) Coming of leaf age: control of growth by hydraulics and metabolics during leaf ontogeny. New Phytol 196: 349-366

Pantin F, Simonneau T, Rolland G, Dauzat M, Muller B (2011) Control of leaf expansion: a developmental switch from metabolics to hydraulics. Plant Physiol 156: 803-815

Parent B, Suard B, Serraj R, Tardieu F (2010) Rice leaf growth and water potential are resilient to evaporative demand and soil water deficit once the effects of root system are neutralized. Plant Cell Environ 33: 1256-1267

Pierik R, Testerink C (2014) The art of being flexible: how to escape from shade, salt, and drought. Plant Physiol 166: 5-22

Poire R, Wiese-Klinkenberg A, Parent B, Mielewczik M, Schurr U, Tardieu F, Walter A (2010) Diel time-courses of leaf growth in monocot and dicot species: endogenous rhythms and temperature effects. J Exp Bot 61: 1751-1759

Ruts T, Matsubara S, Wiese-Klinkenberg A, Walter A (2012) Diel patterns of leaf and root growth: endogenous rhythmicity or environmental response? J Exp Bot 63: 3339-3351

Schurr U, Walter A, Rascher U (2006) Functional dynamics of plant growth and photosynthesis--from steady-state to dynamics--from homogeneity to heterogeneity. Plant Cell Environ 29: 340-352

Seo PJ, Park CM (2011) Cuticular wax biosynthesis as a way of inducing drought resistance. Plant Signal Behav 6: 1043-1045

Shi J, Habben JE, Archilbald RL, Drummond B, Chamberlin MA, Williams R, Lafitte R, Weers B (2015) Over-expression of ARGOS genes modifies plant sensitivity to ethylene, leading to improved drought tolerance in both Arabidopsis and maize. Plant Physiol

Skirycz A, Claeys H, De Bodt S, Oikawa A, Shinoda S, Andriankaja M, Maleux K, Eloy NB, Coppens F, Yoo S-D, Saito K, Inzé D (2011) Pause-and-stop: the effects of osmotic stress on cell proliferation during early leaf development in *Arabidopsis* and a role for ethylene signaling in cell cycle arrest. Plant Cell 23: 1876-1888

Skirycz A, De Bodt S, Obata T, De Clercq I, Claeys H, De Rycke R, Andriankaja M, Van Aken O, Van Breusegem F, Fernie AR, Inzé D (2010) Developmental stage specificity and the role of mitochondrial metabolism in the response of Arabidopsis leaves to prolonged mild osmotic stress. Plant Physiology 152: 226-244

Skirycz A, Vandenbroucke K, Clauw P, Maleux K, De Meyer B, Dhondt S, Pucci A, Gonzalez N, Hoeberichts F, Tognetti VB, Galbiati M, Tonelli C, Van Breusegem F, Vuylsteke M, Inze D (2011) Survival and growth of Arabidopsis plants given limited water are not equal. Nat Biotechnol 29: 212-214

Stitt M, Zeeman SC (2012) Starch turnover: pathways, regulation and role in growth. Curr Opin Plant Biol 15: 282-292

Tang AC, Boyer JS (2002) Growth-induced water potentials and the growth of maize leaves. J Exp Bot 53: 489-503

Tardieu F, Granier C (2000) Quantitative analysis of cell division in leaves: methods, developmental patterns and effects of environmental conditions. Plant Mol Biol 43: 555-567

Tardieu F, Parent B, Caldeira CF, Welcker C (2014) Genetic and physiological controls of growth under water deficit. Plant Physiol 164: 1628-1635

Tardieu F, Simonneau T, Parent B (2015) Modelling the coordination of the controls of stomatal aperture, transpiration, leaf growth, and abscisic acid: update and extension of the Tardieu-Davies model. J Exp Bot 66: 2227-2237

Thain SC, Vandenbussche F, Laarhoven LJ, Dowson-Day MJ, Wang ZY, Tobin EM, Harren FJ, Millar AJ, Van Der Straeten D (2004) Circadian rhythms of ethylene emission in Arabidopsis. Plant Physiol 136: 3751-3761

Tisne S, Serrand Y, Bach L, Gilbault E, Ben Ameur R, Balasse H, Voisin R, Bouchez D, Durand-Tardif M, Guerche P, Chareyron G, Da Rugna J, Camilleri C, Loudet O (2013) Phenoscope: an automated large-scale phenotyping platform offering high spatial homogeneity. Plant J 74: 534-544

Todd J, Post-Beittenmiller D, Jaworski JG (1999) KCS1 encodes a fatty acid elongase 3-ketoacyl-CoA synthase affecting wax biosynthesis in Arabidopsis thaliana. Plant J 17: 119-130

Tresch S, Heilmann M, Christiansen N, Looser R, Grossmann K (2012) Inhibition of saturated very-long-chain fatty acid biosynthesis by mefluidide and perfluidone, selective inhibitors of 3-ketoacyl-CoA synthases. Phytochemistry 76: 162-171

Verslues PE, Agarwal M, Katiyar-Agarwal S, Zhu J, Zhu J-K (2006) Methods and concepts in quantifying resistance to drought, salt and freezing, abiotic stresses that affect plant water status. Plant Journal 45: 523-539

Wang GY, Shi JL, Ng G, Battle SL, Zhang C, Lu H (2011) Circadian clock-regulated phosphate transporter PHT4;1 plays an important role in Arabidopsis defense. Mol Plant 4: 516-526

Westwood JH, McCann L, Naish M, Dixon H, Murphy AM, Stancombe MA, Bennett MH, Powell G, Webb AA, Carr JP (2013) A viral RNA silencing suppressor interferes with abscisic acid-mediated signalling and induces drought tolerance in Arabidopsis thaliana. Mol Plant Pathol 14: 158-170

Wiese A, Christ MM, Virnich O, Schurr U, Walter A (2007) Spatio-temporal leaf growth patterns of Arabidopsis thaliana and evidence for sugar control of the diel leaf growth cycle. New Phytol 174: 752-761

Wilkins O, Brautigam K, Campbell MM (2010) Time of day shapes Arabidopsis drought transcriptomes. Plant J 63: 715-727

Zeller G, Henz SR, Widmer CK, Sachsenberg T, Ratsch G, Weigel D, Laubinger S (2009) Stress-induced changes in the Arabidopsis thaliana transcriptome analyzed using whole-genome tiling arrays. Plant J 58: 1068-1082

Zhang C, Xie Q, Anderson RG, Ng G, Seitz NC, Peterson T, McClung CR, McDowell JM, Kong D, Kwak JM, Lu H (2013) Crosstalk between the circadian clock and innate immunity in Arabidopsis. PLoS Pathog 9: e1003370

Zhou M, Wang W, Karapetyan S, Mwimba M, Marques J, Buchler NE, Dong X (2015) Redox rhythm reinforces the circadian clock to gate immune response. Nature 523: 472-476

Supp. Figure S1. Experimental setup used to measure short term response to mild drought. (A) Arabidopsis plants were grown on the Weighing, Imaging and Watering Machine (WIWAM). (B) Four seedlings were grown per pot to enable growth of 800 young seedlings per experiment. Scale = 2cm. (C) Leaf size was measured in a destructive way by harvesting the third leaf and measuring its size using a light microscope. Scale = 1mm. (D) This setup reproducibly results in a leaf area reduction of 20% in wild type plants at the final harvesting time point, 17 days after stratification (DAS). *** $p < 0.0001$

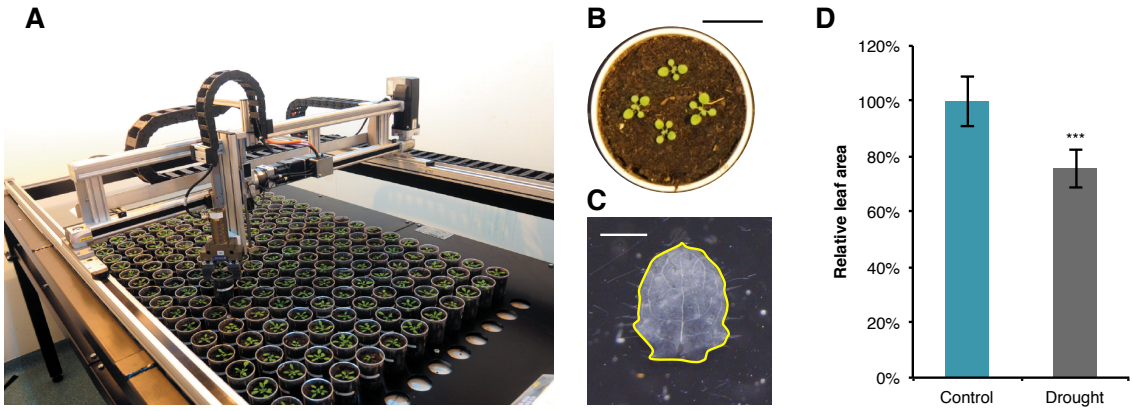

Supp. Figure S2. Relative growth rates (RGR) day and night during the development of the third Arabidopsis leaf. (A) RGR, defined as the generated area per unit of existing area per unit of time, measured along the full developmental time frame of the third leaf; from proliferation stage (9 DAS) until maturity (21 DAS), under well-watered conditions. (B) RGR of the third true leaf calculated from the average leaf area of a pool of 20 leaves harvested at each time point under well-watered (WW) and drought conditions during 5 days since the last watering (DSLW). Error bars represent standard error.

A

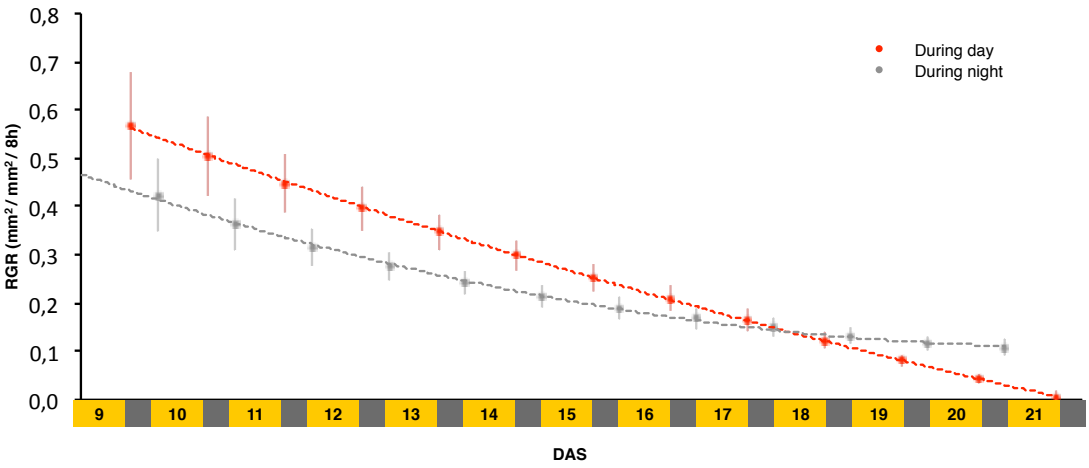

B

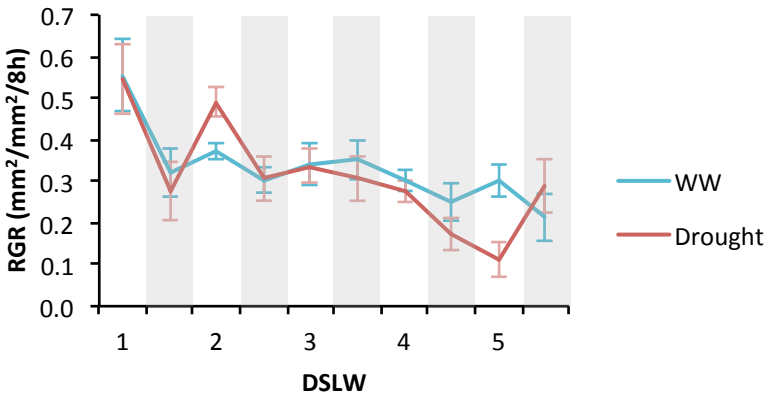

Supp. Figure S3. Imprint setup to measure (cellular) leaf growth over time. (A) Leaf imprints in dental resin enable measurement of leaf size over time of the same leaf. (B) Scanning electron microscopy of nail polish imprints of the resin imprints shown in (A - red square). The selected zones contained about 200 epidermis cells. Growth of individual cells can be tracked over time as illustrated for two cells. Examples of new divisions are shown by white arrowheads. (C) Relative cell expansion rate (RCER) and number of dividing cells within the delimited zone. PCC represents the Pearson Correlation Coefficient between the presented curve and the relative growth rate of the selected zone. "D" = day, "N" = night. (D) Average leaf area of the growing third leaf under well-watered (WW) and drought conditions as measured by the imprint method. DSLW = days since last watering.

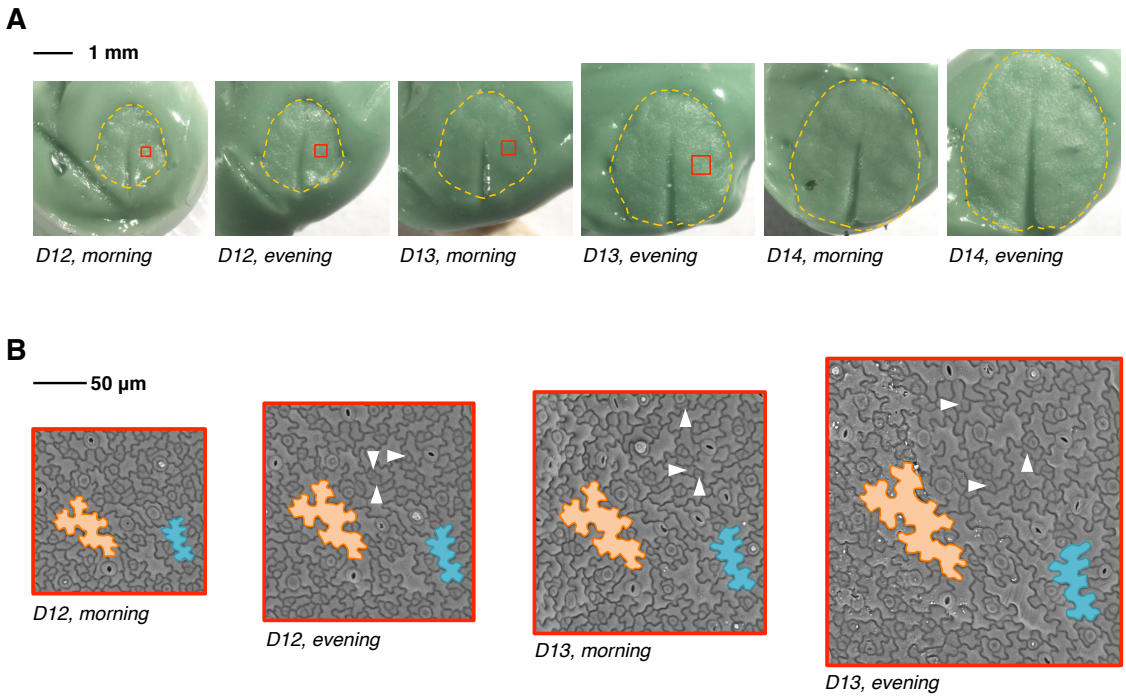

Supp. Figure S4. Principal Component Analysis (PCA) of RNAseq data. PCA plot representing the variation caused by the 'Time of Day' and the 'Treatment' factors in the dataset. Each dataset is represented by a symbol, and the distance between two datasets is representative for the variation between them. As such, datasets of the same Time of Day (04.00 and 04.00') cluster together, while the variation between the 04.00 datasets and 12.00 or 20.00, is clearly more pronounced.

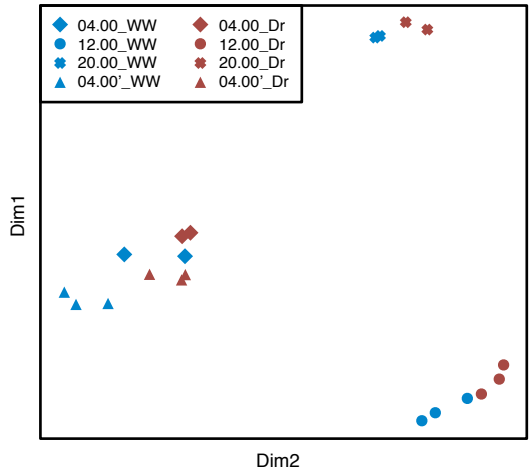

Supp. Figure S5. Overlaps between the datasets of drought-responsive genes. Venn-diagram comparing the significantly differentially expressed genes in drought vs. well-watered conditions at each time point.

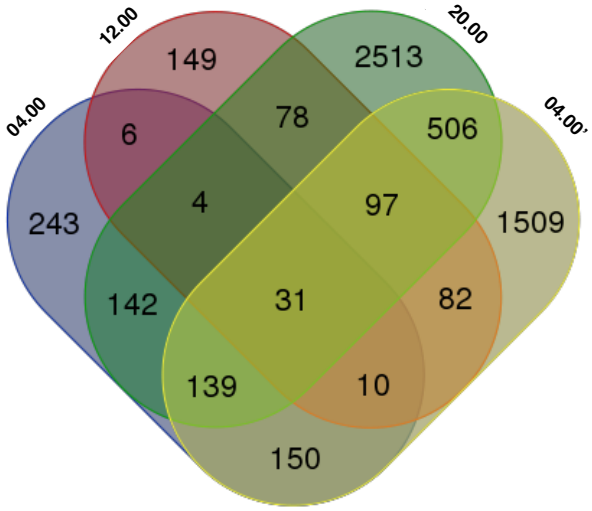

Supp. Figure S6. Expression pattern of *DREB2A* under well-watered (WW) and drought conditions. Expression level of the classical drought stress marker *DREB2A* during 4 days since the last watering (DSLW). Error bars represent standard error.

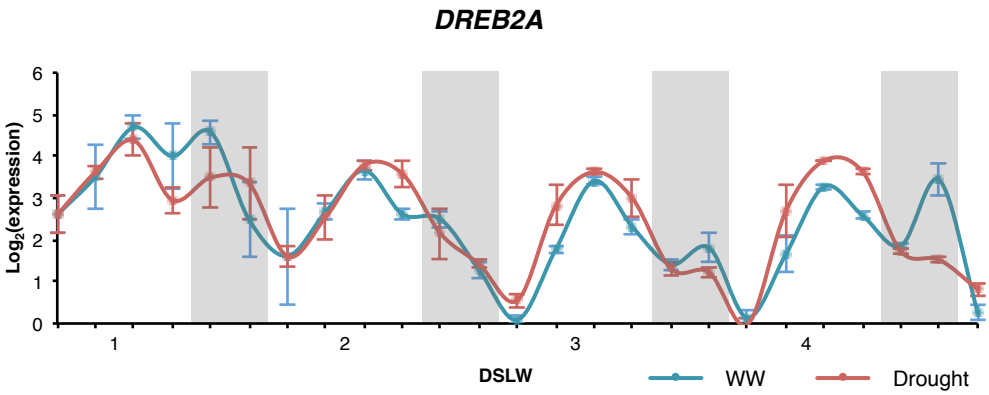

Supp. Figure S7. Phenotypical analysis of *toc1* mutants. (A) Rosette area of wild type and *toc1* mutants at 22 DAS under WW conditions. ** P < 0.001 (B) RGR of wild type and *toc1* mutants during day (D) and night (N) under control and drought conditions around the moment of growth inhibition (14 DAS).

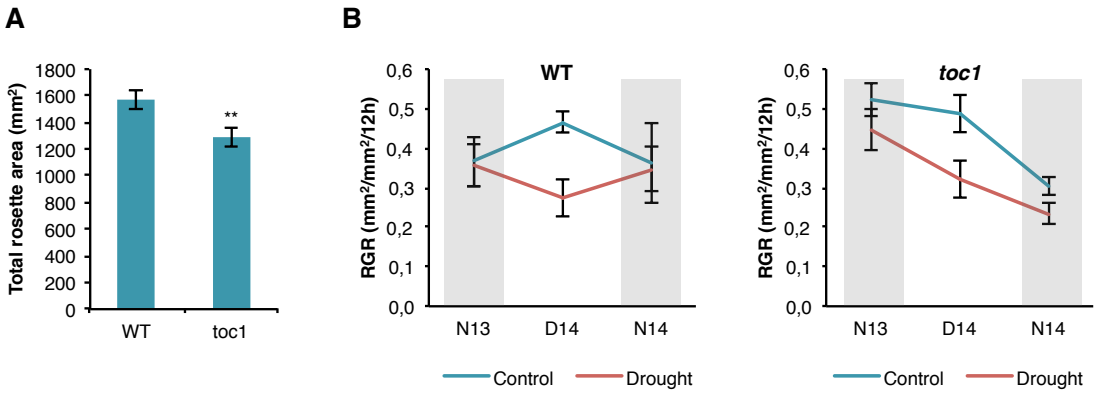

Supp. Figure S8. Confirmation by qPCR of putative positive regulators of leaf growth under drought. Transcription factors selected from the list of Supp. Table 3 containing genes negatively correlated with the dynamics of leaf growth under drought. qPCR was performed on two additional biological repeats of the 20.00 (14 DAS) and 04.00' (15 DAS) time points. The expression was considered as validated (genes in bold) when per time point the up or down-regulation could be reproduced and when the tendency between the two time points (lower expression change on 20.00 compared to 04.00') was reproducible.

Putative positive regulators		RNAseq (Log2-FC)				qPCR (Log2-FC)	
		04.00	12.00	20.00	04.00'	20.00	04.00'
AT2G01760	**ARR14**	0,5	0,1	0,0	0,5	0,0	0,6
AT4G39070	**BBX20**	-0,3	-1,1	-1,2	-0,3	-1,8	-0,3
AT2G42300	**bHLHx**	0,2	0,0	-0,2	0,3	-0,6	0,8
AT3G54810	**BME3**	0,1	-0,1	-0,2	0,8	-0,4	0,6
AT5G67480	**BT4**	0,1	-0,3	-0,6	-0,1	-0,5	0,3
AT4G37610	**BT5**	-0,3	-0,7	-1,5	-0,4	-2,5	-0,4
AT2G42380	**bZIP34**	0,7	-0,4	0,0	0,9	0,1	0,6
AT3G58120	**bZIP61**	0,5	-0,5	-0,1	0,7	-1,0	1,3
AT1G19490	bZIPx	0,5	-0,1	0,0	1,0	1,1	0,5
AT4G23750	**CRF2**	0,0	-0,4	-0,3	0,1	0,1	0,4
AT1G21910	**DREB26**	0,4	-0,6	-1,5	-1,0	0,6	2,0
AT1G25560	**EDF1**	-0,1	-0,7	-0,8	-0,5	-0,3	0,2
AT1G72360	**ERF73**	0,3	0,0	-1,0	-0,6	-0,3	0,2
AT5G07580	**ERFx**	0,2	-0,6	-0,5	0,1	-0,8	0,7
AT4G09180	**FBH2**	0,3	-0,1	-0,1	0,4	0,2	1,5
AT1G76890	**GT2**	0,2	-0,3	-0,3	0,0	-1,5	1,6
AT1G33240	**GTL1**	0,4	-0,2	-0,1	0,3	-0,2	0,4
AT4G17460	**HAT1**	-0,7	-1,3	-0,7	-0,3	0,0	0,9
AT2G18300	**HBI1**	0,6	-0,2	-0,1	0,3	-1,0	1,3
AT3G17609	**HYH**	0,0	-0,3	-0,5	-0,2	0,0	0,9
AT5G61590	**K11J9**	0,2	-0,5	-1,2	0,2	-0,5	0,9
AT3G28910	MYB30	0,3	-0,5	-0,3	0,3	0,1	0,0
AT5G67300	**MYB44**	0,0	-0,3	-0,6	0,4	-0,8	1,1
AT2G23290	**MYB70**	-0,2	-0,5	-1,2	0,1	-0,3	0,9
AT4G37260	**MYB73**	0,2	-0,1	-0,8	0,4	-0,5	0,7
AT3G50060	MYB77	0,5	-0,2	-0,3	0,6	0,5	0,2
AT1G25550	**MYBlike**	0,2	-0,4	-0,5	0,0	-0,9	0,2
AT5G18300	**NAC088**	0,4	-0,6	-1,0	0,0	-0,8	0,8
AT2G22770	**NAI1**	0,0	-0,3	-1,2	-0,6	-0,1	1,0
AT1G64100	PPR-con	-1,0	-1,2	-0,6	2,4	1,9	1,7
AT1G22190	**RAP2.4**	0,5	-0,4	0,0	0,3	-0,5	0,6
AT1G13260	RAV1	-0,3	-0,6	-2,0	-0,4	0,1	-1,3
AT2G39250	**SNZ**	0,4	-0,3	-0,1	0,4	-0,7	0,5
AT5G43270	**SPL2**	0,4	-0,3	-0,1	0,8	-0,8	1,1
AT5G08330	**TCP11**	0,2	-0,2	0,0	0,5	-0,1	0,4
AT1G11850	**Unknown**	0,4	0,0	-0,1	0,3	-0,7	0,4
AT4G23550	Unknown gene 1	0,2	-0,8	-0,4	-0,4	-0,4	0,7
AT5G52830	**WRKY27**	-0,4	-1,2	-0,5	-0,5	-0,3	0,1
AT3G01080	WRKY58	0,6	0,3	-1,1	-0,4	1,1	-0,3

Supp. Figure S9. Confirmation by qPCR of putative negative regulators of leaf growth under drought. Transcription factors selected from the list of Supp. Table 3 containing genes positively correlated with the dynamics of leaf growth under drought. qPCR was performed on two additional biological repeats of the 20.00 (14 DAS) and 04.00' (15 DAS) time points. The expression was considered as validated (genes in bold) when per time point the up or down-regulation could be reproduced and when the tendency between the two time points (higher expression change on 20.00 compared to 04.00') was reproducible.

Putative negative regulators		RNAseq (Log2-FC)				qPCR (Log2-FC)	
		04.00	12.00	20.00	04.00'	20.00	04.00'
AT4G34000	ABF3	0,2	0,4	0,9	0,7	0,4	0,9
AT3G06590	**AIF2**	0,2	0,3	0,5	0,0	1,2	0,3
AT5G67110	ALCATRAZ	-0,1	0,3	0,5	-0,2	0,4	0,9
AT3G61890	**ATHB12**	0,1	0,0	0,6	0,2	1,6	1,3
AT4G40060	ATHB16	0,1	0,2	0,4	0,1	0,5	1,2
AT4G27310	BBX28	-0,6	-0,2	0,8	-0,4	-0,1	0,1
AT3G21330	**bHLHx**	-4,1	-1,1	3,2	-2,4	1,4	-1,1
AT1G28370	**ERF11**	-0,5	0,0	1,0	-4,2	1,0	-0,3
AT5G47220	**ERF2**	-0,2	0,0	1,0	-0,7	1,8	-0,8
AT3G15210	**ERF4**	-0,2	0,2	0,6	0,0	0,7	0,1
AT1G53170	**ERF8**	0,2	0,2	1,1	0,3	1,1	0,9
AT1G11270	F-box	-0,2	-0,1	0,7	0,3	0,7	1,1
AT1G09650	**F-box**	-0,6	-0,1	1,2	-0,4	1,2	0,1
AT2G20570	GRPl1	0,0	0,1	0,4	0,2	0,3	0,9
AT1G17380	JAZ5	-0,2	0,0	1,3	-0,2	1,3	1,5
AT1G31320	LBD4	-0,1	0,4	0,8	0,5	-0,1	0,3
AT2G40970	MYBC1	0,0	0,3	0,7	0,3	0,8	1,1
AT1G32640	MYC2	-0,2	0,4	0,7	0,0	0,6	1,1
AT2G13570	**NFYB7**	0,0	0,0	1,0	0,0	0,9	0,8
AT1G09530	**PIF3**	-0,3	0,1	0,5	0,1	0,5	0,3
AT3G47640	**PYE**	0,1	0,3	0,8	-0,1	0,9	0,8
AT4G36900	**RAP2.10**	-0,3	-0,1	1,0	-0,1	0,8	-0,2
AT2G19810	**TZF2**	-0,2	0,5	0,6	0,2	0,8	-0,5
AT4G29190	**TZF3**	-0,1	0,4	0,9	-0,5	1,1	0,9
AT4G18170	**WRKY28**	-1,4	0,2	1,9	-1,3	2,4	0,0
AT5G28650	**WRKY74**	0,0	-0,5	1,8	1,5	3,1	0,7
AT1G04990	ZnF	0,1	0,3	0,5	0,1	-1,5	0,2
AT5G18550	**ZnF2**	0,1	0,1	0,3	0,2	1,7	0,2

Supp. Figure S10. Genes that were removed from the qPCR validation experiments. Transcription factors selected from the list of Supp. Table 3 but that could not be amplified by qPCR or that were wrongly assigned to the clusters because the expected tendency between the expression level during the day and the expression level during the night was not clear.

Genes wrongly assigned to cluster		RNAseq (Log2-FC)				qPCR (Log2-FC)	
		04.00	12.00	20.00	04.00'	20.00	04.00'
AT1G74890	ARR15	-0,5	-0,5	-0,6	-0,6	-0,7	-0,7
AT5G62920	ARR6	-0,2	-0,6	-0,4	-1,1	-1,3	0,4
AT1G08930	ERD6	0,1	-1,1	-0,7	-0,8	-1,3	-0,2
AT4G09460	MYB6	0,7	-0,2	0,1	0,1	-0,3	0,7
AT1G08810	MYB60	0,1	-0,5	-0,1	-0,2	0,5	0,8
AT5G65210	TGA1	0,2	-0,9	0,1	-0,1	NA	-0,6
AT2G42200	SPL9	-0,3	0,4	0,3	0,3	0,4	0,0

Genes that could not be amplified by qPCR		RNAseq (Log2-FC)				qPCR (Log2-FC)	
		04.00	12.00	20.00	04.00'	20.00	04.00'
AT3G44820	NPH3	0,6	-0,3	-0,1	0,2	NA	NA
AT4G36570	RL3	0,2	-1,8	-0,5	-0,7	NA	NA
AT4G39250	Unknown gene 2	0,3	-2,1	-3,2	-0,5	NA	NA
AT3G04060	ANAC046	-0,6	-0,6	1,4	-0,5	-0,6	NA
AT5G56960	bHLH	-3,4	0,0	2,7	-3,7	NA	NA
AT2G34720	HAP2x	0,0	0,1	0,4	0,2	0,1	NA
AT2G01280	MEE65	-0,8	0,0	1,1	0,2	NA	NA

Supp. Figure S11. Leaf area of the not-retained knock-out lines under well-watered (blue) and drought (red) conditions. Leaf area was measured at 17 days after stratification in two biological repeats.

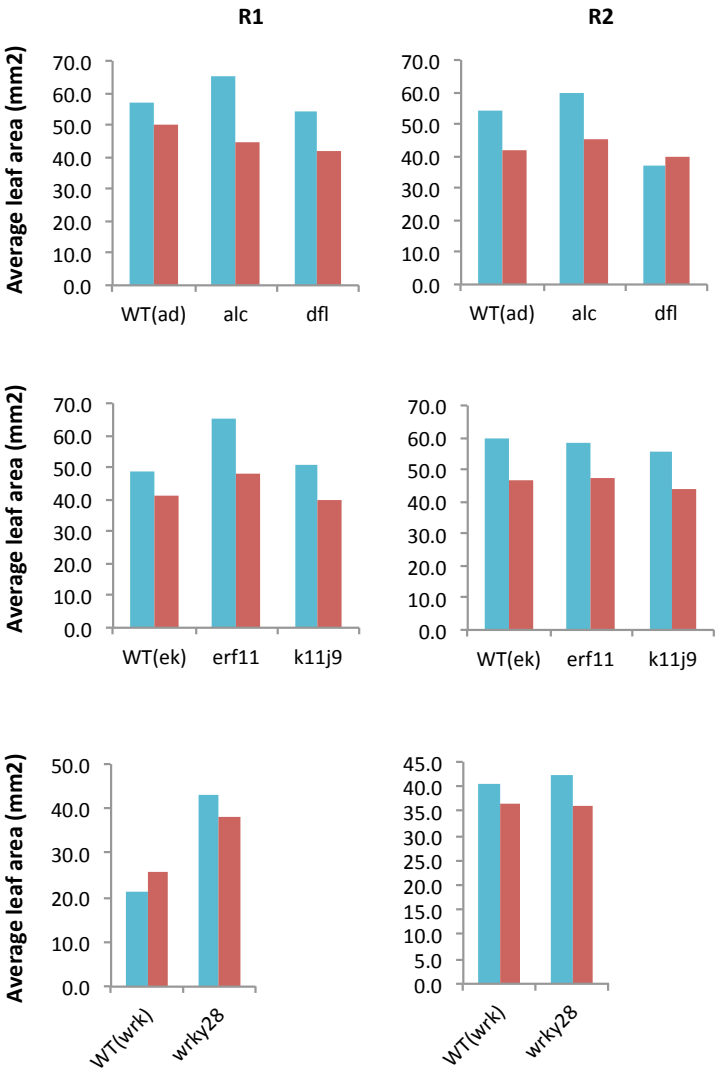

Supp. Table 1. Overview of the 29 genes differentially expressed at all time points from this study. Indicated values are the Log_2(FC) between drought and control at each time points. Colored cells are significant (FDR<0.05). See Supp. Table S2 for more information about the other datasets.

		This study					Baerenfaller			Wilkins				Clauw			Harb		Des marais	
		04.00	12.00	20.00	04.00'	Specific	Transition_EOD	Transition_EON	late expansion_EOD	late expansion_EON	06.00	00.00	18.00	12.00	log(FC) in Col	Common 6 accessions	Proliferation-specific	mDr_day1	mDr_day10	log(FC) in Col	Common 17 accessions
AT1G02205	CER1	0,9	0,7	0,8	3,1		1,4	1,6	1,1	1,4	-0,2	0,0	0,6	0,2	0,1			0,6	-0,2	0,9	X
AT1G08090	ATNRT2	-1,0	-1,4	-2,3	-1,8	X	-0,4	0,0	-0,4	-0,1	0,0	-0,1	0,0	0,0				0,0	0,1	-0,1	
AT1G09240	NAS3	-5,7	-3,4	-5,4	-3,9		0,0	0,2	0,2	0,6	0,2	0,1	0,1	1,4				0,3	0,8	-0,2	X
AT1G10640		0,8	0,6	0,6	1,7		0,5	1,2	-0,2	0,2	0,3	0,3	0,2	0,9	0,3	X		0,6	0,8	0,7	X
AT1G13280	AOC4	0,4	0,3	0,4	0,4		0,2	0,1	0,5	0,6	0,3	-0,1	0,2	0,3	-0,1			0,5	0,0	0,4	
AT1G22570		-0,6	-1,0	-1,2	-0,7		-0,5	-0,6	-0,1	-0,6	0,1	-0,3	-0,4	-0,6	-0,1	X		-0,7	-0,1	0,3	X
AT1G28230	PUP1	0,6	0,5	0,7	1,0		0,5	0,5	0,3	0,5	0,7	0,2	0,5	1,0	0,4			0,3	1,0	0,4	
AT1G51140		0,8	0,5	0,3	1,2		0,3	0,7	0,4	1,5	0,1	0,1	0,7	0,5	0,3	X		1,3	0,4	1,2	X
AT1G60590		0,4	0,4	0,4	0,8		-0,1	0,7	-0,2	1,3	-0,3	0,2	0,0	0,3	0,4	X	X	0,3	0,4	1,1	
AT1G62540	FMOGS-OX2	0,9	1,2	1,8	1,5		0,3	1,3	0,8	1,1	0,1	0,2	0,4	0,3	1,1	X		0,5	0,1	0,7	
AT1G65845		-1,7	-2,5	-2,3	-1,8		-0,4	-0,7	-0,9	-1,4					-0,8						
AT2G21650	MEE3	-0,8	-1,0	-2,5	-0,7		-1,3	-1,2	-1,6	-2,1	1,1	0,6	1,0	0,9	-0,5	X		-0,8	0,8	-2,2	X
AT2G30600		-1,0	-0,9	-1,1	-1,5		-0,4	-1,0	0,0	-0,5	-0,5	0,0	-0,1	-1,0	-0,5	X		-0,8	-0,9	-1,5	
AT2G33380	RD20	1,3	1,1	1,8	2,2		0,2	1,4	0,8	1,9	0,0	-0,1	1,4	0,1	1,1	X		1,2	-1,0	1,6	X
AT2G39800	P5CS1	0,5	1,0	1,5	0,9		0,5	1,4	0,6	2,3					1,1	X					
AT2G40330	PYL6	-0,7	-2,2	-1,9	-1,9		-0,7	-0,5	-0,3	-1,1	0,3	-0,2	-0,1	-0,3	-3,0	X		-0,3	0,0	-0,5	X
AT3G19450	CAD4	-0,2	-0,2	-0,2	-0,2		-0,2	-0,3	-0,4	-0,3	-0,2	0,1	0,4	-0,3	-0,1			-0,1	-0,1	-0,4	
AT3G29575	AFP3	2,2	1,0	2,2	2,4		0,3	0,6	-0,4	1,6	-0,2	-0,5	0,1	-0,5	0,9	X		1,0	0,0	0,9	X
AT3G30775	ERD5	-1,0	-1,7	-2,9	-1,1		-0,4	-1,5	0,1	-0,7	-0,6	0,4	1,9	0,0	-1,0	X		-1,5	-1,3	-3,9	X
AT3G53980		2,4	1,9	2,1	3,1		1,3	1,4	0,8	0,2	0,0	0,3	0,7	0,6	1,1	X		2,2	0,6	3,7	X
AT3G59010	PME61	0,4	0,6	0,4	0,6		-0,1	-0,6	-0,3	0,0	0,3	0,3	0,5	0,6	0,0			0,2	0,3	0,3	X
AT4G11460	CRK30	-0,8	-1,8	-2,2	-1,8		-0,3	-0,3	-0,3	-0,5	-0,2	0,1	-0,1	-0,2	-0,4	X		-0,3	0,0	-0,5	X
AT4G23670		0,4	0,6	0,7	0,9		0,4	0,3	0,8	0,7	0,0	0,3	0,2	0,3	0,2			0,7	0,4	1,2	X
AT5G03190	CPUORF47	0,3	0,5	0,5	0,7		2,0	2,1	2,8	2,5	0,5	0,3	1,3	0,8	0,3	X		1,9	0,7	0,8	
AT5G37300	WSD1	0,9	0,6	0,5	1,7	X	0,4	0,4	0,0	0,2	0,0	0,2	0,3	0,4	0,3			0,4	-0,3	0,1	
AT5G44380		-2,5	-2,5	-2,1	-1,9		0,1	0,0	-0,1	0,0	-0,3	-0,1	0,1	0,0	-0,4			0,1	0,0	-0,3	X
AT5G55930	OPT1	-0,4	-0,5	-0,6	-0,8		-0,1	-0,3	0,0	-0,1	0,3	0,2	0,6	0,5	-0,2	X		0,1	1,0	-1,5	X
AT5G60780	ATNRT2.3	-3,2	-2,9	-5,3	-2,8	X	-0,1	-0,2	-0,1	-0,1	-0,2	-0,1	-0,1	0,0	-0,6			0,0	0,1	0,1	
AT5G64570	XYL4	-0,6	-0,6	-1,2	-0,4		-0,3	-1,3	0,1	-0,1	-0,4	0,0	-0,1	-0,2	-0,6	X		-0,7	-0,6	-1,3	X

Supp. Table 2 . Overview of the datasets used for comparison. Five publicly available datasets were relevant for comparison with this study as they were performed on shoot tissue of plants exposed to mild or moderate drought stress. Severe and desiccation stress studies were excluded. All raw datasets were reanalyzed similarly as the dataset of this study, yielding the indicated amount of differentially expressed genes based on significance (FDR<0.05). Genes with very low fold-changes ($Log_2FC<|0.2|$) were also excluded. Upon reanalysis of the natural variants datasets (Clauw and Des Marais) only 8 and 3 genes were respectively differentially expressed when using only the data for Col; therefore, the originally published list of differentially expressed genes (based on all accessions) was used for further comparison.

	Tissue	Days following drought	Number of genes differentially expressed			
			Morning	Noon	Evening	Night
This study	Proliferating/expanding young leaves	3		460	3661	2406
Baerenfaller (2012)	Proliferating/expanding young leaves	21	121		54	
	Expanding/mature leaves	33	1064		142	
Wilkins (2010)	Full rosettes	4	36	47	822	0
Clauw (2015)	Proliferating/expanding young leaves	7		8 (455)		
Harb (2010)	Expanding/mature leaves	7	114			
	Expanding/mature leaves	17	903			
Des Marais (2012)	Mature leaves	7	3 (1689)			

Part 3:

CONCLUDING REMARKS

Chapter 7

General Discussion

Marieke Dubois [a,b] and Dirk Inzé [a,b]

[a] Department of Plant Systems Biology, VIB, Ghent, Belgium
[b] Department of Plant Biotechnology and Bioinformatics, Ghent University, Belgium

Contributions: M.D. performed the literature study and was the main author of the chapter. D.I. supervised the project and contributed to the writing of this Chapter.

This short chapter integrates the different findings from the previously described research. We first discuss the new insights gained by using *in vitro* assays to unravel the ethylene-centered growth response under stress, and we place our results in a broader context. We further compare the stress response *in vitro* with the response to mild drought stress in soil, and discuss the relevance of *in vitro* setups. Since it's all about timing, we emphasize on the importance of performing time course experiments, both during *in vitro* and in soil assays. Finally, based on the lessons learned from *in vitro* research, we propose possible future paths to follow in order to capture leaf growth regulators under drought.

IN VITRO ASSAYS AS ESSENTIAL TOOLS TO UNRAVEL SHORT TERM STRESS RESPONSES

New insights in ethylene signaling under stress

As introduced in the first chapter, ethylene has very diverse and sometimes contradictory roles during the plant's life cycle (reviewed in Van de Poel et al., 2015). In leaves, the role of ethylene has mainly been characterized under environmental stress conditions, where it represses leaf growth (Chapter 1). Several molecular pathways through which ethylene inhibits cell division and cell expansion were already described. Cell division is known to be repressed by ethylene through transcriptional inhibition of *CYCLIN* genes and of the E2F/RBR-pathway, while inhibition of *EXPANSIN* transcription reduces cell wall loosening and cell expansion. When exposed to *in vitro* osmotic stress, ethylene accumulates and triggers the inactivation of CDKA, resulting in a transient and reversible inhibition of the cell cycle (Skirycz et al., 2011). In parallel, an ethylene response mediated by multiple ETHYLENE RESPONSE FACTORS (ERFs) is initiated in young leaves. ERF6 appears to be central in the stress response in growing leaves, since it has a threefold function. First, ERF6 stimulates the activation of numerous transcription factors with reported roles in stress defense (Chapter 3). Second, ERF6 triggers the downstream inhibition of GA signaling. This occurs through transcriptional induction of the gene encoding the *GA2-OXIDASE6* enzyme which inactivates GA and thereby stabilizes DELLA proteins. The DELLA proteins are the downstream effectors of growth inhibition, as they repress cell division and cell expansion (Achard et al., 2008; Claeys et al., 2012). Third, ERF6 induces a negative feedback loop, involving ERF11, to fine-tune this stress response (Chapter 4). This new pathway fits into the current view of ethylene as a repressor of leaf growth under stress, and highlights an indirect negative effect of ethylene on cell division and expansion, with DELLA proteins as a bridge between ethylene and growth control.

Under mild osmotic stress, ethylene and DELLA proteins thus act together to repress cell expansion and division at multiple level. Accordingly, when exposed to short term osmotic stress, ethylene insensitive mutants and *erf5erf6* mutants grow better than wild type plants (Skirycz et al., 2011 and Chapter 3), and *q-ga2ox* (quintuple mutant; *ga2ox1*, *ga2ox2*, *ga2ox3*, *ga2ox4*, *ga2ox6*) and mutants in DELLA proteins do not show the stress-induced entry in endoreduplication (Claeys et al., 2012). Such crosstalk between ethylene and gibberellins is not restricted to osmotic stress response, but has also been observed during plant development. For example, ethylene represses root growth and flower transition through stabilization of the DELLA proteins (Achard et al., 2003; Achard et al., 2007). While in the case of flower transition ethylene reduces GA biosynthesis, it triggers GA-inactivation in the presented osmotic stress pathway. Similar molecular mechanisms with AP2/EREBP (APETALA2/ETHYLENE RESPONSE ELEMENT BINDING PROTEIN) transcription factors inducing GA-inactivation also occur under freezing and salt stress. In these other stress conditions CBF1 (C-REPEAT BINDING FACTOR 1) and DDF1 (DWARFED AND DELAYED FLOWERING) control the expression of *GA2-OX* genes (Achard et al., 2008; Magome et al., 2008). While specific GA2-OX genes appear to be induced in different environmental conditions, these pathways also converge into the stabilization of DELLA proteins. The unraveled mechanisms thus highlighted a novel context for ethylene/DELLA crosstalk, with ERF6 and GA2-OX6 as osmotic stress induced elements in this pathway.

Incredible complexity emerging around ERF6

When plants are exposed to osmotic stress, hundreds of genes are differentially expressed in actively growing leaves. These genes are enriched for genes encoding transcription factors, suggesting that transcriptional regulation plays a major role under osmotic stress. When identifying the genes downstream of ERF6, we also found a multitude of transcription factors, suggesting the presence of a transcriptional network around ERF6 (Chapter 3) (Figure 7.1). As a follow-up of these observations, research is currently being performed to further characterize these transcription factors and unravel this network. Ongoing experiments on 20 transcription factors thought to be involved in the network show that about ¾ of these genes can influence leaf growth either under stress or under control conditions (Lisa Van den Broeck and Dirk Inzé, unpublished results). A preliminary glimpse on the molecular connections within the network shows that the transcription factors can influence each other's expression level, either positively or negatively. The configuration of this highly interconnected network changes over time upon stress exposure, increasing complexity even more. The antagonistic relationship between ERF6 and ERF11 (Chapter 4), regulating common

target genes in opposite directions, is just one example of a small module within the network.

Additionally, the forward genetics screen presented in Chapter 5 sheds light on putative non-transcriptional mechanisms connecting to the ERF6-pathway. Putative genetic interactions with ERF6 were found for *CPL3*, *HASTY*, and *RST1*, as plants with mutation in these genes can suppress the dwarfism induced by ERF6 overexpression. Further experimental validation of these candidate genes and detailed exploration of the molecular link with ERF6 are the first necessary steps to unravel this network. If validated, these results would show that regulation of transcription, protein localization and perhaps also metabolic control are involved in the ERF6-mediated stress response, since *CPL3*, *HASTY* and *RST1* encode genes with these molecular functions, respectively. Finally, *EIN5* is also connected to ERF6 function, since mutations in *EIN5* suppress the *ERF6* overexpression phenotype. EIN5 is directly implicated in ethylene signaling, but its function in relation to growth has previously been reported to be likely not depending on the classical EIN2-mediated pathway (Dong et al., 2004). Instead, as an exoribonuclease, EIN5 most likely directly controls the transcript levels of growth-related genes, the identity of which still remains to be identified. It is probably through the altered degradation of genes involved in the network around ERF6 that EIN5 is able to suppress the dwarfed phenotype when mutated.

The ERF6-centered growth regulatory pathway as presented in Chapter 3 thus appears to be just a first piece of the puzzle of an incredibly complex stress-responsive network. While the steady states of this network before stress are still easily comprehensible for humans, further rewiring upon stress exposure is hard to visualize and to understand. Differential network visualization is therefore absolutely essential to get insights in these dynamical systems, and we therefore contributed to a new software implementing this (DIFFANY; Van Landeghem et al., in preparation). To understand these dynamics, mathematical approaches such as qualitative and quantitative modeling are necessary. Using such methods, we aim during the coming years to unravel, model, and understand the network, to ultimately circumvent this growth-repressive response to stress.

Broader contexts for the unraveled pathway

As introduced in Chapter 2, several osmotic compounds are routinely used to apply stress *in vitro*. Since salt also induces ionic stress and polyethylene glycol appeared to be less suitable for mild stress setups, our choice fell on the osmoticum mannitol. When stress is applied at mild levels using low concentrations of the compound, the different osmotica trigger responses with little overlap, both in terms of transcriptome (see Chapter 2) and in terms of growth (Claeys et al., 2014). This compound-specificity was

also reflected in the expression of the genes of the ERF6-pathway. The expression of *ERF6* and of several of its target genes was not induced in actively growing leaves of plants exposed to short term salt, polyethylene glycol or sorbitol treatments (unpublished data). Accordingly, *erf5erf6* mutants grow better than wild type plants when exposed to mannitol, but not when exposed to salt, neither when grown under control conditions. Based on these results, we previously concluded that the ERF6-pathway only plays a role in regulating leaf growth under mannitol.

However, several mutants carrying mutations in *EIN5* showed reproducible increased leaf size phenotypes when grown under control conditions (Chapter 5). At least one of these EIN5 mutants was also more tolerant to mild drought stress in soil. This shows that EIN5, or at least these specific alleles of EIN5, are involved in the regulation of leaf growth under conditions other than mannitol-induced osmotic stress. Accordingly, mutations in some genes involved in the transcriptional network around ERF6 were also found to alter leaf growth under control conditions (Lisa van den Broeck and Dirk Inzé, unpublished data). It thus seems that ERF6 is a mannitol-specific central factor controlling a growth-regulatory network, but that the network itself, or at least part of it, likely also functions under a broader range of environmental conditions (Figure 7.1).

Besides its role under abiotic stress, the ERF6-centered network might also form a functional module during biotic stress defense. Ethylene is an important regulator of the biotic stress response, but its function in this process has mainly been characterized in mature Arabidopsis leaves. Necrotrophic pathogens, such as the fungus *Botrytis cinerea*, induce ethylene biosynthesis through posttranslational activation of ACC-SYNTHASES by the MPK3/6 phosphorylation cascade (Meng et al., 2013). MPK3/6 also phosphorylate and thereby activate ERF5 and ERF6. Together with genes involved in JA signaling, also induced by these pathogens, ERF5 and ERF6 are known to regulate the expression of genes encoding for *PLANT DEFENSIN* (PDF) proteins. Accordingly, two studies reported that plants overexpressing *ERF6* are more resistant to necrotrophic fungi (Moffat et al., 2012; Meng et al., 2013), but these results should be interpreted with care as the opposite has also been observed (Son et al., 2012). The network around ERF6 contains several genes of the WRKY family, such as *WRKY15*, *WRKY33* and *WRKY48*, which were also reported to be activated by pathogens (Zheng et al., 2006; Xing et al., 2008; Vanderauwera et al., 2012). Several other members of the transcriptional network, such as MYB51, ERF59, and ERF98, also have been shown to be involved in biotic stress response (Gigolashvili et al., 2007; Zarei et al., 2011; Zander et al., 2014). Finally, also *rst1*, a putative repressor of ERF6-induced growth inhibition, has a reported role in biotic stress defense and *rst1* mutants show enhanced resistance to necrotrophic fungi (Mang et al., 2009). The ERF6-ERF11 regulon, of which the expression is often affected in biotic stress studies (Chapter 4), might thus not only have

roles in the abiotic stress response but could also orchestrate the defense mechanisms under necrotrophe pathogen attack.

Time courses are crucial to unravel short term stress responses

The main advantage of *in vitro* systems is the precise control of stress onset. Controlling stress onset has two main benefits. First, it allows to precisely apply the stress at the chosen developmental stage of the organ of interest, which has previously been shown to be determinant for the specificity of the response. Second, sudden exposure to stress followed by measurements on very short term is possible, and was shown to be essential since part of the stress response is just transient. Following the logic that the subsequent steps of a pathway likely occur in subsequent order with a certain time delay, these *in vitro* assays enabled us to reconstruct a pathway (Figure 7.1). Accumulation of the ethylene precursor ACC occurs within 1 hour after stress exposure (Skirycz et al., 2011). Accordingly, transcriptional induction of *ERF6* was also measured within one hour of stress, or within 45 minutes after ACC-treatment (Chapter 4). Subsequently, induction of the *GA2-OX6* gene occurs 2 to 4 hours upon the activation of ERF6 (Chapter 3). Finally, DELLA proteins stabilize after one day following stress (Claeys et al., 2012) or ERF6 activation (Chapter 3). DELLA proteins trigger exit out of the cell cycle by downregulation of *UVI4/DEL1* and *CYCLIN* genes, whose expression was also clearly downregulated one day after stress (Skirycz et al., 2011). Within the time frame of 24 hours, osmotic stress triggered the inhibition of leaf growth (Skirycz et al., 2011). Two days after the onset of stress, we noticed a reduction in transcript levels of ERF6 and of the transcription factors around ERF6 (Lisa van den Broeck, unpublished data), as well as a decrease in the DELLA levels (Claeys et al., 2012). These results are in accordance with what has been reported in flowers of plants exposed to stress, where DELLA-related responses were only observed in the early stages of mild stress, but not anymore on longer term (Ma et al., 2014). Capturing the growth-inhibitory responses within a short time frame is thus crucial, since leaf growth is partially rescued when mannitol treatment persists (Skirycz et al., 2011). Thus, time courses *in vitro* are essential to uncover the early steps of growth-regulatory pathways.

THE WAY BACK FROM *IN VITRO* TO IN SOIL STRESS TREATMENT IS CHALLENGING BUT FEASIBLE

The overall stress responses triggered by mannitol and mild drought are very different

Once we had explored the molecular pathways regulating leaf growth under *in vitro* osmotic stress, our curiosity brought us to test the role of these pathways when plants are exposed to real drought, in soil. We set up a soil-based assay to measure short term drought response and analyzed the expression of the regulators of growth under mannitol during 5 days following drought. These results clearly showed that *ERF6* is not induced by drought, and is even slightly downregulated after 3 to 4 days of drought (Supp. Figure S1). Accordingly, *erf5erf6* mutants do not grow better than WT plants when exposed to these mild drought conditions (unpublished results). Some target genes of ERF6, such as *STZ* and *GA2-OX6*, also show the tendency to mainly be downregulated by drought, suggesting that they are not involved in the drought stress response in a similar way as under mannitol treatment (Supp. Figure S1). The molecular players important for leaf growth regulation under mannitol (Figure 7.1) are thus clearly not responsible for the inhibition of leaf growth under drought. This also supports our previously described view that ERF5 and ERF6 would be central regulators of the network only in the conditions of mannitol-induced stress.

If mannitol triggers such specific responses, what is the relevance of its use to mimic mild drought? To investigate to what extent mannitol- and drought-triggered responses are similar, we compared our mannitol and drought datasets. While it should be noted that both experiments were performed on leaves that differed 5 days in development, the stress level applied in both datasets is rather similar, since it just mildly affects leaf growth. Overall, the large-scale responses induced by both stresses appear to be very different, as illustrated by the absence of any correlation between the *in vitro* and in soil dataset (PCC = -0.09). This shows that processes that are strongly affected by drought are not responding in a similar way to mannitol, and *vice versa*. For example, genes responsible for proline accumulation were highly responsive to drought stress (Chapter 6), but were not differentially expressed in young leaves of plants exposed to mannitol (Skirycz et al., 2011). Similarly, abscisic acid signaling genes are affected by drought, but under mannitol their induction was restricted to mature leaf tissues, and no differential expression was observed in actively growing leaves (Skirycz et al., 2010). Plants thus activate stress defense responses that are clearly different upon exposure to *in vitro* mannitol-induced stress and in soil mild drought, even when comparable tissues and

severity are used. Thus, overall stress responses indicate that mannitol is not a suitable proxy to mimic mild drought stress in soil.

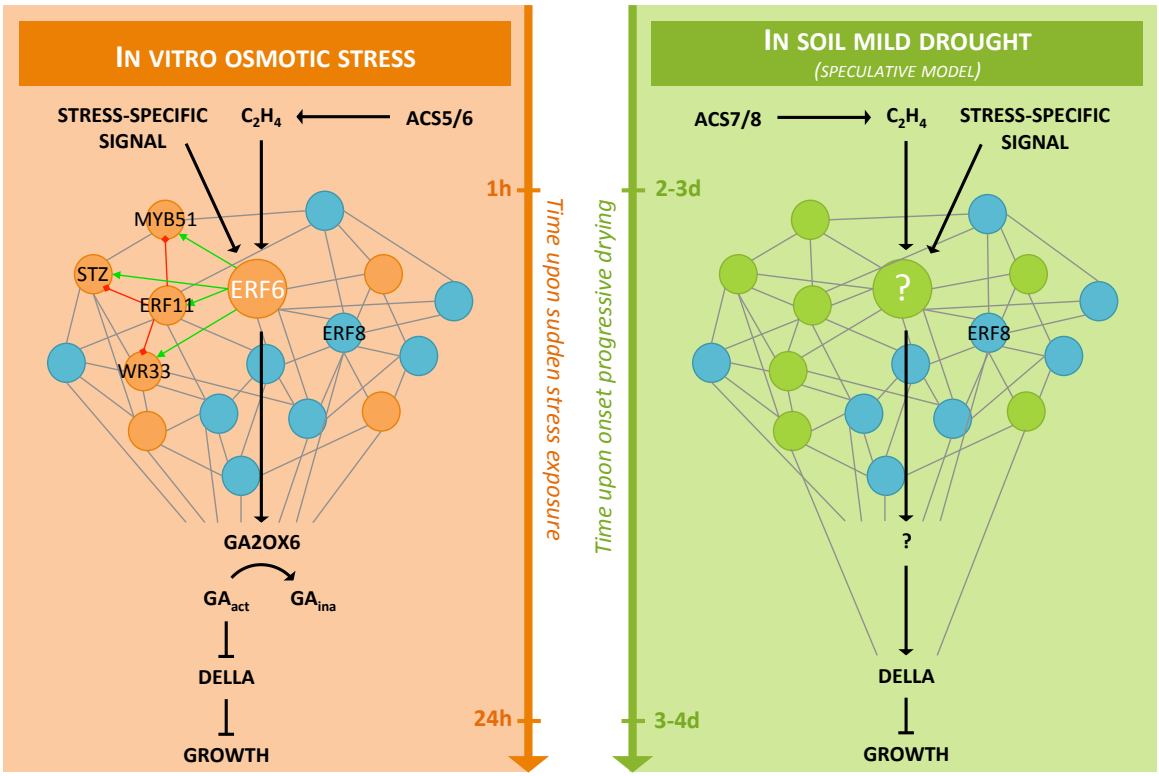

Figure 7.1. Comparison between the growth-regulatory mechanisms under osmotic stress and mild drought. Osmotic stress (left panel) triggers accumulation of the ethylene precursor ACC, within one hour of stress exposure. ACS5 and ACS6 are candidate ACC-synthases to generate ACC under *in vitro* stress. Ethylene induces the expression of several ERFs, but additional stress-specific signals likely determine their exact identity. Under mannitol-induced stress, ERF6 is a central transcription factor in a highly interconnected network of potential growth- and defense-regulators. The ERF6-ERF11 negative feedback loop forms a small module within this network. Several members of the network (orange nodes) are also mannitol-specific. Downstream, ERF6 induces *GA2-OX6*, which inactivates GA, stabilizing DELLA proteins and thereby inhibiting leaf growth within one day. Other members of the network can also affect the growth through yet unknown molecular mechanisms (grey connections). Under mild drought (right panel; speculative model), these general mechanisms underlying leaf growth inhibition might be conserved. ACS7 and ACS8 are candidate activators for ACC-biosynthesis. More downstream, part of the transcriptional network regulating leaf growth is likely conserved (blue nodes), while other drought-specific transcription factors might complete the network under drought (green nodes). The central transcription factor in this network under drought still remains to be identified, since ERF6 is not involved in this response. While the molecular connections with the effectors of growth control are still unknown (grey connections), evidence points toward a role for the DELLA proteins under drought conditions as well.

Basic growth-regulatory mechanisms might be conserved

While mannitol and drought clearly affect different physiological processes, they share the characteristic of reducing the growth of young leaves. To compare the mechanisms underlying leaf growth inhibition, the genes potentially involved in this process first need to be captured out of large transcriptional responses triggered by different stresses. With the *in vitro* setup, this was achieved by focusing on the response in actively growing leaves, at the moment when the growth inhibition occurred (Skirycz et al., 2011). As *in vitro* the onset of stress is controlled, expression changes can be captured within a very short time frame (from 1.5h to 24h after stress onset), thereby reducing the likelihood to measure long term, secondary responses. In soil, however, growth inhibition was observed only three days following the start of progressive drying, and within that time frame other drought-responsive processes were also already strongly induced. Thousands of genes were thus differentially expressed and the subtle growth-related response was diluted in this pool of genes. To extract potential growth-regulating genes under drought, the strategy used was to match the expression patterns with the dynamics of leaf growth under drought. We identified 228 genes putatively involved in growth regulation. Within this group of genes, genes involved in ethylene, GA, and JA synthesis and signaling were overrepresented, while these hormonal processes were not enriched in the overall drought response, demonstrating that the growth response was indeed diluted.

The possible involvement of ethylene and GA specifically in the growth-related response to drought might point towards a similar growth regulation under mannitol and drought. Under *in vitro* stress, the ACC-SYNTHASES ACS5 and ACS6 were shown be important for leaf growth inhibition (Skirycz et al., 2011) and were strongly co-expressed with the expression of the central regulators *ERF5*, *ERF6* and *ERF11* (Chapter 4). In soil, ACS7 and ACS8 might have similar functions under drought; both were identified amongst the 228 genes possibly important for the growth dynamics. ACS7 and ACS8 can be responsible for ethylene accumulation under drought at the moment when leaf growth is inhibited. Similarly as *in vitro* as well, DELLA proteins might be central effectors to induce growth inhibition, since we observed the induction of three of the five DELLA proteins under drought. Interestingly, amongst the 228 genes putatively involved in leaf growth regulation under drought, 81 were transcription factors, which again shows the importance of transcriptional regulation and the possible presence of a growth-related transcriptional network, similarly as under mannitol. What was most striking was that multiple transcription factors figuring amongst the 81 candidates for growth-regulation under drought also belonged to the confined group of 20 transcription factors forming the network centered around ERF6 under mannitol. Several WRKY transcription factors and ERFs, such as ERF11, ERF8, ERF2, and others

were again identified as putative regulators of growth. The expression of *ERF8* was affected similarly by mannitol and drought (Supp. Figure S1). When exposed to mild drought the *erf8* mutant showed a larger leaf phenotype under control conditions as well as under drought (Chapter 6). The same phenotype had previously been observed when *erf8* was grown *in vitro* on MS and mannitol (Lisa Van den Broeck and Dirk Inzé, unpublished results). As also illustrated by the larger phenotype of one of the EMS-induced *ein5* mutants under mild drought, at least part of the growth-regulatory network is conserved between mannitol and drought stress. Future experiments will be essential to determine whether in soil mild drought also triggers the accumulation of ethylene, and subsequently stabilization of the DELLA proteins. However, since the transcriptional data points in this direction, we conclude that while the overall response triggered by mannitol and drought are clearly different, the basic growth-regulatory mechanisms, including ethylene-mediated responses and downstream DELLA effects, are likely conserved. The network, which is centered around ERF6 under osmotic stress, might also be important to regulate leaf growth under drought, but then other regulators which still remain to be identified are controlling this network.

Unraveling growth-regulatory mechanisms directly in soil: additional challenges…

Because *in vitro* setups do not seem to provide the solution to mimic drought in soil, efforts should be made to find suitable setups to measure short term responses to mild drought directly on soil-grown plants, on physiological, phenotypical and transcriptional level. However, additional technical difficulties are popping up with such in soil setups, forming additional challenges and complicating data interpretation.

During the last years, the knowledge gathered from osmotic stress experiments *in vitro* highlighted the importance of precise control of (i) the stress level, (ii) the developmental stage of the studied organ and (iii) the duration of exposure to stress. Measuring the effects of these three factors in relevant drought conditions in soil forms a major challenge, as they can easily be confounded. In drying soil, the stress level and duration of stress exposure are tightly linked, with stress levels increasing with the duration. For example in our data, we observed 728 genes affected by drought during the second night after the start of progressive drying, and 2,538 genes during the third night. This clear increase is likely a combination of increase of one day in stress duration, but also an increase in severity, as the relative humidity of the soil dropped from on average 1.5 to 1.35 g_{water}/g_{soil} between both time points. Moreover, as the progressive drying of the soil takes several days, plant development is often perturbed

during the stress, and is also easily confounded with the duration effect, particularly under long term experiments.

An additional challenge is posed by the seemingly much more complex transcriptional responses encountered when performing transcriptomics in soil. Diurnal expression rhythms are clearly present, since the transcription of more than 60% of the measurable genes fluctuated throughout the day. In soil, the time of day appeared to be of tremendous importance in affecting the extent, the specificity and in some cases also the direction of the drought stress response. In our experiments performed *in vitro*, we did not observe such clear influence of the time of day (Supp. Figure S1). This is likely because our *in vitro* growth medium was supplemented with sucrose, reducing the importance of photosynthesis, and, thus, of effects of the diurnal carbohydrate status in the leaves. In soil, however, diurnal rhythms, clock-controlled leaf growth and transcriptional effects of drought seem to be intimately interconnected, complicating interpretation of such datasets.

… and possible ways to tackle them

Despite several additional technical challenges encountered in soil which are complicating the identification of growth-related drought responses, lessons from *in vitro* research can be used to design adapted experimental setups. To capture pathways involved in leaf growth regulation, the experiments conducted *in vitro* taught us that short term measurements are essential, but defining "short term" in soil poses an additional problem. When soil is dried out progressively, it is unclear at which level of soil humidity the stress response will be activated. Moreover, particular processes within stress response are likely induced when different thresholds in soil humidity are reached. To capture short term drought responses, a technique based on transfer of young seedlings directly to pots with dry soil and to pots with humid soil as a control has been established (Clauw et al., 2015). This technique is suitable to precisely control stress onset and to uncouple stress severity from stress duration. However, *in vitro* assays also taught us that very mild levels of stress can already affect the growth response, and that severe stress predominantly induces survival response (Claeys and Inzé, 2013; Claeys et al., 2014). In such transfer setup, the transfer by itself likely induces considerable stress in such young plants, which might mask or perturb the short term growth-related drought responses.

Finally, *in vitro* studies also showed the importance of performing detailed time course experiments to limit the risk of missing transient responses and to use such data over time to reconstruct the subsequent steps of stress-induced pathways. Based on the lessons learned from the combination of *in vitro* research and the in soil drought

experiments, the following experimental design would, in the opinion of a not yet graduated PhD student with little experience, be suitable to study short term growth-related responses to mild drought. A suitable model leaf should be chosen and plants should be exposed to well-watered conditions until the leaf is still young and actively growing, but has already grown sufficiently to be able easily perform phenotypic, physiological, transcriptional and protein-level measurements. At this time point, progressive drying of the soil can start and this should be accompanied by detailed time course analysis with high-resolution phenotypic, physiological and transcript-level measurements, which should start immediately after stress onset in order to capture the short term response. In this respect, phenotypic measurements performed on the same leaf over time are more powerful to detect subtle changes caused by drought. From the moment that drought triggers small changes in the phenotype, the soil humidity of the drought treatment should be kept constant. The time course experiment can then still be continued for several days, without confusion between stress duration and stress severity. Finally, the dynamics of the drought effects on the phenotype and on the transcriptome can be integrated to uncover possible regulators and effectors of the phenotype of interest. Most likely, mathematical modeling approaches will be of great help to understand these extremely complex but fascinating responses underlying the regulation of leaf growth under drought.

SUPPLEMENTAL DATA

Supplemental Figure S1. Expression analysis of *ERF6*, *ERF8*, *STZ* and *GA2-OX6* during day 15 after stratification upon exposure to stress.

REFERENCES

Achard P, Baghour M, Chapple A, Hedden P, Van Der Straeten D, Genschik P, Moritz T, Harberd NP (2007) The plant stress hormone ethylene controls floral transition via DELLA-dependent regulation of floral meristem-identity genes. Proc Natl Acad Sci U S A 104: 6484-6489

Achard P, Gong F, Cheminant S, Alioua M, Hedden P, Genschik P (2008) The cold-inducible CBF1 factor-dependent signaling pathway modulates the accumulation of the growth-repressing DELLA proteins via its effect on gibberellin metabolism. Plant Cell 20: 2117-2129

Achard P, Vriezen WH, Van Der Straeten D, Harberd NP (2003) Ethylene regulates arabidopsis development via the modulation of DELLA protein growth repressor function. Plant Cell 15: 2816-2825

Claeys H, Inzé D (2013) The agony of choice: how plants balance growth and survival under water-limiting conditions. Plant Physiology 162: 1768-1779

Claeys H, Skirycz A, Maleux K, Inzé D (2012) DELLA signaling mediates stress-induced cell differentiation in Arabidopsis leaves through modulation of anaphase-promoting complex/cyclosome activity. Plant Physiology 159: 739-747

Claeys H, Van Landeghem S, Dubois M, Maleux K, Inzé D (2014) What is stress? Dose-response effects in commonly used in vitro stress assays. Plant Physiology 165: 519-527

Clauw P, Coppens F, De Beuf K, Dhondt S, Van Daele T, Maleux K, Storme V, Clement L, Gonzalez N, Inze D (2015) Leaf responses to mild drought stress in natural variants of Arabidopsis. Plant Physiol 167: 800-816

Dong HP, Peng J, Bao Z, Meng X, Bonasera JM, Chen G, Beer SV, Dong H (2004) Downstream divergence of the ethylene signaling pathway for harpin-stimulated Arabidopsis growth and insect defense. Plant Physiol 136: 3628-3638

Gigolashvili T, Berger B, Mock HP, Muller C, Weisshaar B, Flugge UI (2007) The transcription factor HIG1/MYB51 regulates indolic glucosinolate biosynthesis in Arabidopsis thaliana. Plant J 50: 886-901

Ma T, Li ML, Zhao AG, Xu X, Liu GS, Cheng LQ (2014) LcWRKY5: an unknown function gene from sheepgrass improves drought tolerance in transgenic Arabidopsis. Plant Cell Reports 33: 1507-1518

Magome H, Yamaguchi S, Hanada A, Kamiya Y, Oda K (2008) The DDF1 transcriptional activator upregulates expression of a gibberellin-deactivating gene, GA2ox7, under high-salinity stress in Arabidopsis. Plant J 56: 613-626

Mang HG, Laluk KA, Parsons EP, Kosma DK, Cooper BR, Park HC, AbuQamar S, Boccongelli C, Miyazaki S, Consiglio F, Chilosi G, Bohnert HJ, Bressan RA, Mengiste T, Jenks MA (2009) The Arabidopsis RESURRECTION1 gene regulates a novel antagonistic interaction in plant defense to biotrophs and necrotrophs. Plant Physiol 151: 290-305

Meng X, Xu J, He Y, Yang K-Y, Mordorski B, Liu Y, Zhang S (2013) Phosphorylation of an ERF transcription factor by *Arabidopsis* MPK3/MPK6 regulates plant defense gene induction and fungal resistance. Plant Cell 25: 1126-1142

Moffat CS, Ingle RA, Wathugala DL, Saunders NJ, Knight H, Knight MR (2012) ERF5 and ERF6 play redundant roles as positive regulators of JA/Et-mediated defense against *Botrytis cinerea* in Arabidopsis. PLoS ONE 7: e35995

Skirycz A, Claeys H, De Bodt S, Oikawa A, Shinoda S, Andriankaja M, Maleux K, Eloy NB, Coppens F, Yoo S-D, Saito K, Inzé D (2011) Pause-and-stop: the effects of osmotic

stress on cell proliferation during early leaf development in *Arabidopsis* and a role for ethylene signaling in cell cycle arrest. Plant Cell 23: 1876-1888

Skirycz A, De Bodt S, Obata T, De Clercq I, Claeys H, De Rycke R, Andriankaja M, Van Aken O, Van Breusegem F, Fernie AR, Inzé D (2010) Developmental stage specificity and the role of mitochondrial metabolism in the response of Arabidopsis leaves to prolonged mild osmotic stress. Plant Physiology 152: 226-244

Son GH, Wan J, Kim HJ, Nguyen XC, Chung WS, Hong JC, Stacey G (2012) Ethylene-responsive element-binding factor 5, ERF5, is involved in chitin-induced innate immunity response. Molecular Plant-Microbe Interactions 25: 48-60

Van de Poel B, Smet D, Van Der Straeten D (2015) Ethylene and hormonal crosstalk in vegetative growth and development. Plant Physiol

Vanderauwera S, Vandenbroucke K, Inze A, van de Cotte B, Muhlenbock P, De Rycke R, Naouar N, Van Gaever T, Van Montagu MC, Van Breusegem F (2012) AtWRKY15 perturbation abolishes the mitochondrial stress response that steers osmotic stress tolerance in Arabidopsis. Proc Natl Acad Sci U S A 109: 20113-20118

Xing DH, Lai ZB, Zheng ZY, Vinod KM, Fan BF, Chen ZX (2008) Stress- and pathogen-induced Arabidopsis WRKY48 is a transcriptional activator that represses plant basal defense. Mol Plant 1: 459-470

Zander M, Thurow C, Gatz C (2014) TGA Transcription Factors Activate the Salicylic Acid-Suppressible Branch of the Ethylene-Induced Defense Program by Regulating ORA59 Expression. Plant Physiol 165: 1671-1683

Zarei A, Korbes AP, Younessi P, Montiel G, Champion A, Memelink J (2011) Two GCC boxes and AP2/ERF-domain transcription factor ORA59 in jasmonate/ethylene-mediated activation of the PDF1.2 promoter in Arabidopsis. Plant Mol Biol 75: 321-331

Zheng Z, Qamar SA, Chen Z, Mengiste T (2006) Arabidopsis WRKY33 transcription factor is required for resistance to necrotrophic fungal pathogens. Plant J 48: 592-605

Supp. Figure S1. Expression analysis of *ERF6*, *ERF8*, *STZ* and *GA2-OX6* during day 15 after stratification upon exposure to stress. Expression of *ERF6* (A) and *ERF8* (B) during *in vitro* growth (left) on control (MS) and osmotic stress (Mann; mannitol) conditions, and during in soil growth (right) under well-watered (WW) and mild drought conditions. Osmotic stress was applied suddenly in the morning of day 15. Progressive soil drying was started at 12 days after stratification. The blue arrow represents the amplitude of diurnal ERF6 and ERF8 fluctuations under control conditions. (C) Expression of *STZ* and *GA2-OX6* during in soil growth under WW and drought conditions as described in (A,B). The gray zone represents the dark period at night. Values are the means of three biological repeats with their standard error.

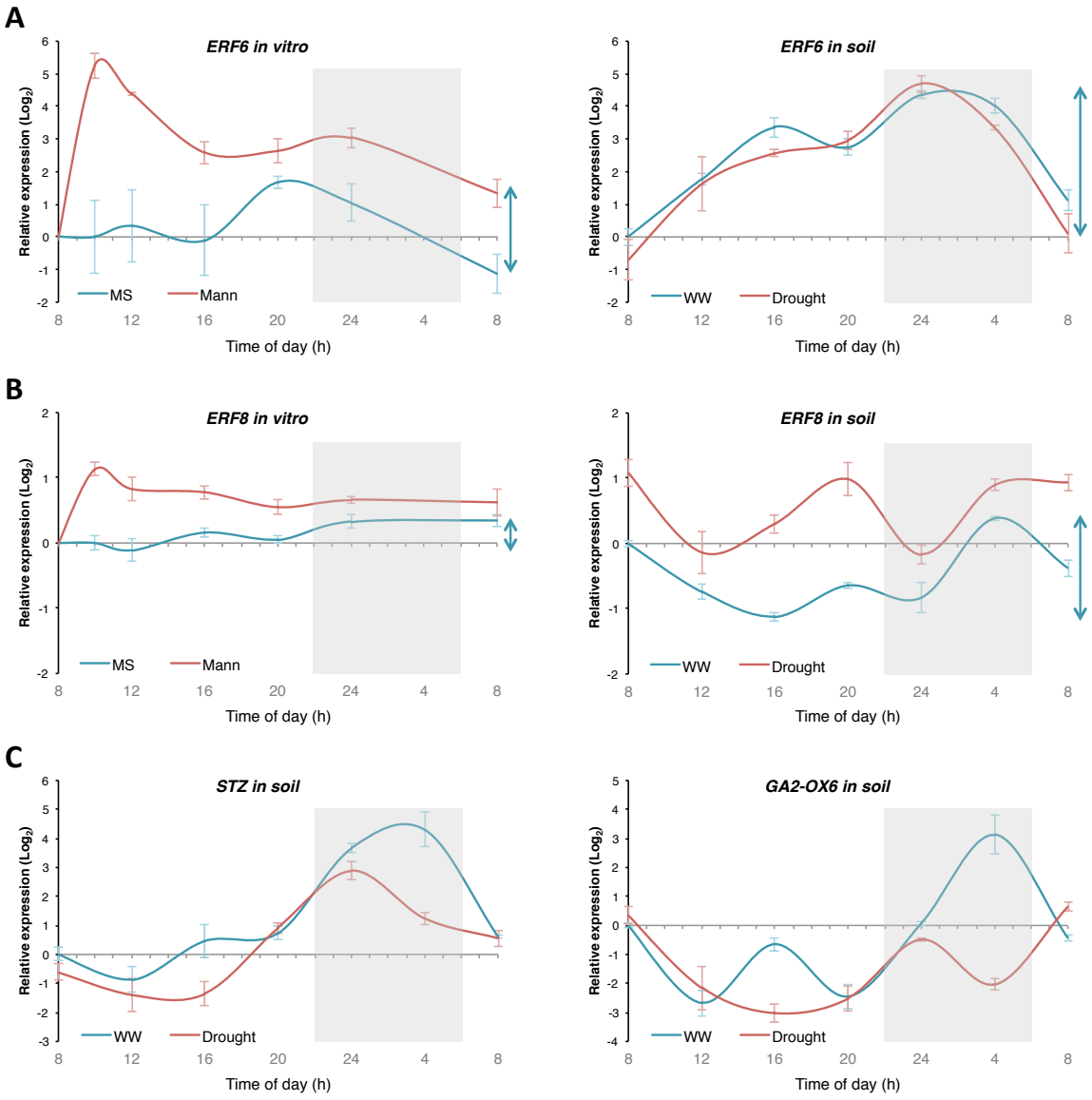

Summary

Drought stress forms a major constraint for agriculture worldwide as it is responsible for tremendous yield losses every year. In moderate climates, drought stress does not threaten the survival of plants but severely affects plant growth. Even when the water availability is only slightly reduced, mechanisms are induced to shut down growth. In the presented work, we studied the regulation of this growth inhibition at the molecular level. We used young leaves of Arabidopsis plants exposed to mild osmotic stress as model organs to explore the drought-induced changes in growth and the transcriptome.

Upon exposure to osmotic stress *in vitro*, which is used as a proxy for drought, the phytohormone ethylene rapidly accumulates specifically in the young, actively growing leaves. Since ethylene is a known negative regulator of cell division and cell growth in various other contexts, this hormone is a plausible candidate to repress leaf growth under osmotic stress as well. Several ETHYLENE RESPONSE FACTORs (ERFs), the transcription factors downstream of the ethylene-signaling pathway, are induced within one hour of exposure to stress and are central regulators of the early stress response.

We first characterized ERF6, a transcriptional activator, which plays a dual role in growing leaves of plants exposed to stress. On the one hand, ERF6 activates the *GA2-OXIDASE6* gene, encoding an enzyme that inactivates gibberellins (GA), thereby stabilizing DELLAs, important growth-repressing proteins. As a result, plants overexpressing *ERF6* are extremely dwarfed and hypersensitive to stress, while loss-of-function *erf5erf6* mutants grow better than wild type plants when exposed to stress. On the other hand, ERF6 also activates a plethora of well-known stress-related transcription factors, which are thought to be involved in stress tolerance mechanisms.

Amongst the target genes of ERF6, many other ERFs were found and we subsequently characterized the function of ERF11, a transcriptional repressor induced by ERF6. While overexpression or loss-of-function of *ERF11* alone did not dramatically affect plant growth or gene expression, mainly its relationship with ERF6 appeared to be important under stress. Being a repressor, ERF11 inhibits the growth- and tolerance-related genes that were induced by ERF6 when stress was perceived. As a result of this antagonism, plants simultanously overexpressing *ERF6* and *ERF11* do no longer exhibit the ERF6-

induced dwarfism. We speculated that this negative feedback mechanism was established to fine-tune the stress response and to block it when stress decreases. Together, these experiments showed that rapid ethylene accumulation under stress and downstream inhibition of the GA-pathway are connected by several ERFs, which act together to induce and subsequently fine-tune the stress response in growing Arabidopsis leaves.

Considering the complexity of the mechanisms underlying leaf growth and of the response to stress, it was however very unlikely that this simple pathway would be the sole regulator of leaf growth under stress. To expand the network around ERF6 and identify new genes involved in growth under stress, we performed a forward genetics screen for mutants suppressing the ERF6-induced dwarfism. Up to now, seven suppressor-mutants were identified and the causal mutations suppressing the ERF6 function are being confirmed. Amongst the mutants suppressing ERF6-induced dwarfism, several were mutated in *ETHYLENE INSENSITIVE 5* (EIN5). EIN5 is a regulator of transcript stability within the ethylene signaling pathway, and loss-of-function of EIN5 results in ethylene insensitivity and suppression of the ERF6-overexpression phenotype. Interestingly, several specific alleles of *EIN5* identified during the screen generate plants with increased leaf sizes, both under control and drought stress conditions. Hence, EIN5 is clearly linked with the ERF6-function and, more generally, with the control of leaf growth, through still unknown molecular mechanisms.

Finally, after exploring the mechanisms underlying leaf growth inhibition under osmotic stress *in vitro*, we investigated whether similar mechanisms were important for the response to real drought, in soil. We therefore first developed a setup that enabled capturing the early drought responses in actively growing Arabidopsis leaves, by tracking leaf growth over time and measuring expression changes with a high time-resolution. Surprisingly, the growth and transcriptional responses to drought were extremely complex, with the time of day as a crucial factor influencing not only the extent and the specificity, but also the direction of the expression changes. While the response to drought in soil does not seem to involve the same molecular players as compared to stress *in vitro*, the general mechanisms, including ethylene- and gibberelin-mediated growth inhibition, seem to be most likely conserved. Accordingly, several ERF transcription factors were identified as putative candidates to orchestrate the growth-regulatory mechanisms under drought stress in soil.

Samenvatting

Droogte vormt wereldwijd een grote bedreiging voor de jaarlijkse landbouwopbrengsten. In gematigde klimaten heeft droogte weinig effect op het overleven van de plant, maar het wel zorgt voor een dramatische vermindering in plantengroei. Zelfs als de droogte nog zeer mild is, activeert de plant mechanismen om zijn groei stil te leggen. In deze studie onderzochten we de moleculaire mechanismen die dergelijke groei-inhibitie reguleren. We gebruikten jonge bladeren van Arabidopsis planten blootgesteld aan milde osmotische stress, om de groei en de transcriptionele responsen onder stress in kaart te brengen.

Bij blootstelling aan *in vitro* osmotische stress, die gebruikt wordt om droogte na te bootsen, wordt het hormoon ethyleen uitsluitend in jonge, actief groeiende bladeren zeer snel geïnduceerd. Van ethyleen is reeds geweten dat het een groei-represserende functie kan uitoefenen in verschillende andere biologische contexten; het vormt dus een geschikte kandidaat om ook in jonge bladeren de respons op stress te reguleren. Meerdere Ethyleen Respons Factoren (ERFs), transcriptiefactoren die geactiveerd worden door ethyleen, worden geïnduceerd na slechts één uur blootstelling aan stress en staan centraal in deze respons.

In deze studie karakteriseerden we eerst de functie van ERF6, een transcriptionele activator die een tweezijdige rol blijkt te spelen in de respons onder stress. Enerzijds activeert ERF6 het *GA2-OXIDASE6* gen, dat codeert voor een enzym dat gibberellines (GA) inactiveert. Dalende GA-niveaus zorgen ervoor dat de DELLA-eiwitten gestabiliseerd worden, wat groei-inhibitie veroorzaakt. Planten die *ERF6* tot overexpressie brengen vertonen extreme dwerggroei en zijn hypersensitief voor stress, terwijl *erf5erf6* mutanten beter groeien ten opzichte van wild-type planten wanneer ze onder stress gegroeid worden. Anderzijds induceert ERF6 ook talrijke andere transcriptiefactoren, waarvan sommige reeds gekende functies hebben in stresstolerantie.

Een van de transcriptiefactoren die door ERF6 geactiveerd wordt, is ERF11, een transcriptionele repressor. Hoewel overexpressie of neerregulatie van *ERF11* op zich geen dramatische effecten heeft op plantengroei, bleek ERF11 voornamelijk belangrijk

te zijn in relatie tot ERF6. Onder stress represseert ERF11 de groei- en stresstolerantiegenen die door ERF6 geactiveerd werden. Als gevolg van het antagonisme tussen beide transcriptiefactoren, vertonen planten die zowel *ERF6* als *ERF11* tot overexpressie brengen geen dwerggroei meer. Vermoedelijk kwam dit negatieve feedbackmechanisme tot stand om de stressrespons af te stellen en deze snel te kunnen remmen wanneer de stress opnieuw afneemt. Deze experimenten toonden aan dat de snelle ethyleenaccumulatie en de daaropvolgende inhibitie van de GA-pathway gelinkt kunnen worden door meerdere ERFs, die samen de groei onder stress nauwkeurig reguleren.

Aangezien bladgroeiregulatie en stressrespons zeer complex kunnen zijn, lijkt het onwaarschijnlijk dat bladgroei onder osmotische stress enkel door de simpele ERF6/ERF11-pathway beïnvloed wordt. Om het netwerk rond ERF6 verder uit te breiden, voerden we een grootschalige screen uit voor mutanten die de ERF6-gemedieerde dwerggroei kunnen onderdrukken. Tot nu toe werden zeven suppressor-mutanten geïdentificeerd en de mutaties die aan de basis liggen van het herstel van het dwergfenotype worden momenteel bevestigd. Meerdere suppressor-mutanten vertoonden een mutatie in het EIN5-gen (ETHYLENE INSENSITIVE5), dat codeert voor een eiwit dat transcripten degradeert in de ethyleensignalisatie pathway. Verlies van de functie van EIN5 maakt planten ongevoelig voor ethyleen en onderdrukt het ERF6-fenotype. Echter, sommige specifieke mutaties in *EIN5* genereren *EIN5*-allelen die niet enkel ERF6-gemedieerde dwerggroei herstellen maar bovendien ook grotere rozetten vertonen, zowel onder controle condities als onder droogtestress. EIN5 is dus duidelijk gelinkt aan het ERF6-netwerk, en speelt wellicht ook een belangrijke rol in de regulatie van bladgroei.

Nadat we de mechanismen die bladgroei inhiberen onder osmotische stress uitvoerig geanalyseerd hadden, onderzochten we of gelijkaardige mechanismen ook een functie hebben onder echte droogte, in aarde. Hiervoor ontwikkelden we een nieuwe setup die het mogelijk maakt om bladgroei en expressieveranderingen over tijd te volgen met hoge tijdsresolutie. Na blootstelling aan droogte, bleken de groei- en transcriptionele responsen bijzonder complex te zijn. Beide waren bovendien zeer sterk beïnvloedbaar door het moment van de dag waarop de metingen gebeurden, met zeer verschillende responsen ‘s morgens, ‘s middag, en ‘s nachts. Hoewel de responsen op echte droogte niet dezelfde moleculaire factoren betrekken als de responsen op osmotische stress, blijken de algemene mechanismen toch behouden te zijn. Ethyleen en gibberellines spelen ongetwijfeld ook onder droogte een cruciale rol, aangezien een aantal ERFs opnieuw geïdentificeerd werden als potentiële regulatoren van bladgroei onder echte droogte.

Acknowledgements

Cold Spring Harbor, NY, 28/07/2015

I have just been enjoying the 34°C and sun for more than an hour, but some little voices in my head keep on reminding me of the reason for being here. I need to write, these holidays were meant for writing and my introduction is still not finished (actually, only one paragraph done since noon). It's nearly the last day of my writing holiday, the fourth of this year and likely the last one (unless something goes really wrong...). I was recalling some memories of these 4.5 really amazing years; crazy how time flies when passion and friends drive you through it. I'm savoring the sun and the home-made iced tea (thanks, Hansie!), trying in the mean time to spot another deer, with the sound of squirrels springing from tree to tree, and our cat Lauryn laying at my feet. It thought I would postpone that part till the end, but this suddenly feels like the ideal timing for writing the most popular part of my thesis, and express some big thank you.

Dirk, « for giving me the opportunity to do my PhD in his group »… No, for so much more. For believing in me since years, giving me so much freedom and for supporting every crazy idea. For guiding me through fascinating science for four years, and for setting me back on the right path when I lost it, but also for being so human when it came to non-scientific things. Thank you Dirk, I couldn't have wished for a better PhD promoter!

Hannes, at the moment I'm writing you are on your field. I need to be fast as soon you'll come back and we'll have to leave for diner tonight. Northporth, it's gonna be perfect, as always. We will talk about science while enjoying diner at candlelight, and discuss about our list of future trips to make around the world, while looking at the sunset on the ocean. I think I don't need more words; I've found the best friend, most amazing scientist, greatest post-doc and most fantastic travel partner ever. I will never thank you enough for pulling me through this whole PhD, so I will not even try. You know how grateful I am, anyway.

Hannes, the other one, the one who always manages to make me smile in every situation; thank you for this! I really enjoyed having a neighbor like you, and I hope that our separating future paths will be brought back together by new, exciting science. Thanks to

you, and to Liesbeth, for the nice lunch-break chats and the hour-long gossiping, I really loved sharing all these moments with you.

Lisa, for the very nice collaboration during these last 2,5 year. For your great enthusiasm, passion, seriousness, motivation, but also for your trust. You really taught me a lot. Besides Lisa, I also want to thank every other student who ever shared a part of my project: Kaatje, Michiel, Ting, Isabelle, Pieter, Fien, Catarina, Katrien and Ryan. Even though not all experiences were equally positive, I learned from all of you.

Aleksandra, for building the foundations of a project that I really loved, and for sharing all her know-how, passion, and genius.

Nathalie, for taking so well care of me and everyone else of our group, and for always making time for a chat or for advice, whenever I needed it. I wish you a great scientific future, and hope you will not forget to also take care of yourself.

Katrien, Twiggy, Liesbeth, and Mattias, for all the big or little helps, I really appreciated your enthusiasm, advice, support, and actually all moments shared with you at the bench. Mattias, for being so flexible when it comes to cleaning my bench. Judith, for the good chats, scientific or not, it was good to have you nearby. Raf, for being the best example that a silent person can be incredibly funny and crazy. Jasmien, for being always so positive and for sharing this when needed; I wish you all the best with your crazy project. Chrystalla, for sharing late evenings in the lab but also for always being willing to save my experiments during the weekends. Alexandra, for the frietjes-evenings with long chats during my night experiments. Pieter, for introducing me to the world of real drought and leaving behind an already optimized machine. Youn Jeong, for the highly appreciated chats on late evenings. Jonas, for sharing your passion for science and see, I will not forget the messages you transmitted. Stijn and Nathalie W., for always being willing to spend some time when I had troubles with a robot. To all of you, so many thanks! I really enjoyed all scientific and non-scientific moments with everyone of the Yield group, so a big big thank you to all great yielders.

An equally big thank you to all the non-yielders who taught me so much during these years or who just made my time in PSB a bit greater by being there. Robin, for making me discover the world of luciferase assays, spending hours of time to solve my robot problems and make my assays work. Brecht, for the same reasons actually (yes, I really struggled in the beginning). All the people of the TAP-group for their first aid with all the western blot problems I encountered. Frederik, for solving the statistics or sequencing emergencies. Wilson, because it is so nice to work with smiling people around you. Also all people that make me feel less lonely during night experiments: Wim, Matthias, Zubing, Lorin and more sporadic night-workers. Everyone that made working at PSB so easy by their great

support: Nathalie VdH, Kristof, Jacky, Peter, Nico, Miguel, and the whole logistic and support team. A big thank you to Karel, for the last-minute cover picture!

To all people who ever rescued the WIWAM robot during the weekend: many thanks for saving my experiments!

The members of the Jury of my PhD, and Geert De Jaeger for being the perfect Chair of it. Thanks for taking the time to read this work, for providing highly appreciated useful feedback, and for being so flexible in planning the defenses.

And last but certainly not least, my family and friends, mom, dad, Quentin and Jeroen, for giving me all this love, all these opportunities, but also all this freedom. Marie, Catherine, Sophie, Caro and my lovely dancers of Cie A Pieds Nus, for all these highly appreciated relaxing and wonderful moments during the weekends. I guess this perfect balance between work and distraction was the key of 4 years of happiness.

I had a wonderful time, met so many fantastic people who taught me great science in a so pleasant environment. I think I have filled my knowledge luggage, at least enough for the next trip, and I just need friends to guide me, a boss to support me, and importantly, a bit of luck, to bring the future plans to a good end!

Curriculum Vitae

Marieke DUBOIS
488, Rue de la gare
59299 Boeschepe
FRANCE
madub@psb.ugent.be
+32 (0) 475 33 78 19

Date of birth: October 24, 1987
Place of birth: Croix (59), France
Nationality: French
Marital status: Unmarried

Current position

Predoctoral fellow, in the "Systems biology of yield" group headed by Prof. Dirk Inzé.
Department of Plant Systems Biology, VIB Ghent, Belgium

Education

2011 – 2015 **PhD., Plant biotechnology**
Ghent University, Ghent, Belgium
Dissertation: "Unraveling the molecular mechanisms underlying leaf growth inhibition under drought: it's all about timing"
Promotor: Prof. Dr. Dirk Inzé

2005 – 2010 **B.Sc. and M.Sc., Biochemistry and biotechnology**
Major: Plant biotechnology
Ghent University, Ghent, Belgium
Graduated 'with great distinction'
Dissertation: "Systems biology of drought in Arabidopsis"
Promotor: Prof. Dr. Dirk Inzé

Skills

Languages: French (native), Dutch (native), English (good), German (basic)
Software: MS Office Word – Excel – Powerpoint (very good), Linux (basic), Shore (basic)
Programming languages: Perl (basic)
Statistics: R (basic)

Publications in peer-reviewed journals

Dubois M*, Skirycz A*, Claeys H, Maleux K, Dhondt S, De Bodt S, Vanden Bossche R, De Milde L, Yoshizumi T, Matsui M, Inzé D. (2013) Ethylene Response Factor6 acts as a central regulator of leaf growth under water-limiting conditions in Arabidopsis. Plant Physiology 162(1):319-332.

Dubois M, Van den Broeck L, Claeys H, Van Vlierberghe K, Matsui M, Inzé D. (2015) The ETHYLENE RESPONSE FACTORS ERF6 and ERF11 antagonistically regulate mannitol-induced growth inhibition in Arabidopsis. Plant Physiology 169(1):166-179.

Dubois M*, Claeys H*, Inzé D. Time of day determines Arabidopsis transcriptome and growth dynamics under mild drought. Nature Plants, under review.

Claeys H, Van Landeghem S, Dubois M, Maleux K, Inzé D. (2014) What Is Stress? Dose-Response Effects in Commonly Used in Vitro Stress Assays. Plant Physiology 7;165(2):519-527.

Van Landeghem S, Van Parys T, Dubois M, Inzé D, Vandepeer Y. Diffany: an ontology-driven framework to infer, visualise and analyse differential molecular networks. BMC Bioinformatics, under review.

Patents

"Mutant alleles for yield increase", by D. Inzé, H. Nelissen and M. Dubois. Filed 3/10/2014. EP 14187614.4.

"Methods and means to produce abiotic stress tolerant plants", by D. Inzé, M. Dubois and A. Skirycz. 16/09/2011. PCT/EP2012/068100.

Presentations at international conferences

SPS Conference 2013, Paris: Plant signaling in a changing environment. Selected short talk entitled "How drought affects leaf growth: ERF5/6 and DELLAs act together to regulate growth inhibition under stress."

EPSR Conference 2013, Ghent: European Plant Science Retreat. Selected short talk entitled "Molecular mechanisms underlying leaf growth inhibition under stress."

Salt and drought stress Gordon Research Conference 2015, Maine, US. Poster presentation entitled "From *in vitro* to in soil: unraveling leaf growth under drought."

Organisation of international conferences

EPSR Conference 2013, Ghent: European Plant Science Retreat. As a member of the organizing committee.

Supervising activities

PhD projects

"Unraveling the growth-regulatory network under stress" - Lisa Van den Broeck
"Identifying the early regulators of leaf growth under drought" - Kaatje Van Vlierberghe
"Identification of new genes involved in leaf growth under stress" - Ting Li

Master thesis projects

"ERFs as central regulators of leaf growth under stress" – Kaatje Van Vlierberghe
"Identification of new genes for leaf growth under drought" – Michiel Rydant
"Unraveling the network underlying leaf growth under stress" – Lisa Van den Broeck

Undergraduate projects

"Upstream regulators of ERF6 under stress" – Katrien Dewolf
"Identification of ERF6 target genes" – Lisa Van den Broeck
"Natural variation of leaf growth under drought in Arabidopsis" – Isabelle Van de Velde
"Building the network of genes around ERF6" – Catarina Cascais
"Unraveling the connection between ERF6 and ERF11" – Kaatje Van Vlierberghe
"Investigating the link between ERF6 and ERF11" – Pieter Heeremans
"Unraveling the ERF6-induced transcriptional network" – Fien Christiaens